

University of St Andrews



Full metadata for this thesis is available in
St Andrews Research Repository
at:

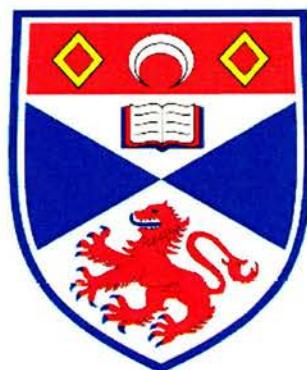
<http://research-repository.st-andrews.ac.uk/>

This thesis is protected by original copyright

SYNTHETIC STUDIES ON THE SMALL MOLECULE TOOL (S)-(-)-BLEBBISTATIN

Thesis submitted to the University of St Andrews in application for the degree of
Doctor of Philosophy

Cristina Lucas-Lopez



School of Chemistry
University of St Andrews
Fife, Scotland

July 2005



Th
F85

DECLARATION

I, Cristina Lucas Lopez, hereby certify that this thesis, which is approximately 54,123 words in length, has been written by me, that it is the record of work carried out by me and that it has not been submitted in any previous application for a higher degree.

Date: 21/07/05

Signature of candidate:

I was admitted as a research student in November, 2001 and as a candidate for the degree of Doctor of Philosophy in July, 2005; the higher study for which this is a record was carried out in the University of St Andrews between 2001 and 2005.

Date: 21/07/05

Signature of candidate:

I hereby certify that the candidate has fulfilled the conditions of the Resolution and Regulations appropriate for the degree of Doctor of Philosophy in the University of St Andrews and that the candidate is qualified to submit the thesis in application for that degree.

Date: 21/07/05

Signature of supervisor:

(Dr. N. J. Westwood)

COPYRIGHT DECLARATION

Unrestricted access

In submitting this thesis to the University of St Andrews I understand that I am giving permission for it to be made available for use in accordance with the regulations of the University Library for the time being in force, subject to any copyright vested in the work not being affected thereby. I also understand that the title and abstract will be published, and that a copy of the work may be made and supplied to any *bona fide* library or research worker.

Date: 21/07/05

Signature of candidate:

ABSTRACT

Small molecules that can perturb the function of a specific target protein are useful tools in basic cell biology research. Important areas in biology, such as cytokinesis (the last step in cell division), have not been extensively explored due to the lack of suitable small molecule tools that target their relevant proteins. Non-muscle myosin II has been identified as a protein component necessary for cell division. A recent programme focused on identifying novel inhibitors of non-muscle myosin II has been developed at Harvard University and screening of a commercially available compound library led to the discovery of the novel small molecule inhibitor, (-)-blebbistatin.

This thesis describes an efficient and flexible synthetic approach to highly optically enriched (-)-blebbistatin. The bioactive compound is synthesised from 2-amino-5-methylbenzoic acid in a four step procedure. The key step is the asymmetric hydroxylation of a quinolone intermediate using the Davis oxaziridine methodology. For the first time, we have proved that the absolute stereochemistry of (-)-blebbistatin is *S* by X-ray analysis of a heavy atom containing analogue of blebbistatin.

Subsequent studies on the core structure of blebbistatin show that it is possible through chemical modification to prepare analogues. Further biological testing of these compounds show which parts of (*S*)-(-)-blebbistatin are important to retain its inhibitory activity.

In addition, it is shown that the incorporation of a nitro functional group into the blebbistatin core structure modifies its fluorescence properties. This is of importance since this analogue can therefore be used in fluorescence-based microscope imaging experiments on live cells where (-)-blebbistatin cannot.

To my parents and to the memory of Pepa

ACKNOWLEDGEMENTS

I would like to thank Dr Nicholas Westwood for his help, advice, and encouragement during my project. I am very indebted to him for giving me the opportunity to join his group.

I would like to thank the EPSRC and the University of St Andrews for funding my project.

Thanks also to Dr David Smith for his support and constant wise advice. Thanks to Prof. Alexandra Slawin for being so much help with solving the crystal structures and for her kindness. Many thanks to Dr Nwaf Al-Maharik for his help and advice. I am grateful to Mrs Melanja Smith and Dr Tomas Lebl for their patience with answering my non-ending NMR questions. Also thanks to Dr Catherine Botting for teaching me all I needed to run HPLC, Mrs Carolyn Horsburgh for helping me with the MS and Mrs Sylvia Williamson for her help with the microanalysis.

My thanks to the post-docs in my lab; special thanks to Dr Stephen Patterson (Pupo), for suffering all my stress and his ability to always calm me down. Thanks, Pupo for all the good advice in both chemistry and life you have given to me and many thanks for being a good friend. I am also thankful to my other post-docs, Till Blum (for being there whenever I needed him and his nice company), Jon Hollick (for his good ideas), David Taddei (for cheering me up during my time writing up) and Russell Pearson (always ready to help).

I must also thank all the people in my lab, Nico (for the long chats), Neil (for his smile), Richard (for his great sense of humour), Kathryn and Rachel (for the good suggestions) and Nick. Thanks to all of them for the great time we have shared in the lab.

Many thanks to my 'Spanish family', Alejandro, Alvaro, Belen and Cristina, for always being there, for the good and bad moments, for taking care of me and for putting up with my variable mood...gracias por haber sido mi familia durante todo este tiempo y por esa gran amistad que hemos tenido. Thanks also to my other family 'the Italians',

Franco, Cosimo, La Fede, Davide and Walter, for their happiness and for their constant support, making me feel as one of them.

My thanks to Vasso and Jana (for their friendship), Mark (for helping me so much with the computers), Charlotte (for allowing me to bother Pupo during dinner time with chemistry), Mairead, Gareth, Jose, Mayca, Alberto, Fernando, Vanesa, Eduardo and Carina.

Thanks to my friends in Spain, Emi, Raquel, Espe, Monica, Chuvi, Laura, Pepa, Eva, Sonia, Francisco, Maria Jesus, Rocio and Juan ('el pelos'). Gracias por haber mantenido el contacto y no olvidaros de mi durante todo este tiempo fuera. Sin vuestro apoyo, la vida en este pais se me hubiera hecho un poco mas dura.

A mis abuelas, a mis tios, Reme, Jose, Paqui y Chelo, a mis primos y hermano Susana, Carina, Pepe y David, por apoyarme en todo momento y por toda la fuerza que me han dado para seguir adelante.

Finally, this thesis would not have been possible without all the support, help, and love of my parents. They have been encouraging me during all these years of study and have given to me the best advices to keep my mind sane. Todo lo que he conseguido en esta vida y lo que pueda conseguir en un futuro os lo debo a vosotros, gracias.

ABBREVIATIONS

Å	angstrom
Ac	acetyl
ADP	adenosine diphosphate
ATP	adenosine triphosphate
Bz	benzoyl
°C	degrees centigrade, temperature unit
CAN	cerium (IV) ammonium nitrate, $[\text{Ce}(\text{NH}_4)_2(\text{NO}_3)_6]$
CD	circular dichroism
CDCl_3	deuterated chloroform
CD_3OD	deuterated methanol
CHCl_3	chloroform
CH_3O	methoxy radical, $\text{OCH}_3\cdot$
CI	chemical ionisation
COSY	proton-proton correlation spectroscopy
DABCO	1,4-diazabicyclo[2,2,2]octane
DCC	1,3-Dicyclohexylcarbodiimide
DCM	dichloromethane
D6-DMSO	deuterated dimethyl sulfoxide
d.e	diastereomeric excess
δ	chemical shift
DMAP	4-dimethylaminopyridine
DMF	<i>N,N</i> -dimethylformamide
DMPU	1,3-dimethyl-3,4,5,6-tetrahydro-2(1 <i>H</i>)-pyrimidinone
DMSO	dimethylsulfoxide

D8-THF	deuterated tetrahydrofuran
ee	enantiomeric excess
EI	electron impact, ionisation technique
equiv	equivalents
ES ⁺	positive electrospray
Et	ethyl radical, CH ₃ CH ₂ -
EtOAc	ethyl acetate
g	grams
Gly	Glycine
h	hours
HMBC	Heteronuclear Multiple Bond Connectivity
HMPA	hexamethylphosphoramide
HOBt	1-hydroxybenzotriazole
HPLC	high performance liquid chromatography
HR	high resolution
HSQC	Heteronuclear Single Quantum Coherence
HTS	highthrough-put screening
IC ₅₀	concentration at which 50% enzyme inhibition is observed
IR	infrared
<i>J</i>	coupling constant
LCMS	liquid chromatography mass spectrometry
LDA	lithium diisopropylamide
Leu	Leucine
LiHMDS	lithium bis(trimethylsilyl)amide
M	concentration, mol.L ⁻¹

<i>m</i> -CPBA	<i>m</i> -chloroperbenzoic acid
Me	methyl radical, CH ₃ -
MeCN	acetonitrile
MeI	methyl iodide
MeOH	methanol
MHz	MegaHertz
min	minutes
μL	microlitres
mL	millilitres
mmol	millimol
mp	melting point
MS	mass spectroscopy
MTPA	α-methoxy-α-(trifluoromethyl)phenylacetyl chloride
<i>m/z</i>	mass over charge ratio
NADH	nicotinamide adenine dinucleotide (reduced form)
NAD(+)	nicotinamide adenine dinucleotide (oxidised form)
NBS	<i>N</i> -bromosuccinimide
NEt ₃	triethylamine
NaHMDS	sodium bis(trimethylsilyl)amide
nm	nanometres
NMMII	non-muscle myosin II
NMR	nuclear magnetic resonance
NOE	nuclear Overhauser effect
NOESY	nuclear Overhauser effect spectroscopy technique
ORD	optical rotatory dispersion
PBS	phosphate-buffered saline

Pd/C	palladium on carbon
Ph	phenyl radical, C ₆ H ₅ -
Pi	inorganic phosphate
ppm	parts per million
Py	pyridine
R _f	retention factor, chromatography
RNAi	ribonucleic acid interference
RT	room temperature
Selectfluor TM	1-chloromethyl-4-fluoro-1,4-diazoniabicyclo[2.2.2] octane bis(tetrafluoroborate)
THF	tetrahydrofuran
TLC	thin layer chromatography
t _R	retention time
UV	ultraviolet
v	wavenumber, cm ⁻¹

CONTENTS

DECLARATION

COPYRIGHT DECLARATION

ABSTRACT

ACKNOWLEDGEMENTS

ABBREVIATIONS

CONTENTS

CHAPTER 1: INTRODUCTION

1.1	SMALL MOLECULES: DISCOVERY AND OPTIMISATION.....	1
1.2	CHEMICAL GENETICS	5
1.3	SMALL MOLECULES INVOLVED IN STUDYING THE CYTOSKELETON.....	10
1.4	TARGET PROTEIN: THE MYOSINS	12
1.4.1	Classification of Myosins	12
1.4.2	Inhibitors of Myosins	16
1.4.3	Identification of (\pm)-Blebbistatin: a novel small molecule inhibitor of <i>non-muscle</i> myosin II	18
1.4.3.1	Preliminary biological characterisation of (\pm)-Blebbistatin	20
1.4.3.2	Specificity of (\pm)-Blebbistatin	23
1.4.3.3	Mechanism of action of (\pm)-Blebbistatin.....	24
1.5	AIMS AND OBJECTIVES OF THE PROJECT	24
1.6	REFERENCES	26

CHAPTER 2: RESULTS AND DISCUSSION

2.1	SYNTHESIS OF RACEMIC 3a-HYDROXY-6-METHYL-1-PHENYL-2,3,3a,4- TETRAHYDRO-1 <i>H</i> -PYRROLO[2,3- <i>b</i>]-QUINOLIN-4-ONE	32
2.1.1	<i>Via</i> Azatacrine Degradation	32
2.1.2	An overview of the synthetic approach to (\pm)-Blebbistatin	33

2.1.3	Preparation of the cyclisation precursors	34
2.1.3.1	The Vilsmeier reaction.....	35
2.1.3.2	Initial attempts to prepare amidine	38
2.1.3.3	Empirical approaches to improving the yield of the coupling reaction.....	42
2.1.3.4	NMR studies on the formation of the Vilsmeier intermediate.....	45
2.1.3.4.1	NMR studies on <i>N</i> -lactams and phosphorus oxychloride	46
2.1.4	Synthesis of Quinolones.....	50
2.1.4.1	Attempts to cyclise amidine analogues.....	54
2.1.5	Synthesis of (±)-Blebbistatin.....	56
2.1.5.1	Air Oxidation	56
2.1.5.2	Photolysis.....	56
2.2	ASYMMETRIC HYDROXYLATION: AN ALTERNATIVE ROUTE FOR THE SYNTHESIS OF THE CORE STRUCTURE OF (–)-BLEBBISTATIN	58
2.2.1	Overview of chemical methods in asymmetric hydroxylation.....	58
2.2.2	Oxaziridines.....	59
2.2.2.1	Synthesis of oxaziridines	60
2.2.2.2	Oxaziridines as oxygen transfer reagents	62
2.2.2.3	Examples of the use of oxaziridines	63
2.2.3	Synthesis of (–)-Blebbistatin using Davis methodology.....	66
2.3	REFERENCES.....	70

CHAPTER 3: RESULTS AND DISCUSSION

3.1	GENERAL METHODS FOR THE DETERMINATION OF ENANTIOMERIC EXCESS	74
3.1.1	Determination of the enantiomeric excess for (–)-Blebbistatin by chiral liquid chromatography (HPLC).....	78
3.1.2	Optimisation of the asymmetric hydroxylation reaction.....	80
3.1.3	Preparation of highly optically enriched samples of (–)-Blebbistatin and (+)-Blebbistatin.....	88
3.2	DETERMINATION OF THE ABSOLUTE CONFIGURATION	91
3.2.1	Proof of absolute stereochemistry of (<i>S</i>)-(–)-Blebbistatin.....	93
3.3	ASYMMETRIC HYDROXYLATION OF METHYL ANALOGUES OF (<i>S</i>)-(–)-BLEBBISTATIN	101

3.4	PROPOSED MODEL FOR ASYMMETRIC INDUCTION	103
3.5	REFERENCES.....	110

CHAPTER 4: RESULTS AND DISCUSSION

4.1	SPECIFICITY AND POTENCY OF (<i>S</i>)-(-)-BLEBBISTATIN.....	115
4.2	INTRODUCTION OF DIVERSITY INTO THE (<i>S</i>)-(-)-BLEBBISTATIN CORE STRUCTURE	115
4.3	PREPARATION OF (<i>S</i>)-(-)-BLEBBISTATIN ANALOGUES SUBSTITUTED IN THE AROMATIC RING (R^3).....	116
4.3.1	Synthesis of analogues with $R^3 = \text{Me}$	118
4.3.2	Preparation of an analogue of (<i>S</i>)-(-)-Blebbistatin incorporating a nitro substituent in the aromatic ring (R^3)	124
4.3.3	Summary section	128
4.4	INTRODUCTION OF DIVERSITY AT THE QUATERNARY CARBON (3a) POSITION	129
4.4.1	Incorporation of Halogens at the R^1 position	129
4.4.1.1	Synthesis of 3a-Chloro analogue	130
4.4.1.2	Synthesis of 3a-Fluoro analogue.....	134
4.4.1.3	Synthesis of 3a-Bromine analogue	139
4.4.2	Attempts to derivatise the Blebbistatin core structure at position 3a	140
4.4.2.1	Acylation of the tertiary alcohol	140
4.4.2.2	Alkylation of the 3a alcohol.....	147
4.4.3	Carbon-Carbon bond formation	148
4.5	CHANGE IN THE OXIDATION STATE OF THE HETEROCYCLIC CORE STRUCTURE	152
4.6	INCORPORATION OF DIVERSITY AT THE <i>N</i> -PHENYL RING (R^2).....	159
4.7	REFERENCES.....	162

CHAPTER 5: RESULTS AND DISCUSSION

5.1	CRYSTAL STRUCTURE OF BLEBBISTATIN AND MYOSIN II	166
5.2	BIOLOGICAL ACTIVITY OF (<i>S</i>)-(-)-BLEBBISTATIN, (<i>R</i>)-(+)-BLEBBISTATIN AND NITROBLEBBISTATIN	169
5.3	PRELIMINARY BIOLOGICAL TESTING OF BLEBBISTATIN ANALOGUES.....	171
5.4	SECTION SUMMARY	178
5.5	REFERENCES.....	179

CHAPTER 6: CONCLUSIONS AND FUTURE WORK.....	180
CHAPTER 7: EXPERIMENTAL.....	183
APPENDIX.....	242

CHAPTER 1
INTRODUCTION

THE USE OF SMALL MOLECULE TOOLS TO STUDY CELLULAR PROCESSES

1.1. SMALL MOLECULES: DISCOVERY AND OPTIMISATION

The use of small molecules as tools to perturb biological systems has had an enormous impact in the field of cell biology.^{1,2} There have been a considerable number of pharmacological reagents, both natural products and synthetic compounds, developed over the years for use in biology laboratories (Figure 1 shows some important examples). In addition, the use of small molecule tools is gaining momentum in other fields such as neurobiology and cellular microbiology.³

The term 'small molecule' is usually applied to organic, non-peptide compounds with a molecular weight of less than 1500 Da.^{3,4} Small molecules are preferably cell-permeable and can perturb (either enhance or inhibit) the function of a specific target protein in place of a genetic mutation.⁵ Knowing the mode of action of the small molecule in one system could also lead to the investigation of the role of its target protein in other systems and processes.⁶

Small molecules come from several sources such as complex mixtures of natural products extracted from plants, fungi and bacteria,⁷ commercial compound collections (*e.g.* Maybridge) or 'in house libraries' (*e.g.* from target orientated synthesis (TOS) libraries and diversity orientated synthesis (DOS) libraries).⁸

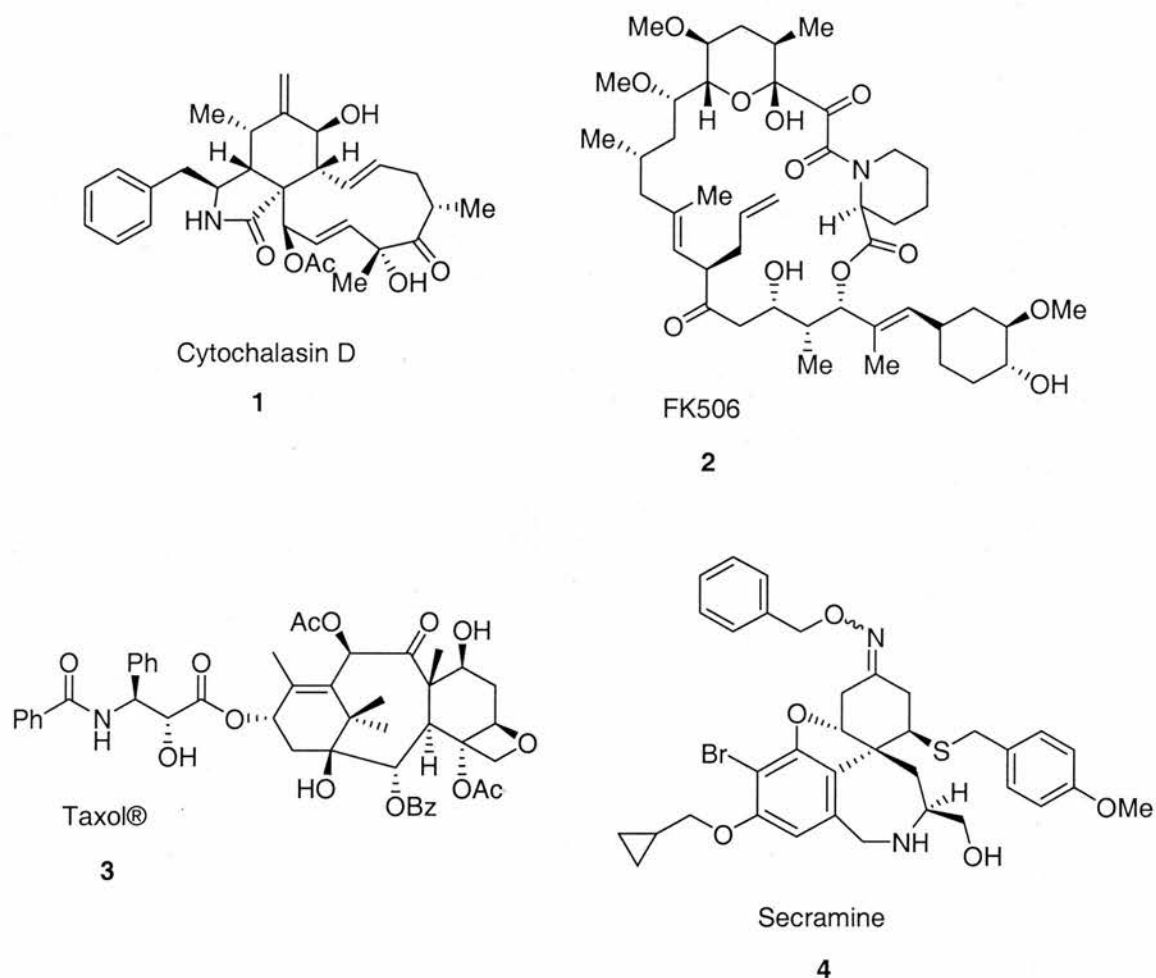


Figure 1. Examples of bioactive small molecules. a) Cytochalasin D (1), a natural product isolated from a fungal species. This molecule inhibits whole-cell migration through a direct effect on actin⁹ and disrupts the cell margin and the cytoplasmic cleavage of dividing cells¹⁰ b) FK506 (2), a natural product that inhibits the production of many cytokines (*e.g.* the protein calcineurin) which are produced in cells during an immune response. In addition this immunosuppressant molecule is used to prevent organ transplant rejection¹¹ c) Taxol® (3), a natural product with an antileukemic and antitumor activity. This compound stimulates the polymerisation of microtubules (tubulin stabiliser)¹⁰ d) Secramine (4), a small molecule identified from a DOS library that is known to block protein trafficking from the Golgi apparatus to the plasma membrane, although the protein target is unknown.¹²

Small molecule natural products can be obtained by extraction of plants or microbes with different solvents. Subsequently, the resulting crude extracts can be assayed for the biological activity of interest. Further rounds of purification and screening are repeated until the pure bioactive compound is isolated. Although natural products have been used as a source of bioactive small molecules for many years, the purification of single bioactive entities from complex crude mixtures is laborious and difficult. This is one of the factors that has resulted in commercial collections of compounds becoming more popular. Large, chemically diverse and high purity collections of small molecules can be purchased from different companies (*e.g.* ChemBridge and ChemDiv) and they are also available from non commercial sources such as the National Cancer Institute. These compound collections are often provided as individual dry films/powders or as stock solutions in DMSO, formatted in multi-well plates ready for high-throughput screening. Common features of these compounds are often their low molecular weight (average 350 Da) and the relative absence of stereogenic centres. Not all bioactive compounds identified from these collections can be used in a straightforward manner as a tool to study the biological processes of interest, as the identified compounds do not always have all the desired properties (chemical, biological or physical). At this stage, the synthetic organic chemist plays a very important role by carrying out *chemical optimisation* of the target molecule to improve its properties. A key challenge is to modify the structure of the compounds by incorporation of diverse building blocks (*i.e.* preparing a large collection of analogues).^{4,13}

Finally, small molecules can be prepared in the laboratory as large collections of novel compounds. This work has been intensively developed by Schreiber and co-workers at Harvard University.⁸ The preparation of small molecule collections using solid phase organic chemistry affords not only the initial hit compounds but also large numbers of structurally related analogues. Work in this field is termed diversity-orientated synthesis (DOS), which has the aim of preparing large collections of compounds with a high level of structural complexity and diversity to explore a specific biological process.¹⁴ This approach contrasts with target-orientated synthesis (TOS), which has as its main goal the synthesis of a defined target (*e.g.* a natural product synthesis).^{8,15}

The search for novel small molecule modulators of protein function has been mainly an approach developed in pharmaceutical companies although it is gaining momentum in academia. This revival in the use of small molecules in academic biology has occurred because they provide a method of dissecting biological processes that is often complementary to classical genetics and RNAi technology.¹⁶ The success of the chemical genetic approach and the increasing access in academia to high-throughput screening equipment and collections of small molecules will allow the rapid discovery of potential novel therapeutics and biological probes.^{17, 18} Figure 2 lists the advantages of using small molecules and therefore the importance of the chemical genetics approach.

Advantages	Disadvantages
<ul style="list-style-type: none"> • Cell permeability. • Fast acting. • Use of small molecules in combination (multiple knock-outs/ins). • Easily applicable to cross-species studies. • Used to study systems where standard genetic tools are unavailable, rudimentary or difficult to use. • Study of the function of essential or recessive genes. • Excellent temporal resolution (particularly important in the study of rapid cellular processes). • The ability to observe biological responses following release from a small molecule block (due to reversibility of action of most small molecules). • Can be used in most experimental situations including <i>in vitro</i> (e.g. purified protein studies), in the cell type of the researcher's choosing or <i>in vivo</i>. • Precise temporal and spatial control of activity using caging techniques.¹⁹ • Leads for drug discovery. 	<ul style="list-style-type: none"> • Lack of sufficient selectivity. • Timescale, for identification/validation

Figure 2. Advantages and disadvantages of using small molecules.⁴

1.2. CHEMICAL GENETICS

The investigation of the role of a protein in a cellular process requires the alteration of its function. A ‘genetic approach’, widely used in biology, involves the incorporation of inactivating (*e.g.* ‘knock out’) or activating mutations in the gene encoding the protein of interest. However, small molecules bind directly to proteins and can therefore be used in complementary studies to the genetic approach to alter protein function (Figure 3). The use of small molecules as biological probes is not a new concept. Since the eighteenth century where the first active compound (morphine) was isolated from a plant, natural product extracts have been used as the main available tool for perturbing biological systems. Nevertheless, a recent field has emerged at the interface between chemistry and biology which has been termed ‘chemical genetics’ with the aim of systematising the discovery and use of small molecule tools. This approach could also be considered as a reinvention of classical pharmacology using chemistry to generate biologically relevant small molecules.^{2, 5, 11, 13, 20, 21}

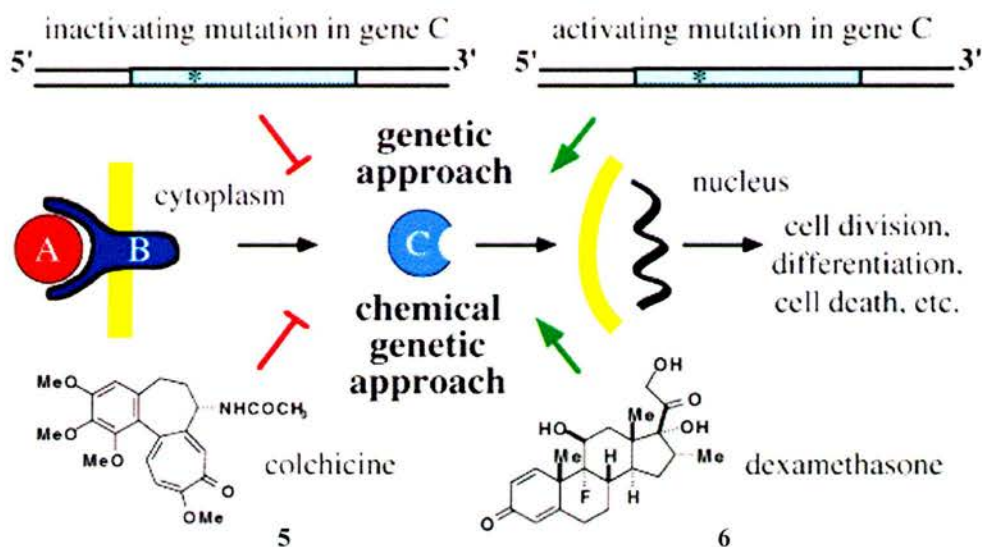


Figure 3. Schematic representation of the relationship between chemical genetics and classical genetics, using both small molecules and mutations to explore protein function. In the case of the genetic approach, inactivating or activating mutations in genes that encode the protein of interest are used. The chemical genetic approach uses small molecules to alter the function of the protein of interest by binding to it. These molecules can either inactivate the function of the protein (*e.g.* colchicine, which inactivates the function of tubulin) or activate the function of the protein (*e.g.* dexamethasone, a steroid hormone that activates the transcriptional properties of nuclear hormone receptors). (Figure taken from Schreiber, S. L., *Bioorganic & Medicinal Chemistry*).¹¹

In addition, this approach requires the development of new synthetic methods both to help to discover novel small molecules and to optimise the potency and specificity of the initially identified bioactive compounds.^{22, 23}

The chemical genetics approach is divided into two types:^{22, 24} a) *Forward chemical genetics*, where chemical libraries of compounds are tested in cells with the aim of finding small molecules that can cause the desired effect on the cell (produce a phenotype of interest), b) *Reverse chemical genetics*, where the small molecules are used to determine the biological function of a single target protein by inhibiting its activity.

Both *forward* and *reverse chemical genetics* (Figure 4) are essentially three step procedures: a) a collection or 'library' of compounds is obtained, b) a high-throughput screen (HTS) or assay is carried out to identify relevant compounds, c) a final step that is different for forward and reverse chemical genetics. *Forward chemical genetics* involves the use of an appropriate methodology to identify the target protein, the activity of which has been affected by the bioactive compound (*protein target identification*).²⁵ Protein target identification usually uses biochemical and molecular biological techniques. In *reverse chemical genetics* it is necessary to show that the *in vitro* activity of the small molecule is applicable in cells. This also involves target validation studies.^{1, 13, 20, 25}

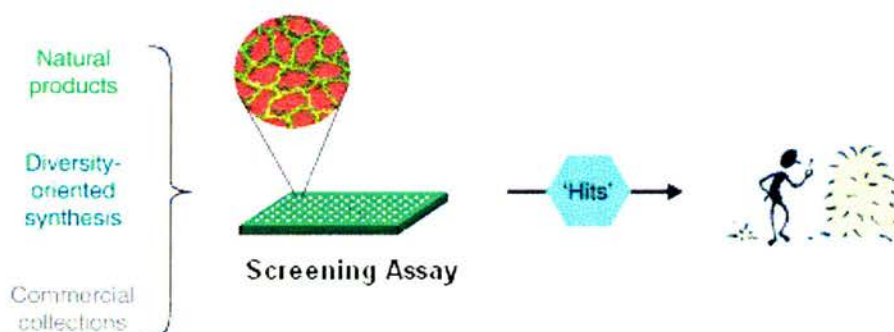


Figure 4. Chemical genetics approach. A schematic representation of the three step procedure: a) source of the small molecules, b) screening assay, c) target identification (*forward chemical genetics*) or target validation in cells (*reverse chemical genetics*).¹³

a) The chemical genetics approach: Collections or ‘libraries’ of compounds

The different methodologies used to prepare such libraries include solution phase (automated parallel synthesis) and solid phase (solid support such as a polystyrene bead). The use of solid phase methods is empowered by the ‘split and pool’ procedure (Figure 5) which enables the synthesis of large diverse collections of compounds by combining different building blocks (monomers).²⁶

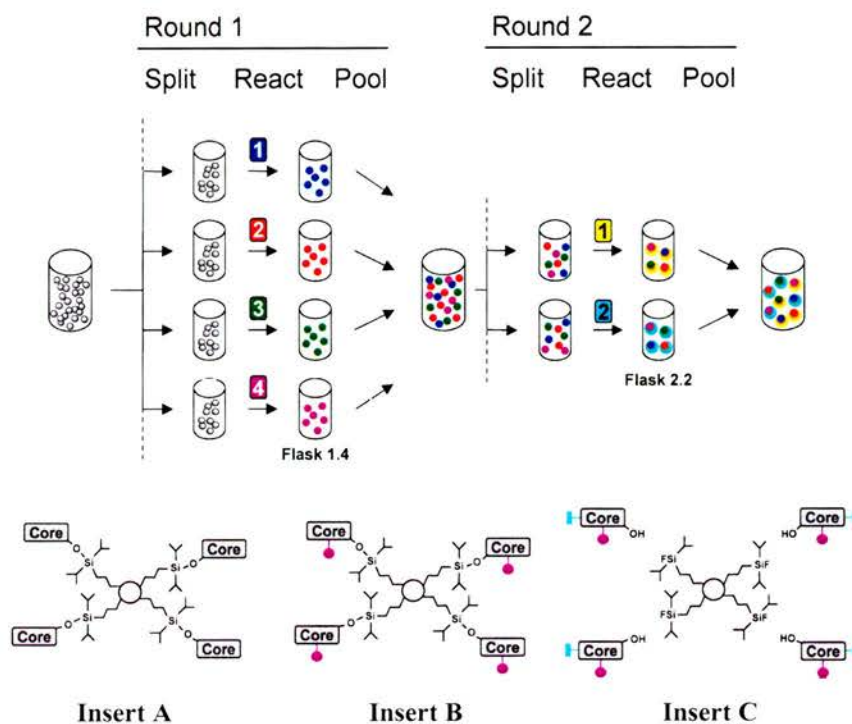


Figure 5. An example of the combinatorial chemistry approach. ‘Split and pool’ methodology to prepare large number of compounds.³ The reaction starts with copies of the same core small molecule attached to a set of beads (grey colour and insert A). The beads are then split out into different reaction flasks (in this example, four). Similar chemical reactions are carried out in order to attach a different building block to the small molecules on the beads, contained in each flask (purple colour and insert B). The beads from each flask are then pooled together into the same flask. Subsequently, they are split out again into a new set of reaction flasks (in this example, two). Second set of building blocks is added to the small molecules on the bead, using the same chemistry in each reaction. The beads from each flask are then pooled into the same flask again. Two rounds of split-pool synthesis have been completed. Insert A: example of the representation of a solid phase synthesis on a bead. The core small molecule is attached to the bead through a linker system (covalently attached to the small molecule). Insert B: example of a bead after one round of ‘split and pool’ synthesis. Insert C: at the end of the synthesis, the small molecule is cleaved from the bead after each bead is separated from each other. Finally, the small molecules are ready to be analytically and biologically tested.

This approach has yielded a wide range of chemical structures, although the compounds sometimes appear relatively simple compared with the complexity presented in natural products, which target diverse proteins with high affinity and selectivity. Although there is not an optimal structure to affect all biological system, it seems that efforts to synthesise small molecules have focused on heterocyclic aromatic compounds, which have a good background as drug leads. Recently studies led by Schreiber have focused on the synthesis of natural product-like libraries.^{1, 20, 25}

b) The chemical genetics approach: High-throughput screening (HTS)

Once a collection of compounds has been established, the next step is to assay them in order to find compounds with the desired biological activity. In the case of the *forward chemical genetics* approach, the compound collection is added to cell cultures whereas for the *reverse chemical genetics* approach, the library of compounds is added to a purified protein of interest. The technology used is often automated and miniaturised.²⁷ In general assays are performed in 96 well plates at 100 μL /assay or in 384 well plates at ~ 20 μL /assay. On rare occasions 1536 well plates at ~ 2 -4 μL /assay are used. The transfer of microlitre and also nanolitre volumes of liquid containing compounds from the collection into wells can be carried out by the use of parallel pipetting systems and pin arrays linked to a robotic system respectively (Figure 6). Control compounds (both positive and negative) are added to each plate where possible. Assays are usually monitored in a plate reader using either absorbance, luminescence, radioactivity or different fluorescence-based formats. In addition, automated microscopy approaches can be used.³ The collection of compounds is screened at a fixed concentration (typically 100 μM) hopefully yielding hit rates of 0.5-2.0%. All hits are retested several times to obtain validated preliminary hits (a new sample of the hit compound is either repurchased or resynthesised). Furthermore once the bioactive compounds have been discovered in the screen, they will often have to be structurally modified in order to increase their affinity for the target and to aid in protein target identification studies.³

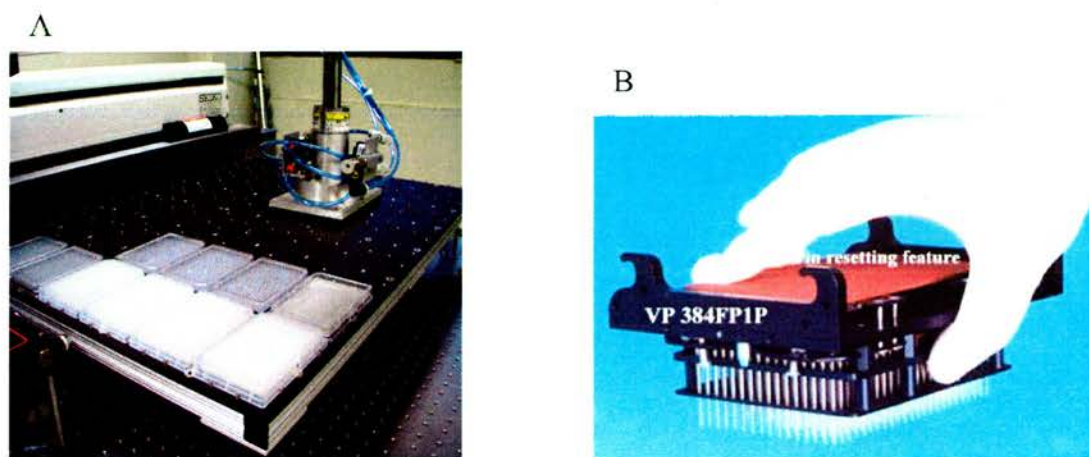


Figure 6. Compound transfer using a robot. An example of the pin array which can be attached to a robot.

c) Chemical genetics tools: Target validation in cells

This section briefly describes the third step in *reverse chemical genetics* as this was the approach used to identify the small molecule, (*S*)-(-)-blebbistatin (**7**) which is the subject of this thesis.

Once the active small molecule has been selected from a chemical library, the next step is to test whether the hit binds to and modifies the activity of its protein target in cells. This is the first step in a process referred to as *target validation*. A further step involves efforts to study the *specificity* of the small molecule for its target protein in the presence of multiple other possible targets. This specificity assessment is often carried out by testing whether the small molecule inhibits other closely related proteins in *in vitro* assays. Finally the specificity of the small molecule must be tested in cells although this is considerably more challenging.²⁸

In summary, the continuous effort by chemists and biologists to co-operate together and the improvement of techniques involved in chemical genetics is generating a series of powerful small molecule tools to help investigate biological questions. Furthermore, small molecules that have been screened for a human disease pathway can also function as drug leads.²⁵ Additionally, Schreiber has proposed a new goal for the chemical genetics approach, where the chemistry plays an important role in identifying a small molecule partner for every protein.¹¹

1.3. SMALL MOLECULES INVOLVED IN STUDYING THE CYTOSKELETON

One aspect of cell biology research involves the study of the cytoskeleton (Figure 7). The cytoskeleton is a complex network of protein filaments that extends throughout the cytoplasm to control the shape and movement of the cell. The cytoskeleton is also involved in intracellular transport and chromosome segregation. Two main groups of proteins that form the cytoskeleton are the protein filaments known as microtubules (made of tubulin) and microfilaments (made of actin). Other proteins present in the cytoskeleton include the intermediate filaments and motor proteins (myosins, kinesins, dyneins).²⁹ Many essential cell biological processes require the correct functioning of the cytoskeleton. Therefore, cell biologists have been interested in the search for small molecules that can modulate the activity of the *cytoskeletal proteins* in order to help them study the cytoskeleton.¹⁰

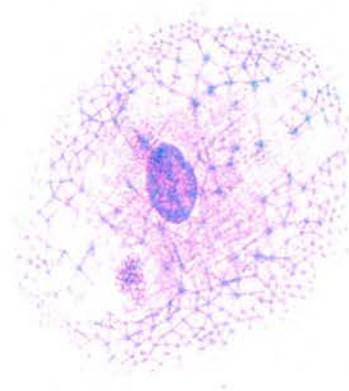


Figure 7. Coomassie stained cell showing extent of network of protein filaments throughout the cell (picture taken from Alberts *et al.*, Molecular Biology of the Cell).²⁹

The existing literature includes several examples of small molecules that target the cytoskeleton. For instance, the latrunculin family (Figure 8, A (**8**) and B (**9**)) has been widely used to study the cellular role of the actin cytoskeleton, as these inhibitors modify the ability of actin to polymerise.^{10,30} Furthermore, colchicine (**5**), a plant natural product has been used as a tubulin targeting tool to study the role of the microtubule cytoskeleton of cells. In addition some of these chemical inhibitors have been used as drugs for the treatment of diseases (*e.g.* colchicine (**5**) has been used in the treatment of gout).¹⁰

The recent discovery of the small molecule tool, (*S*)-monastrol (**10**) has been of great interest due to the fact that it is one of the few molecules shown to disrupt mitosis without acting on tubulin. (*S*)-Monastrol (**10**) was discovered from a commercially available compound collection (using a *forward chemical genetics* approach) and subsequently identified as a selective inhibitor of the motor protein Eg5 (a mitotic kinesin). This molecule has therefore become an important molecular tool for studying mitotic mechanisms.³¹ Other small molecules that have been used to study the cytoskeleton included Taxol® (**3**), the cytochalasins (**1** and **11**) and nocodazole (**12**) amongst others (Figures 1 and 8).¹⁰

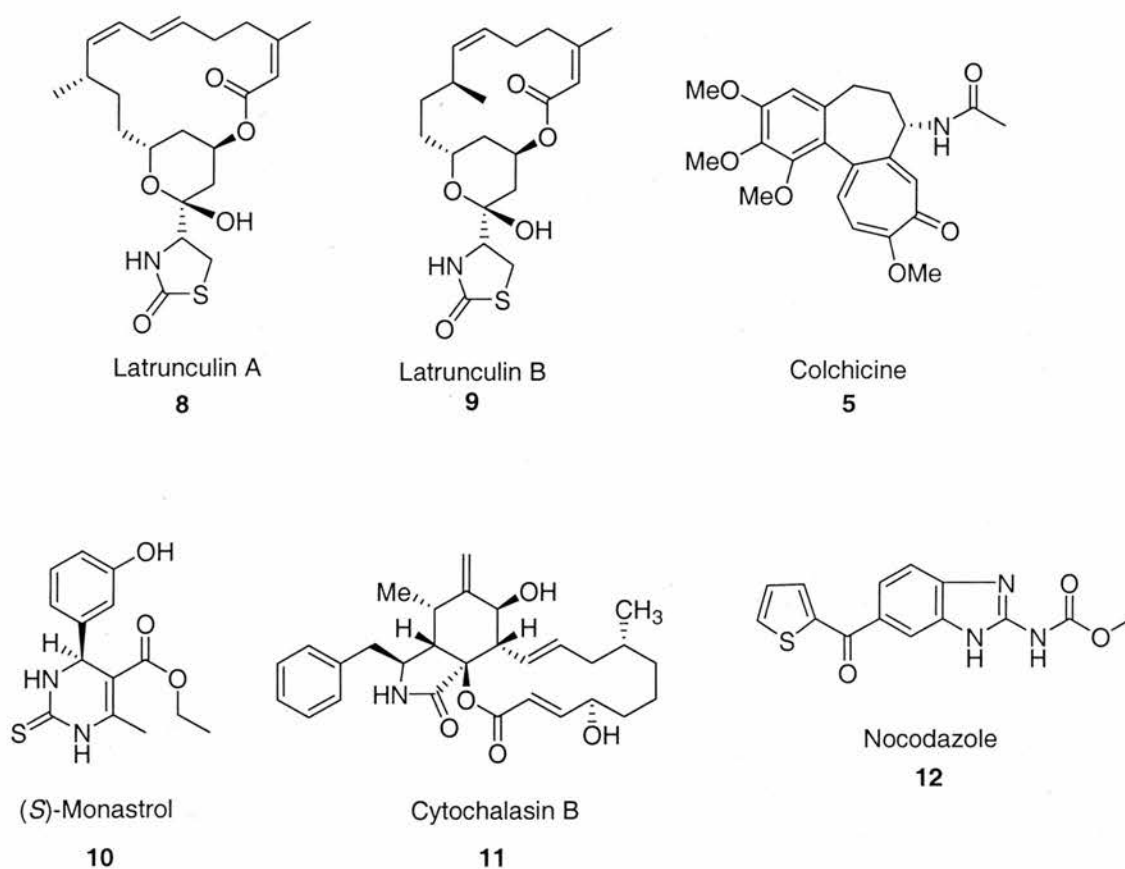


Figure 8. Structures of small molecules that target cytoskeletal proteins.

Advances in combinatorial chemistry and high-throughput screening should speed up the identification of small molecules that target cytoskeletal proteins.¹⁰ This is of great importance for many areas of cytoskeletal research which have not yet been explored due to the lack of suitable small molecule tools. For example, the detailed study of *cytokinesis* in mammalian cells would benefit from a small molecule that is

capable of preventing ingression of the cleavage furrow without preventing furrow assembly.³²

Cytokinesis is described as the final stage of cell division that leads to the formation of two daughter cells from one mother cell. This process is possible due to the formation of a contractile ring. The contractile ring must be assembled at the beginning of cell division and contains proteins such as actin,³³ myosin³⁴ and anillin (Figure 9).³⁵ This ring appears below the plasma membrane and it compresses the middle of the cell leading to the separation of the cell into the daughter cells (the process in which the cytoplasm is divided is also termed ‘cleavage’).²⁹

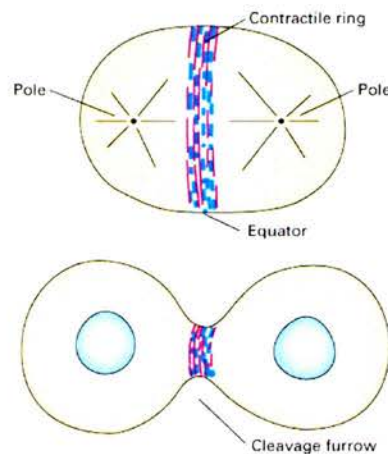


Figure 9. Actin and myosin in cytokinesis. Formation of the contractile ring containing an actin-myosin complex and subsequent cleavage of the cell into the two daughters (picture taken from Lodish, H., *et al.*, *Molecular Cell Biology*).³⁶

It has been shown using an anti-myosin II antibody that it is possible to stop the cell cycle during cytokinesis by inhibiting the action of non-muscle myosin II.³⁴ Therefore, in order to study cytokinesis in more detail using a chemical genetic approach it was necessary to *discover* a small molecule that inhibits the activity of non-muscle myosin II. This thesis has its origins in attempts to identify small molecules of this type.

1.4. TARGET PROTEIN: THE MYOSINS

1.4.1. Classification of Myosins^{37, 38}

The myosins are a large superfamily of molecular motor proteins that interact with actin filaments. There are at least 18 different classes of myosins^{39, 40} found in

eukaryotic cells (Figure 10). Sometimes within a single class, myosins isoforms are named with the letters A, B, etc. Only myosin classes I, II and V have been extensively biochemically characterised. The class II myosins have been widely studied and much is known about their function.^{37,38} Furthermore over 40 myosins are expressed in humans and their involvement in many cellular processes makes them potential drug targets.³⁹

Myosin II

The class II myosins are the most abundant in animal cells and are mainly located in muscle cells and the cytoplasm of most non-muscle cells. The myosin II class is divided into subclasses such as skeletal muscle, cardiac muscle, smooth muscle and non-muscle. Non-muscle myosin II contains three isoforms referred to as non-muscle IIA, non-muscle IIB and non-muscle IIC.⁴¹ Although, myosin II appears in all non-muscle cells, its concentration is lower than in muscle cells. The function of myosin II in skeletal and cardiac muscles is the generation of force necessary for muscle contraction. Non-muscle myosin II (found mainly in stress fibres within cells) is involved in several cellular processes such as membrane blebbing, cell migration, controlling cell polarity and cytokinesis.

Other myosin classes

Myosins are also essential in sensory systems such as hearing, balance and vision. Myosin classes I, III, VI and VII have roles in sensory function. Myosin III and VII are required for vision whereas myosins I, VI and VII are necessary for hearing.⁴² Therefore, mutations in these myosins are linked to human disorders such as deafness. Myosin class XIV is involved in host cell invasion by protozoan parasites including *Plasmodium falciparum*, the causative agent of malaria.^{43,44}

Figure 10 shows a schematic representation of the myosin superfamily. Although 18 classes have been identified so far, the scheme only shows 17 classes of myosins and their subclasses.

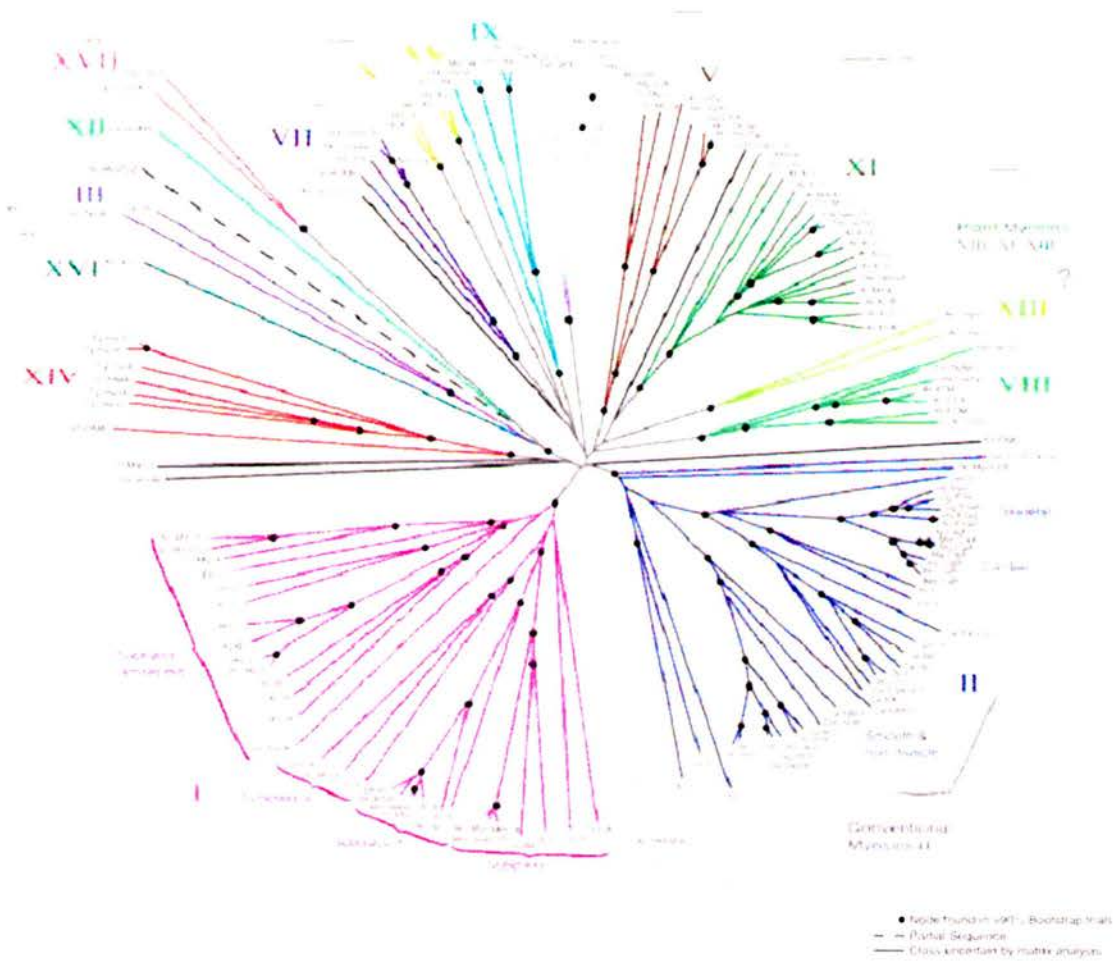


Figure 10. Myosin superfamily tree.⁴⁵

The common characteristic of all the myosins is their ability to bind reversibly to actin filaments. They all hydrolyse ATP to produce the energy for movement along actin filaments (Figure 11). The ATPase activity of the myosins alone is low but when myosin interacts with actin filaments its ATPase activity increases significantly.

Figure 11 shows a schematic representation of how myosin II is believed to move along actin filaments.

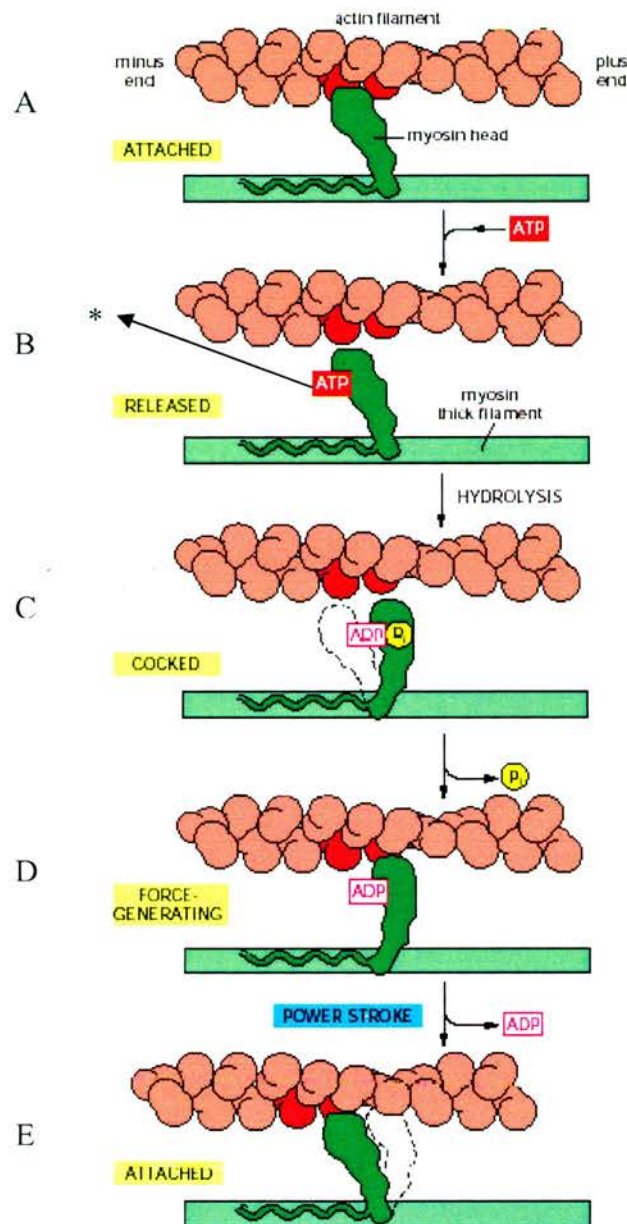


Figure 11. Movement of myosin along actin filaments: cycle of conformational changes of the myosin head during ATP binding, hydrolysis and inorganic phosphate release.^{29, 46} A) The head of myosin is bound to the actin filament but does not bind to ATP (short-lived state which is ended by the binding of ATP). B) A molecule of ATP binds to the head of myosin (on the cleft* situated on the back and the furthest side to the actin filament). A slight change in the conformation of the domains is produced with the consequence of reducing the affinity of the myosin head for actin, leading to the movement of myosin along the actin filament. C) The cleft closes around the ATP molecule and then due to a large shape change, the head is displaced along the filament. After that ATP is hydrolysed, although the ADP and inorganic phosphate produced remain tightly bound to myosin. D) Release of the inorganic phosphate occurs due to the now weak binding of the myosin head to a new site on the actin filament. Therefore the head recovers its origin conformation and loses its bound ADP. E) The myosin head is tightly bound to the actin filament although the head has moved to a new position on the actin filament. *The cleft is extended from the actin-binding site to the base of the ATP binding site.

Myosins contain three functional domains: a) a globular head or motor domain, which contains the actin and ATP binding sites, b) a neck domain, which binds to light chain subunits or calmodulin, c) a tail domain which serves to anchor and position the head of myosin interaction with actin (Figure 12).^{37, 38}

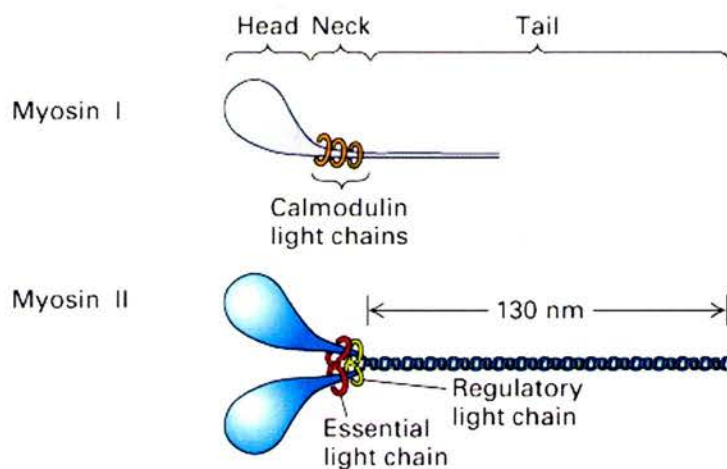


Figure 12. Functional domains of myosin I and II: head, neck and tail. Note that myosin II has two heads (each head contains both ATPase and motor activity), two pairs of light chains on the neck and a long tail (picture taken from Lodish, H., *et al.*, Molecular Cell Biology).³⁶

1.4.2. Inhibitors of Myosins

Due to the fundamental importance of myosins in many cellular processes, one important long term goal is the identification of a series of small molecules that *specifically* inhibit the biological activity of different sub-classes of myosins (a small molecule for each member of the superfamily). Through the specific inhibition of the activity of these proteins it will be possible to learn which biological processes are controlled by each myosin (Section 1.3). To date, only a few examples of inhibitors of myosins have been reported in the literature (see below).⁴⁷

Only two small molecule inhibitors of myosin II; 2,3-butanedione monoxime (**13**) (BDM)⁴⁸ and *N*-benzyl-*p*-toluene sulfonamide (**14**) (BTS)⁴⁹ have been studied extensively (Figure 13).

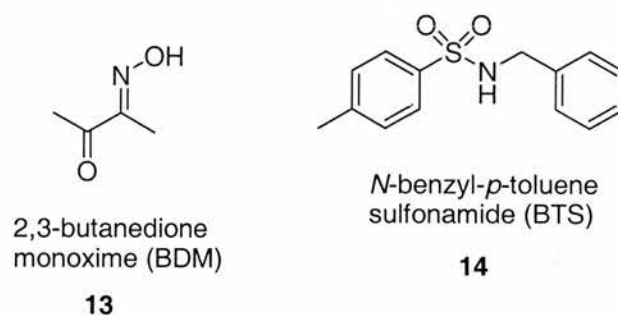


Figure 13. Inhibitors of skeletal muscle myosin II.

BDM (**13**) is a non-competitive inhibitor of skeletal *muscle* myosin II and inhibits myosin II ATPase activity.^{48, 50, 51} Previous results in the literature report this molecule as a 'general' myosin inhibitor.⁵² However later reports call this into question due to the fact that **13** was found to be non specific and to affect the function of other proteins.^{49, 53} It was observed that **13** seems to slow the release of inorganic phosphate following the ATP hydrolysis cycle.^{50, 51} BTS (**14**) is a relatively specific inhibitor of skeletal muscle myosin II which inhibits myosin ATPase activity. BTS (**14**) does not compete with ATP for the nucleotide-binding site of skeletal muscle myosin II. **14** decreases the affinity of myosin-ADP-Pi and myosin-ADP complexes for actin.⁵⁴ In addition BTS (**14**) also decreases the rate of phosphate release from skeletal muscle myosin II. It is suggested that BTS (**14**) could bind within the cleft between the ATP binding pocket and the actin.⁵⁴

Xestoquinone (**15**), a natural product extracted from a sea sponge was found to inhibit the ATPase activity of skeletal muscle myosin II (Figure 14).⁵⁵ In addition, analogues of xestoquinone (**15**) retaining the quinone moiety were also found to have the same inhibitory activity as **15**.⁵⁶ Analogues of **15** where the quinone was chemically converted into a quinol dimethyl ether (**16**) did not inhibit the ATPase activity. These results suggest that the quinone moiety is essential for the inhibitory activity of **15**.⁵⁶ A recent report has described the dual effect of thymol (**17**) upon myosin II. **17** is a plant natural product which is used as an antiseptic. Thymol (**17**) (Figure 14) acts as an inhibitor reducing the contraction of skeletal muscle fibres, but at the same time it enhances the ATPase activity of myosin.⁵⁷ The molecular mechanism of this interaction has currently not been determined.

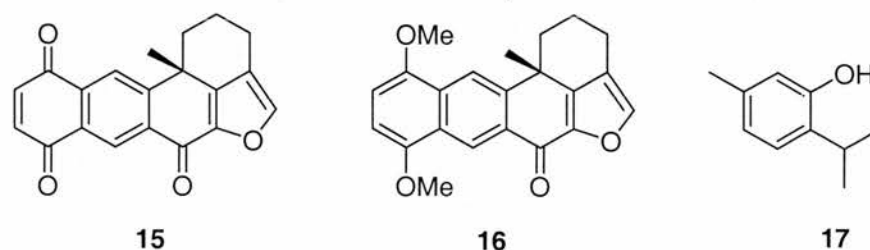


Figure 14. Chemical structure of xestoquinone (**15**), a dimethyl ether analogue (**16**) and thymol (**17**).

1.4.3. Identification of (\pm)-Blebbistatin (**18**): a novel small molecule inhibitor of *non-muscle* myosin II

Mitchison and co-workers have developed a programme at Harvard University to screen commercially available chemical libraries in order to discover selective inhibitors of myosin protein subfamilies (a *reverse chemical genetics* approach). This approach employs HTS of small molecules against the actin stimulated ATPase activity of myosins (Figure 15, panel A).⁴⁹ A recent application of this approach was to study the role of *non-muscle* myosin II in cytokinesis.³² A commercially available compound library of 16,300 chemical compounds was screened. This led to the identification of four preliminary hits as inhibitors of non-muscle myosin IIA (NMIIA) ATPase activity (Figure 15, panel B) of which compound **18** was the most potent.

In this type of approach, once hits have been identified, the next step is to confirm the chemical structure of the initially identified hit. Therefore, more material is purchased or prepared for subsequent biological testing. Interestingly, the structure of the compound present in the hit well was azatacrine **22**. However, when a repurchased and freshly dissolved sample of **22** was tested again it did *not* inhibit the activity of non-muscle myosin II. In addition, it was observed that when a solution of **22** was stored at room temperature in DMSO it decomposed from a colourless to a bright yellow solution. This result suggested that the screening sample of **22** had decomposed to produce a mixture of compounds that was active in this assay.

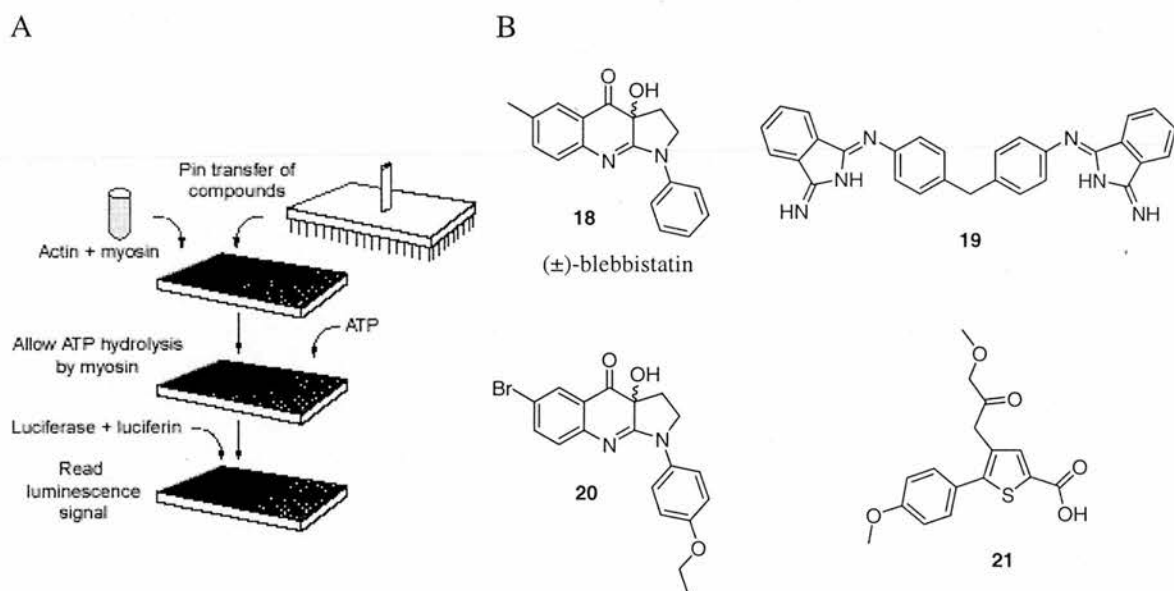


Figure 15. A reverse chemical genetic approach to discover novel small molecule tools: A) A diagrammatic representation of the coupled assay procedure used to identify inhibitors of non-muscle myosin IIA. The assay was performed by adding DMSO solutions of small molecules to wells containing a solution of actin and human platelet NMIIA. The assay was performed in a 1536 well format, with nanolitre volumes of solutions being transferred using an automated pin transfer device. The assay was then initiated by the addition of ATP. The assay plates were incubated to allow ATP hydrolysis to occur prior to the addition of a solution of luciferase and luciferin. The resulting luminescence was then recorded as a direct measure of the inhibitory effect of each small molecule; the greater the luminescence the more ATP present and therefore the more effective an inhibitor the small molecule was. B) The four inhibitors of NMIIA identified by HTS.^{32, 49}

Whilst not the first time that a degradation product or contaminant of the intended inhibitor has proved to be the bioactive component,⁵⁸ these cases are relatively rare. Preliminary studies carried out in the Mitchison laboratory, showed that an ‘aged’ DMSO solution of **22** degrades to **18** (Figure 16).

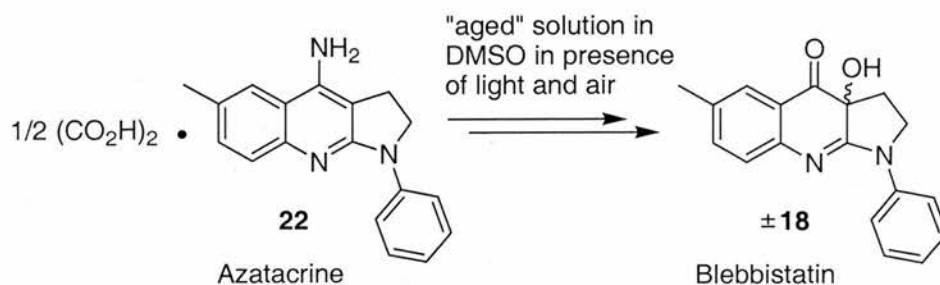


Figure 16. Decomposition of azatacrine (**22**) to give blebbistatin (\pm **18**).

The chemical structure of **18** was confirmed based on the following spectroscopic evidence:

- ^1H NMR on a very small sample of **18** (<1 mg). However, the interpretation of the spectra was relatively difficult due to the structural isolation of the sets of protons.
- The conjugated system in the molecule produced an intense colour.
- Mass spectrometric analysis (ES+) was consistent with **18**, although the peak appeared to have a mass corresponding to the mass of **18** plus water $[\text{M}+\text{H}+18]^+$.

Unfortunately, the initial lack of material made it impossible to obtain a ^{13}C NMR or X-ray analysis on the compound. Furthermore, there is no literature precedent for heterocycles of this type.

1.4.3.1. Preliminary biological characterisation of (\pm)-blebbistatin (**18**)

Once the hit molecule has been identified from the compound collection, the next step in this *reverse chemical genetics* programme was to determine the biological effect of **18** upon non-muscle myosin II in cells. **18** was found to inhibit several myosin II-dependent processes in vertebrate cells. It blocks, reversibly and rapidly, cell blebbing, cell migration and cytokinesis (Figure 17).³² Due to the fact that **18** inhibits blebbing of the cell membrane it was given the name **blebbistatin**. 100 μM (\pm)-blebbistatin (**18**) blocked contraction of the cleavage furrow in dividing cells without affecting mitosis or contractile ring assembly (localisation of myosin II, microtubules and anillin was unaffected during assembly). Therefore, in the presence of (\pm)-blebbistatin (**18**) the two daughter cells cannot be separated into individual cells. However, the progression of the furrow ingression and therefore the completion of cytokinesis was possible after ‘washing out’ (\pm)-blebbistatin (**18**).

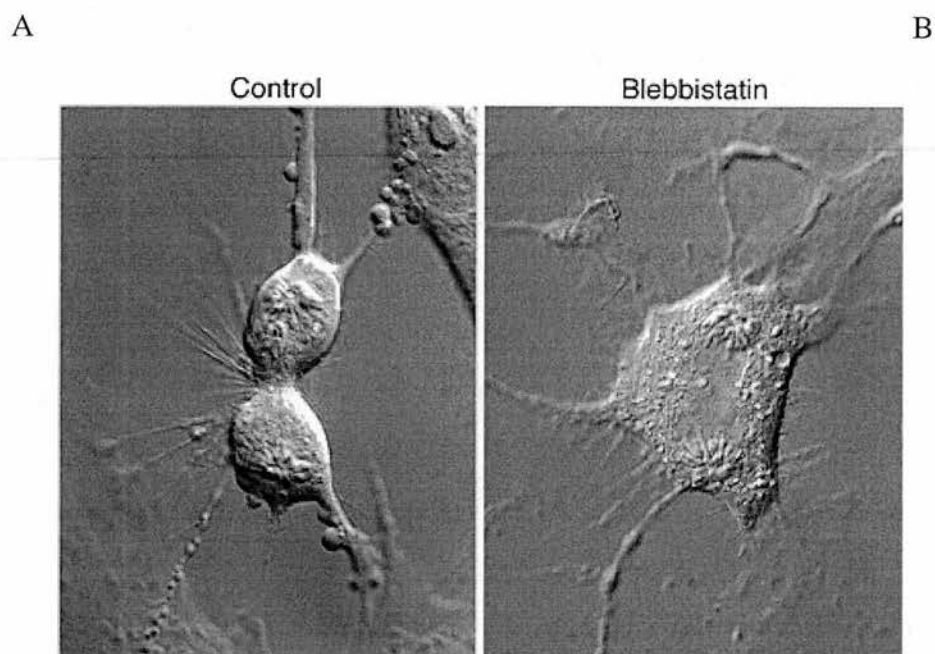


Figure 17. The effect of (\pm)-blebbistatin (**18**) on cytokinesis. Image A shows a vertebrate cell undergoing normal cell division in the absence of drug treatment (control cell), note the presence of the contracted cleavage furrow. Image B shows the same cell type treated with 100 μ M (\pm)-blebbistatin (**18**). Note the complete absence of cleavage furrow contraction despite successful chromosome segregation.³²

It is important to note that (\pm)-blebbistatin (**18**) contains a stereogenic centre. It is therefore of interest to test the inhibitory activity of each enantiomer separately, as it is common to find that one enantiomer of a bioactive molecule is more potent than the other. Therefore, the two enantiomers of (\pm)-blebbistatin (**18**) were separated by chiral HPLC and assigned according to the direction in which each enantiomer rotates the plane of plane polarised light. It was found that (–)-blebbistatin (**7**) (for structure see page 88) was active against non-muscle myosin II with an IC_{50} value of approximately half that of racemic **18**, whereas (+)-blebbistatin (**23**) was inactive. However, the (+)-enantiomer (**23**) (for structure see page 88) can be used as a useful control compound for biological studies.³²

In summary, (\pm)-blebbistatin (**18**) was found to be a novel specific, cell permeable, reversible small molecule inhibitor of *non-muscle* myosin II. This compound inhibits cytokinesis by blocking the contraction of the cleavage furrow without disrupting mitosis or contractile ring assembly.³²

Interestingly, the importance of (–)-blebbistatin (**7**) as a molecular tool, in biology and medicine, increased dramatically after its initial publication in March 2003.³² Twenty seven research papers were published from 2004 to date, focusing on the use of the small molecule (–)-blebbistatin (**7**) or (±)-blebbistatin (**18**) as a tool to study other non-muscle myosin II-dependant cellular process. In addition, the compound is now commercially available as a (±)-**18**, (–)-**7** and (+)-**23** blebbistatin for use in cell biology research.

An interesting application to examine the effects of (S)-(–)-blebbistatin (**7**) as a molecular tool in different processes has been reported recently by Duxbury *et al.*⁵⁹ The effects of (S)-(–)-blebbistatin (**7**) were tested on pancreatic adenocarcinoma cellular migration invasion, adhesion and spreading. Pancreatic adenocarcinoma is a malignant and aggressive type of cancer that is very difficult to treat due to its rapid metastasis. Cancer cell invasion and metastasis, is a multi-step process that involves changes in cellular morphology, motility, and interaction with extracellular matrix components. The components of the cytoskeleton such as microtubules, actin microfilaments and other proteins including non-muscle myosin II play an important role upon malignant cellular behaviour. The (–)-enantiomer (**7**) was used in these experiments in order to investigate the role of non-muscle myosin II in migration, invasiveness and the extracellular matrix interaction. The results from this study showed that **7** potently inhibited pancreatic adenocarcinoma cellular migration and invasiveness. In addition, proliferation of the cancer in mice was affected with high concentrations of **7**.

Another example on the use of (±)-blebbistatin (**18**) as a molecular tool to dissect biological processes is in neurological studies. Recently it has been shown that myosin II plays an important role in the nervous system.⁶⁰ (±)-Blebbistatin (**18**) was used to determine whether myosin II activity is required for axon retraction (a process that occurs as part of the axons response to an injury). The results showed an inhibitory effect of (±)-blebbistatin (**18**) on axon retraction. Therefore, this confirmed the importance of myosin II in this process.

In summary, neurological and cancer biology studies using (±)-blebbistatin (**18**) and (–)-blebbistatin (**7**) have identified myosin II as a key protein in biological process of therapeutic relevance.^{59, 60} As a result the (–)-enantiomer of blebbistatin (**7**) could be

considered as a lead compound for pharmaceutical development to treat these and other diseases or injuries.

1.4.3.2. Specificity of (\pm)-Blebbistatin (**18**)

The specificity of (\pm)-blebbistatin (**18**) was tested in order to observe its ability to inhibit different classes of myosin. Straight *et al.* reported that when different classes of myosin (I, V and X) were treated with (\pm)-blebbistatin (**18**), their ATPase activities were unaffected, except for myosin V that was slightly inhibited.³² However, a recent study reported in the literature by Sellers and co-workers showed that the activity of myosin V was not inhibited at all.⁶¹ They also re-assessed the ATPase activity of different classes of myosins (I, X and XV), in the presence of **18**. None of these myosins were inhibited by **18** even when the concentration of the compound was at 100 μ M, consistent with the earlier report.⁶¹ These results suggest that **18** is *specific* for the class II myosins, but other myosin family classes remain to be tested.

The specificity of (\pm)-blebbistatin (**18**) was also tested within myosin class II. It was found that **18** inhibits the ATPase activity of rabbit *skeletal muscle* myosin, porcine β -*cardiac muscle* myosin, human *non-muscle* myosin IIA and chicken *non-muscle* myosin IIB (Figure 18). In contrast, turkey *smooth muscle* myosin was only weakly inhibited by **18** (IC_{50} 80 μ M).

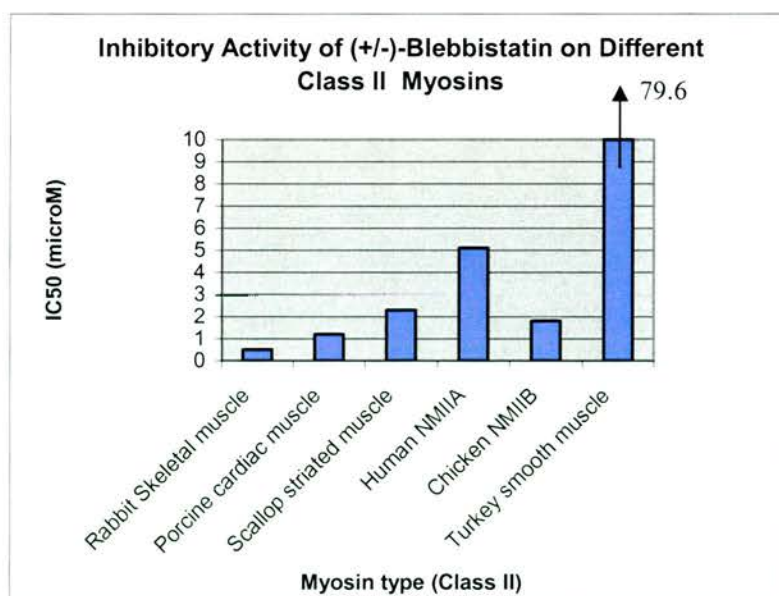


Figure 18. Assessment of (\pm)-blebbistatin (**18**) selectivity within the myosin II class.⁶¹

In summary, it was shown that (\pm)-blebbistatin (**18**) has a limited selectivity within the myosin class II and subclasses, being an inhibitor of both muscle and non-muscle myosin II.⁶¹ In addition, this compound is becoming a popular molecular tool especially in the fields of cell motility and muscle physiology. Therefore it is interesting to note, that the role for the organic chemist remains as important in preparing novel analogues of **18** with improved potency and specificity (see Chapter 4).

1.4.3.3. Mechanism of action of (\pm)-Blebbistatin (**18**)

Until recently only two papers were reported describing the mechanism of action of (\pm)-blebbistatin (**18**).^{62,63} These papers involve assessment of the effect of **18** on the kinetics of skeletal muscle and non-muscle myosin IIB function.^{62,63} In brief, these investigations conclude that **18** does not compete with ATP at the ATP binding site of the motor domain of the myosin and that **18** does not interfere with the binding of myosin to actin. Instead (\pm)-blebbistatin (**18**) binds with high affinity to a complex that contains ADP and Pi bound to myosin and therefore slows down the release of inorganic phosphate (see cycle of ATP binding and its hydrolysis in Figure 11, Section 1.4). The complex formed between myosin and ADP-Pi represents a long-lived state where the force-generating step is catalysed by the release of phosphate when myosin binds again to actin. Therefore, the results suggested that ($-$)-blebbistatin (**18**) affects specific steps in the motility cycle. Molecular simulations proposed that the binding site of ($-$)-blebbistatin (**18**) to the myosin head is within the aqueous cavity between the nucleotide and actin binding sites (referred to as the cleft).⁶³ Although this result was not conclusive it was envisaged that this information could be useful in developing an appropriate strategy for preparing inhibitors of myosin II or other myosin classes.

1.5. AIMS AND OBJECTIVES OF THE PROJECT

From the initial results relating to the discovery of (\pm)-blebbistatin (**18**),³² it was clear that ($-$)-**18** will become a powerful molecular tool to dissect cellular processes. Therefore, it is at this stage of a chemical genetics project that synthetic organic chemistry can play an important role, firstly to prove the chemical structure of (\pm)-blebbistatin (**18**) and also for the preparation of analogues in order to find more *potent* and *specific* inhibitors of myosin II or other myosin classes. In addition, it is of

importance to take into account that the two enantiomers of blebbistatin differed in biological activity with only (*S*)-(-)-enantiomer of blebbistatin (**7**) being *active*. Therefore, a stereoselective synthesis was required.

The goals of the project were therefore clearly established. Although initial attempts to prepare **18** provided support for its structure based on spectroscopic methods, the lack of material made the complete assignment of its structure difficult (Section 1.4.3). Thus, the initial goal of the project was:

1. To prepare a sufficient amount of the proposed bioactive compound **18** (Section 1.4.3) to confirm its chemical structure by X-ray crystallographic techniques (Chapter 2).

In addition, other goals to be achieved in the project were as follows:

2. To design a synthetic route to prepare optically pure enantiomers of (-)- and (+)-blebbistatin (**18**) (Chapter 3).
3. To determine and optimise the degree of asymmetric induction (*ee*) achieved during the preparation of optically enriched samples of **18** (Chapter 3).
4. To develop a methodology to determine the absolute configuration of the bioactive enantiomer of (-)-blebbistatin (**7**) (Chapter 3).
5. To introduce diversity in the (-)-blebbistatin (**7**) core structure in order to prepare more active and selective analogues (Chapter 4).
6. To test the biological activity of the different analogues of **7**, which were prepared (Chapter 5).

1.6. REFERENCES

- 1 Mayer, T. U., *Trends Cell Biol.*, **2003**, *13*, 270-277.
- 2 Yeh, J-R. J. and Crews, C. M., *Developmental Cell*, **2003**, *5*, 11-19.
- 3 Ward, G. E., Carey, K. L., Westwood, N. J., *Cell. Microbiol.*, **2002**, *4*, 471-482.
- 4 Westwood, N. J., *Philos. Trans. R. Soc. London, Ser. A*, **2004**, *362*, 2761-2774.
- 5 Mitchison, T. J., *Chem. Biol.*, **1994**, *1*, 3-6.
- 6 Carey, K. L., Westwood, N. J., Mitchison, T. J., Ward, G. E., *Proc. Natl. Acad. Sci.*, **2004**, *101*, 7433-7438.
- 7 Clark, A. M., *Pharm. Res.*, **1996**, *13*, 1133-1144.
- 8 Schreiber, S. L., *Science*, **2000**, *287*, 1964-1969.
- 9 Ohmori, H. and Toyama, S., *J. Cell Biol.*, **1992**, *116*, 933-941.
- 10 Peterson, J. R. and Mitchison, T. J., *Chem. Biol.*, **2002**, *9*, 1275-1285.
- 11 Schreiber, S. L., *Bioorg. Med. Chem.*, **1998**, *6*, 1127-1152.
- 12 Pelish, H. E., Westwood N. J., Feng, Y., Kirchhausen, T., Shair, M. D., *J. Am. Chem. Soc.*, **2001**, *123*, 6740-6741.
- 13 Lokey, R. S., *Curr. Opin. Chem. Biol.*, **2003**, *7*, 91-96.
- 14 Koehler, A. N., Shamji, A. F., Schreiber, S. L., *J. Am. Chem. Soc.*, **2003**, *125*, 8420-8421.
- 15 Burke, M. D. and Lalic, G., *Chem. Biol.*, **2002**, *9*, 535-541.

- 16 Wang, S., Sim, T. B., Kim, Y-S., Chang, Y-T., *Curr. Opin. Chem. Biol.*, 2004, 8, 371-377.
- 17 Strausberg, R. L. and Schreiber, S. L., *Science*, **2003**, 300, 294-295.
- 18 Crews, C. M. and Shotwell, J. B., *Prog. Cell Cycle Res.*, **2003**, 5, 125-133, and references therein.
- 19 Politz, J. C., *Trends Cell Biol.*, **1999**, 9, 284-287.
- 20 Stockwell, B. R., *Trends in Biotechnology*, **2000**, 18, 449-455.
- 21 MacBeath, G., *Genome Biology*, **2001**, 2, 2005.1-2005.6.
- 22 Alaimo, P. J., Shogren-Knaako, M. A., Shokato, K. M., *Curr. Opin. Chem. Biol.*, **2001**, 5, 360-367.
- 23 King, R. W., *Chem. Biol.*, **1999**, 6, 327-333.
- 24 Thorpe, D. S., *Combinatorial Chemistry & High Throughput Screening*, **2003**, 6, 623-647.
- 25 Kim, T. K., *J. Biochem. Mol. Biol.*, **2004**, 37, 53-58.
- 26 Furka, A., Sebestyen, F., Asgedom, M., Dibo, G., *Int. J. Pept. Protein Res.*, **1991**, 37, 487-493.
- 27 Stockwell, B. R., Haggarty, S. J., Schreiber, S. L., *Chem. Biol.*, **1999**, 6, 71-83.
- 28 Stockwell, B. R., *Nature Rev. Genet.*, **2000**, 1, 116-125.

- 29 Alberts, B., Bray, D., Lewis, J., Raff, M., Roberts, K., Watson, J. D., *Molecular Biology of The Cell*, **1994**, Third Edition, Garland Publishing, Inc., New York.
- 30 Coue, M., Brenner, S. L., Spector, I, Korn E. D., *FEBS Lett.*, **1987**, *213*, 316-318.
- 31 Mayer, T. U., Kapoor, T. M., Haggarty, S. J., King, R. W., Schreiber, S. L., Mitchison, T. J., *Science*, **1999**, *286*, 913-914.
- 32 Straight, A. F., Cheung, A., Limouze, J., Chen, I., Westwood, N. J., Sellers, J. R., Mitchison, T. J., *Science*, **2003**, *299*, 1743-1747.
- 33 Schroeder, T. E., *Proc. Natl. Acad. Sci.*, **1973**, *70*, 1688-1692.
- 34 Mabuchi, I. and Okuno, M., *J. Cell Biol.*, **1977**, *74*, 251-263.
- 35 Oegema, K., Savoian, M. S., Mitchison, T. J., Field, C. M., *J. Cell Biol.*, **2000**, *150*, 539-551.
- 36 Lodish, H., Baltimore, D., Berk, A., Zipursky, S. L., Matsudaira, P., Darnell, J., *Molecular Cell Biology*, **1995**, Third Edition, Scientific American Books, Inc, New York.
- 37 Sellers, J. R., *Myosins*, **1999**, Second Edition, Oxford University Press, New York.
- 38 Sellers, J. R., *Biochim. Biophys. Acta*, **2000**, *1496*, 3-22.
- 39 Berg, J. S., Powell, B. C., Cheney, R. E., *Mol. Biol. Cell*, **2001**, *12*, 780-794.

-
- 40 Thompson, R. F. and Langford, G. M., *The Anatomical Record*, **2002**, 268, 276-289.
- 41 Golomb, E., Ma, X., Jana, S. S., Preston, Y. A., Kawamoto, S., Shoham, N. G., Goldin, E., Conti, M. A., Sellers, J. R., Adelstein, R. S., *J. Biol. Chem.*, **2004**, 279, 2800-2808.
- 42 Mermall, V., Post, P. L., Mooseker, M. S., *Science*, **1998**, 279, 527-533.
- 43 Tardieux, I., Baines, I., Mossakowska, M., Ward, G. E., *Mol. Biochem. Parasitol.*, **1998**, 93, 295-308.
- 44 Dobrowolski, J. M., Carruthers, V., Sibley, D. L., *Mol. Microbiol.*, **1997**, 26, 163-173.
- 45 Hodge, T. and Cope, M. J. T. V., *J. Cell Sci.*, **2000**, 113, 3353-3354.
- 46 Rayment, I., Holden, H. M., Whittaker, M., Yohn, C. B., Lorenz, M., Holmes, K. C., Milligan, R. A., *Science*, **1993**, 261, 58-65.
- 47 Literature search done in PubMed and Web of Science, July 2005 (key words: myosin inhibitors).
- 48 Higuchi, H. and Takemori, S., *J. Biochem.*, **1989**, 105, 638-643.
- 49 Cheung, A., Dantzig, J. A., Hollingworth, S., Baylort, S. M., Goldmann, Y. E., Mitchison, T. J., Straight, A. F., *Nature Cell Biol.*, **2002**, 4, 83-88.

- 50 Herrmann, C., Wray, J., Travers, F., Barman, T., *Biochemistry*, **1992**, *31*, 12227-12232.
- 51 McKillop, D. F. A., Fortune, N. S., Ranatunga, K. W., Geeves, M. A., *J. Muscle Res. Cell Motil.*, **1994**, *15*, 309-318.
- 52 Cramer, L. P. and Mitchison, T. J., *J. Cell Biol.*, **1995**, *131*, 179-189.
- 53 Ostap, E.M., *J. Muscle Res. Cell Motil.*, **2002**, *23*, 305-308.
- 54 Shaw, M. A., Ostap, E. M., Goldman, Y. E., *Biochemistry*, **2003**, *42*, 6128-6135.
- 55 Sakamoto, H., Furukawa, K., Matsunaga, K., Nakamura, H., Ohizumi, Y., *Biochemistry*, **1995**, *34*, 12570-12575.
- 56 Nakamura, M., Kakuda, T, Oba, Y., Ojika, M., Nakamura, H., *Bioorg. Med. Chem.*, **2003**, *11*, 3077-3082.
- 57 Tamura, T. and Iwamoto, H., *Biochem. Biophys. Res. Commun.*, **2004**, *318*, 786-791.
- 58 Talaga, P., *Drug Discovery Today*, **2004**, *9*, 51-53.
- 59 Duxbury, M. S., Ashley, S. W., Whang, E. E., *Biochem. Biophys. Res. Commun.*, **2004**, *313*, 992-997.
- 60 Gallo, G., *Exp. Neurol.*, **2004**, *189*, 112-121.
- 61 Limouze, J., Straight, A. F., Mitchison, T. J., Sellers, J. R., *J. Muscle Res. Cell Motil.*, **2004**, *25*, 337-341.

- 62 Ramamurthy, B., Yengo, C. M., Straight, A. F., Mitchison, T. J., Sweeney, H. L., *Biochemistry*, **2004**, *43*, 14832-14839.
- 63 Kovacs, M., Toth, J., Hetenyi, C., Malnasi-Csizmadia, A., Sellers, J. R., *J. Biol. Chem.*, **2004**, *279*, 35557-35563.

CHAPTER 2

RESULTS AND DISCUSSION

SYNTHETIC APPROACHES TO S-3a-HYDROXY-6-METHYL-1-PHENYL-2,3,3a,4-TETRAHYDRO-1H-PYRROLO [2,3-*b*]QUINOLIN-4-ONE

2.1. SYNTHESIS OF RACEMIC 3a-HYDROXY-6-METHYL-1-PHENYL-2,3,3a,4-TETRAHYDRO-1H-PYRROLO[2,3-*b*]QUINOLIN-4-ONE (18)

2.1.1. Via Azatacrine (22) Degradation

Initial studies carried out in the Mitchison laboratory, showed that an “aged” DMSO solution of the azatacrine analogue **22** degrades to (±)-blebbistatin (**18**), although the mechanism of this reaction was not studied (Figure 19) (see Chapter 1, Section 1.4.3. for more details).¹

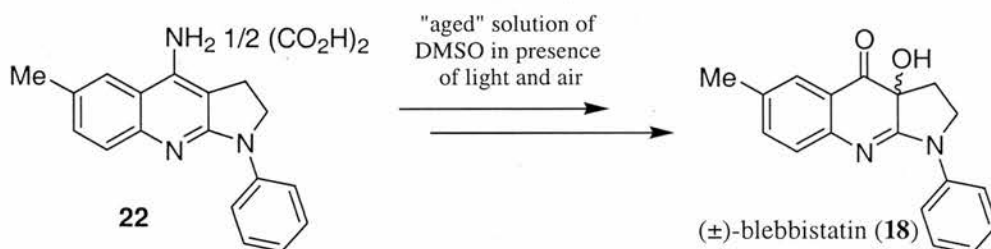


Figure 19. Degradation of **22** into **18** in the presence of light and air.

¹H NMR experiments were carried out in order to follow this decomposition and to enable the proposal of a possible reaction mechanism. It was first envisaged that **22** could hydrolyse to afford quinolone **24**. **24** could then oxidise in the presence of air to the corresponding (±)-blebbistatin (**18**) (Figure 20).

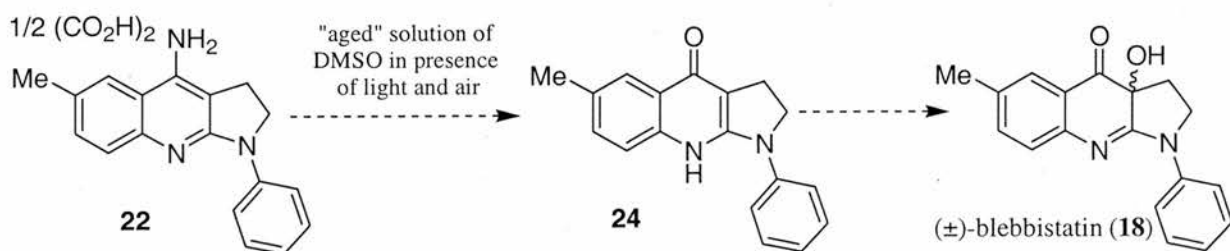


Figure 20. Proposed degradation of **22** into **18** in the presence of light and air.

Azatacrine **22** was dissolved in d^6 -DMSO in the absence of air and was analysed by ^1H NMR each day for 12 days. The same procedure was carried out for a sample of quinolone **24**. No decomposition and no hydrolysis of **22** was observed over this period of time. In the case of **24** it was observed that the sample was stable to oxidation over that period of time, without any change on the ^1H NMR. It was then decided to add a small amount of deuterium oxide to the sample of **22** and to analyse the resulting solution by ^1H NMR and ^{13}C NMR. Whilst minor changes were observed in both spectra, it was not possible to assign these changes to the formation of a new compound. These results are tentatively explained by a solvent dependence in the NMR spectra of **22**. It is clear, however, that even when excess D_2O is added to the d^6 -DMSO solution of **22** hydrolysis of **22** to **24** does not occur over a two day period. The two samples were then opened to the air for 16 hours resulting in their oxidation (samples turned bright yellow). A mass spectroscopic analysis (ES^+ mode) of both samples afforded a signal corresponding to (\pm)-blebbistatin (**18**) (m/z 293). In a similar experiment a sample of azatacrine **22** in d^6 -DMSO without D_2O was exposed to the air for 16 hours. The result was the oxidation of the sample to give **18**.

It is therefore proposed that a sample of azatacrine **22** could first oxidise in a slow step in the presence of air to give **25**, this is then followed by the rapid hydrolysis of **25** to give **18** (Figure 21).

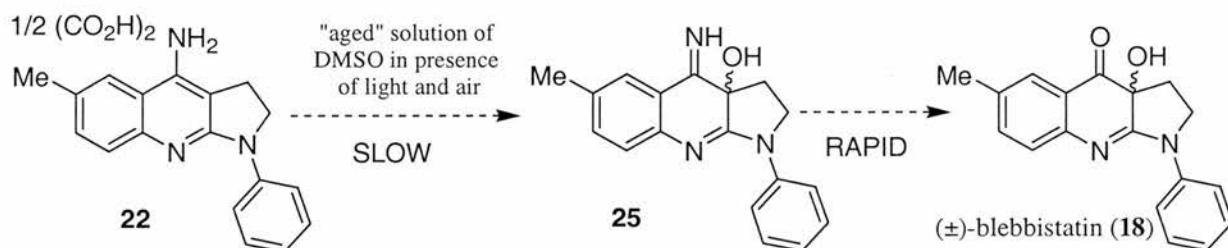


Figure 21. Proposed mechanism for the oxidation of azatacrine **22**.

2.1.2. An overview of the synthetic approach to (\pm)-Blebbistatin (**18**)

In an attempt to confirm the chemical structure of (\pm)-blebbistatin (**18**) and to prepare larger amounts of **18**, a more efficient route, *via* quinolone **24**, was developed. The synthetic approach comprised of a four step reaction sequence. In brief, the route starts with the esterification of commercially available methyl anthranilic acid² **26**

(Figure 22). A coupling reaction between 5-methyl anthranilate (**27**) and commercially available 1-phenyl-2-pyrrolidinone (**28**) affords amidine **29**, which could be followed by a base induced intramolecular cyclisation of **29** to give **24**. Finally the proposed structure **18** would be prepared by oxidation of **24**. On completion of the synthesis of **18**, the plan was to prove the chemical structure by single X-ray crystal analysis and to show that it was identical to the bioactive decomposition product (Chapter 1, Section 1.5. goal 1). An analogous route was also planned for the synthesis of a blebbistatin analogue **30**.

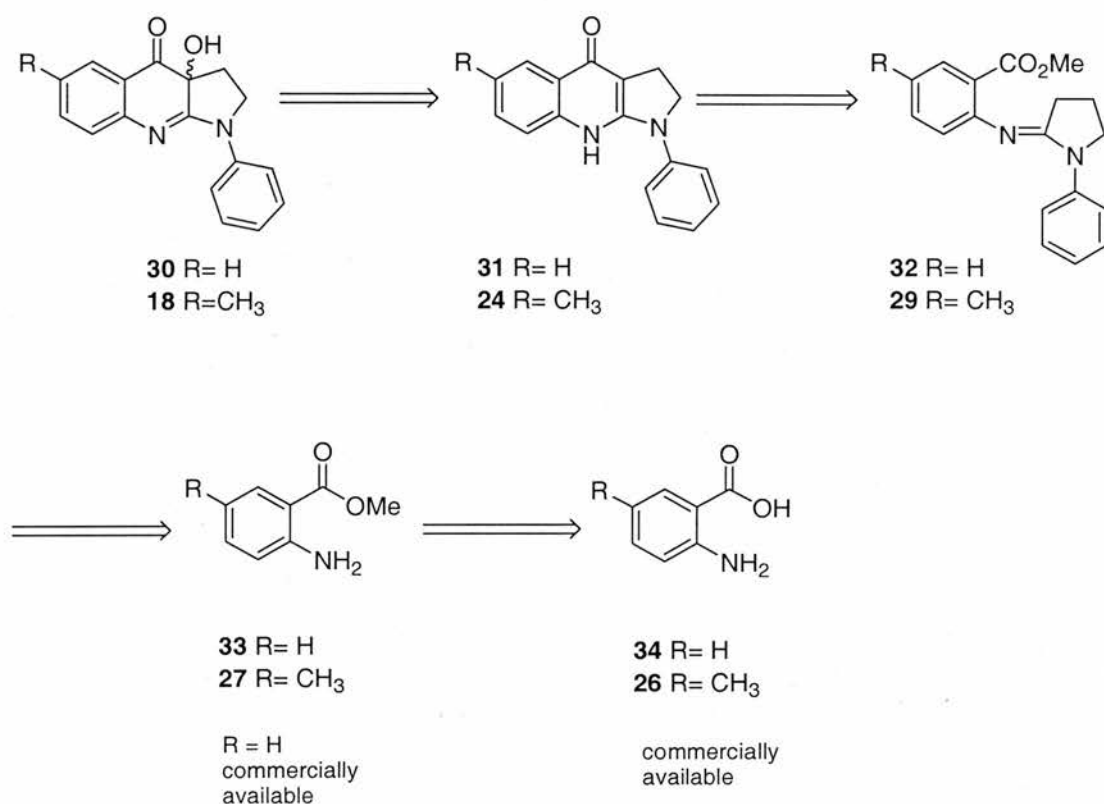


Figure 22. A retrosynthetic analysis to (±)-blebbistatin **18** and **30**.

2.1.3. Preparation of the cyclisation precursors **29** and **32**

The first step in the synthesis of (±)-blebbistatin (**18**) was the preparation of the anthranilate ester **27** as starting material (Figure 23). Although **27** is commercially available now, initial attempts involved the esterification of the commercially available 2-amino-5-methyl carboxylic acid (**26**) to the corresponding methyl ester **27**. The esterification was carried out using concentrated sulphuric acid in methanol at reflux for

48 hours. Purification by flash column chromatography gave **27** in excellent yield (94%) with its structure being confirmed by ^1H NMR analysis. The anthranilate **33** was commercially available. It was envisaged that reaction of the lactam **28** with phosphorus oxychloride could afford an intermediate that was activated towards nucleophilic attack by anthranilates **27** and **33**. This step would afford the desired amidines **29** and **32**.

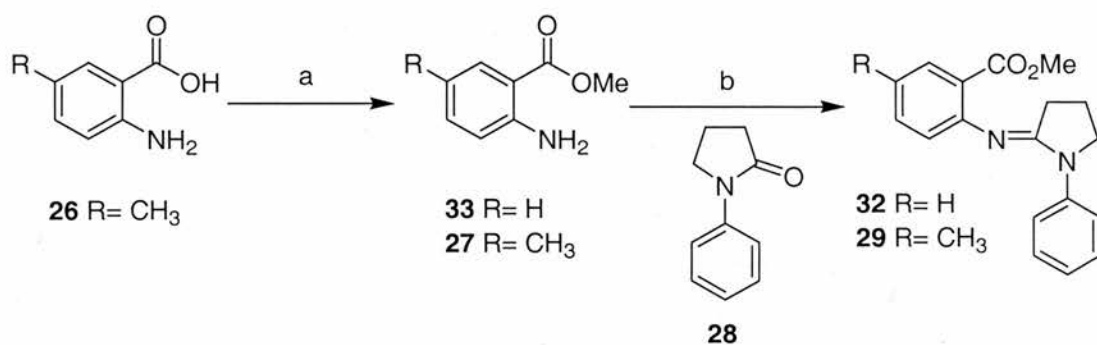


Figure 23. Preparation of the amidines **29** and **32**. Reagents and conditions: a) MeOH, H₂SO₄, 80 °C, 48 hours, basic work-up, 94%, b) i) **28** (1.0 equiv), POCl₃ (1.2 equiv), DCM, RT, 16 hours, ii) Anthranilate ester **27** or **33** (1.1 equiv), DCM, 40 °C, 16 hours, 10% (**29**), 16% (**32**).

2.1.3.1. The Vilsmeier reaction

The initial idea for activation of the lactam **28** with phosphorus oxychloride was based on results reported by Kuehne *et al.*³ These authors proposed that this reaction led to the formation of an iminium intermediate **35** (Figure 24) by conversion of an amide or lactam of general structure **36** in the presence of phosphorus oxychloride.

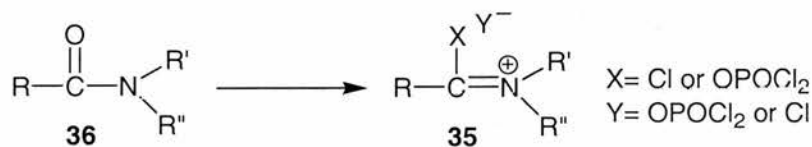


Figure 24. Formation of an iminium intermediate where X and/or Y can be OPOCl₂ and/or Cl.³

It is well known that the Vilsmeier reaction converts amides to electrophilic intermediates, iminium ions, which are very reactive species and therefore may react with weakly nucleophilic groups.⁴ A Vilsmeier salt is formed when a disubstituted

amide, most often *N,N*-dimethylformamide (DMF), is treated with an inorganic acid halide, such as phosphorus oxychloride (POCl_3), thionyl chloride (SOCl_2) or phosgene (COCl_2).⁵ The general representation of the Vilsmeier salt derived from the reaction between *N,N*-dimethylformamide and phosphorus oxychloride is shown in Figure 25, as the β -chloroiminium phosphate (**37**) which has been proved by IR and both ^1H and ^{31}P NMR analysis.^{5, 6, 7, & 8} However a third structure, β -phosphoryliminium chloride, has also been proposed as being more reactive than the β -chloroiminium phosphate (Figure 26), although the structure of **38** has been called into question during measurements by ^{31}P NMR analysis.^{5, 8}

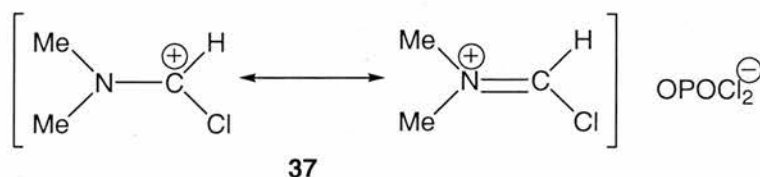


Figure 25. β -Chloroiminium phosphate **37** intermediate formed from the reaction with phosphorus oxychloride and DMF.^{5, 6}

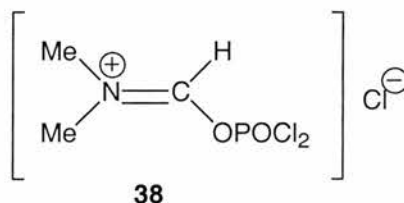


Figure 26. Proposed structure for β -phosphoryliminium chloride **38**.⁵

Kuenhe followed the formation of the iminium derivatives in his work by ^1H NMR analysis in CDCl_3 . The results showed a downfield shift of 0.8-1.0 ppm for the protons α to nitrogen in tertiary amides and 0.4-0.6 ppm in secondary amides in the ^1H NMR spectra. Table 1 shows the conversion of the lactams into the corresponding iminium derivatives at different reaction times and their corresponding chemical shifts.

Other examples of the use of phosphorus oxychloride to activate amides and lactams, *via* Vilsmeier-type chloro iminium ion intermediates have been reported in the literature.^{4, 9, 10} One of these examples is the formation of amidine pseudodisaccharides from the *N*-methyl lactam **39** (Figure 27).

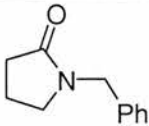
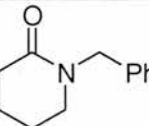
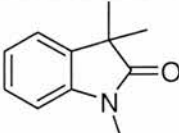
Entry	Compound	Reaction time (h)	Lactam Conc ^a (M)	Lactam (δ ppm)	Iminium derivative (δ ppm)	$\Delta\delta$, ppm
1		0.25	1.0	(s) 4.5	(s) 5.48	0.98
2		0.25	1.0	(s) 4.6	(s) 5.60	1.0
3		24.0*	1.0	(s) 3.26	–	–

Table 1. Reaction of different lactams with phosphorus oxychloride. The reaction times are expressed in hours and the chemical shifts in ppm. The concentration of the lactam are given in units of Molarity. In general, the reactions were carried out at room temperature. * Reaction run at reflux, although no formation of the iminium derivative was observed. The value for the protons α to the nitrogen atom, corresponds to the benzylic protons (entry 1 and 2).³

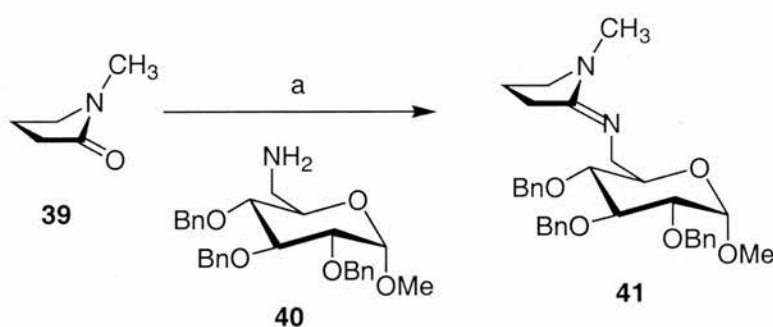


Figure 27. Literature example of the formation of amidine **41**. Reagents and conditions: a) i) POCl_3 , benzene, 23 °C, 24 hours, ii) **40**, benzene, 60 °C, 5 hours.¹⁰

An example from the literature reported that amidine **42** could be accessed from the condensation of 2-cyanoaniline derivative **43** and a lactam derivative **44** in the presence of various condensing agents such as phosphorus oxychloride (POCl_3), phosphorus pentachloride (PCl_5) or thionyl chloride (SOCl_2) in either dichloromethane or chloroform (Figure 28).¹¹

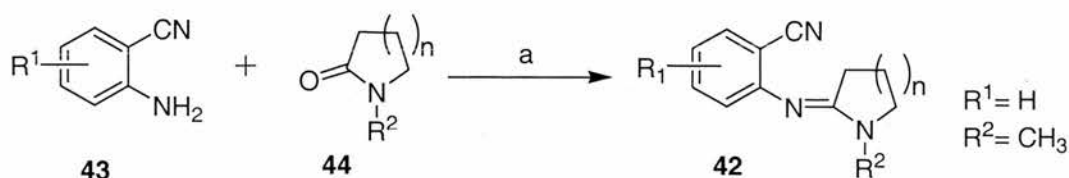


Figure 28. Literature example for the preparation of the amidine **42**. Reagents and conditions: a) i) *N*-methyl-2-pyrrolidinone (**44**, $R^2 = \text{CH}_3$, $n=1$) (1.0 equiv), POCl_3 (1.1 equiv), CHCl_3 , RT, 30 min, ii) **43** ($R = \text{CH}_3$) (1.0 equiv), 60°C , 3 hours, 98%.¹¹

Another example from the literature also reported the synthesis of an amidine following this procedure. The preparation of amidine **45** was carried out by the reaction of 1-phenyl-2-pyrrolidinone (**28**) and the corresponding *ortho*-trifluoromethyl toluidine (**46**) in the presence of phosphorus oxychloride (Figure 29).¹² Interestingly the yield for the reaction was not reported by the authors.

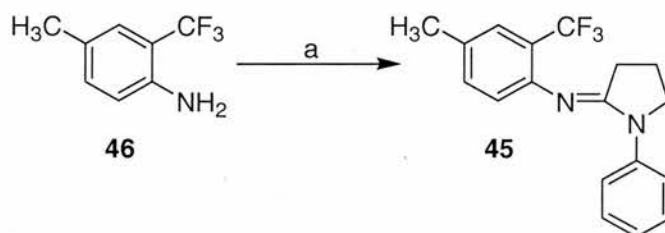


Figure 29. Literature example for the preparation of amidine **45**. Reagents and conditions: a) 1-phenyl-2-pyrrolidinone (**28**), POCl_3 , CHCl_3 , 60°C , 4 hours.¹²

2.1.3.2. Initial attempts to prepare amidine **29**

The first attempts to form the amidine functionality **29** are summarised in Table 2. The reactions were carried out by following the literature procedure.¹³ Phosphorus oxychloride was added to a solution of commercially available 1-phenyl-2-pyrrolidinone (**28**) in benzene, and the reaction was stirred for 16 hours at room temperature. Subsequently anthranilate **27** was added and the reaction was refluxed for 16 hours. Unfortunately none of the desired amidine **29** was identified by ^1H NMR analysis of the crude reaction mixture (entry 1). A second attempt was carried out with the only major change being in the concentration of the reaction. Again none of the desired product **29** was present in the crude reaction mixture (entry 2). However when the solvent was changed from benzene to dichloromethane a 10% yield of **29** was

obtained (entry 3). The desired product **29** was obtained after purification by flash column chromatography. ^1H NMR analysis confirmed the presence of the desired compound **29**. The sample was recrystallised from ethyl acetate/hexane affording high quality crystals suitable for X-ray analysis, which confirmed the structure of **29** (Figure 30).

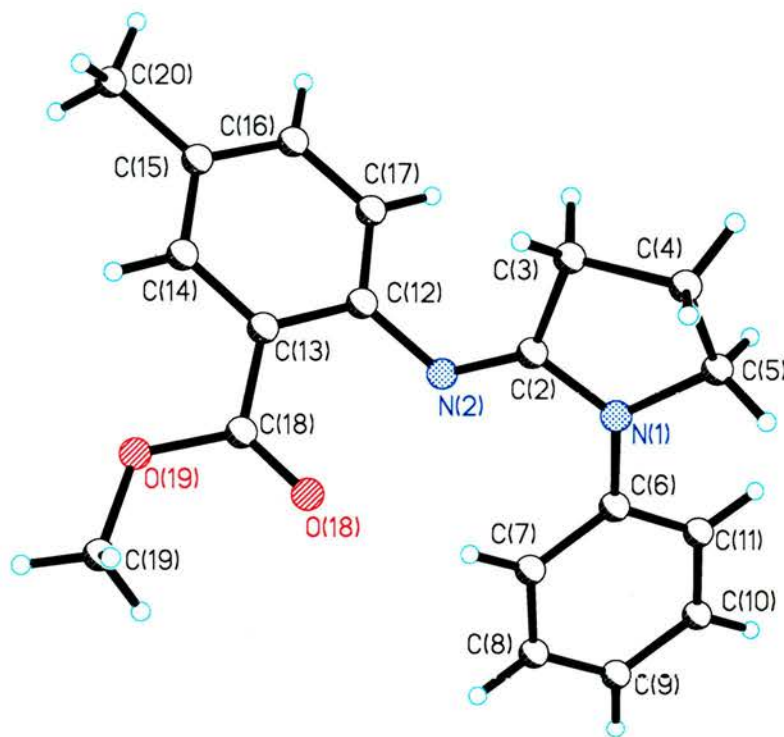


Figure 30. X-ray of amidine **29**. CDC number 243020.

In a further attempt (entry 4) using dichloromethane as the solvent but at the same concentration as entry 1, none of the desired product **29** was obtained. It was concluded that the concentration of the reaction as well as the solvent played an important role in the formation of the amidine moiety.

Entry	Solvent	Time ^a (h)	equiv ^b (29)	equiv ^b POCl ₃	equiv ^b (28)	Conc ^c	Yield (%)
1	Benzene	16	1.0	1.2	1.1	0.12	–
2	Benzene	16	1.0	1.2	1.2	0.62	–
3	DCM	16	1.0	1.2	1.1	0.62	10
4	DCM	16	1.0	1.2	1.1	0.12	–

Table 2. Preparation of the amidine **29** at different concentrations and solvents. The time^a of the reaction is expressed in hours and indicates time of stirring at room temperature prior to addition of **27**. The amount of the starting material is given in equivalents^b. Concentration^c is expressed in Molarity based on **28**. Reagents and conditions: a) i) 1-phenyl-2-pyrrolidinone (**28**), POCl₃, Benzene or DCM, RT, 16 hours, ii) anthranilate **27**, benzene or DCM, heat, 16 hours.

In addition to the atom connectivity, the geometry of the N(2)=C(2) double bond was shown by X-ray analysis to be the *E* regioisomer. Spatial proximity of the protons in amidine **29** was explored by nOe (nuclear Overhauser enhancement) experiments (Figure 31). The NOESY experiment was also consistent with the *E*-isomer being the only isomer present in solution. A nOe was observed between the signals corresponding to the OCH₃ protons δ_{H} 3.82 and the protons on C(7)/C(11) δ_{H} 7.82. Another two nOes were found between protons on C(5) and the protons on C(7)/C(11) and also between protons on C(7)/C(11) and protons on C(10). Enhancement between the signals corresponding to the proton on C(3) and the protons of OCH₃ was not observed. This is also consistent with the *E*-isomer being present in **29**.

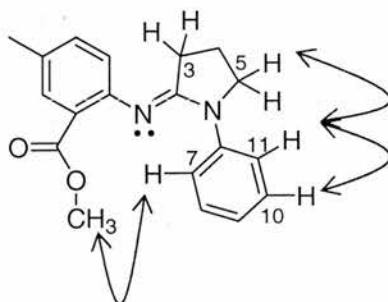


Figure 31. nOe Enhancements observed in amidine **29**. The observed nOes are indicated by arrows.

In order to study further the importance of the formation of a Vilsmeier intermediate on the coupling reaction a series of attempts were carried out. When the reaction of the anthranilate **27** and the lactam **28** in dichloromethane was heated at 40 °C for 16 hours in the absence of POCl₃, none of the desired amidine **29** was obtained. In a similar attempt carried out by Dr Blum in our laboratory, the reaction between **27** and **28** was carried out under microwave irradiation in the absence of POCl₃. Again, none of the desired amidine **29** was formed even in the presence of a dehydrating agent. In addition, attempts to optimise this reaction by using alternative reagents (SOCl₂, MeOTf, PCl₅) proved unsuccessful.

¹H NMR experiments (on a Bruker Avance 300 (300.1 MHz) spectrometer) were carried out in order to study the formation of a possible Vilsmeier intermediate, inspired by the results reported by Kuehne *et al.*³ (Table 1). The reaction was carried out between lactam **28** and phosphorus oxychloride at room temperature where aliquots were withdrawn at different times for ¹H NMR spectroscopic analysis. Unfortunately, ¹H NMR analysis of the reaction did not provide evidence in support of the formation of an iminium intermediate, making these preliminary results difficult to interpret.

Finally, different approaches for preparing amidine **29** were attempted. The first attempt commenced with the coupling between the lactam **28** and anthranilate **33** in the presence of the coupling reagent, DCC (**47**) (Figure 32). The reaction was heated for 24 hours, although as judged by TLC, only starting material was detected. It was decided then to heat the reaction another day. ¹H NMR confirmed the presence of unreacted starting materials.

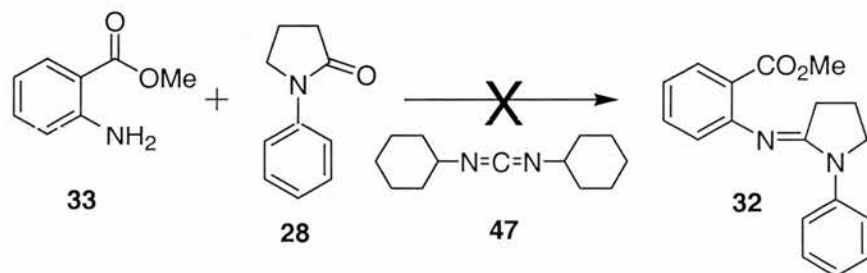


Figure 32. Attempted preparation of the amidine **32**. Reagents and conditions: a) **33** (1.0 equiv), **28** (2.0 equiv), DCC (**47**) (1.0 equiv), DCM, 40 °C, 48 hours.

According to literature precedent¹⁴ the amidine functionality has been prepared in the presence of piperidine instead of phosphorus oxychloride. Dr Blum developed experiments in order to verify the formation of the amidine moiety following this literature protocol. The reactions were carried out with anthranilic acid **34** and either pyrrolidinone (**48**) or 1-phenyl-2-pyrrolidinone (**28**) (Figure 33), respectively, in the presence of piperidine (**49**) and they were heated in ethanol for 5 hours. As judged by ¹H NMR only unreacted starting material was obtained.

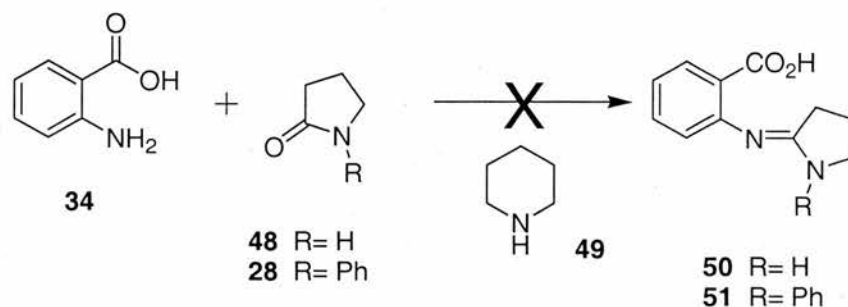


Figure 33. Attempted preparation of the amidines **50** and **51**. Reagents and conditions: a) **34** (1.0 equiv), lactam **28** or **48** (1.0 equiv), **49** (1.0 equiv), EtOH, 80 °C, 5 hours.

2.1.3.3. Empirical approaches to improving the yield of the coupling reaction

In the light of the results obtained previously it was decided to attempt the improvement of the yield of the reaction empirically. Several attempts at this reaction were carried out during the course of this project. Table 3 summarises the results from these experiments (between lactam **28** and phosphorus oxychloride) when the solvent (see Section 2.1.3.2), time and concentration were changed. It is worth noting that a systematic study was not carried out and that the reaction conditions used were different in each case and are therefore not directly comparable. Nevertheless, a number of trends can be discussed from the results.

First, it was found that similar yields were obtained for the coupling reactions when they were carried out at different time, 3 and 16 hours, respectively. Second, no significantly improvement in the isolated yield of the reaction was observed when different conditions were attempted (entries 1-9).

Entry	Amidine	Solvent	Time ^a	equiv ^b (28)	equiv ^b POCl ₃ ^b	equiv ^b (27), (33)	Conc ^c	Yield (%)
1	29	DCM	16	1.0	1.2	1.1	0.60	10
2	29	DCM	3	5.0	1.0	1.2	0.60	7
3	29	DCM	3	5.0	1.0	1.2	0.30	4
4	29	DCM	3	10	1.0	1.2	1.5	11
5	29	DCM	3	10	1.0	1.2	2.5	6
6	29	DCM	3	10	1.5	1.2	1.5	10
7	29	DCM	3	1.1	1.0	1.0	1.1	41
8	32	DCM	3	1.0	1.0	1.0	1.5	16
9	32	DCM	3	1.1	1.0	1.0	1.0	26

Table 3. Preparation of the amidines **29** and **32**. The time^a of the reaction is expressed in hours and indicates time of stirring at room temperature prior to addition of **27** or **33**. The amount of the starting material is given in equivalents^b. Concentration^c is expressed in Molarity based on **28**. Reagents and conditions: a) i) 1-phenyl-2-pyrrolidinone (**28**), POCl₃, DCM, RT, 16 and 3 hours, ii) Anthranilate **27** or **33**, DCM, 40 °C, 16 hours.

In all cases, the purification of the amidines **29** and **32** was carried out without the use of flash column chromatography. Once the reaction was complete, as judged by TLC analysis, the reaction solvent was removed *in vacuo*. The residue was then dissolved in dilute hydrochloric acid (pH 2) (to protonate the amidine carrying it into the aqueous phase) and extracted three times with dichloromethane. The aqueous extract was then basified (pH 8) (to recover the amidine from the aqueous phase) and subsequently extracted three times with ethyl acetate. ¹H NMR analysis confirmed the structure of the product with no minor impurities detected. In cases where the extraction procedure was repeated two more times (starting with the dichloromethane extracts, entries 7 and 9), it was found that the isolated yield was increased. However, the extraction procedure suggested that the poor yield of the reaction could be rationalised by loss of product into dichloromethane during the work-up procedure.

In addition, it was envisioned that perhaps an excess of hydrochloric acid could be produced during the condensation reaction and therefore a possible protonation of the anthranilate would take place, decreasing the yield. Therefore in order to remove any hydrochloric acid, a base was added to the reaction. Anthranilate **27** was added to a

crude reaction mixture of **28** and phosphorus oxychloride that had been stirred for 48 hours and the reaction was heated for 16 hours. Diisopropylethylamine (Hunig's base) was then added. After refluxing the reaction mixture for a further 16 hours an aliquot was taken from the reaction in order to check for the formation of the desired product (**29**). Although ^1H NMR analysis showed the presence of a small amount of **29**, purification by flash column chromatography of the rest of the reaction gave only a different product. By comparing the analytical data with literature precedent^{15,16} a possible structure for this compound, **52**, was proposed (Figure 34). Mass spectrometric analysis of the compound showed the molecular weight (m/z (Cl^+) 305) to be consistent with the proposed structure. ^1H NMR and COSY data were also consistent with **52**. The geometry of the double bond in **52** was not determined. Therefore, it was decided to draw **52** as the *Z*-isomer according to the literature.^{15,16} In a subsequent reaction it was found rerunning this reaction, but in absence of anthranilate **27**, also gave **52**.

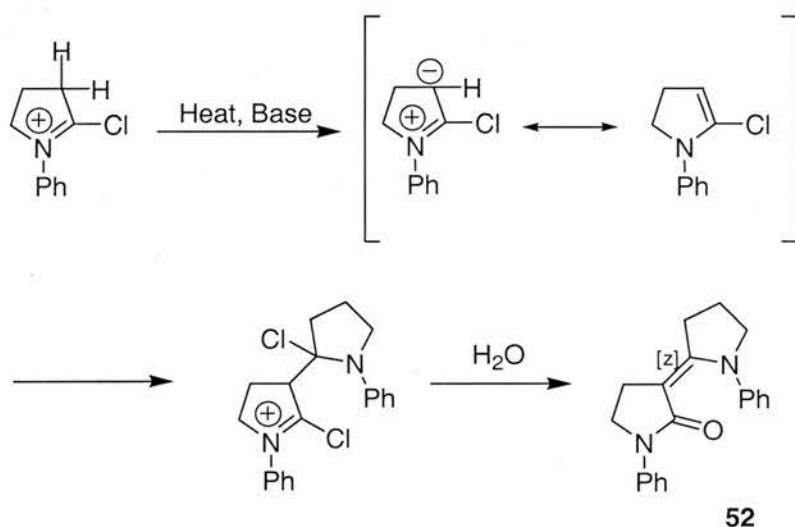


Figure 34. Proposed mechanism for the formation of **52**.¹⁶

In conclusion, despite the low yield for the coupling reaction, it was decided to use the conditions described in the table (entry 7 and 9) as optimal for preparation of amidines **29** and **32**.

2.1.3.4. NMR studies on the formation of the Vilsmeier intermediate

In the light of the low yields previously obtained for the coupling reaction, it was decided to revisit the NMR experiments in order to study the reaction in more detail. In this case, the NMR spectra were obtained in collaboration with Dr Tomas Lebl and were recorded on a Bruker Avance 500 (499.9 MHz) spectrometer.

The first issue was to find a system that would work under the reaction conditions to enable subsequent analysis by ^1H and possibly ^{31}P NMR. Based on literature precedent³ (Section 2.1.3.1), it was envisaged that the type of lactams that should work well in these reactions would contain an electron-donating groups on the nitrogen atom, such as *N*-alkyl lactams **39** and **53**. Therefore, the first aim was to prepare *N*-alkyl amidines **54** and **55** (Figures 35 and 36), under the optimised work-up procedure previously described in Section 2.1.3.3.

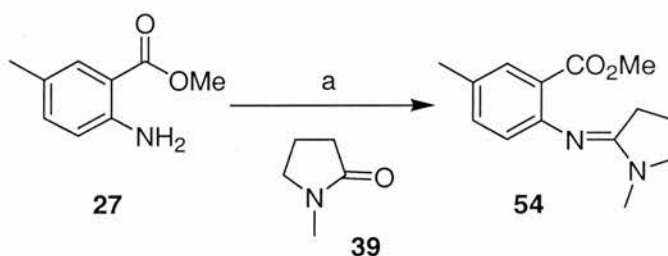


Figure 35. Preparation of the amidine **54**. Reagents and conditions. a) i) **39** (1.1 equiv), POCl₃ (1.0 equiv), DCM, RT, 3 hours, ii) **27** (1.0 equiv), DCM, 40 °C, 16 hours, 79%.

N-methyl-2-pyrrolidinone (**39**) and *N*-ethyl-2-pyrrolidinone (**53**) were activated in the presence of phosphorus oxychloride and then reacted with anthranilate ester **27** at 40 °C for 16 hours. The solvent was removed *in vacuo* and the residue was dissolved in aqueous hydrochloric acid. The aqueous phase was extracted with dichloromethane and then basified and extracted with ethyl acetate. The reactions gave the desired products in moderate yields, 46% for **54** and 29% for **55**, respectively. When this extraction protocol was repeated one more time, there was a significant increase in the final yield of **54** (79%) whereas in the case of **55** the final yield was almost the same (31%). Further attempts to recrystallise these compounds to determine their structure and geometry were unsuccessful due to the fact that the samples were thick oils.

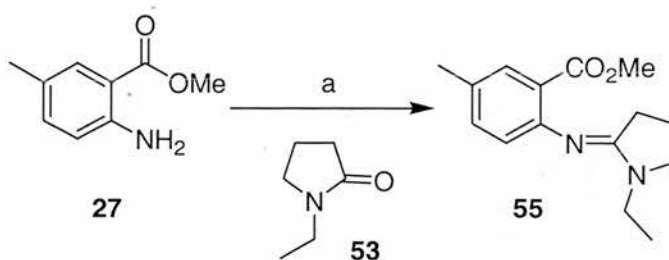


Figure 36. Preparation of the amidine **55**. Reagents and conditions. a) i) **53** (1.1 equiv), POCl₃ (1.0 equiv), DCM, RT, 3 hours, ii) **27** (1.0 equiv), DCM, 40 °C, 16 hours, 31%.

¹H NMR analysis confirmed the presence of compounds **54** and **55** respectively. However attempts to determine the geometry of the double bond in **54** by measuring spatial proximity of the protons by NOESY were unsuccessful. Although some nOes were observed, the free rotation of the single bonds between the aromatic ring and the nitrogen and between the lactam nitrogen and the methyl group, made this molecule flexible and therefore a possible assignment of the geometry proved difficult.

These results showed that the presence of an electron-donating group (*e.g.* alkyl group) on the lactam nitrogen increased significantly the yield of the coupling reaction as required for these sections of research. It was therefore decided to carry out ¹H NMR experiments on the reaction of lactam **39** with phosphorus oxychloride. These experiments were carried out in CD₂Cl₂ in order to mirror the preparative scale reaction. The results from these experiments and from analogous studies using the *N*-phenyl lactam **28** are presented below.

2.1.3.4.1. NMR studies on *N*-lactams **28** and **39** and phosphorus oxychloride

The reaction was carried out between lactam **39** (1.1 equivalents) and phosphorus oxychloride (1.0 equivalents) in CD₂Cl₂, at a concentration of 25 mM. ¹H spectra were recorded at 15 minute intervals (not all data points are shown in Figure 37). Two interesting observations were made: i) the signals corresponding to starting lactam **39** shifted downfield as the time course progressed with the shift for the signals corresponding to the H-3 protons being the most dramatic; ii) a new set of signals was observed to increase in intensity with time having first become visible at *t* = 130 minutes.

An analogous set of experiments were carried out using *N*-phenyl lactam **28** (Figures 38 and 39). Signals corresponding to the lactam **28** were observed to shift downfield in analogous manner to those for **39**. However, this shift was less pronounced in the case of **28**. In addition no formation of a second set of signals was observed.

Attempts to synthesise amidines **29** and **54** gave significantly different results. Amidine **54** was produced in much higher yield than amidine **29**. One possible explanation for the difference in yields of these two reactions is that it reflects a difference in the reaction of the two lactams (**28** and **39**) with phosphorus oxychloride. In fact when the reaction of **28** and **39** with phosphorus oxychloride is followed by ^1H NMR, a clear difference is observed. At first sight, the reaction of **39** with phosphorus oxychloride appears to be consistent with previous observations made by Kuehne.³ However, the fact that no analogous peaks are observed in the reaction with **28**, despite knowing that formation of **29** occurs, suggests that the situation may be much more complicated than previously suggested. Whilst ultimately difficult to interpret, these experiments do at least identify a clear difference in the reactivity of **28** and **39**. This almost certainly results from the presence of the aromatic substituent on the nitrogen in **28** which causes a delocalisation of the lone pair of electrons into the ring. Further studies to aid the explanation of these observations are continuing within the Westwood laboratory.

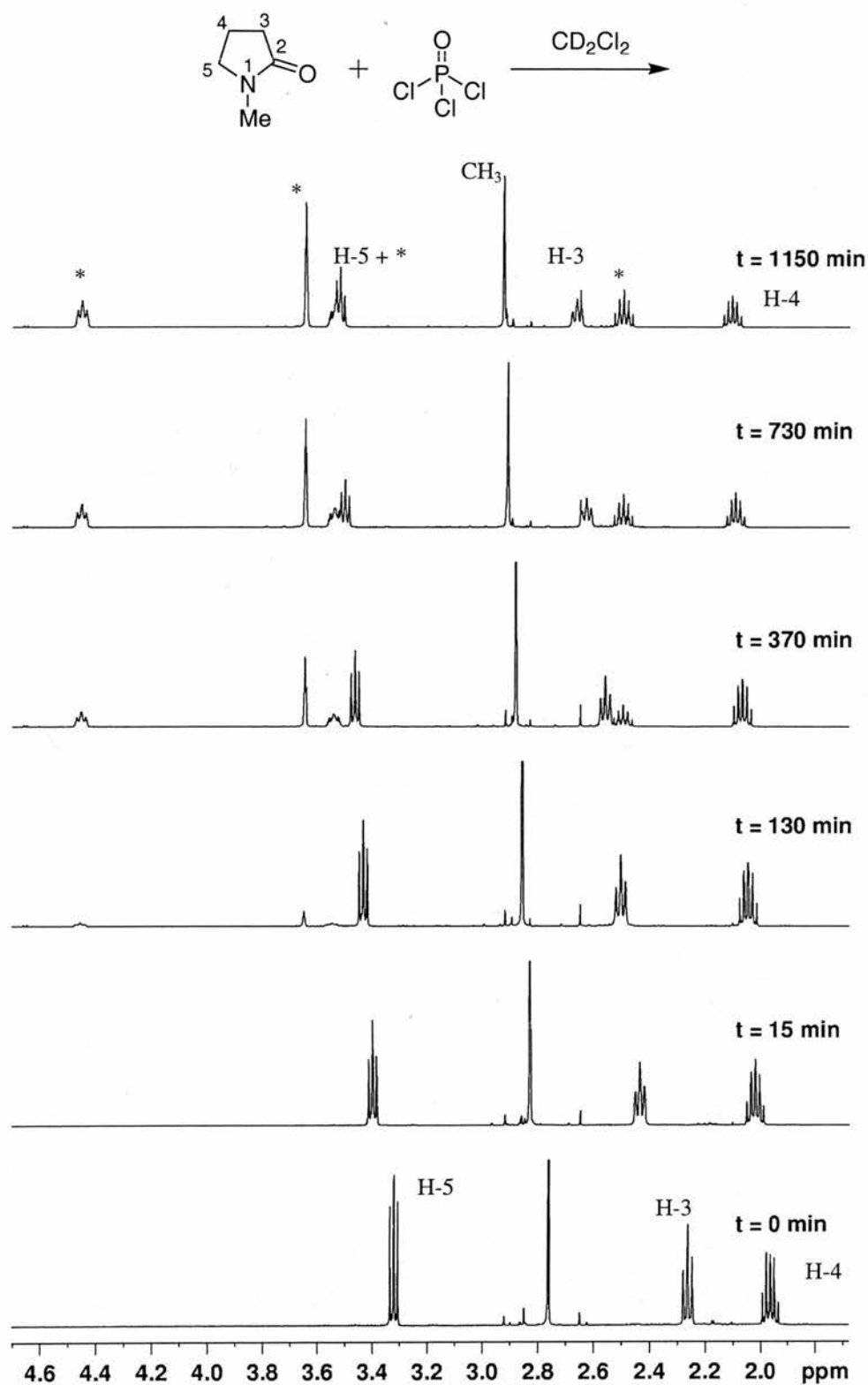


Figure 37. ¹H NMR spectrum of reaction of **39** in CD₂Cl₂ after 19 hours. * Signals corresponding to the protons for the new chemical species.

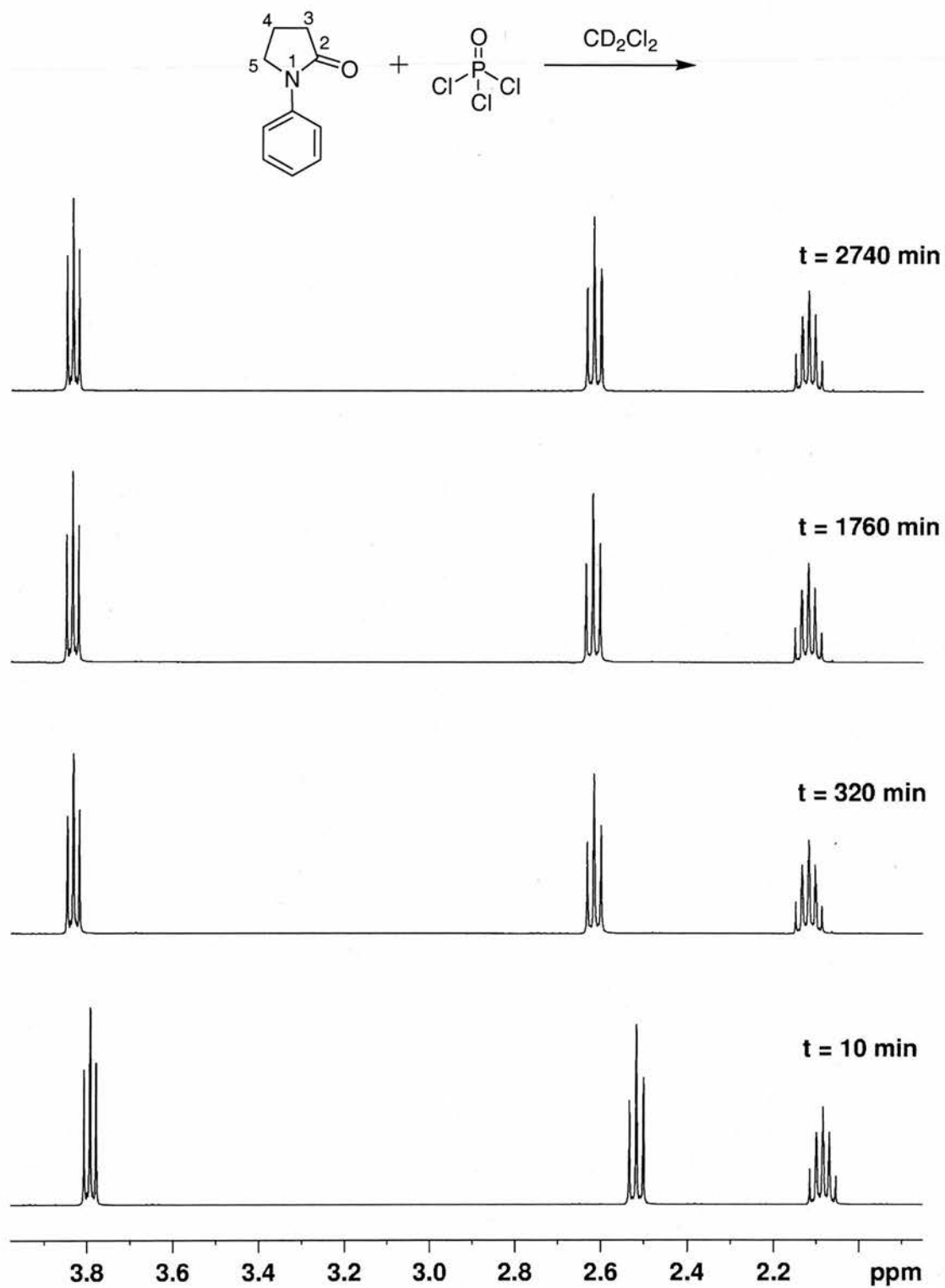


Figure 38. ^1H NMR spectrum of the aliphatic region, of reaction of **28** in CD_2Cl_2 after 2 days.

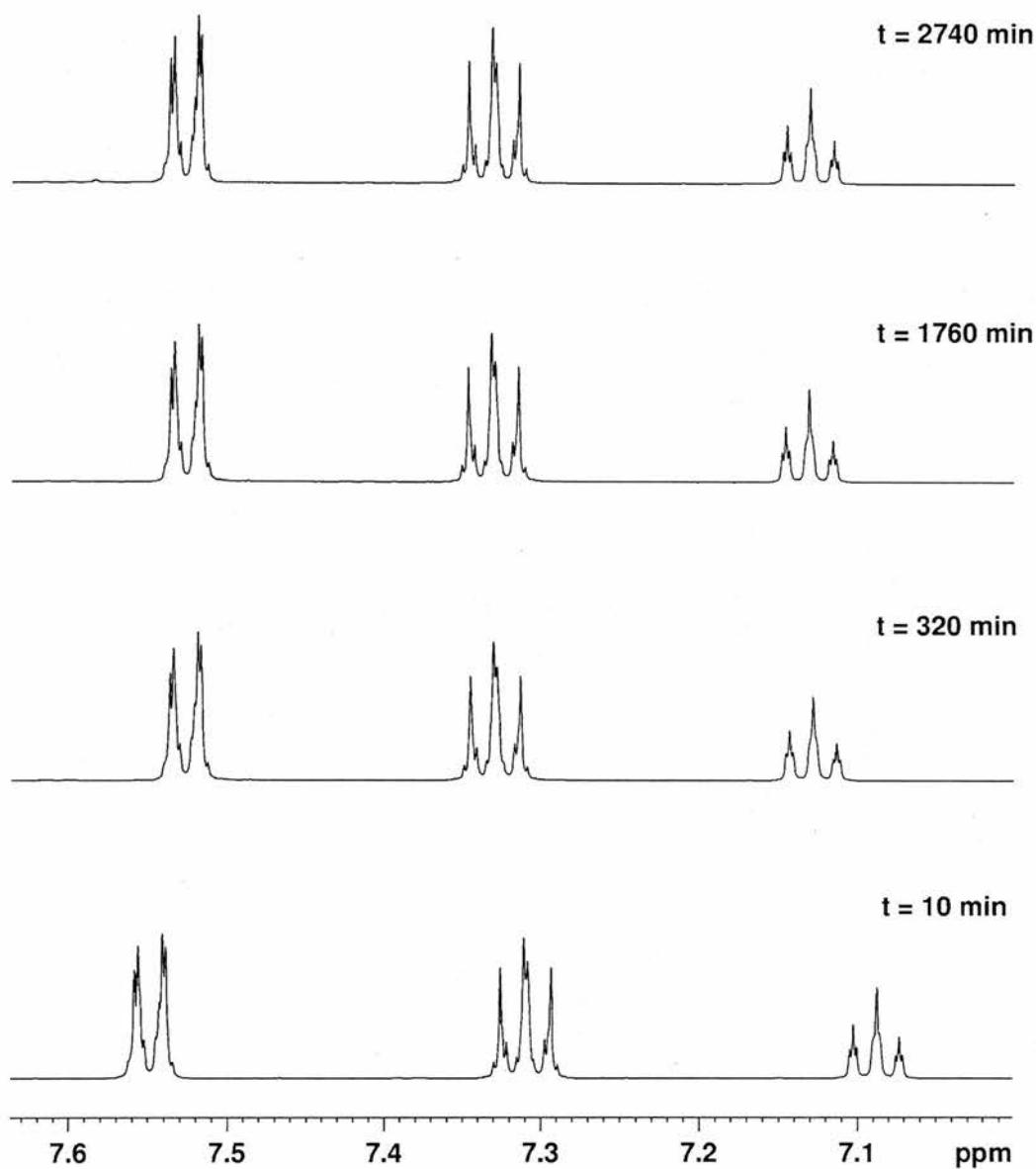


Figure 39. ^1H NMR spectrum of the aromatic region, of reaction of **28** in CD_2Cl_2 after 2 days.

2.1.4. Synthesis of Quinolones **24** and **31**

Quinolone **24** was prepared from amidine **29** en route to the final product (\pm)-blebbistatin (**18**). Several analogous transformations have been reported in the literature and are briefly reviewed here. Interestingly it was found that tacrine **56**, a quinoline-based heterocycle of relevance to the treatment of Alzheimer's disease, could be synthesised using the reaction of amidine **42** with ZnCl_2 (Figure 40).¹¹

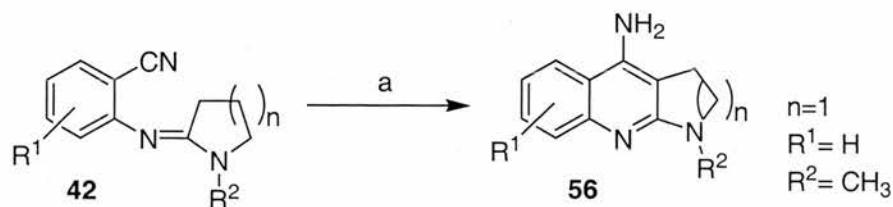


Figure 40. Literature example for the preparation of tacrine **56**. Reagents and conditions: a) ZnCl_2 , nitrobenzene, 140°C , 50 min.¹¹

A different approach to a tacrine heterocycle **57** proceeded through the formation of a quinone methide intermediate **58** (Figure 41).¹²

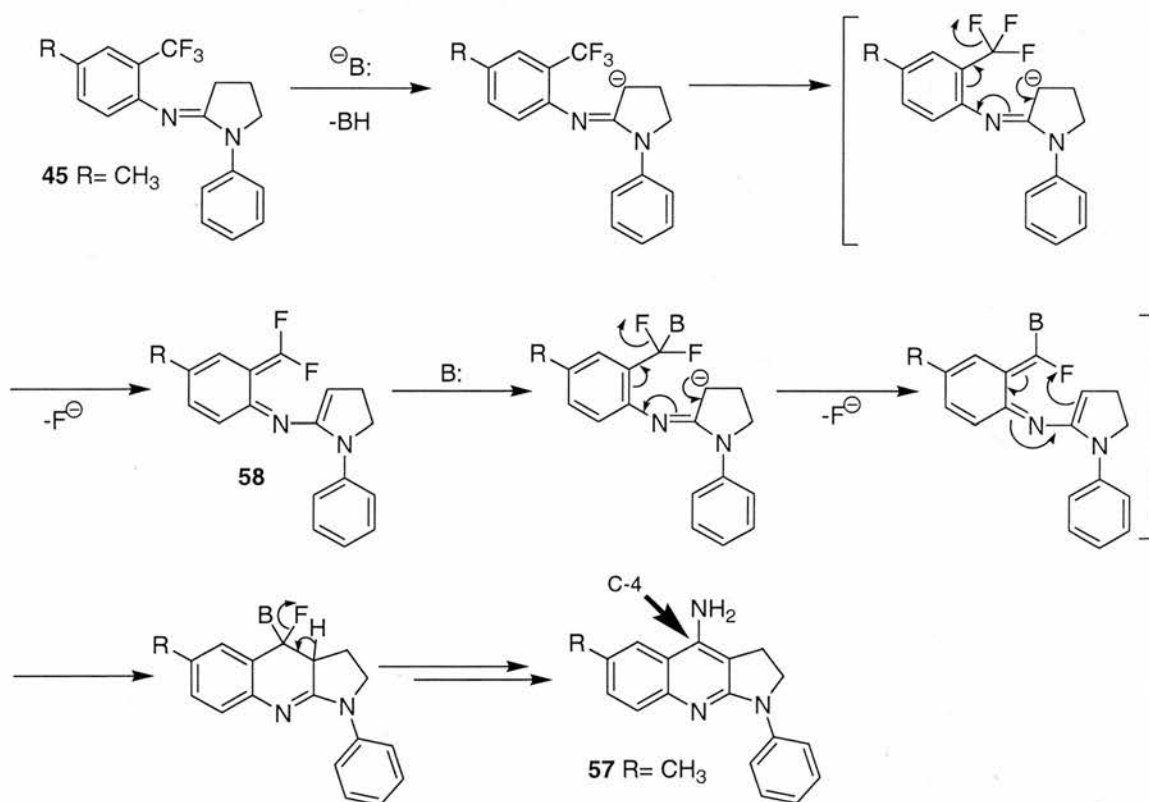


Figure 41. Proposed mechanism for the preparation of tacrine **57**. Reagents and conditions: a) NaHMDS (1M in THF), -78°C -RT, 4 hours, 81% (**57**).¹²

In this case, the amidine **45** was reacted in the presence of 4 equivalents of base (NaHMDS) to afford the desired heterocycle **57** in excellent yield. They found that THF was the optimal solvent for the cyclisation reaction compared with diethyl ether, dioxane or 2-methyltetrahydrofuran. Temperature and time also played a very important role in the reaction. Low yields were found when the reaction mixture was

allowed to warm to room temperature rapidly whereas the optimal range for the cyclisation temperature was found to be -35 to -15 °C. However the nature of the base counteranion did not affect the reaction.

It was also found that the nature of the substituents in the trifluoromethylaniline (either mildly electron-donating or mildly electron withdrawing) did not affect the progress of the reaction.¹² Surprisingly, a previous report suggested that the presence of either a nitrogen or oxygen group at C-4 position of **57** comes directly from the base utilised for cyclisation (*e.g.* lithium diisopropylamine (LDA) or potassium *tert*-butoxide (*t*-BuOK), although it is important to point out that these bases are not nucleophiles).¹⁷

In our case, the preparation of quinolone **24** was carried out by base-induced cyclisation of the amidine **29** (Figure 42). Therefore **29** was treated with an excess of lithium bis(trimethylsilyl)amide at -78 °C. The reaction mixture was then warmed to 0 °C for 3 hours until no starting material (**29**) was detected by TLC. The crude reaction mixture was purified by flash column chromatography eluting with 100% ethyl acetate to afford the desired quinolone **24** in high yield (90%). Quinolone **24**, an off-white solid, was found to be stable in the absence of air and light and could be stored for extended periods of time in multigram quantities. The same protocol was carried out for the preparation of **31** from **32**.

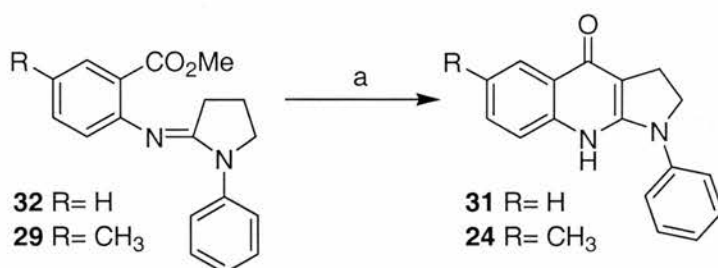


Figure 42. Preparation of the quinolones **24** and **31**. Reagents and conditions: a) LiHMDS (3.0-2.5 equiv), THF, -78 °C-0 °C, 3 hours, 90% (**24**) and 95% (**31**).

During the cyclisation reaction (Figure 43) it was assumed that the base, lithium bis(trimethylsilyl)amide, would remove the most acidic proton to form the enamine anion which would attack the ester carbonyl carbon, with methoxide acting as a leaving group. In theory, therefore, only one equivalent of base is required in this reaction. In

practice, however, it was necessary to use an excess of base in order to push the reaction to completion.

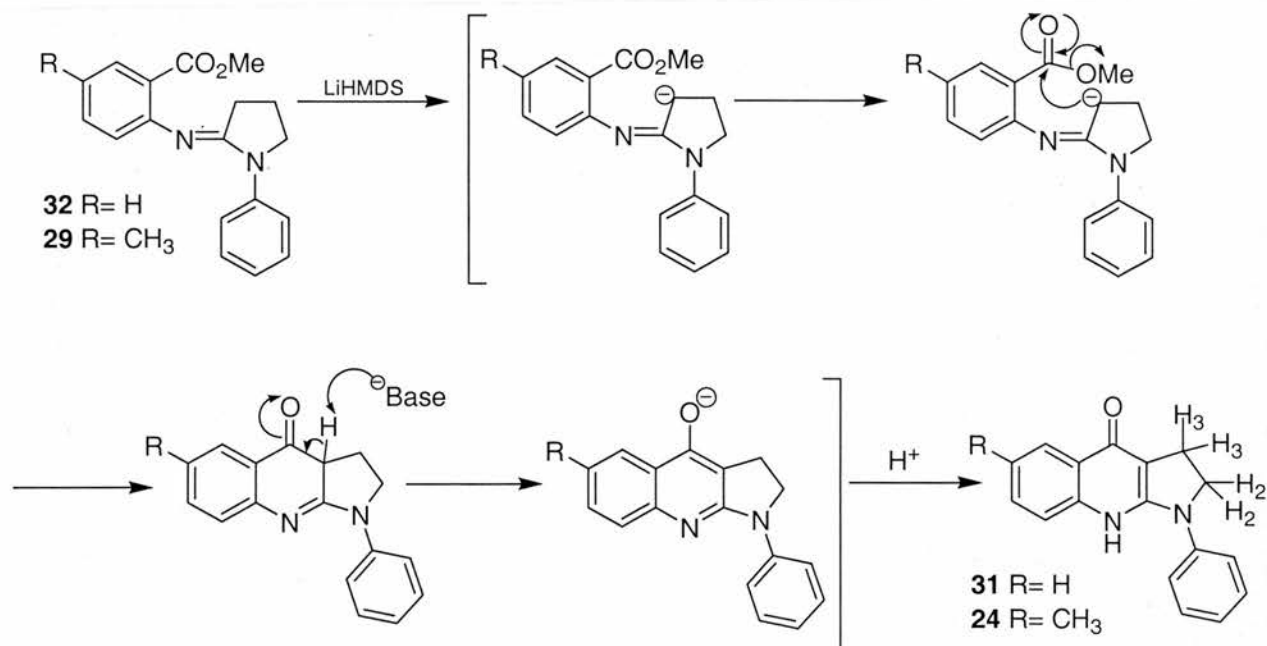


Figure 43. Proposed mechanism for the cyclisation reaction.

The structure of the product **24** was confirmed by ¹H NMR analysis which showed the presence of two triplets with chemical shifts of 3.17 ppm for H-3 and 4.06 ppm for H-2. A report in the literature discusses the presence of ketone-enol tautomerism associated with the quinolone structure (Figure 44). It is argued that only two tautomers are possible, the oxo or keto form (**24**) and the hydroxyl or enol form (**59**). However **24** is preferred in solution.¹⁸ A third form **60** was ruled out based on spectroscopic evidence. Infrared analysis showed the presence of a band at 1571 cm⁻¹, which is assumed to correspond to the ketone.

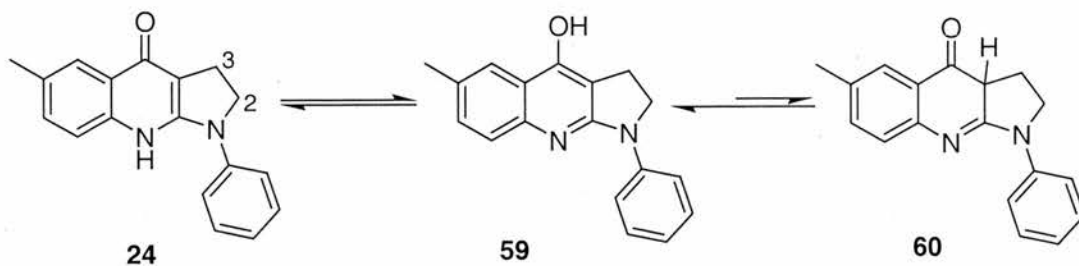


Figure 44. Tautomeric forms of quinolone **24**.

It was shown that the cyclised product **24** could decompose in the presence of molecular oxygen and light to give (\pm)-blebbistatin (**18**). Therefore it was decided to investigate its stability by ^1H NMR. Quinolone **24** was dissolved in CDCl_3 , covered with parafilm and left at room temperature under natural light in the absence of atmospheric oxygen. ^1H NMR spectra were taken at regular intervals over twenty five days. It was found that quinolone **24** was stable towards oxidation in the absence of air and could be stored for long periods of time without degradation.

2.1.4.1. Attempts to cyclise amidine analogues **54** and **55**

After the successful preparation of quinolones **24** and **31**, it was decided to carry out the cyclisation of the amidines **54** and **55**. The first attempts at these reactions followed the procedure described in Section 2.1.4. Unfortunately none of the desired quinolones were obtained after purification of the crude reaction mixture by flash column chromatography.

The cyclisation reaction for amidine **54** (Figure 45) was carried out at $-78\text{ }^\circ\text{C}$ and the reaction was warmed to room temperature for 3 hours. However, it was found that the starting material was consumed at $-40\text{ }^\circ\text{C}$ as judged by TLC analysis. This reaction was therefore repeated at $-40\text{ }^\circ\text{C}$ with 2 equivalents of base for 16 hours and then quenched at $-40\text{ }^\circ\text{C}$. TLC analysis showed the presence of one major new compound. ^1H NMR analysis of the crude reaction mixture suggested the possible presence of the dimer **61** (Figure 47). Mass spectroscopic analysis of the crude reaction mixture showed the presence of a peak at m/z (EI) 460 consistent with this assignment. Again, purification by flash column chromatography proved difficult. The same conditions were attempted for the cyclisation of **55** (Figure 47). TLC analysis of the reaction showed a complex mixture of products and no purification attempts were made.

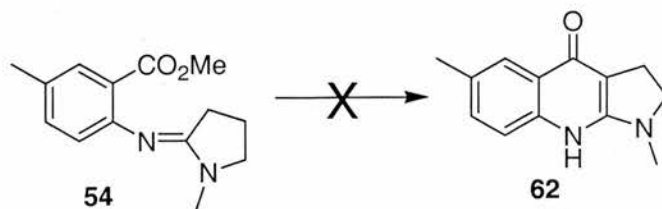


Figure 45. Attempt to cyclise *N*-methyl amidine **54**. Reagents and conditions: a) LiHMDS (2.0 equiv), THF, $-40\text{ }^\circ\text{C}$, 16 hours.

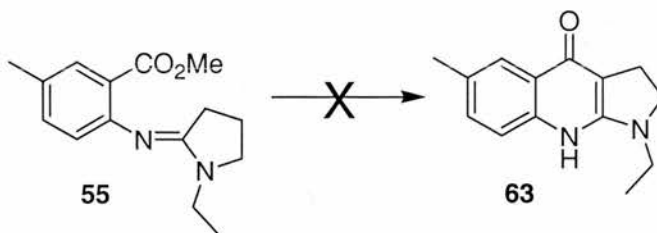


Figure 46. Attempt to cyclise *N*-ethyl amidine **55**. Reagents and conditions: a) LiHMDS (2.0 equiv), THF, -40 °C, 16 hours.

In a final attempt to cyclise amidine **54** an additive, DMPU (**64**) was included. It is known that solvents such as HMPA (**65**) and DMPU (**64**) (Figure 47) can disrupt metal chelation,¹⁹ therefore it was envisioned that addition of this co-solvent might avoid formation of dimer **61**, in favour of the quinolone formation by destabilising a chelate of structure **66**. To a solution of amidine **54** in THF at -78 °C was added 3 equivalents of lithium bis(trimethylsilyl)amide and 1 equivalent of DMPU. The reaction mixture was warmed to 0 °C for 16 hours and TLC analysis confirmed the consumption of the starting material **54**. Mass spectrometric analysis of the crude reaction mixture exhibited a positive ion mass peak at m/z (ES+) 461, being consistent with the mass of the dimer **61**. In addition, high resolution mass analysis on that peak was consistent with the formation of a compound with the molecular formula $C_{27}H_{33}N_4O_3$, which was the same as that for dimer **61** (Figure 47). No other products were identified and the reaction was therefore abandoned.

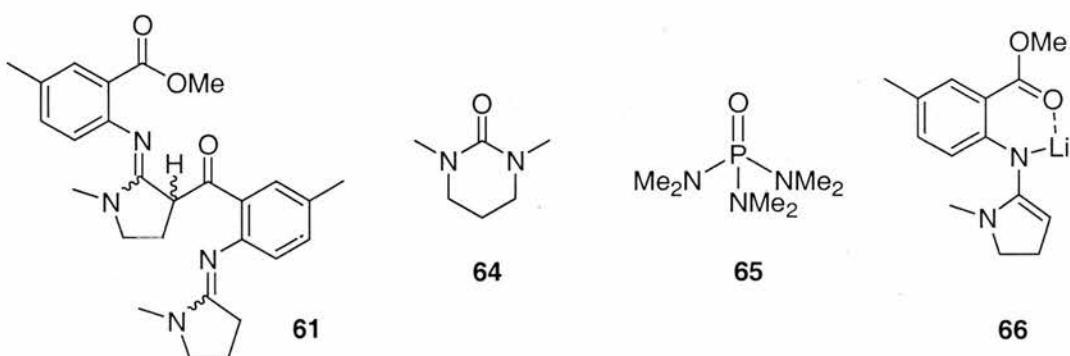


Figure 47. Structure of the dimer **61**, DMPU (**64**), HMPA (**65**), and chelate **66**.

2.1.5. Synthesis of (±)-Blebbistatin (18)

The last step of the reaction sequence to the blebbistatin core structure was the oxidation of quinolone **24**. This section focuses on the oxidation of **24** to (±)-blebbistatin (**18**) by two different methods.

2.1.5.1. Air Oxidation

It was observed that a DMSO solution of quinolone **24** slowly decomposed in air in the presence of light to give (±)-blebbistatin (**18**) (Figure 48). The experiment was followed for 40 days and initial TLC analysis mainly showed the presence of **24**, although an additional less polar spot was detected and increased during the course of the experiment. The resultant product was purified by flash column chromatography to afford the desired (±)-blebbistatin (**18**) in a low yield (22%). ¹H NMR analysis confirmed the structure of **18** and the measurement of the optical rotation gave a value of zero ($[\alpha]_D^{25} = 0$), as expected.



Figure 48. Oxidation of quinolone **24** to (±)-blebbistatin (**18**). Reagents and conditions: a) O₂, light, DMSO, RT, 40 days, 22%.

2.1.5.2. Photolysis

The rate of this transformation was increased by irradiation of **24** in DMSO or THF using a medium pressure mercury lamp (400 W, unfiltered) or upon irradiation (365 nm) of **24** supported on silica gel (Figure 49).

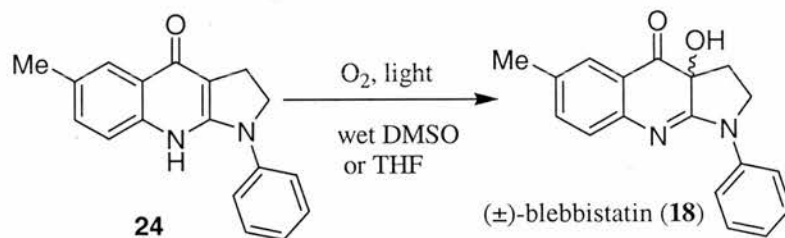


Figure 49. Oxidation of quinolone **24** to the (±)-blebbistatin (**18**). Reagents and conditions: a) O_2 , light, DMSO or THF, RT, 3 hours, 29% and 26% respectively.

A solution of **24** in DMSO in the presence of air was irradiated for 1 hour. The reaction was followed by TLC analysis which showed a very weak yellow spot corresponding to the product **18**. It was then decided to increase the time of irradiation for another hour and more of the yellow spot was formed as judged by TLC analysis. Finally after 3 hours of reaction, no further change was observed. The crude material was purified by flash chromatography to afford the desired compound **18** as a yellow solid in 29% of yield. 1H NMR and optical rotation values ($[\alpha]_D^{25} = 0$) were consistent with the previous result.

Due to the inconvenience of removing DMSO during the work up, the use of an alternative solvent to carry out the degradation process was attempted. THF was judged to be the most suitable solvent as quinolone **24** was soluble in this solvent. Distilled THF was required for the reaction due to the fact that commercially available bottles contained a radical inhibitor. The reaction followed the same procedure as described above for DMSO. In this case (±)-blebbistatin (**18**) was obtained in 26% of yield. An analogous experiment using the photosensitiser, Rose Bengal, was carried out in an attempt to improve the yield of the reaction. Unfortunately no significant differences were observed. Furthermore it was found that when quinolone **24** was irradiated in the presence of argon, (±)-blebbistatin (**18**) was not formed, as judged by 1H NMR analysis, consistent with the essential role of molecular oxygen in this transformation.

In summary, the degradation of **24** to **18** occurred in a slightly better yield and in much less time when the reaction is irradiated using a mercury lamp. The use of THF as a solvent helped work up as the reaction could be concentrated in *vacuo* directly allowing for immediate purification of **18**. The use of a photosensitiser (Rose Bengal) did not improve the yield of the reaction.

2.2. ASYMMETRIC HYDROXYLATION: AN ALTERNATIVE ROUTE FOR THE SYNTHESIS OF THE CORE STRUCTURE OF (-)-BLEBBISTATIN (7)

Stereochemical control in the formation of stereogenic centres presents a significant challenge to the organic chemist. It is well established that for many chiral compounds the two enantiomers show different biological properties. For instance it can happen that one enantiomer of a bioactive compound is more potent than the other, or even that one enantiomer is inactive or induces a different unrelated phenotype. Mitchison *et al.*¹ (Chapter 1, Section 1.4.3.1) observed in *in vitro* assays that (-)-blebbistatin (7) was active against non-muscle myosin II whilst (+)-blebbistatin (23) was inactive. In light of these results, it became desirable to develop a highly efficient route for synthesising enantiomerically enriched samples of (-)-blebbistatin (7) and (+)-blebbistatin (23).

The α -hydroxy carbonyl functionality in (-)-blebbistatin (7) is common in many biologically active molecules, as well as in chiral building blocks and in key intermediates in the synthesis of natural products.^{20, 21, 22, & 23} In many of these examples this functional group is prepared by direct oxidation of an enolate to the desired α -hydroxy ketone (Figure 50). The stereoselective creation of the new stereogenic centre can be achieved by the reaction with a chiral reagent.

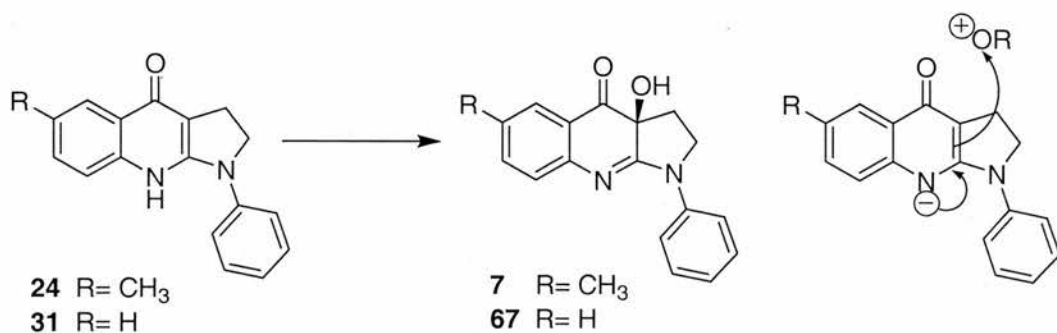


Figure 50. Proposed mechanism for the oxidation of the quinolone.

2.2.1. Overview of chemical methods in asymmetric hydroxylation

Several methods have been developed for the synthesis of α -hydroxy carbonyl compounds, although most of them involve multistep transformation of a carbonyl

group.²⁴ Examples reported in the literature involve, among others, the conversion into the hydroperoxy compound and subsequent reduction to the α -hydroxy compounds as developed by Barton *et al.*²⁵ or the pre-formation of a silyl enol ether from the carbonyl compound followed by oxidation with reagents such as *m*-chloroperbenzoic acid (*m*-CPBA) as developed by Rubottom.²⁶ The most straightforward way to α -hydroxy carbonyl compounds is direct enolate hydroxylation. Two reagents that have been studied in detail for this transformation are molecular oxygen (O₂)²⁷ and Vedejs' reagent [molybdenum peroxide-pyridine-hexamethylphosphoramide, MoO₅ Py HMPA (MoOPH)].^{28, 29} Nevertheless, these two reagents do not induce asymmetry (they are not chiral) and their use also lead to the formation of byproducts.²⁴ α -Hydroxy ketones can also be prepared by catalytic enantioselective oxidation of achiral ketones using molecular oxygen with a chiral phase transfer catalyst, affording up to 79% of enantiomeric excess.³⁰ The enantioselective α -hydroxylation of β -ketoesters, has been reported in the literature by using titanium catalyst complexes and an oxaziridine as the oxidising reagent, affording enantioselectivities up to 94%.³¹ Several other examples of this approach using chiral *N*-sulfonyloxaziridines have been reported.^{23, 24, 30} These reagents afforded the α -hydroxy carbonyl compounds in high yield with excellent stereoselectivity. The advantages of these reagents are that they are aprotic, therefore they will not be destroyed by the enolate prior to oxidation, and are very stable thus easy to store. In addition, over-oxidation to α -dicarbonyl compounds are not detected as side products in the oxidation reaction (where relevant).

Therefore it was decided to focus our attention on exploring the asymmetric synthesis of (–)-blebbistatin (**7**) using the Davis oxaziridine reagents.²¹

2.2.2. Oxaziridines

The oxaziridines (Figure 51) are a class of oxidising reagents employed for the asymmetric α -hydroxylation of enolates. These reagents are heterocyclic compounds containing an oxygen, nitrogen and carbon atom in a three-membered ring which leads to an unusually high reactivity and also results in the weak N-O bond. In addition, if the substituents at the ring carbon in the oxaziridines are identical ($R^2 = R^3$ and R^1 does not contain a stereogenic centre), the only possible centre of asymmetry is the nitrogen atom.³² This class of compounds was introduced by Franklin A. Davis, and extensive

literature exists for their use and synthesis. The features of these reagents are that they are neutral, aprotic, electrophilic, stable, easy to prepare, in some cases commercially available and they frequently afford high stereoselectivities in asymmetric oxidations. *N*-sulfonyloxaziridines are soluble in different solvents such as tetrahydrofuran, dichloromethane, chloroform and insoluble in water and hexane.²¹

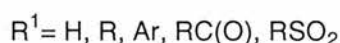
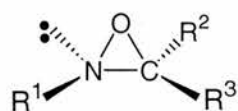


Figure 51. General structure of oxaziridines.

2.2.2.1. Synthesis of oxaziridines

The main group of oxaziridines is the *N*-sulfonyloxaziridines **68** (Figure 52) which are widely studied in asymmetric synthesis. They can be prepared from biphasic buffered oxidation of sulfonimine (**69**) with *m*-chloroperbenzoic acid (*m*-CPBA) or Oxone (potassium peroxymonosulfate), affording racemic *trans*-*N*-sulfonyloxaziridine **68** in excellent yields.^{21, 23, 33}

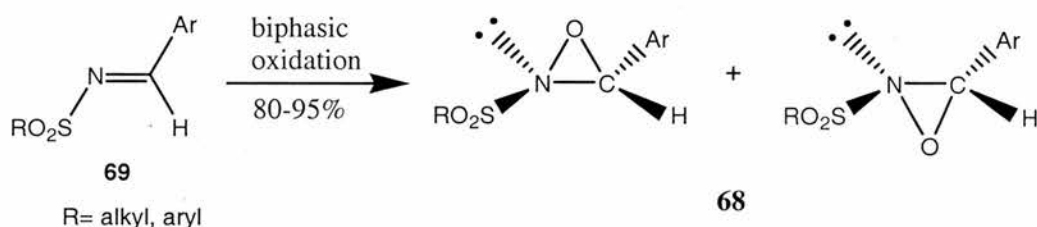


Figure 52. Preparation of *N*-sulfonyloxaziridines **68**.

The *N*-sulfonyloxaziridines are classified as followed.^{21, 23}

a) Optically active *N*-sulfonyloxaziridines; they can be prepared by biphasic oxidation of optically active sulfonimines **70** (Figure 53) using achiral peracids (*m*-CPBA) to give mixtures of oxaziridine diastereoisomers **71** and **72** or oxidation of an achiral sulfonimine with a chiral peracid. These oxaziridines can only be separated by recrystallisation due to their instability to chromatographic techniques.³⁴

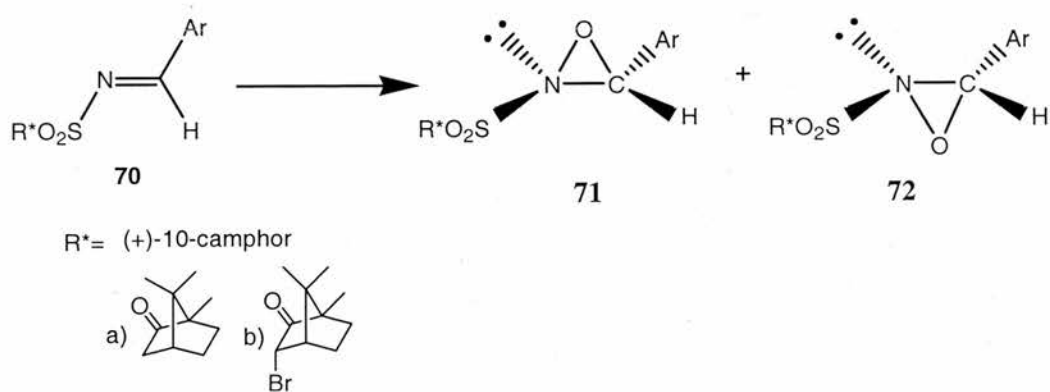


Figure 53. Preparation of optically active *N*-sulfonyloxaziridines **71** and **72**.

b) Diastereomeric *N*-sulfamyloxaziridines; they can be prepared by biphasic oxidation of sulfamimines **73** (Figure 54) using *m*-CPBA/NaHCO₃, to give a mixture of the two diastereomeric 2-sulfamyloxaziridines **74** and **75** in high yield. The diastereomers are stable to chromatography and therefore they can be separated by crystallisation or preparative HPLC into their optical pure forms.³⁵

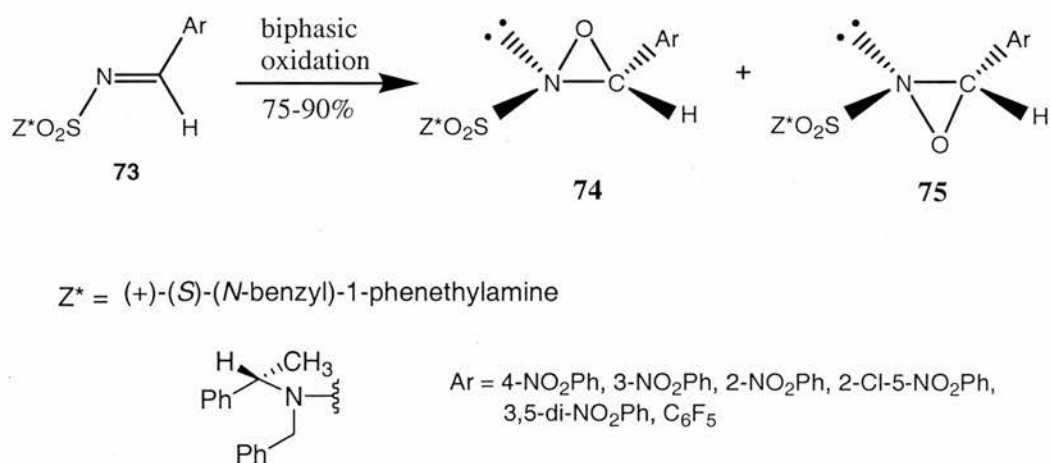


Figure 54. Preparation of diastereomeric *N*-sulfamyloxaziridines **74** and **75**.

c) (Camphorylsulfonyl)oxaziridines; they can be prepared by biphasic oxidation of the sulfonimine **76** (Figure 55) with potassium peroxymonosulfate (Oxone), *m*-chloroperbenzoic acid (*m*-CPBA), buffered with saturated K₂CO₃ to afford a single oxaziridine isomer ((-)- or (+)-(camphorylsulfonyl)oxaziridines). The oxidation has also been developed using peracetic acid or magnesium monoperoxyphthalate with K₂CO₃ in the presence of a phase-transfer catalyst.³⁶ The enantiomerically pure forms

of several (camphoryl-sulfonyl)oxaziridines are commercially available from the Aldrich Chemical Co. and Fluka.

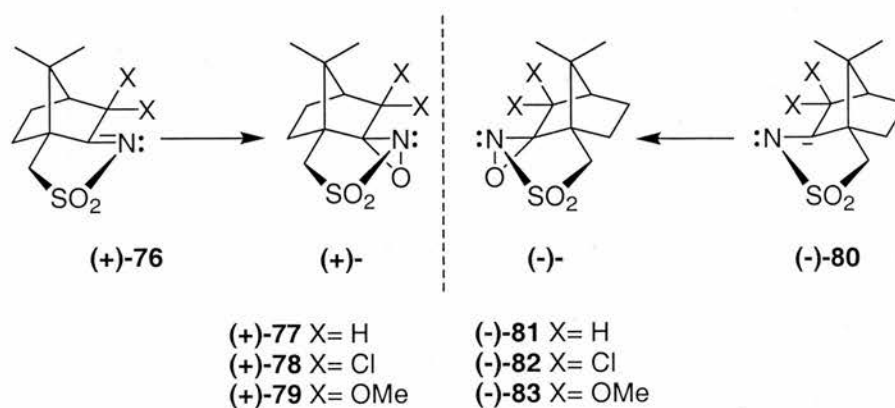


Figure 55. Preparation of (camphorylsulfonyl)oxaziridines.

2.2.2.2. Oxaziridines as oxygen transfer reagents

N-Sulfonyloxaziridines contain a highly electrophilic oxygen atom. The main reaction in which *N*-sulfonyloxaziridines are involved is with nucleophiles as oxidising reagents. The mechanism of the transfer of oxygen from *N*-sulfonyloxaziridine to the nucleophile is *via* an S_N2 process. The oxaziridine oxygen atom is attacked by the carbon atom of the enolate **84** with simultaneous N-O bond cleavage to give the hemiaminal intermediate **85** which fragments to the sulfonimine **86** (by-product) and alkoxide **87** (Figure 56).

In some cases when *N*-sulfonyloxaziridines (**88**) react with lithium enolates (Figure 56), in addition to the α -hydroxy carbonyl compound, the imino-aldol product **89** is also obtained as a side product, resulting from the addition of the enolate **84** to the carbon atom of the sulfonimine **86**. However, the formation of the imino-aldol product **89** could be avoided by using sodium or potassium enolates or (camphorylsulfonyl)-oxaziridines.²³

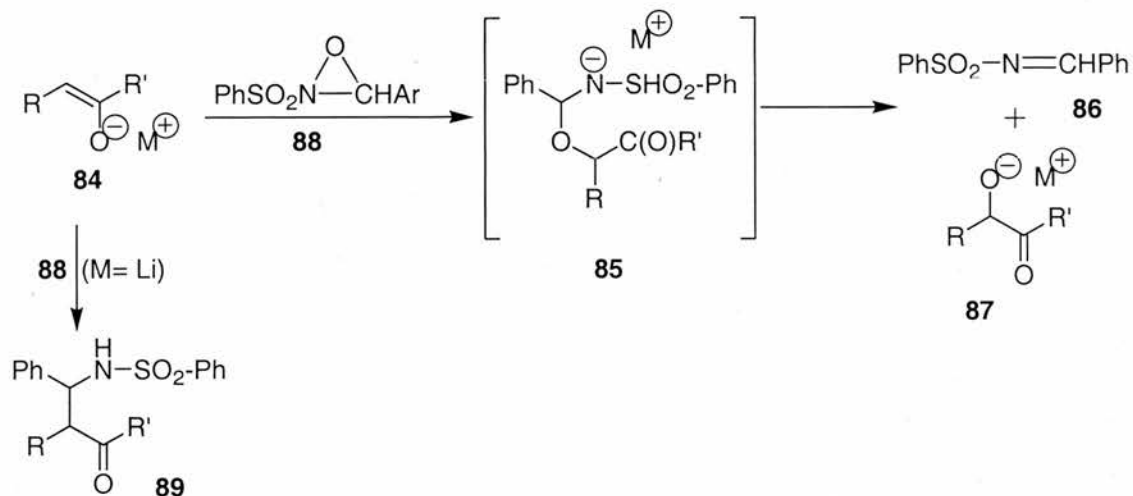


Figure 56. General mechanism for enolate oxidation with *N*-Sulfonyloxaziridine **88**.²³

The *N*-sulfonyloxaziridines are highly chemoselective oxidising reagents in reactions such as the oxidation of organosulfur compounds, organoselenium compounds, organonitrogen compounds, carbon-carbon double bonds and organometallic reagents.²¹ The enantiomerically pure samples of *N*-sulfonyloxaziridines are used, mainly as asymmetric oxidising reagents for the asymmetric oxidation of sulfides (66 to $\geq 95\%$ of enantiomeric excess), for the epoxidation of alkenes (up to 65% of enantiomeric excess), and for asymmetric oxidation of enolates to optically active α -hydroxy carbonyl compounds (55-95% of enantiomeric excess). These reagents afford high stereoselectivities in asymmetric oxidations and the configuration of the oxaziridine three-membered ring controls the product stereochemistry.³⁷

2.2.2.3. Examples of the use of oxaziridines

One example of the use of enantiomerically pure *N*-sulfonyloxaziridines is in the asymmetric oxidation to afford α -hydroxy β -dicarbonyl compounds (Figure 57). This moiety is a common feature of many biological molecules such as antibiotics and it is also an intermediate for the asymmetric synthesis of natural products. Therefore (+)-[(8,8-dimethoxycamphoryl)sulfonyl]oxaziridine (**79**) was used to prepare α -hydroxy β -ketoester **90** a precursor of the AB ring segment of the antitumor anthracycline antibiotic Daunomycin, in 70% yield and $>95\%$ of enantiomeric excess.^{38, 39, & 40}

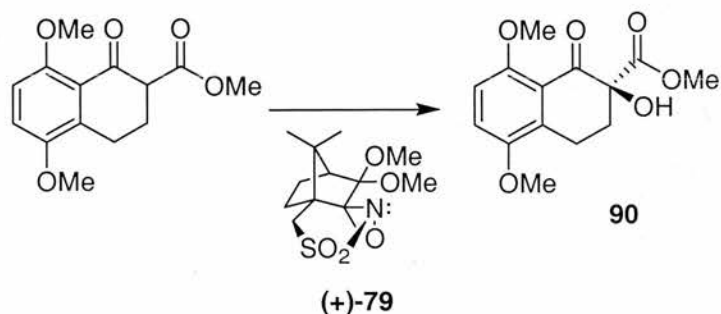


Figure 57. Literature example for the synthesis of α -hydroxy β -dicarbonyl compound **90** with Davis reagent **79**.³⁸

Another example that has been reported is the asymmetric oxidation of the azaenolate anion of deoxyvasicinone **91** (Figure 58). Vasicinone (*S*)-**92** is one of the pyrrolo[2,1-*b*]-quinazoline alkaloid family which includes medicines for bronchitis and asthma. One route employed for the synthesis of Vasicinone (**92**) is by the asymmetric hydroxylation of deoxyvasicinone (**91**) with oxaziridines (1*S*)-(+)-**77** or (1*R*)-(–)-**81**. The reaction afforded the two pure enantiomers of Vasicinone (**92**) in a 71% and 62% of enantiomeric excess, respectively. The optical purity was analysed by chiral HPLC.⁴¹ It is surprising that these two values are not equal and opposite to each other.

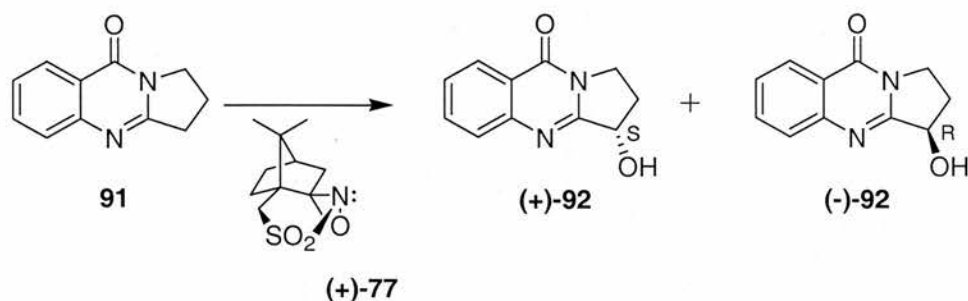


Figure 58. Literature example for the synthesis of Vasicinone (**92**) with Davis reagent **77**.⁴¹

Chiral tetrasubstituted enolates can also be oxidised in the presence of enantiomerically pure *N*-sulfonyloxaziridines. The diastereoselective oxidation of the amide enolate of **94** gave acyclic tertiary α -hydroxy amide **95** in high optical purity (88-91% *de*) (Figure 59).²¹

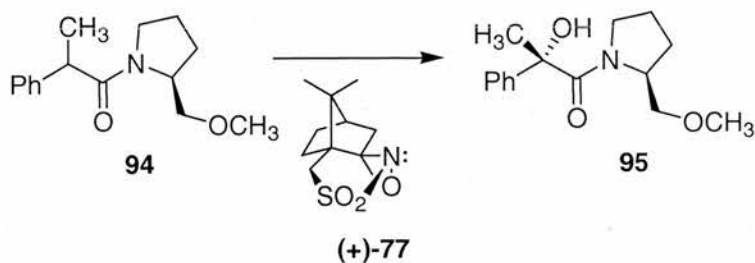


Figure 59. Literature example for the synthesis of tertiary α -hydroxy amide **95** with Davis reagent **77**.²¹

An interesting example which shows the importance of using oxaziridines in asymmetric synthesis arises from the synthesis and application of new chiral non-racemic reagents such as 3-aryl-*N*-alkoxycarbonyloxaziridine (**96**) (Figure 60). This reagent has been reported as a tool for the asymmetric electrophilic amination of enolates.⁴² Therefore in this case, **96** reacts with the enolate of **97** to introduce nitrogen into the product **98** instead of the oxygen. However the aminated products were obtained in low diastereoselectivities of up to 21% *d.e.* (diastereomeric excess).

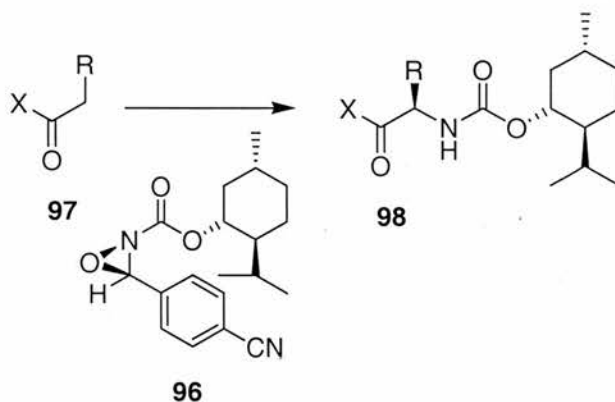


Figure 60. Literature example of the asymmetric amination of the enolate of **97** with the chiral reagent **96**.⁴²

Our attention was focused on the asymmetric hydroxylation of enolates to enantiomerically enriched α -hydroxy carbonyl compounds using enantiopure *N*-sulfonyloxaziridines. This reaction was applied to study the asymmetric synthesis of the target molecule (–)-blebbistatin (**7**).

2.2.3. Synthesis of (-)-Blebbistatin (**7**) using Davis methodology

It was envisaged that optically enriched (-)-blebbistatin (**7**) or (+)-blebbistatin (**23**) could be prepared from quinolone **24** using the Davis methodology.^{19, 21} This late stage oxidation was attractive as both enantiomers could be prepared in a single step from a common intermediate.

Our first step in establishing a standard asymmetric hydroxylation protocol was to focus on determining the temperature at which the Davis reagent reacted with the ketone enolate. Frequently, lower temperatures allow for higher levels of stereoselectivity.⁴³

The first attempt to prepare the 5-hydro analogue of (-)-blebbistatin (**67**) was carried out using a one pot reaction with the base-induced cyclisation of the amidine **32** to form the corresponding enolate followed by asymmetric hydroxylation (Figure 61). Lithium bis(trimethylsilyl)amide was added to a solution of amidine **32** in THF at -78 °C and the reaction was warmed to 0 °C and stirred until no starting material was detected by TLC analysis. A solution of Davis reagent **81** in THF was then added to the enolate at -78 °C. The reaction was followed by TLC analysis to find the optimum of temperature at which the Davis reagent reacted with the enolate. It was found that when the reaction was warmed to -10 °C a very bright yellow spot was detected by TLC analysis. It was decided to warm the reaction to room temperature to afford complete conversion to the oxidised product **67**. The reaction was quenched at room temperature with saturated aqueous NH₄Cl. The crude residue was purified by flash column chromatography (20% ethyl acetate/hexane) to give the desired oxidised product **67** in low yield 18%, as a very bright yellow solid. The same procedure was used for the oxidation of **29** affording the product **7** in 25% yield.

¹H NMR analysis confirmed the presence of **67** and (-)-blebbistatin **7** respectively in these two reactions. The optical rotation for compound **67** afforded a negative value ($[\alpha]_D^{25} = -107$, concentration of 0.1 g/100mL in dichloromethane) which was consistent with the sign found for the biologically active enantiomer of blebbistatin (Chapter 1, Section 1.4.3.1).

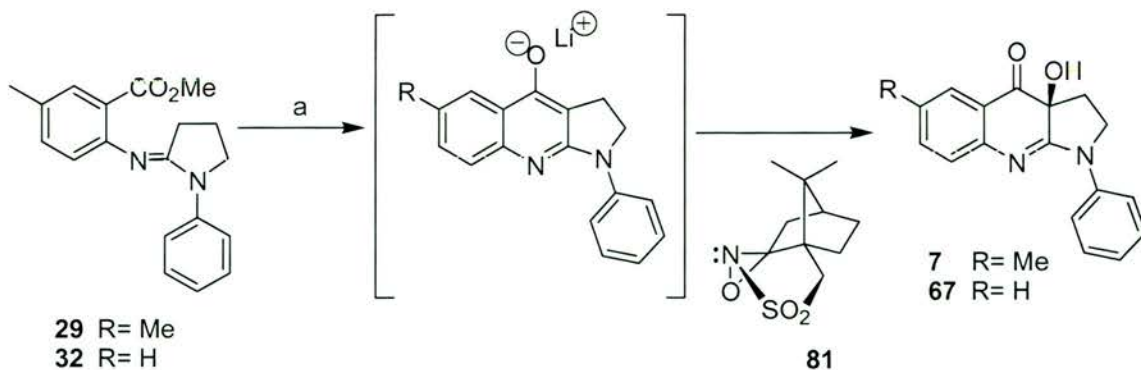


Figure 61. Preparation of (-)-blebbistatin **7** and **67** in a one pot reaction. Reagents and conditions: a) i) LiHMDS (1.1-3.0 equiv), THF, -78 °C to 0 °C, ii) **72** (2.0 equiv), THF, -78 °C to RT, 25% (**7**), 18% (**67**), respectively.

Furthermore **67** was recrystallised from ethyl acetate/hexane to afford crystals suitable for X-ray analysis. Surprisingly two different types of crystals were obtained from the recrystallisation of **67**, one set appeared yellow and the other set green (Figures 62 and 63). Both of these X-ray analyses confirmed the structure of **67** but they differ in the intermolecular hydrogen bonding network. In addition in both sets of crystals only one enantiomer was present although it was not possible to assign the absolute stereochemistry due to the lack of a heavy atom. In contrast the reaction for **7** did not yield enough material either for recrystallisation or for measuring the optical rotation.

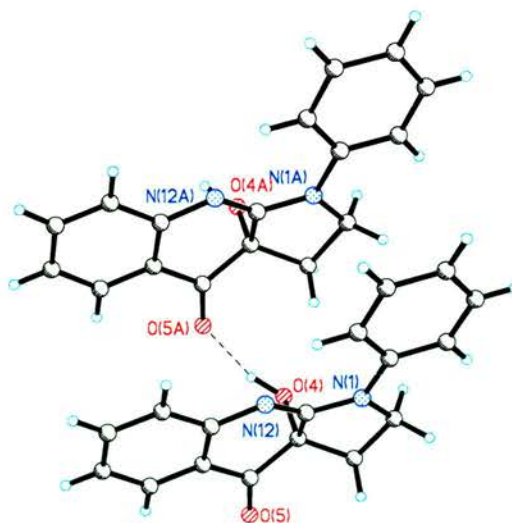


Figure 62. X-Ray structure of **67** (yellow crystals). The figure shows the intermolecular hydrogen bonding network between hydrogen (from the 4-oxygen) and 5A-oxygen.

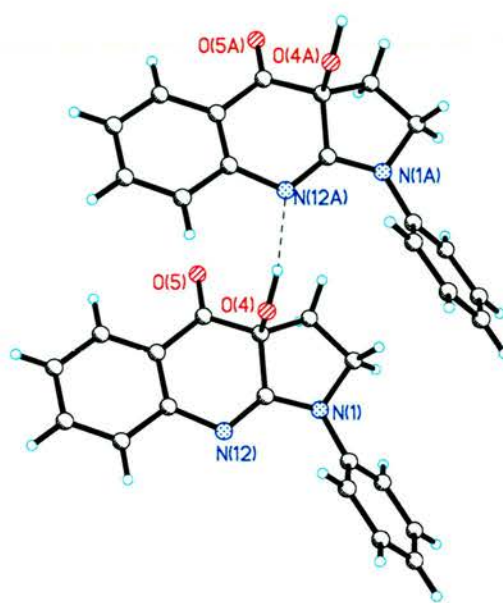


Figure 63. X-Ray structure of **67** (green crystals). The figure shows the intermolecular hydrogen bonding network between hydrogen (from the 4-oxygen) and 12A-nitrogen.

Despite the fact that the first attempt led to the synthesis of **67** and **7** and confirmed the structure of **67**, there was a need to optimise the yield of the reaction and also to prepare sufficient amounts of **7** for a complete assignment. In addition, the use of the one pot procedure, which required excess reagents, could lead to a situation in which unwanted counter ions negatively influence the enantiomeric excess of the reaction. In order to avoid this, it was decided to hydroxylate quinolone **24** directly. Quinolone **24** was deprotonated at $-78\text{ }^{\circ}\text{C}$ with one equivalent of LiHMDS. The reaction was then warmed from $-78\text{ }^{\circ}\text{C}$ to $-10\text{ }^{\circ}\text{C}$, until no starting material was detected by TLC analysis. A solution of **81** (2.0 equivalent) was added at $-78\text{ }^{\circ}\text{C}$ and the reaction mixture was warmed slowly. Although TLC analysis showed the presence of a new bright yellow spot corresponding to the desired product at $-10\text{ }^{\circ}\text{C}$, the reaction was warmed to room temperature and quenched with saturated aqueous NH_4Cl . The crude residue was purified by flash column chromatography (20% ethyl acetate/hexane) to afford (–)-blebbistatin (**7**) in an improved yield (48%). The optical rotation for **7** gave a negative value of $[\alpha]_{\text{D}}^{25} = -56$ (concentration of 0.1 g/100mL in dichloromethane). The structure of the compound was confirmed by ^1H NMR.

In summary, a synthetic route to access enantioselectively the bioactive enantiomer, (-)-blebbistatin (**7**), was established *via* quinolone **24**. However with the new procedure the yield of the reaction was still moderate. Optimisation of the reaction conditions to improve the yield and also establishment of an optimal methodology to determine the enantiomeric excess of the reaction were the next goals of the project (see Chapter 3).

2.3. REFERENCES

- 1 Straight, A. F., Cheung, A., Limouze, J., Chen, I., Westwood, N. J., Sellers, J. R., Mitchison, T. J., *Science*, **2003**, 299, 1743-1747.
- 2 Cai, S. X., Zhou, Z., Huang, J., Whittemore, E. R., Egbuwoku, Z., Lu, Y., Hawkinson, J. E., Woodward, R. M., Weber, E., Keana, J. F. W., *J. Med. Chem.*, **1996**, 39, 3248-3255.
- 3 Kuehne, M. E. and Shannon, P. J., *J. Org. Chem.*, **1977**, 42, 2082-2087.
- 4 Smith, D. C., Lee, S. W., Fuchs, P. L., *J. Org. Chem.*, **1994**, 59, 348-354.
- 5 Marson, C. M., *Tetrahedron*, **1992**, 48, 3659-3726.
- 6 Martin, G. and Martin, M., *Bull. Soc. Chim. Fr.*, **1963**, 1637-1646.
- 7 Filleux-Blanchard, M. L., Quemeneur, M. T., Martin, G. J., *J. Chem. Soc., Chem. Commun.*, **1968**, 836-837.
- 8 Martin, G. J. and Poignant, S., *J. Chem. Soc., Perkin Trans. 2*, **1972**, 1964-1966.
- 9 Rahman, A., Basha, A., Waheed, N., *Tetrahedron Lett.*, **1976**, 3, 219-222.
- 10 Knapp, S., Choe, Y. H., Reilly, E., *Tetrahedron Lett.*, **1993**, 34, 4443-4446.
- 11 Kuroki, Y., Fujiwara, H., Nishino, S., Nakamura, I., Tokunaga, H., EU patent #EP0430485A2 (1990).
- 12 Smith, L. and Kiselyov, A. S., *Tetrahedron Lett.*, **1999**, 40, 5643-5646.
- 13 Acheson, R. M., Ferris, M. J., Sinclair, N. M., *J. Chem. Soc., Perkin Trans. 1*, **1980**, 579-585.

- 14 Gaur, S., Ranga, S. P., Sharma, S., Mehta, R. K., *Indian J. Chem.*, **1988**, 27A, 806-808.
- 15 Buchel, K. H., Bocz, A. K., Korte, F., *Chem. Ber.*, **1966**, 99, 724-735.
- 16 Eilingsfeld, H., Seefelder, M., Weidinger, H., *Angew. Chem*, **1960**, 72, 836-845.
- 17 Streckowski, L., Wydra, R. L., Cegla, M. T., Czarny, A., Harden, D. B., Patterson, S. E., Battiste, M. A., Coxon, J. M., *J. Org. Chem.* **1990**, 55, 4777-4779.
- 18 De la Cruz, A., Elguero, J., Goya, P., Martinez, A., Pflleiderer, W., *Tetrahedron*, **1992**, 48, 6135-6150.
- 19 Davis, F. A., Sheppard, A. C., Chen, B-C., Haque, M. S., *J. Am. Chem. Soc.* **1990**, 112, 6679-6690
- 20 Davis, F. A. and Sheppard, A. C., *Tetrahedron Lett.*, **1988**, 29, 4365-4368.
- 21 Davis, F. A. and Sheppard, A. C., *Tetrahedron*, **1989**, 45, 5703-5742.
- 22 Enders, D. and Brushan, V., *Tetrahedron Lett.*, **1988**, 29, 2437-2440.
- 23 Davis, F. A. and Chen, B-C., *Chem. Rev.*, **1992**, 92, 919-934.
- 24 Davis, F. A., Vishwakarma, L. C., Billmers, J. M., *J. Org. Chem.*, **1984**, 49, 3243-3244.
- 25 Bailey, E. J., Barton, D. H. R., Elks, J., Templeton, J. F., *J. Chem. Soc.*, **1962**, II, 1578-1591.
- 26 Rubottom, G. M., Vazquez, M. A., Pelegrina, D. R., *Tetrahedron Lett.*, **1974**, 49-50, 4319-4322.

- 27 Gardner, J. N., Carlon, F. E., Gnoj, O., *J. Org. Chem.*, **1968**, *33*, 3294-3297.
- 28 Vedejs, E., *J. Am. Chem. Soc.*, **1974**, *96*, 5944-5946.
- 29 Vedejs, E., Engler, D. A., Telschow, J. E., *J. Org. Chem.*, **1978**, *43*, 188-196.
- 30 Masui, M., Ando, A., Shioiri, T., *Tetrahedron Lett.*, **1988**, *29*, 2835-2838.
- 31 Toullec, P. Y., Bonaccorsi, C., Mezzetti, A., Togni, A., *PNAS*, **2004**, *101*, 5810-5814.
- 32 Boyd, D. R. and Graham, R., *J. Chem. Soc., Chem. Commun.*, **1969**, 2648-2650.
- 33 Davis, F. A. and Stringer, O. D., *J. Org. Chem.*, **1982**, *47*, 1774-1775.
- 34 Davis, F. A., Jenkins, R. H., Awad, S. B., Stringer, O. D., Watson, W. H., Galloy, J., *J. Am. Chem. Soc.*, **1982**, *104*, 5412-5218.
- 35 Davis, F. A., McCauley, J. P., Chattopadhyay, S., Harakal, M. E., Towson, J. C., Watson, W. H., Tavanaiepour, I., *J. Am. Chem. Soc.* **1987**, *109*, 3370-3377.
- 36 Mergelsberg, I., Gala, D., Scherer, D., DiBenedetto, D., Tanner, M., *Tetrahedron Lett.*, **1992**, *33*, 161-164.
- 37 Davis, F. A., Towson J. C., Vashi, D. B., Reddy, R. T., McCauley, J. P., Harakal, M. E., Gosciniak, D. J., *J. Org. Chem.*, **1990**, *55*, 1254-1261.
- 38 Davis, F. A., Liu, H., Chen, B-C., Zhou, P., *Tetrahedron*, **1998**, *54*, 10481-10492.
- 39 Davis, F. A., Kumar, A., Chen, B-C., *Tetrahedron Lett.*, **1991**, *32*, 867-870.

- 40 Davis, F. A., Clark, C., Kumar, A., Chen, B-C., *J. Org. Chem.*, **1994**, *59*, 1184-1190.
- 41 Eguchi, S., Suzuki, T., Okawa, T., Matsushita, Y., *J. Org. Chem.*, **1996**, *61*, 7316-7319.
- 42 Armstrong, A., Atkin, M. A., Swallow, S., *Tetrahedron: Asymmetry*, **2001**, *12*, 535-538.
- 43 Davis, F. A., Weismiller, M, C., Murphy, C, K., Reddy, R. T., Chen, B-C., *J. Org. Chem.*, **1992**, *57*, 7274-7285.

CHAPTER 3

RESULTS AND DISCUSSION

ABSOLUTE STEREOCHEMICAL ASSIGNMENT OF (-)-BLEBBISTATIN (7)

3.1. GENERAL METHODS FOR THE DETERMINATION OF ENANTIOMERIC EXCESS

The previous chapter described preliminary results on the enantioselective preparation of (-)-blebbistatin (7) using Davis chiral oxaziridines (Chapter 2, Section 2.2.3). Although it was known that 7 prepared by this route was neither racemic ($[\alpha]_D^{25} \neq 0$) nor enantiomerically pure but enantiomerically enriched, it was necessary to develop a method to determine accurately the ratio of the two enantiomers (enantiomeric excess (*ee*)). The enantiomeric excess (*ee*) can be defined as the excess of one isomer over the other. It can be calculated with the following formula: $ee = 100 \times (X_R - X_S) / (X_R + X_S)$, where $X_R > X_S$ and X_R and X_S representing the molarity of each enantiomer.

Well established methods have been developed for determining enantiomeric excess (*ee*) in asymmetric synthesis.¹ The classical methods include the use of NMR spectroscopy² which usually requires the intervention of a chiral reagent to convert a mixture of enantiomers into the corresponding mixture of diastereomers. The three types of chiral reagents are: a) enantiomerically pure derivatising reagents^{3,4} in achiral solvents, b) chiral lanthanide shift reagents,^{5,6} c) chiral solvating agents.^{7,8} Other techniques, which involve diastereomeric interactions for the separation of the two enantiomers, include the use of chiral stationary phases in gas and liquid chromatography (GC and HPLC).⁹ Methods such as optical rotation, optical rotatory dispersion (ORD) and circular dichroism (CD) can also be used to determine the enantiomeric excess due to the ability of the chiral molecules to rotate the plane of plane-polarised light, although the enantiomers cannot be separated with these techniques.

Chiral derivatisation and NMR analysis remains the most widely used technique for determination of enantiomeric excess. The studied chiral molecule (*e.g.* alcohols

and amines) is derivatised with optically active acids to afford the corresponding diastereoisomeric esters and amides, respectively. The first chiral derivatising reagent [(R)-(-)-*O*-methylmandeloyl chloride (**99**)] (Figure 64) was introduced by Raban and Mislow¹⁰ and extensively used by others.^{11, 12} The diastereomers can be identified by NMR due to differences in chemical shift values (*e.g.* difference in the chemical shift of the CH_3O groups) in the ^1H NMR spectrum. Therefore, the ratio of both diastereomers can be measured by the integration of the areas under their corresponding peaks. However, the use of this reagent was limited by the observed epimerisation at the hydrogen α to the acid chloride carbonyl, presumably *via* the corresponding ketene.¹³

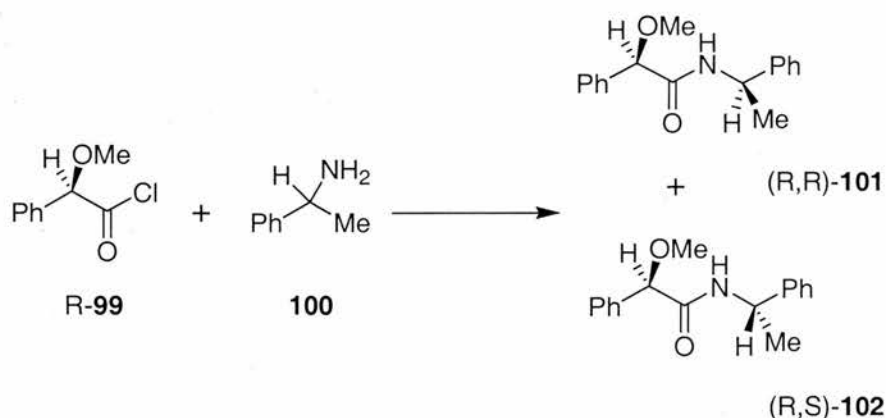


Figure 64. Literature example of the derivatisation of an amine with the chiral derivatising reagent, (*R*)-(-)-*O*-methylmandeloyl chloride (**99**).^{11, 12}

In order to avoid the problem of racemisation, Mosher *et al.*,^{3, 4} developed the well known chiral derivatising reagent, Mosher's acid (α -methoxy- α -trifluoromethyl-phenyl-acetic acid) (MTPA). This reagent is stable to racemisation because it contains a CF_3 group instead of the α -hydrogen atom (Figure 65). The enantiomers of the molecule under analysis are converted into diastereomers as before. The advantage of these reagents is the presence of CF_3 which enables the determination of the enantiomeric excess by ^{19}F NMR analysis. This approach leads to fewer signals (normally only two peaks) than ^1H NMR analysis, avoiding the problem of overlapping signals.

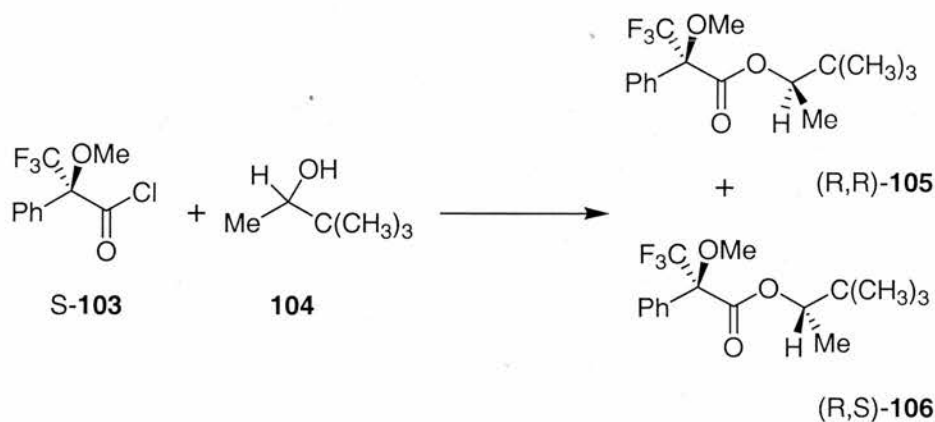


Figure 65. Derivatization of the secondary alcohol (3,3-dimethylbutan-2-ol) with Mosher's acid chloride **103** [(*S*)-(+)-MTPA-Cl].¹⁴

Chiral lanthanide shift reagents^{5,15} form diastereomeric association complexes with the enantiomers in solution resulting in an induced shift in certain resonances in the NMR spectrum. The most common reagents are the perfluoroalkyl camphorato chelates tris-(3-trifluoromethyl-hydroxymethylene-(1*R*)-camphorato)europium (III) [Eu(thd₃)] (**107**) and tris-(3-heptafluorobutyryl-hydroxymethylene-(1*R*)-camphorato)-europium (III) [Eu(hfc)₃] (**108**) (Figure 66) and they have been used with chiral alcohols, aldehydes, ketones, esters, oxiranes and sulphonamides.⁵ The measurement of the enantiomeric excess is by integration of the peaks corresponding to the diastereomeric complexes.

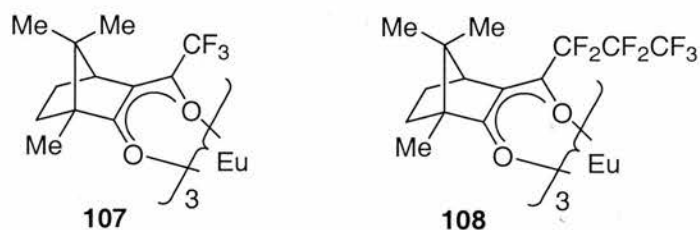


Figure 66. Chiral lanthanide shift reagents [Eu(thd₃)] (**107**) and [Eu(hfc)₃] (**108**).^{5,15}

The use of chiral solvating agents in NMR to determine the enantiomeric excess has been studied on lactones.⁷ This method is based on the stereochemical interaction between the homochiral solvating agent and the chiral compound (Figure 67), and therefore the formation of diastereomeric solvation complexes with the enantiomers. The enantiomeric excess can be determined on the basis of such interactions.

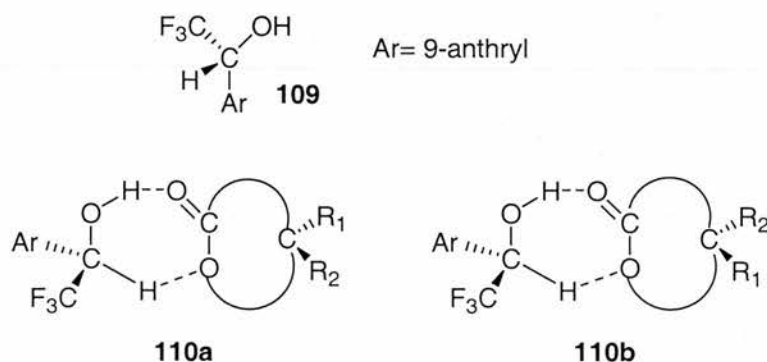


Figure 67. Example of the interaction between the chiral solvating agent (2,2,2-trifluoro-1-(9-anthryl)ethanol) (**109**) and γ -lactone enantiomers **110a** and **110b**.⁷

Polarimeter based methods have also been used to determine optical purity. ORD and CD are more powerful techniques than optical rotation. These techniques are based on the variation of the optical rotation (α) with the wavelength of the light. CD is a complementary technique in which the differential absorption of polarised light by the chromophore is studied.⁵ However, polarimeter measurements are often unreliable because they depend on a number of factors such as temperature, solvent, and concentration (massive errors can be introduced due to the presence of small amount of chiral impurities).⁵

The separation of enantiomers can be carried out by chromatographic methods such as chiral HPLC and GC. Both methods use a chiral stationary phase which contains an auxiliary resolving agent of high enantiomeric purity.⁵ The comparison of relative peak areas provides the measurement of the enantiomeric excess. Chiral gas chromatography (GC) on capillary columns is an important tool for determining the optical purity of chiral compounds and its advantages are high resolution, precision and reproducibility.¹⁶ It is based on the separation of volatile substances, therefore only volatile compounds are suitable for this technique. The main chiral compounds analysed by this technique contain hydroxyl (alcohols and phenols) and carbonyl (aldehydes and ketones) groups. Separation by GC is carried out at high temperatures therefore the studied compound also needs to be thermally stable.¹⁷

A number of techniques have been described to determine the enantiomeric excess (*ee*) of chiral compounds. However, there is no general rule as to which specific methodology is most appropriate for a particular chiral compound therefore two independent methods should be carried out if possible to verify the observed enantiomeric excess.⁵

3.1.1. Determination of the enantiomeric excess for (-)-Blebbistatin (7) by chiral liquid chromatography (HPLC)

This section describes our main method for determining the enantiomeric excess (*ee*) of the Davis hydroxylations using chiral high performance liquid chromatography (HPLC). This approach was chosen to determine the enantiomeric excess of samples of (-)-blebbistatin (7) due to its reliability in our system compared with the other techniques described in Section 3.1. HPLC differs from GC in several ways, probably the most important of which is that liquid chromatography is carried out at room temperature. The possibility of racemisation or sample degradation during the separation is therefore negligible.^{17, 18}

The determination of enantiomeric excess by HPLC is divided into two categories:¹⁷ a) direct measurement using a chiral stationary phase (CPS), b) indirect measurement, which involves derivatisation of the chiral compound with a suitable chiral derivatising reagent. In the second of these, separation of the resulting diastereomers occurs on an achiral column. The most common method used is the direct separation, which is based on the diastereomeric interactions between the chiral stationary phase and each enantiomer. The diastereomeric complexes formed have different stabilities which lead to elution at different times (the enantiomer that forms the complex of higher stability will be eluted second). This methodology is more efficient and less problematic than the indirect method.⁵

The separation of the two enantiomers of (-)-blebbistatin (7) was performed using the direct separation method (monitored by diode array and mass spectrometry). The column was a commercially available analytical reverse phase column packed with amylose tris(3,5-dimethylphenylcarbamate) (**111**), coated on a 10 μm silica gel substrate (Figure 68). The optimal conditions for the resolution of 7 were found to be in

isocratic mode (solvent conditions held constant). The mobile phase was a mixture of two eluents (acetonitrile and water) without the presence of acid (for more details see Experimental Section).

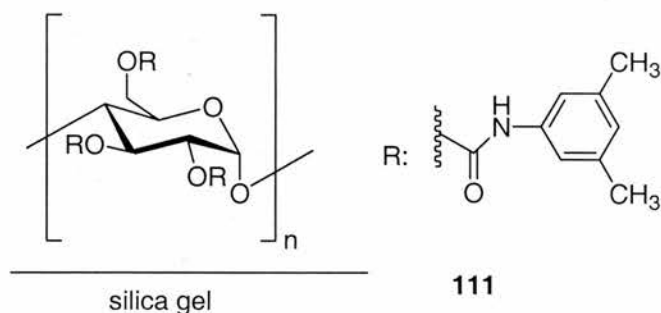


Figure 68. Composition of the chiral reverse phase column for the resolution of **7**.

A standard provided by the HPLC company (2-methyl-1-tetralone) was first measured to ensure that the column was working properly and subsequently, a sample of racemic blebbistatin **18** was analysed to confirm the retention time of the two blebbistatin enantiomers (Figure 69). Chiral liquid chromatography (HPLC) showed the presence of two peaks of equal integration (50:50), indicating a racemic mixture of the two enantiomers of **18** ($ee=0\%$).

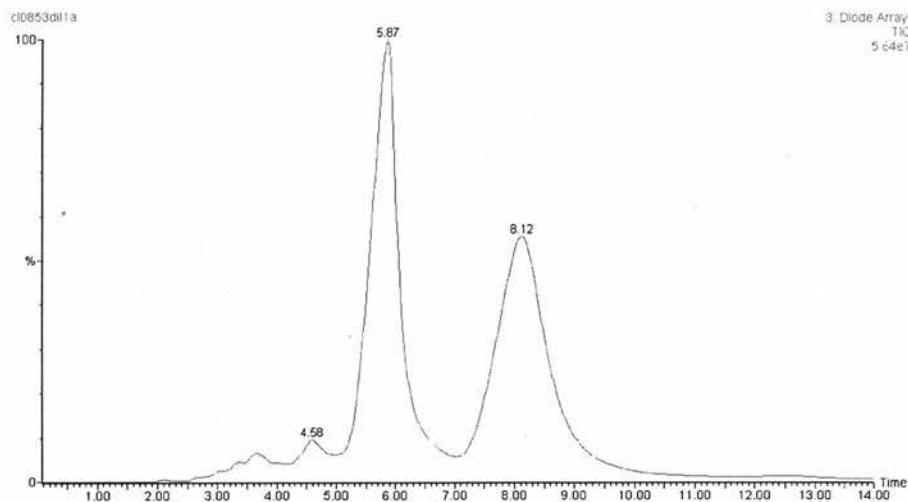


Figure 69. Determination of the enantiomeric excess of racemic (\pm)-blebbistatin (**18**) by chiral HPLC analysis. Conditions: Daicel Chiralpak AD-RH, Acetonitrile/Water 50:50, flow rate 0.8 mL min^{-1} , $\lambda=254 \text{ nm}$. Chromatogram of the purified product (**11**): first enantiomer $t_R=5.87 \text{ min.}$, $\lambda_{\text{max}}=249 \text{ nm}$ and second enantiomer $t_R=8.12 \text{ min.}$, $\lambda_{\text{max}}=249 \text{ nm}$.

3.1.2. Optimisation of the asymmetric hydroxylation reaction

The selective formation of stereogenic centres presents a significant challenge to the organic chemist. However, precedent exists for the use of (camphorylsulfonyl)-oxaziridines such as **77** and **78** (Figure 71) to perform asymmetric hydroxylations of ketone enolates in high yield and with excellent enantiomeric excesses (*ee*).¹⁹ It was envisaged that optically enriched (–)-blebbistatin (**7**) could be prepared from quinolone **24** using the methodology described in Chapter 2, Section 2.2.3. In order to optimise the stereoselectivity for the asymmetric hydroxylation of (–)-blebbistatin (**7**), it was decided to carry out a number of experiments to find the best reaction conditions.

A number of factors are involved in determining the stereoselectivity of asymmetric hydroxylation reactions using chiral *N*-sulfonyloxaziridines. Initial studies to find new oxidising reagents in asymmetric synthesis, showed the influence of the oxaziridine structure on the stereoselectivity of the asymmetric oxidation of sulfides to sulfoxides.²⁰ For instance, asymmetric oxidation of sulfides to sulfoxides resulted in higher enantioselectivities using *N*-sulfamyloxaziridines **74** (53-91% *ee*, determined by a chiral HPLC column) compared with (camphorylsulfonyl)oxaziridines **77** and *N*-sulfonyloxaziridines **71** (Figure 70 and 71).^{20, 21}

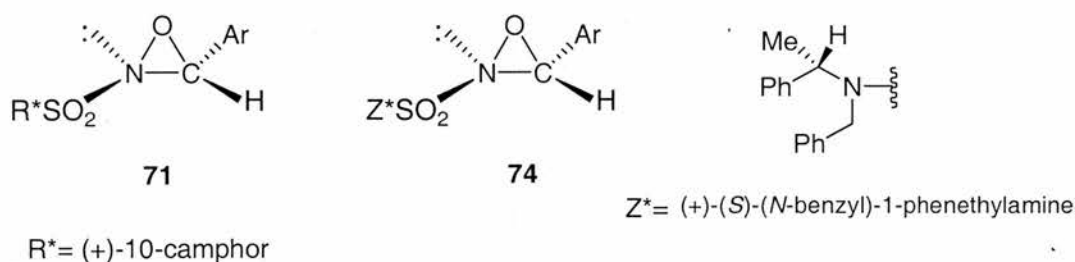


Figure 70. Structures of *N*-sulfonyloxaziridine **71** and *N*-sulfamyloxaziridine **74**.

In contrast, for the asymmetric oxidation of metal enolates to optically active α -hydroxy carbonyl compounds, (camphorylsulfonyl)oxaziridines of type **77** are the most frequently used reagents because they are more stable and easier to prepare than **71** and **74**. Additionally (camphorylsulfonyl)oxaziridines of type **77** gave high enantioselectivities (60-95% *ee*, determined by using the chiral shift reagent $Eu(hfc)_3$ and chiral HPLC column) for the asymmetric oxidation of enolates.^{19, 22, 23, 24}

Davis *et al.*,^{19,25,26} reported an improvement of the stereoselection for the oxidation of tetrasubstituted cyclic ketone enolates (tetralone enolates) (Figure 91, Section 3.3) with a new reagent, (+) ((8,8-dichlorocamphoryl)sulfonyl)oxaziridine (**78**) (Figure 71). This reagent showed higher enantioselectivities of 90-95% *ee* (determined by chiral HPLC column and chiral shift reagent $\text{Eu}(\text{hfc})_3$), compared with (camphorylsulfonyl)oxaziridines of type **77** (Figure 71) (16-30% *ee*, determined by chiral HPLC column and chiral shift reagent $\text{Eu}(\text{hfc})_3$). They considered that this resulted from either stereoelectronic and/or metal chelation effects due to the presence of the electronegative chlorine atoms in **78**. In another attempt to improve stereoselectivities in the asymmetric oxidation of enolates, it was reported that (+)-[(8,8-dimethoxycamphoryl)sulfonyl]oxaziridine (**79**) (Figure 71) also led to an increase in stereoselectivity (better than 94%*ee*), compared to (+)-((8,8-dichlorocamphoryl)sulfonyl)oxaziridine (**78**), because of the presence of the chelating methoxy groups.²⁷ Although it was found that oxidation of 8-methoxy-tetralone gave higher enantioselectivities with this new reagent **79** than **78** and **112**, it was necessary to have the 8-methoxy group in the substrate for this result. This conclusion arose from the observation that oxidation of 2-substituted 1-tetralone enolates (Figure 91, Section 3.3) lacking the 8-methoxy group, when they are treated with dimethoxy oxaziridines of type **79**, gave lower stereoselectivities (2-36%) than those obtained with the dihalo oxaziridine of type **78**. However, this result could not be explained due to the inability to relate the enolate solution structure with reactivity.²⁷

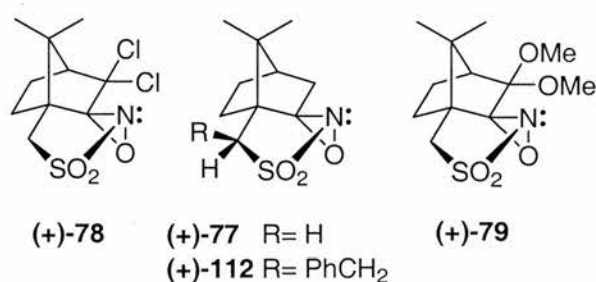


Figure 71. Structure of (+)-(camphorylsulfonyl)oxaziridines.

Furthermore it was found that the enolate substitution pattern has a strong influence on the asymmetric induction. For instances, for the oxidation with (camphorylsulfonyl)oxaziridines of type **77** and **78** (Figure 71), acyclic ketone enolates generally gave higher enantioselectivities than cyclic ketone enolates.^{22,28}

Another factor which affects the degree of asymmetric induction is the enolate counterion. The oxidation of lithium enolates of esters and amides with optically active dihydro oxaziridines of type **77** and **81** (Figures 71 and 74) gave better enantiomeric excesses (up to 85% *ee*) than the sodium and potassium enolates.²⁸ In contrast, the sodium enolates of ketones gave the highest stereoselectivities with the dihydro oxaziridines of type **77** and **81**, respectively.^{22, 28} Furthermore sodium enolates from **113** are more reactive than lithium or zinc enolates at low temperatures (from -78 °C to -40 °C) whereas the tetrasubstituted sodium enolates from **116** were not completely oxidised at -78 °C (Figure 72). The reactions required warming to 0 °C affording good yields although the stereoselectivities were low. In these cases dihydro oxaziridines of type **77** and **81** were used.²⁴

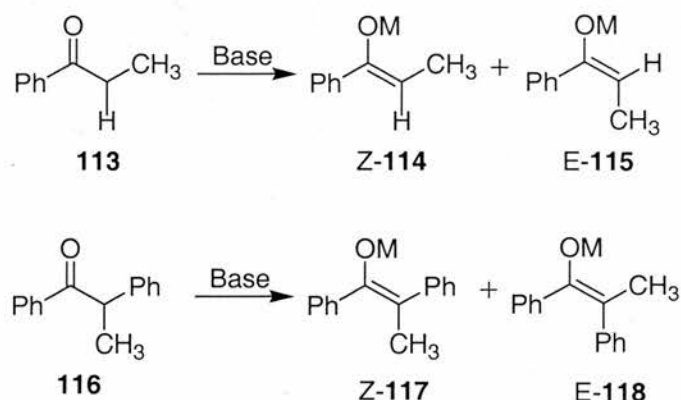


Figure 72. Example of enolates type **113** and tetrasubstituted **116** enolates.²⁴

It was also envisaged that the solvent could affect significantly the stereoinduction. Optimisation of the reaction conditions for the oxidation of ketone enolates has been reported to result in only modest improvement in the stereoinduction when the solvent was changed from THF to toluene.²⁵

Finally, temperature plays an important role in the asymmetric induction. When the temperature of oxidation is lowered from 25 to -78 °C, the degree of asymmetric induction for conversion of sulfides to sulfoxides, increases using 2-sulfamyloxaziridines of type **74**. This effect is related to the increase in the rigidity of the substrate and oxaziridine in the transition state.²⁰ Higher reactivity was exhibited with the dihalo oxaziridines of type **78** allowing enolate hydroxylations to proceed at -78 °C instead of 0 °C for acyclic trisubstituted enolates. However, in the case of

2-methyl-1-tetralone enolates, it was necessary to warm the reaction with dihalo oxaziridines of type **78**, to 0 °C.²⁶

Summarising the results reported in the literature (see above), it was found that the stereoselectivities are mainly influenced by the choice of oxaziridine, the enolate substitution pattern, the enolate solution structure (counterion) and the reaction temperature.

In our case, it was decided to carry out a number of reactions to prepare (–)-blebbistatin (**7**) in an attempt to identify the optimal conditions. The reactions were carried out in THF as the main solvent but some conditions were changed following the literature examples described above, including temperature, oxaziridine and base. The enantiomeric excess of the reaction was determined by chiral HPLC. Optical rotation measurements were also used in each case and the values for the enantiomeric excess were calculated using these values.

The results for the asymmetric hydroxylation of quinolone **24** are summarised in Table 4. The kinetic enolate anions were formed by the slow addition of the quinolone **24** to a solution of 1.2 equivalents of the base at -78 °C. A solution of 2.4 equivalents of the Davis oxaziridines of type **81** and **82** (Figure 74) was then added to the preformed enolate after 30 minutes stirring at -78 °C. The progress of the reaction was monitored by TLC. When the reactions were complete (0.5-16 hours), they were quenched at different temperatures by addition of aqueous NH₄I, to reduce the excess oxaziridine to the (camphorylsulfonyl)imine **80** (Figure 73). This procedure was used to facilitate, if necessary, chromatographic isolation of (–)-blebbistatin (**7**) which was found to have a similar R_f to the dihalo oxaziridine **82**.²⁴

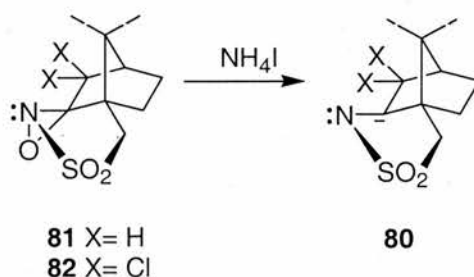


Figure 73. Reduction of (camphorylsulfonyl)oxaziridine **81** and **82** to camphorsulfonylimine **80**.

It is interesting to note that often the purification of the crude residue did not require flash column chromatography. The crude residue was dissolved in dilute acid (pH 2) and extracted three times with dichloromethane. The aqueous extract was then basified (pH 8) and extracted three times with ethyl acetate to give (-)-blebbistatin (**7**) in good yields (65-90%) (Table 4).

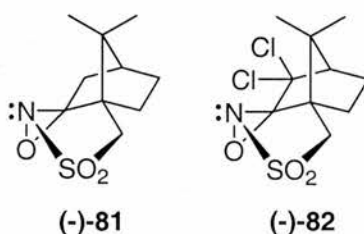


Figure 74. Structure of (-)-(Camphorylsulfonyl)oxaziridines.

Entry	Davis oxaziridine	Base	Temperature (°C)	Time (h)	% yield	% ee (HPLC)	$[\alpha]_D^{25}$	%ee*
1	81	LiHMDS	-78	16	0	n/a	n/a	n/a
2	81	LiHMDS	-40	16	0	n/a	n/a	n/a
3	81	LiHMDS	-10	16	73	42	-183	34
4	81	LiHMDS	RT	1.5	74	44	-181	34
5	81	NaHMDS	-78	16	0	n/a	n/a	n/a
6	81	NaHMDS	-40	16	81	36	-105	20
7	82	LiHMDS	-78	16	0	n/a	n/a	n/a
8	82	LiHMDS	-40	16	74	74	-345	65
9	82	LiHMDS	-10	16	82	86	-461	87
10	82	NaHMDS	-78	16	65	82	-385	73
11	81	LDA	0	16	90	31	-107	20
12	81	LDA	RT	16	83	37	-105	20

Table 4. Optimisation of the asymmetric oxidation using the Davis oxaziridine methodology. Reagents and conditions: a) i) LiHMDS or LDA or NaHMDS (1.2 equiv), THF, 30 min, ii) oxaziridine **81** or **82** (2.4 equiv). The table summarises the yield and enantiomeric excess (*ee*) obtained as a function of base, temperature and reagent. All *ee* values were determined using chiral HPLC analysis of the crude reaction mixture. Optical rotation values were measured in DCM on the purified material. *Calculated *ee* based on optical rotation values.

The results summarised in Table 4 suggested a number of trends that agreed with the results reported by Davis *et al.*²⁶ in the literature for the preparation of α -hydroxy carbonyl compounds.

1. Lithium enolates are less reactive than the sodium enolates (entries 7 and 10). When reactions are carried out at low temperatures in the presence of the lithium base, no reaction was observed (entries 1, 2 and 7). Therefore, the reactions using lithium enolates needed to be warmed for complete consumption of **24** (entries 3, 4, 8, 9, 11 and 12).
2. The dihalo oxaziridine **82** was more reactive than the dihydro reagent **81**. Reaction with **82** gave the desired (-)-blebbistatin (**7**) at low temperature (entries 8 and 10) whereas in the corresponding experiment using **81** (entries 2 and 5) no reaction was observed. The highest stereoselectivities (74-86% *ee*) for the asymmetric oxidation of **24** were observed when the reactions were carried out with either lithium or sodium enolates and dihalo oxaziridine **82** at -10 °C, -40 °C and -78 °C (entries 8, 9 and 10), although the reaction with the lithium enolate at -10 °C gave the best yield.
3. It is interesting to note that whereas in literature²⁶ precedent the hydroxylations with dihalo oxaziridines are carried out at -78 °C, in our case it was observed no formation of product at that temperature using the dihalo oxaziridine **82** (entry 7).
4. In contrast the dihydro oxaziridine **81** was less stereoselective for the asymmetric oxidation of **24** (31-44% *ee*, entries 3, 4, 6, 11 and 12). It is interesting to note that when the oxidation was carried out in the presence of LDA, the lowest temperature for the formation of (-)-blebbistatin (**7**) was found to be at 0 °C.
5. Table 5 summarises the results obtained by Davis *et al.*²⁶ for the hydroxylation of 2-methyl-1-tetralone (**119**) in order to compare them with the data obtained for (-)-blebbistatin (**7**). In this case the enolates were formed at 0 °C during 30 minutes and then the reaction was cooled to -78 °C before adding the

oxaziridine. However, the reactions need to be warmed to 0 °C before quenching, when dihydro oxaziridine **77** was used. In contrast, when the reaction was carried out with dihalo oxaziridine **78**, the necessary temperature was -78 °C. The main difference observed from these results is in the enantiomeric excess. The hydroxylation reactions carried out with dihydro oxaziridine **77** gave lower values of enantiomeric excess than the dihalo oxaziridines **78**. In addition the lowest enantioselectivities were found for the potassium enolates (see entries 3 and 6). Davis rationalised the observed difference in enantiomeric excess as a function of oxaziridine and the differences in the temperature that the two reactions were carried out. It is interesting to note that the stereochemistry obtained for the hydroxylation of **119** with the (+)-enantiomer of the oxaziridines **77** and **78** is *R* (see Section 3.4 for more details).

It is worth pointing out that the difference in enantiomeric excess observed by Davis was also found for the preparation of (-)-blebbistatin (**7**). When the asymmetric hydroxylation was carried out with oxaziridines **81** and **82** at the same temperature, it was observed that the enantiomeric excesses for both reactions were different (Table 4, entries 3 and 9).

Entry	Davis oxaziridine	base	Temperature (°C)	% ee	configuration	% yield
1	77	LDA	0	30	R	82
2	77	NaHMDS	0	16	R	90
3	77	KHMDS	0	6	R	76
4	78	LDA	-78	>95	R	60
5	78	NaHMDS	-78	>95	R	66
6	78	KHMDS	-78	60	R	61

Table 5. Hydroxylation of 2-methyl-1tetralone (**119**) by Davis et al.²⁶

6. Davis *et al.*,¹⁹ found in the asymmetric oxidation of 3-methyl-4-chromanone (**120**) with (+)-(8,8-dichlorocamphorylsulfonyl)oxaziridine (**78**) that the

absolute stereochemistry of the product was dependent on the counterion with the sodium enolates giving the *R* product (96% *ee*), whereas the lithium enolates afforded the *S* enantiomer (64% *ee*) (Figure 75).

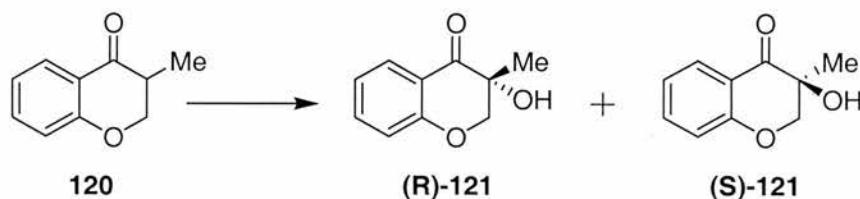


Figure 75. Asymmetric hydroxylation of the sodium enolate of 3-methyl-4-chromanone (**120**) with **78**. The reaction afforded (*R*)-**121** in 96% *ee* and 64% yield.¹⁹

However, this counterion dependency was not detected for the asymmetric oxidation of the lithium and sodium enolates of tetralone **119** with (+)-(8,8-dichlorocamphorylsulfonyl)oxaziridine (**78**) (Figure 76).¹⁹

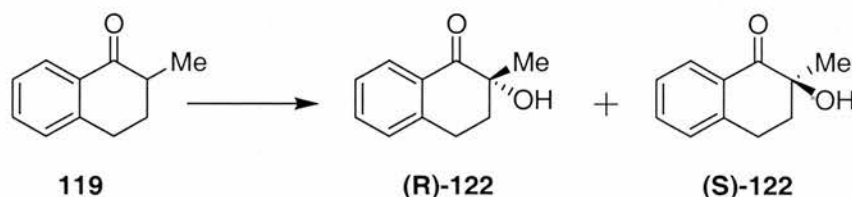


Figure 76. Asymmetric hydroxylation of the sodium and lithium enolate of 2-methyl-1-tetralone (**119**) with **83**. The reaction afforded (*R*)-**122** in $\geq 95\%$ *ee* and 66% yield with NaHMDS and (*R*)-**122** in $\geq 95\%$ *ee* and 60% yield with LDA.¹⁹

In the case of the asymmetric oxidation to give (–)-blebbistatin (**7**) with (–)-(8,8-dichlorocamphorylsulfonyl)oxaziridine (**82**) it was found that for both lithium and sodium enolates the stereochemistry of the product was the same as judged by the sign of the optical rotation (entries 9 and 10).

In summary, the asymmetric oxidation of the quinolone **24** gave the highest stereoselectivities with the dihalo oxaziridine **82**. Furthermore the sodium enolates were more reactive at low temperatures than the lithium enolates. Finally the best result was found for the reaction with **82** and the lithium enolate at $-10\text{ }^{\circ}\text{C}$, where both enantiomeric purity and yield of the reaction were good although it was not possible to obtain *ee* > 90% without further purification (see next section).

3.1.3. Preparation of highly optically enriched samples of (-)-Blebbistatin (**7**) and (+)-Blebbistatin (**23**)

In the light of the results obtained from Section 3.1.2., this section describes the preparation of highly optically enriched (-)-blebbistatin (**7**) and (+)-blebbistatin (**23**). The reaction conditions described in Table 4, entry 9 were used to prepare **7** in 82% yield and with high stereoselectivity (86% *ee*) (Figure 77). The optical rotation for (-)-blebbistatin (**7**) was determined as $[\alpha]_D^{25} = -461$ (concentration of 0.1 g/100mL in dichloromethane). A single recrystallisation from acetonitrile of the crude reaction product provided essentially optically pure **7** in >99% *ee* ($[\alpha]_D^{25} = -530$, concentration of 0.1 g/100mL in dichloromethane). The crystals were suitable for X-ray analysis and confirmed the structure of (-)-blebbistatin (**7**) (Figure 78). It is important to note that the enantiomer drawn in Figure 77, for (-)-blebbistatin (**7**), was chosen arbitrarily.

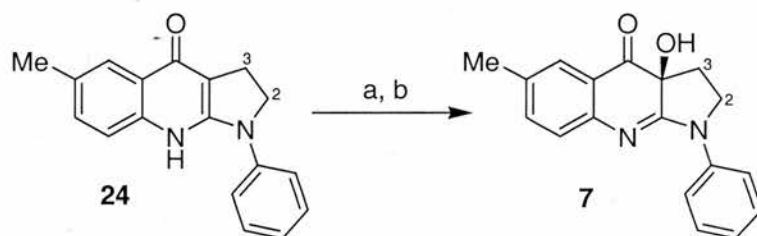


Figure 77. Asymmetric hydroxylation of quinolone **24**. Reagents and conditions: a) i) LiHMDS (1.2 equiv), THF, -78 °C, 30 min, ii) **82** (2.4 equiv), THF, -10 °C, 16 hours, 82%, 86% *ee*, b) recrystallisation from MeCN, >99% *ee*, $[\alpha]_D^{25} = -530$ (c=0.1 in DCM).

In addition, ^1H NMR and ^{13}C NMR analysis confirmed the structure of **7**. The triplets corresponding to the protons H-2 and H-3 (Figure 77) from the starting material **24** disappeared to give more complicated signals. The introduction of a stereogenic centre into the molecule resulted in chemical shift nonequivalence of the diastereotopic protons H-2 (δ 3.79-3.88 and δ 3.96) and H-3 (δ 2.15-2.30 and δ 2.44) (Figure 79).

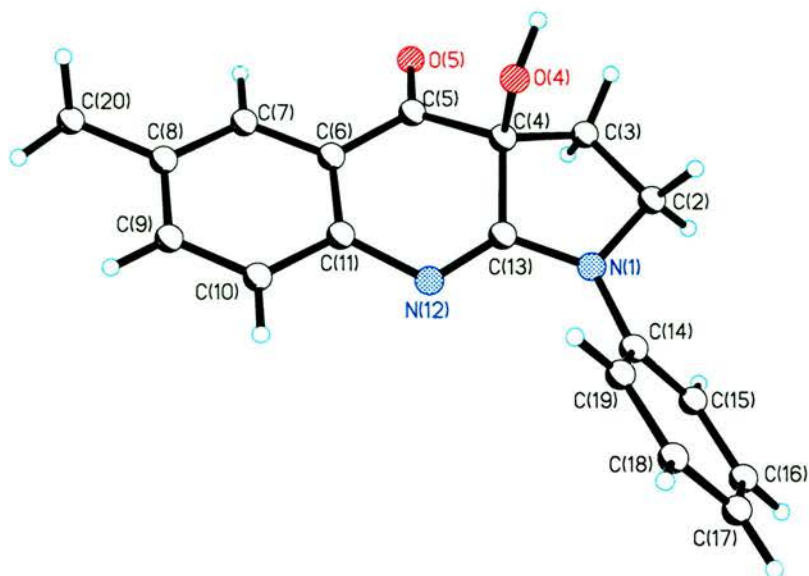


Figure 78. X-Ray of (-)-blebbistatin (7).CCDC number 238391.

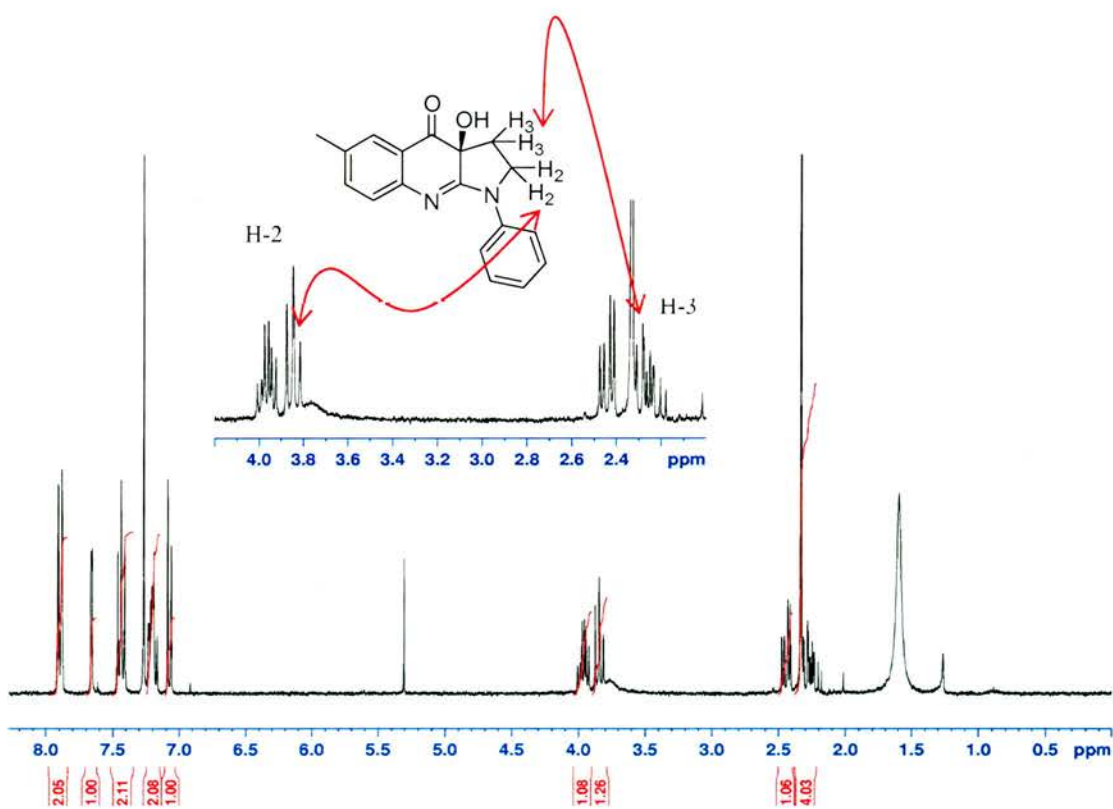


Figure 79. ¹H NMR of (-)-blebbistatin (7) in CDCl₃. Expansion of the aliphatic region to show the diastereotopic protons corresponding to H-2 and H-3.

In addition, the (+)-blebbistatin enantiomer (**23**) was also prepared following the same procedure, except for replacement of **82** by its enantiomer **78**, in a 76% yield and 86% *ee* as judged by HPLC analysis. A single recrystallisation from acetonitrile gave highly optically enriched **23** in >99% *ee* ($[\alpha]_D^{25} = +525$, concentration of 0.2 g/100mL in dichloromethane).

Chiral HPLC analysis of both the crude reaction mixture and the recrystallised material **7** demonstrate how effective this purification procedure was (Figure 80).

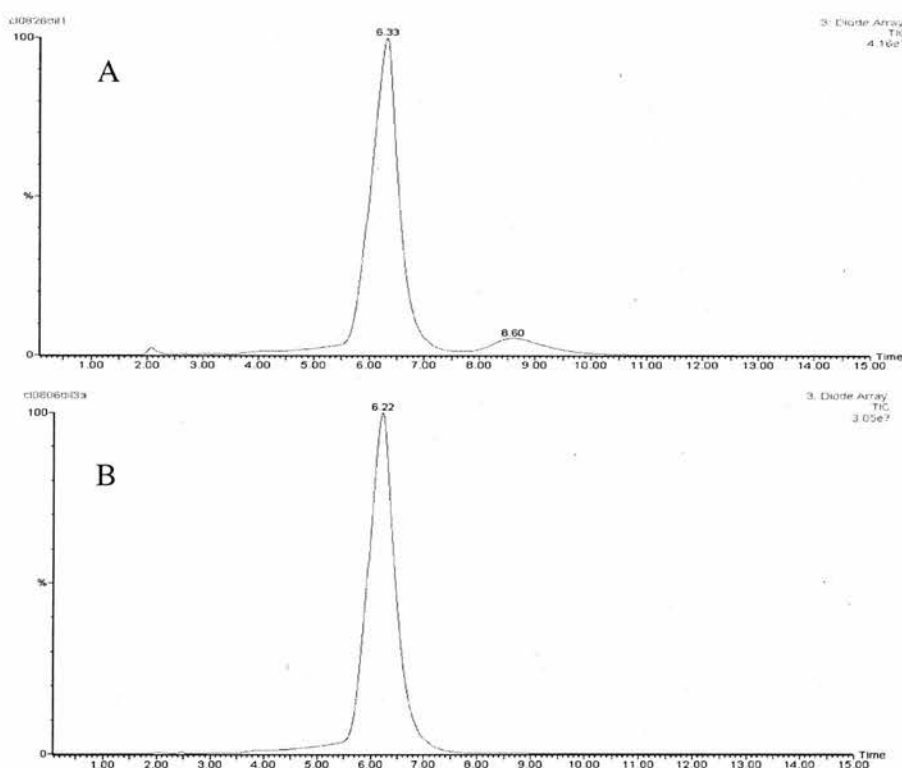


Figure 80. Determination of the enantiomeric excess of (-)-blebbistatin **7** detected by chiral HPLC analysis. Conditions: Daicel Chiralpak AD-RH, Acetonitrile/Water 50:50, flow rate 0.8 mL min⁻¹, $\lambda=254$ nm. A) Chromatogram of the crude mixture of **7**: major enantiomer $t_R=6.33$ min., $\lambda_{max}=249$ nm. and minor enantiomer $t_R=8.60$ min., $\lambda_{max}=249$ nm. B) Chromatogram of crystallised **7**: major enantiomer $t_R=6.22$ min., $\lambda_{max}=249$ nm.

In summary, this section has described a flexible and efficient route to highly optically enriched (-)-blebbistatin (**7**) and (+)-blebbistatin (**23**) (>99% *ee*) using the Davis oxaziridine methodology. In addition the structure of **7** has been proved by X-ray crystallographic techniques. The next goal of the project is to determine the absolute configuration of (-)-blebbistatin (**7**).

3.2. DETERMINATION OF THE ABSOLUTE CONFIGURATION

One challenge in organic chemistry is determination of the absolute configuration of optically pure organic molecules.²⁹ Therefore, the development of different methodologies to determine the absolute configuration is of importance. The classical methods for determining absolute configuration include: a) X-ray diffraction,¹³ b) optical rotation,¹³ c) methodologies which require initial derivatisation into the diastereomeric derivatives, such as circular dichroism (CD) exciton chirality, pioneered by Nakanishi *et al.*,³⁰ and NMR analysis of diastereomeric esters introduced by Mislow *et al.*,^{2,31} and developed latter by Mosher^{14,32} and others.^{33,34, & 35}

Small molecule X-ray crystallographic analysis is a very useful tool to determine absolute configuration. This can be achieved through the methodology developed by Bijvoet *et al.*,³⁶ using anomalous X-ray scattering, for substances that are crystalline and contain an appropriate heavy atom. In cases where there is no heavy atom, the methodology used is multiple scattering X-ray experiments for light atom molecules.^{18,37,38}

Circular dichroism exciton chirality is based on the absorption of the circularly polarised light by chiral molecules, therefore on the variation of the optical rotation (α) with the wavelength of the light. The assignment is based on the sign of the CD at a suitable wavelength.

NMR spectroscopic methods are extensively used in the literature to assign the absolute configuration of organic molecules. The general procedure involves the derivatisation of the compound of unknown configuration with the two enantiomers of an auxiliary reagent to afford the corresponding diastereomers. The most common auxiliary reagents are methoxyphenylacetic acid (MPA), α -methoxy- α -trifluoromethylphenylacetic acid (MTPA) (Mosher's reagent) and *O*-methylmandelic acid (described in Section 3.1).^{14,33} The configuration of the desired compound can be deduced from the correlation of the NMR spectral data with the configuration of the alternative diastereomers. Therefore, the proton NMR spectra of the resulting diastereoisomeric derivatives are compared and the differences are measured in chemical shifts as $\Delta\delta^{\text{RS}}$ values. The sign of the $\Delta\delta^{\text{RS}}$ values is used to assign the

absolute configuration. The determination of the configuration with these methods has been possible for primary alcohols, secondary alcohols, primary amines and carboxylic acids.^{39, 40, & 41}

However, the techniques described have some limitations when they are used on their own. Literature precedent shows examples of how contradictory these methodologies can be for determining the stereochemistry of organic compounds. For instance, although the Mosher esters have been shown as a reliable method involving an easy preparation, their use can be unsuccessful for sterically hindered alcohol groups.⁴²

Additionally an example reported in the literature describes the use of both CD and NMR analysis of Mosher's derivatives for determining the absolute configuration of the tricyclic **123** (Figure 81).²⁹

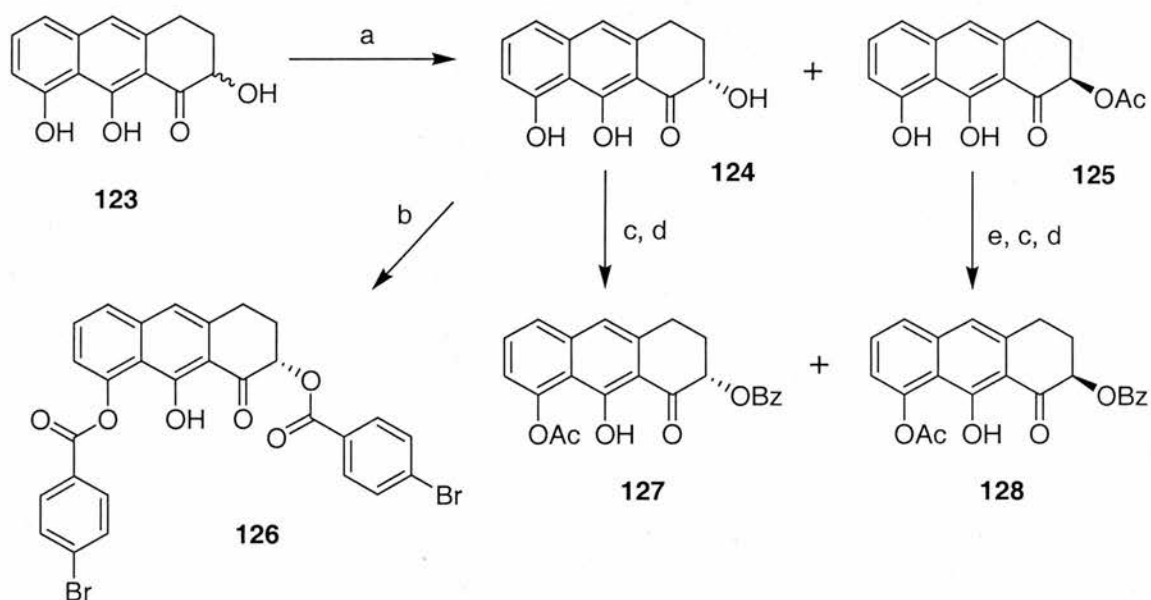


Figure 81. Derivatization of **123** to the corresponding benzoate esters **126**, **127** and **128** to determine their absolute configuration. Reagents and conditions: a) PFL (*Pseudomonas fluorescens* lipase), vinyl acetate, RT, 4h, 53%, b) *p*-bromobenzoyl chloride (2 equiv), *N*-methylimidazole (3 equiv), 2:1 DCM/propylene oxide, RT, 30 min, 60%, c) Acetyl chloride (1 equiv), *N*-methylimidazole (0.2 equiv), 2:1 DCM/propylene oxide, RT, 2.5 h, 74%, d) Acyl chloride, *N*-methylimidazole 2:1 DCM/propylene oxide, RT, 2 h, 50-70%, e) PFL, 50mM phosphate buffer, pH=7, RT, overnight, 40%.²⁹

The two techniques (CD and NMR analysis) gave opposite results (*R* and *S*, respectively).²⁹ Attempts to establish finally the determination of the configuration of **123** by a third method were based on the use of calculated and experimental optical rotatory dispersion (ORD) data, which was consistent with the Mosher ester analysis. Subsequently, they decided to prepare a bromobenzoate analogue of **123** to confirm the absolute configuration by X-ray analysis. A single-crystal X-ray diffraction of the ester **126** established the absolute configuration as *S*, consistent with Mosher's and ORD methodologies. Therefore, it was concluded that the use of the CD method must be treated with care when determining absolute configuration.

3.2.1. Proof of absolute stereochemistry of (*S*)-(-)-Blebbistatin (**7**)

In our case it was initially decided to solve the absolute configuration of (-)-blebbistatin (**7**) by X-ray diffraction. Absolute structures of light-atom containing organic systems can normally be achieved by X-ray diffraction with Cu-K α radiation when the molecule contains sufficient oxygen atoms.^{43,44} Although the preparation of crystals for X-ray analysis was successful and also the absolute structure parameter was close to zero, (see Chapter 3, Section 3.1.3. and Appendix for X-ray details), the described method failed to determine the absolute configuration due to the fact that the crystals were not of high enough quality.

Therefore, it was decided to try and use Mosher's methodology to determine both the enantiomeric excess and the absolute configuration. It is worth noting that this methodology has been used mainly for secondary alcohols (see Section 3.1) and in our case the molecule of interest contains a tertiary alcohol. Unfortunately attempts to derivatise **7** into the corresponding ester with the Mosher's reagent (**103**) [(*R*)-(-)- α -methoxy- α -(trifluoromethyl)phenylacetyl chloride] (Figure 82) were unsuccessful (see in more detail Chapter 4, Section 4.4.1.1).

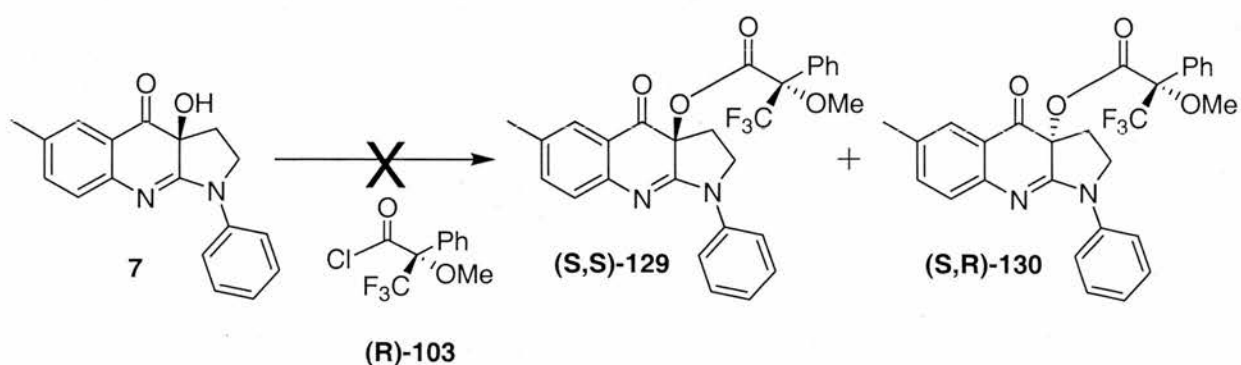


Figure 82. Attempted preparation of the Mosher's esters **129** and **130**. Reagents and conditions: a) DMAP (catalytic amount), Et₃N, (*R*)-(-)-Mosher acid chloride (**103**) (25 equiv), DCM, RT, 2 hours.

Another attempt to prepare the ester was through coupling reaction with HOBT and DCC (Figure 83). A solution of Mosher's acid ((*S*)-(-)- α -methoxy- α -(trifluoromethyl)phenylacetic acid) (**131**) and HOBT in THF was added to optically enriched (-)-blebbistatin (**7**) (86% *ee*), followed by addition of DCC. The reaction mixture was stirred for 16 hours at room temperature. TLC analysis showed only the presence of starting material. The reaction was then heated for 16 hours at 80 °C. TLC analysis showed mainly starting material from the reaction.

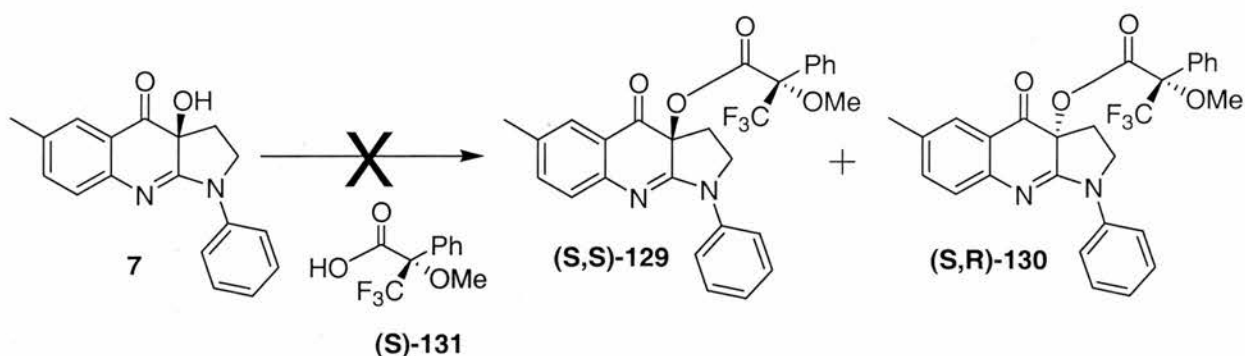


Figure 83. Attempted preparation of the Mosher's esters **129** and **130**. Reagents and conditions: a) (*S*)-Mosher's acid (*S*)-**131** (5.0 equiv), HOBT (5.0 equiv), DCC (5.0 equiv), THF, RT, 16 hours and 80 °C, 16 hours.

Finally, it was decided to try and prepare a heavy atom containing derivative in order to assign the absolute configuration. The incorporation of a bromine atom was selected. Therefore, a heavy atom (bromine)-containing analogue of (-)-blebbistatin (**7**) was prepared.

The most well known way to introduce bromine into a system that contains an aromatic ring is by electrophilic substitution with bromine. However, several problems can occur. For example, the use of bromine can afford a complex mixture of polysubstituted bromo compounds and when *N*-bromosuccinimide is used as the brominating reagent, the reaction often affords the dibromo derivatives.⁴⁵ The polarity of the solvent used with the brominating reagent is also very important.⁴⁶ While bromination with *N*-bromosuccinimide, in carbon tetrachloride or benzene, can introduce a bromine atom on a methyl group (as is possible in this case) or methylene group adjacent to the aromatic ring, the use of *N*-bromosuccinimide in a polar solvent, mainly gives the aromatic substituted products.⁴⁶ However, the use of *N*-bromosuccinimide in polar solvents such as DMF at room temperature is reported to be a mild, selective monobrominating reagent for reactive aromatic compounds.⁴⁷ Additionally, the latter brominating reagent is reported to be more selective than bromine and thallium (III) acetate⁴⁸ and cupric bromide⁴⁹ for the bromination of aromatic systems.⁴⁷

In our case initial attempts to brominate (–)-blebbistatin (**7**) with NBS at room temperature in DMF were unsuccessful. Purification of a mixture of brominated isomers resulting from the reaction proved difficult. An equally complex mixture was obtained when bromination of amidine **29** was attempted.

During attempts to acylate the tertiary alcohol functionality in **7** with various bromobenzoyl chlorides, the desired products were isolated, but in initial studies did not yield sufficiently high quality crystals for X-ray analysis (Chapter 4, Section 4.4.2.1). Attempts to prepare an analogue of **7** with a bromine atom in place of the methyl substituent also proved unsuccessful due to the low yield of the reaction between methyl 5-bromoanthranilate and 1-phenyl-2-pyrrolidinone **28**.

After failed attempts to brominate directly **7** and amidine **29** to give **135** and **133** respectively, it was decided to prepare **135** from the lactam **28** using an analogous approach to that used to prepare (–)-blebbistatin (**7**) (Figure 84) (Chapter 3, Section 3.1.3). Therefore, **28** was dissolved in DMF and treated with NBS. The reaction mixture was stirred at room temperature for 2 days. The compound was purified by recrystallisation in hexane/ethyl acetate to afford white needles in 50% yield. In this case the selective monobromination was achieved at the *para* position on the aromatic

ring. ^1H NMR of **132** showed an AA'BB' system on the aromatic region due to the presence of the *para*-bromine. The coupling reaction was carried out in 16 hours affording the corresponding bromo amidine **133** in low yield (26%). The quinolone **134** was then prepared in 62% yield after purification by flash column chromatography using neat ethyl acetate. Finally the desired oxidised bromine-containing analogue **135** was prepared using the optimised asymmetric hydroxylation in good yield (69%) as a red solid.

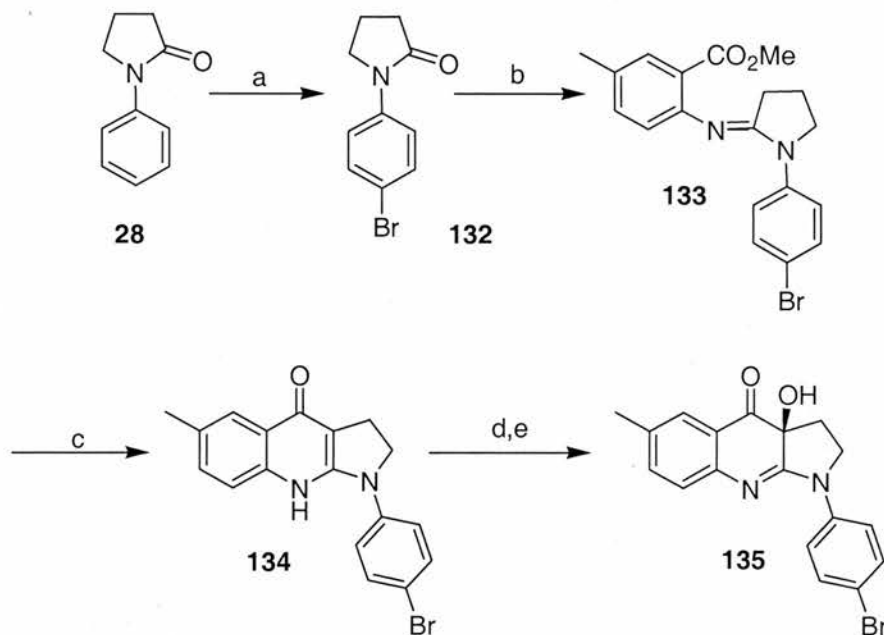


Figure 84. Assignment of the absolute stereochemistry of (-)-blebbistatin (**7**). Reagents and conditions: a) NBS (1.0 equiv), DMF, RT, 2 days, 50%; b) i) POCl_3 (0.90 equiv), DCM, RT, 3 hours; ii) **27** (1.0 equiv), DCM, 40°C , 16 hours, 26%; c) LiHMDS (3.0 equiv), THF, -78°C to 0°C , 3 hours, 62%; d) i) LiHMDS (1.2 equiv), THF, -78°C , 30 min; ii) **82** (2.4 equiv), THF, -10°C , 16 hours, 69%, 88% *ee*; e) recrystallisation from MeCN >99% *ee*; $[\alpha]_{\text{D}}^{25} = -526$ ($c=0.1$ in DCM).

The enantiomeric excess of the asymmetric oxidation was determined by chiral HPLC which showed that **135** was prepared in a high enantiomeric excess (88% *ee*) (Figure 85). Recrystallisation from acetonitrile gave **135** as essentially one enantiomer (>99% *ee*) as confirmed by chiral HPLC analysis (Figure 85). ^1H NMR and ^{13}C NMR spectra were consistent with the formation of **135**. ^1H NMR showed the presence of an AA'XX' system in the aromatic region which is consistent with the presence of a bromine atom at the *para* position. The optical rotation value of optically pure **135** showed a negative value of $[\alpha]_{\text{D}}^{25} = -526$ (concentration of 0.1 g/100mL in

dichloromethane). The synthesis of highly optically enriched (>99% *ee*) **135** was achieved with an overall yield for the synthetic route of 5.3%.

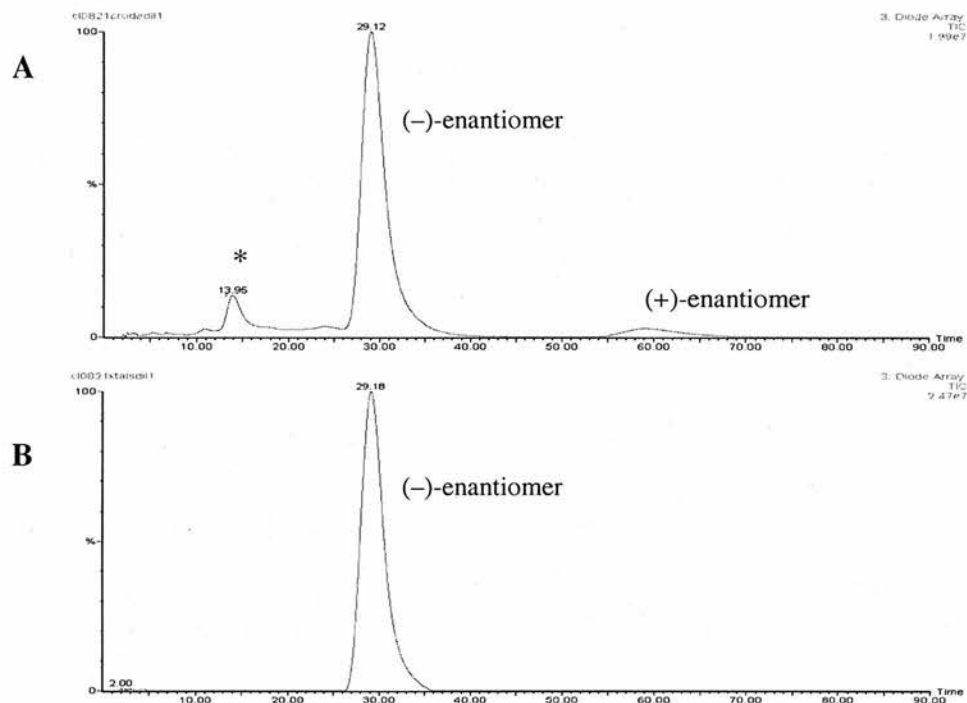


Figure 85. Determination of the enantiomeric excess of **135** by chiral HPLC analysis. Conditions: Daicel Chiralpak AD-RH, Acetonitrile/Water 50:50, flow rate 0.8 mL min^{-1} , $\lambda=254 \text{ nm}$. A) Chromatogram of the crude mixture of **135**: major enantiomer $t_R=29.12 \text{ min}$, $\lambda_{\text{max}}=244 \text{ nm}$. and minor enantiomer $t_R=59.25 \text{ min}$, $\lambda_{\text{max}}=244 \text{ nm}$. B) Chromatogram of the crystallised bromo-blebbistatin analogue **135**: major enantiomer $t_R=29.18 \text{ min}$, $\lambda_{\text{max}}=244 \text{ nm}$. * Minor impurity at $t_R=13.95 \text{ min}$. For more details see Appendix.

Sufficiently high quality crystals of the bromine-containing analogue **135** were successfully prepared to enable X-ray analysis. As shown in Figure 86, the *absolute configuration of (-)-bromo-blebbistatin (135) is S*. Figure 87 shows an intermolecular hydrogen bond between the oxygen atom of the carbonyl group O(5A) and the hydrogen H(O4) of an adjacent molecule.

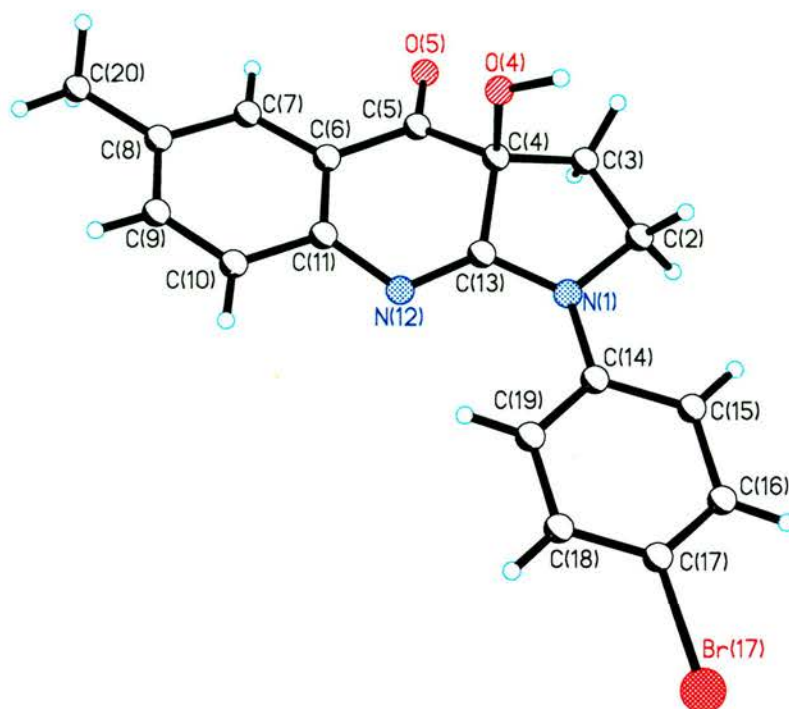


Figure 86. X-Ray of bromo containing analogue of blebbistatin 135. CCDC number 238392.

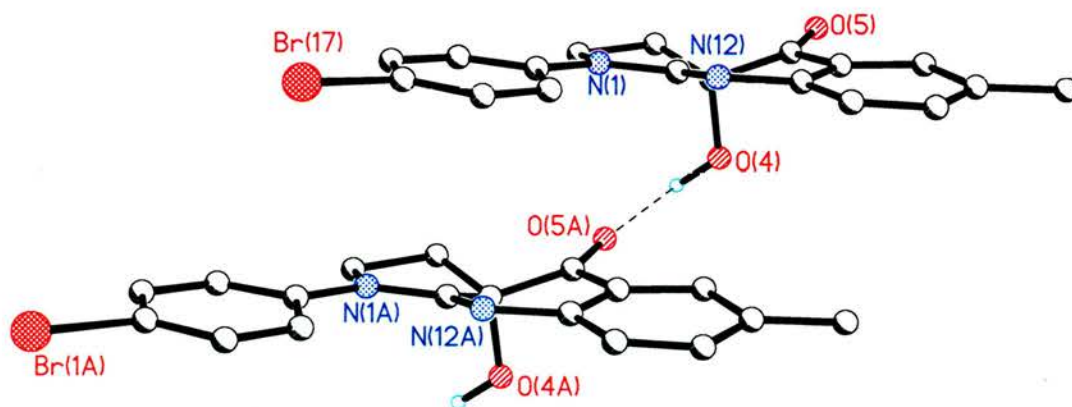


Figure 87. Intermolecular hydrogen bonding between Hydrogen (from the 4-Oxygen) and the 5-Oxygen in 135.

Hydrogenation of a highly enantiomerically enriched sample of **135** (>99% *ee*) was then carried out (Figure 88). **135** was dissolved in a 1:1 mixture of MeOH:DMF in the presence of triethylamine and a catalytic amount of 1% Pd/C.⁵⁰ The reaction was treated with hydrogen gas and stirred at room temperature for 24 hours. Purification of the residue by flash column chromatography gave (–)-blebbistatin (**7**) in an essentially quantitative yield (100%). In addition, during initial attempts at this reaction, it was found that the blebbistatin core structure could be reduced in the presence of H₂/Pd/C (Chapter 4, Section 4.5).

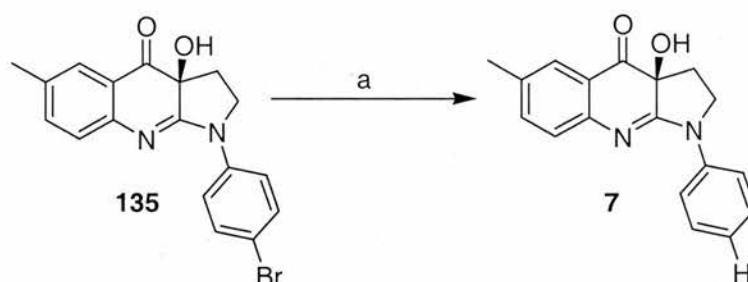


Figure 88. Hydrogenation of (–)-bromo-blebbistatin (**135**). Reagents and conditions: a) H₂, 1% Pd/C, Et₃N, DMF/MeOH, RT, 24 hours, 100% (quant).

Chiral HPLC analysis of the crude reaction mixture showed that reduction of **135** afforded **7** as the only peak in the chromatogram (Figure 89C). Samples of enantiomerically pure (+)-blebbistatin (**23**) (Figure 89A) and (–)-blebbistatin (**7**) (Figure 89B) were first run as references. Comparison with the product from the hydrogenation of **135** ($t_R=6.18$ min) showed that reduction of **135** gave a product that was identical to **7** ($t_R=6.22$ min). When **23** was mixed with the reduced product, two different peaks were observed (Figure 89D). Finally it was decided to mix the three samples to ensure the presence of only two peaks corresponding to the (–)-blebbistatin and (+)-blebbistatin enantiomers (Figure 89E). These results confirmed that when **135** was reduced by hydrogenation it afforded (–)-blebbistatin (**7**) and hence that as the absolute stereochemistry of **135** is known to be *S*, the absolute stereochemistry of (–)-blebbistatin (**7**) must be *S*.

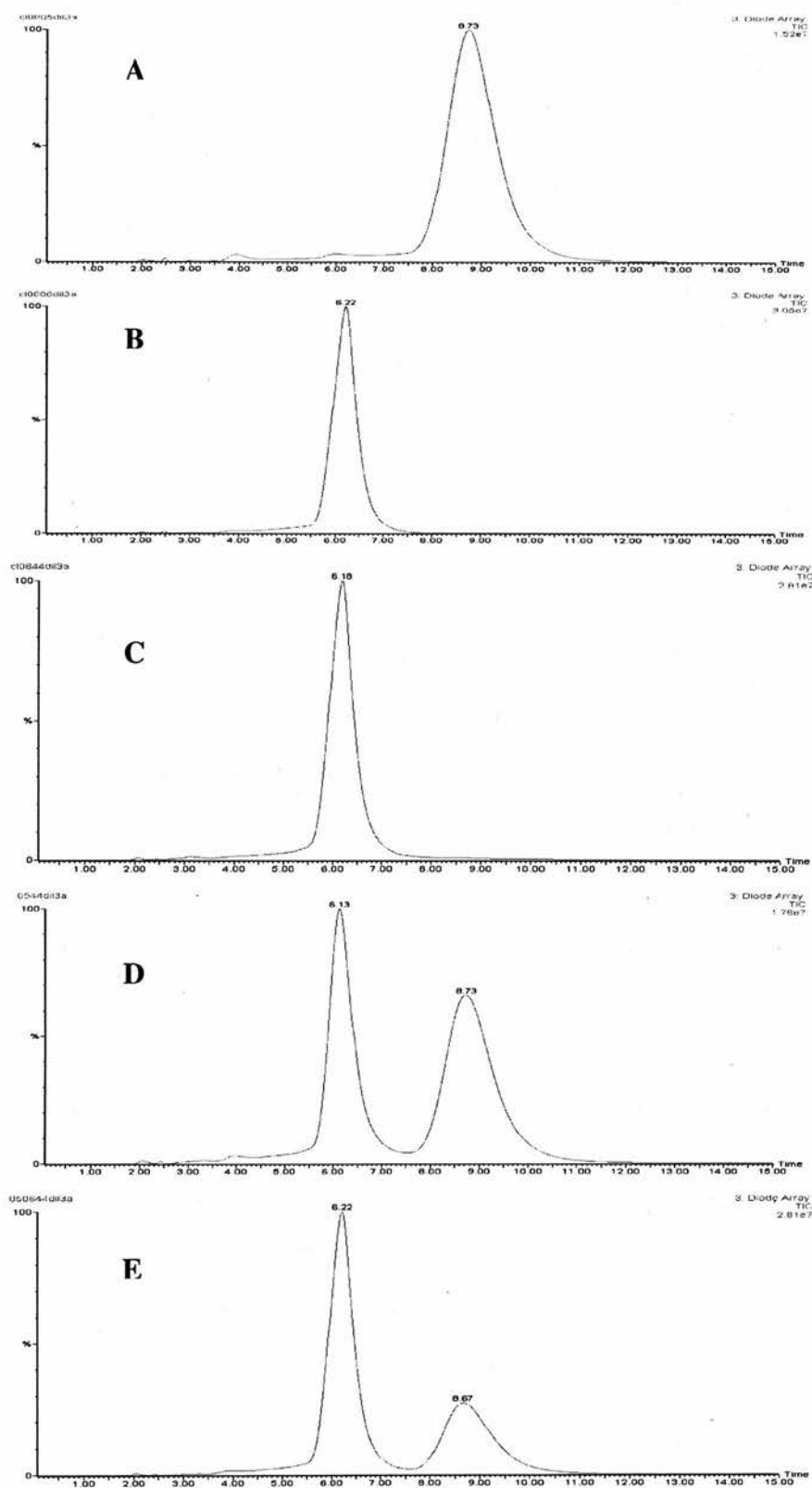


Figure 89. Determination of the absolute configuration of **135** by chiral HPLC chromatography. Conditions: Daicel Chiralpak AD-RH, Acetonitrile/Water 50:50, flow rate 0.8 mL min^{-1} , $\lambda=254 \text{ nm}$. Chromatograms; A) crystallised material **23**, $t_R=8.73 \text{ min}$, B) crystallised material **7**, $t_R=6.22 \text{ min}$, C) reduced bromo-blebbistatin $t_R=6.18 \text{ min}$, D) A+C, $t_R=6.13 \text{ min}$, $t_R=8.73 \text{ min}$. E) A+B+C, $t_R=6.22 \text{ min}$, $t_R=8.67 \text{ min}$.

In summary, the preparation of an essentially optically pure bromine-containing analogue of blebbistatin **135** was achieved. The structure of **135** was confirmed by X-ray analysis and the *absolute configuration* was solved, due to the presence of the heavy-atom, as *S*. Subsequent replacement of the bromine in (*S*)-(-)-**135** with a hydrogen atom using catalytic hydrogenation gave exclusively (-)-blebbistatin (**7**) (confirmed by comparison with authentic material using chiral HPLC). Therefore, *the absolute stereochemistry of (-)-blebbistatin (7) is S*.

Additionally blebbistatin analogue **135** can also function as a useful precursor for the synthesis of a radiolabelled derivative of **7** (*via* palladium catalysed tritiation) and for the preparation of (*S*)-(-)-blebbistatin (**7**) analogues functionalised at C4'. Preliminary data on the activity of compounds substituted at C4' shows that they retain non-muscle myosin II ATPase inhibitory activity.⁵¹

3.3. ASYMMETRIC HYDROXYLATION OF METHYL ANALOGUES OF (*S*)-(-)-BLEBBISTATIN (**7**)

In order to study the effect that the position of the methyl substituent has on the enantiomeric excess for the asymmetric hydroxylation of the methyl analogues of (-)-(*S*)-blebbistatin (**7**) (Chapter 4, Section 4.3.1) a series of asymmetric hydroxylations were carried out. The asymmetric hydroxylation of the different ketone enolates were carried out by treatment of the corresponding quinolones with 1.2 equivalents of the appropriate base at -78 °C followed, after 30 minutes, by the addition of 2.4 equivalents of the Davis oxaziridine (**78**, **81**, **82**) (Figure 90) to the preformed enolate at -78 °C. The reactions were stirred at -10 °C for 16 hours. The progress of the reaction was monitored by TLC and the reactions were quenched at -10 °C by addition of aqueous NH₄I. The enantiomeric excess (*ee*) was determined in each case by chiral HPLC. The results are summarised in Table 6.

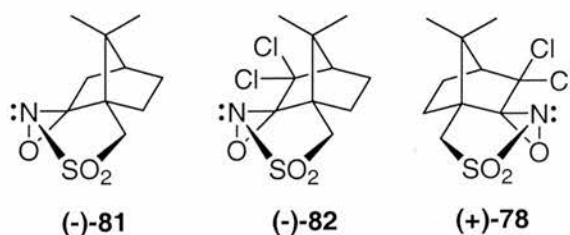
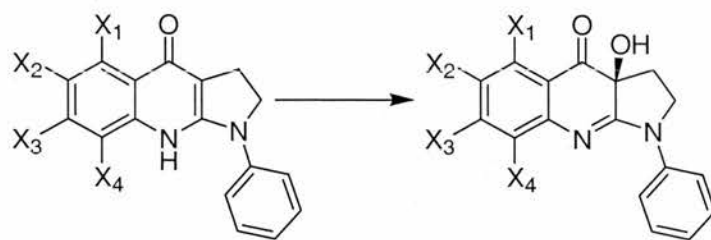


Figure 90. Structure of (Camphorylsulfonyl)oxaziridines.



136 $X_1 = \text{Me}, X^{2,3,4} = \text{H}$

24 $X_2 = \text{Me}, X^{1,3,4} = \text{H}$

137 $X_3 = \text{Me}, X^{1,2,4} = \text{H}$

138 $X_4 = \text{Me}, X^{1,2,3} = \text{H}$

31 $X^{1,2,3,4} = \text{H}$

139 $X_1 = \text{Me}, X^{2,3,4} = \text{H}$

7 $X_2 = \text{Me}, X^{1,3,4} = \text{H}$

140 $X_3 = \text{Me}, X^{1,2,4} = \text{H}$

141 $X_4 = \text{Me}, X^{1,2,3} = \text{H}$

67 $X^{1,2,3,4} = \text{H}$

Entry	Product	% ee (81)	% ee (82)	% ee (78)	% yield (81)	% yield (82)	% yield (78)
1	139	17	64	65	76*	87	87
2	7	42	86	86	73	82	76
3	140	28	90	90	72	83	67
4	141	40	86	88	33	63	77
5	67	55	86	85	65	78	74

Table 6. Comparison on the enantiomeric purity (*ee*) of the different methyl analogues of (–)-blebbistatin (**7**). Reagents and conditions: a) i) LiHMDS (1.2 equiv), THF, -78 °C, 30 min, ii) oxaziridines **81**, **82** and **78** (2.4 equiv), THF, -10 °C, 16 hours. The table summarises the yield and enantiomeric excess (*ee*) obtained as a function of base and reagent. All *ee* values were determined using chiral HPLC analysis. *Reaction carried out by Dr Stephen Patterson.

The results summarised in Table 6 suggest a number of trends. First, it was found that asymmetric oxidation carried out by dihydro oxaziridine **81** showed low stereoselectivities for each analogue of (–)-blebbistatin (**7**) (17-55% *ee*). However, an improvement was observed with the use of dihalo oxaziridine **82** (64-90% *ee*). These results were consistent with the results obtained by Davis *et al.*,²⁵ where they found that ((8,8-dichlorocamphoryl)sulfonyl)oxaziridine gave the highest stereoselectivities. It is interesting to note that the asymmetric induction for **139** gave the lowest *ee* with both reagents dihydro **81** and dihalo **82** and **78** oxaziridines (see entry 1). Furthermore the asymmetric hydroxylation of the lithium enolates gave good yields for all the analogues except in the case of formation of **141** with dihydro oxaziridine of type **81** (entry 4).

These results suggest the position of the methyl group can influence the enantioselectivity of the reaction. Davis *et al.*,^{19, 26} reported that enolate structure is very important for the hydroxylation stereoselectivity. In one example Davis focuses attention on the asymmetric hydroxylation of tetralones with dihalo oxaziridine **78** (Figure 91). High enantioselectivities were observed (>90%) for 2-substituted 1-tetralones having a variety of groups at C-2 (R= Me, Et, PhCH₂). However, it was found that when a methoxy group is placed at the C-8 position the stereoselectivity decreased to 83% (*ee*).

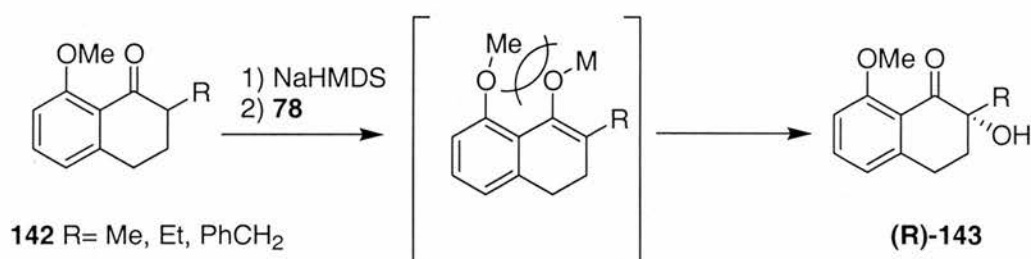


Figure 91. Asymmetric oxidation of 2-substitued 1-tetralone (**142**) with OMe at C-8 position.^{19,26}

In summary, the asymmetric hydroxylation of analogues of quinolone **24** in which the methyl group has been placed in all possible positions, resulted in good yields for each analogue. In addition, variations in the enantiomeric excess did occur, with special attention being drawn to the hydroxylation of **136** to give **139**.

3.4. PROPOSED MODEL FOR ASYMMETRIC INDUCTION

Formation of (*S*)-(-)-blebbistatin (**7**) presumably proceeds through an analogous transition state to the one proposed by Davis.^{24, 26} After extensive discussion of the possible transition state, Davis²⁶ concluded that an “open” or “nonchelated” transition state of the type TS1 and TS2 was the most favoured for the hydroxylation of 2-methyl-1-tetralone (**119**). However, these studies found that in fact TS1 is more favoured than TS2, and therefore TS1 was used as a model to explain the stereochemistry of the product (Figure 92).

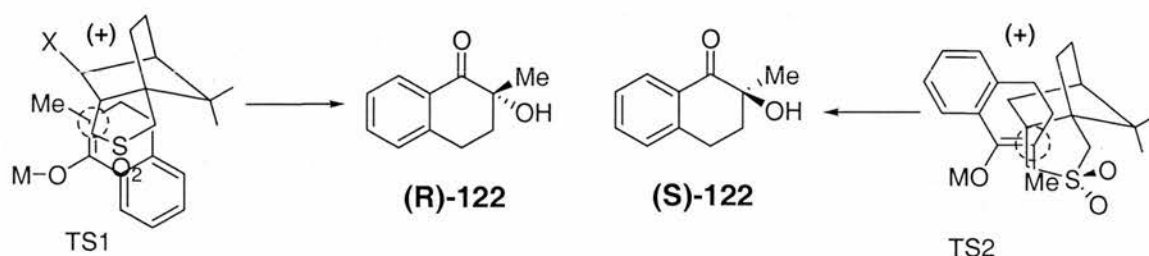


Figure 92. Transition state structures for the hydroxylation of 2-methyl-1-tetralone (**119**).²⁶

In the case of (*S*)-(-)-blebbistatin (**7**) it was decided to reproduce the proposed Davis model for the transition state of type TS1 (Figure 93). The transition state (TS1) corresponding to the approach of the enolate of 1-methyl-2-tetralone (**119**) to the dihalo oxaziridine **78** affording the *R* configuration is shown in Figure 93A. Therefore, when the same rationalisation was applied to (*S*)-(-)-blebbistatin (**7**), using dihalo oxaziridine **78**, the predicted configuration should correspond to *R* (Figure 93B). In contrast, when dihalo oxaziridine **82** is used, the predicted configuration should correspond to *S* (Figure 93C). These predictions were consistent with the results previously described for the synthesis of (*S*)-(-)-blebbistatin (**7**).

In addition, Davis²⁶ also rationalised the variation observed in the enantiomeric excess for the hydroxylation of the 2-methyl-1-tetralone (**119**) using dihydro **81** and dihalo **82** oxaziridines. Davis proposed that it was the difference in the temperature at which the hydroxylation reaction was carried out with the two oxaziridines that had the major influence on the enantiomeric excess. The reaction of the lithium enolate with dihydro oxaziridines afforded 30% *ee* when the temperature of the reaction was 0 °C, whereas the dihalo oxaziridine gave >95% *ee* at -78 °C. In the case of (*S*)-(-)-blebbistatin (**7**), it was observed that the enantiomeric excess for the hydroxylation reaction using dihydro **81** and dihalo **82** oxaziridines, were different even when the reaction was carried out at the same temperature (-10 °C) (see Table 4, entries 3 and 9). Therefore the difference in the enantiomeric excess must result from the presence of halogen atoms in the oxaziridine which must have a differential effect on the TS1 and TS2. Davis²⁶ and co-workers also suggested that the metal of the enolate could chelate to the halogen of the oxaziridines although further experiments with fluorine showed that the enantiomeric excess for the hydroxylation of 2-methyl-1-tetralone (**119**) was lower (62% *ee*) compared with the dichloro oxaziridines (>95% *ee*). Unfortunately due

to time constraints it was not possible to carry out a further hydroxylation of quinolone **24** with difluoro oxaziridines to help investigate further the origins of observed difference in enantiomeric excess.

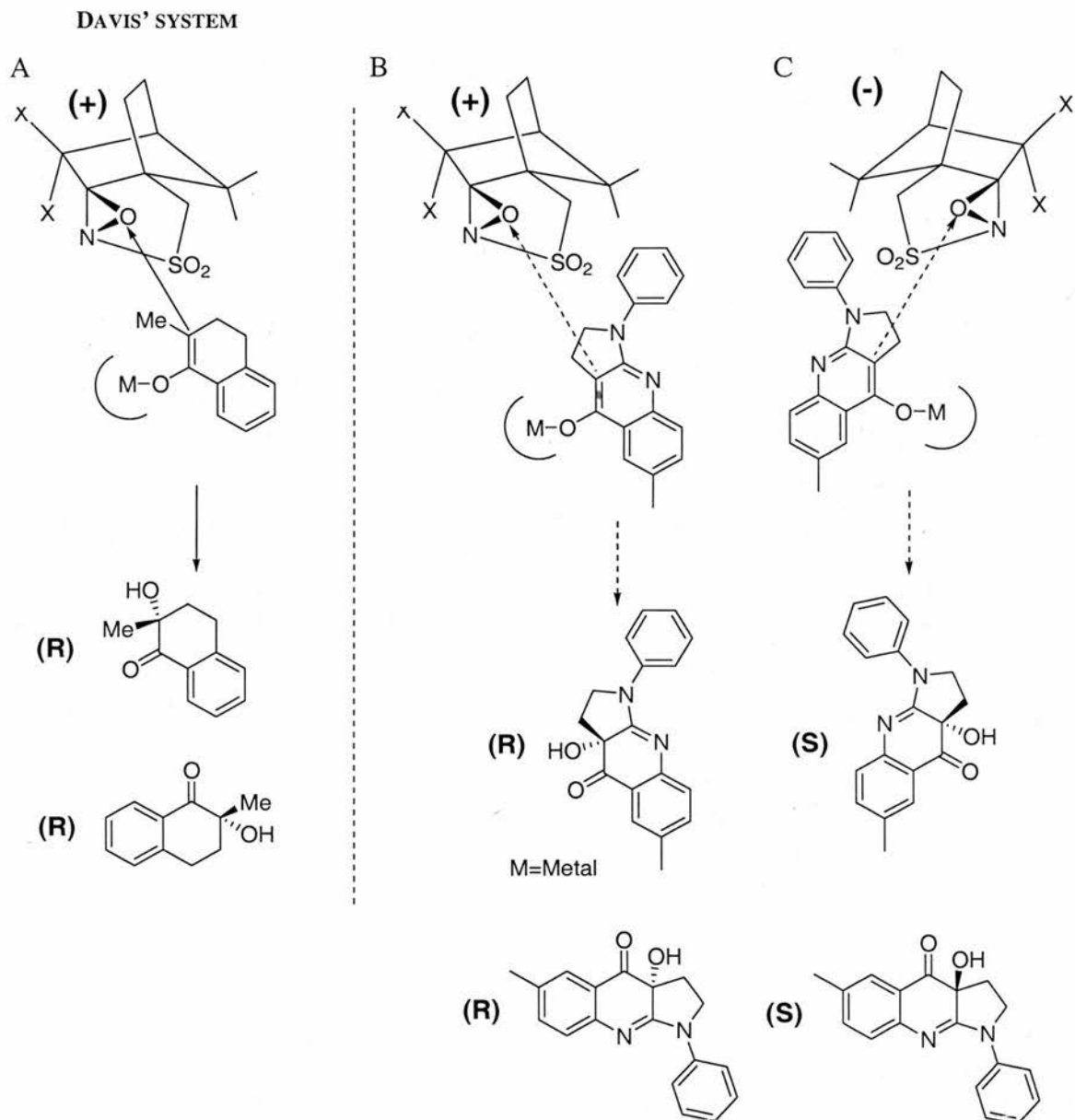


Figure 93. A schematic representation of Davis' rationalisation of the sense of asymmetric induction and its application to (*S*)-(-)-blebbistatin (**7**) compared with the literature example. Proposed approach of the enolate to the oxaziridine from the less hindered direction. OM (Metal= Li, Na), the most sterically demanding group.

In order to provide further information to rationalise the observed differences in the asymmetric induction for the different methyl analogues of (*S*)-(-)-blebbistatin (**7**) (Section 3.3), ^7Li NMR analysis of the corresponding enolates was carried out. It was proposed that these studies would afford some limited spectroscopic information about the lithium enolates of the quinolones (**136**, **137**, **138** and **24**).

The fact that **139** gave the lowest enantiomeric excess of the methyl blebbistatin analogues could possibly be explained by differences in the structure of their lithium enolates. Therefore, it was decided to prepare four samples of the enolate anions using the four quinolone analogues **136**, **137**, **138** and **24**. The reactions were carried out in NMR tubes under an inert atmosphere in dry tetrahydrofuran. Thus, 1.2 equivalents of the base (LiHMDS) were added to each quinolone at $-78\text{ }^\circ\text{C}$ and the formation of the lithium enolates was examined by ^7Li NMR (116.6 MHz), at $-78\text{ }^\circ\text{C}$. The ^7Li NMR spectra from these experiments are presented in Figure 94.

The ^7Li NMR showed the presence of a signal with the same chemical shift (0.69 ppm) for the enolates of **137**, **138** and **24**. The chemical shift observed for the enolate of **136** was different (0.33 ppm). It is important to take into account that ^7Li NMR is difficult to interpret due to its small chemical shift scale (around 6 ppm for salt solution) and it is also solvent, temperature and concentration dependent.⁵² Nevertheless, the difference observed in the NMR is consistent with a difference in the structure of the enolate formed from **136** compared with those formed from **137**, **138** and **24**. This difference in enolate structure mirrors the low value of enantiomeric excess for the formation of **139** from **136**, compared to the high enantiomeric excess for **140**, **141** and **7** from **137**, **138** and **24** respectively.

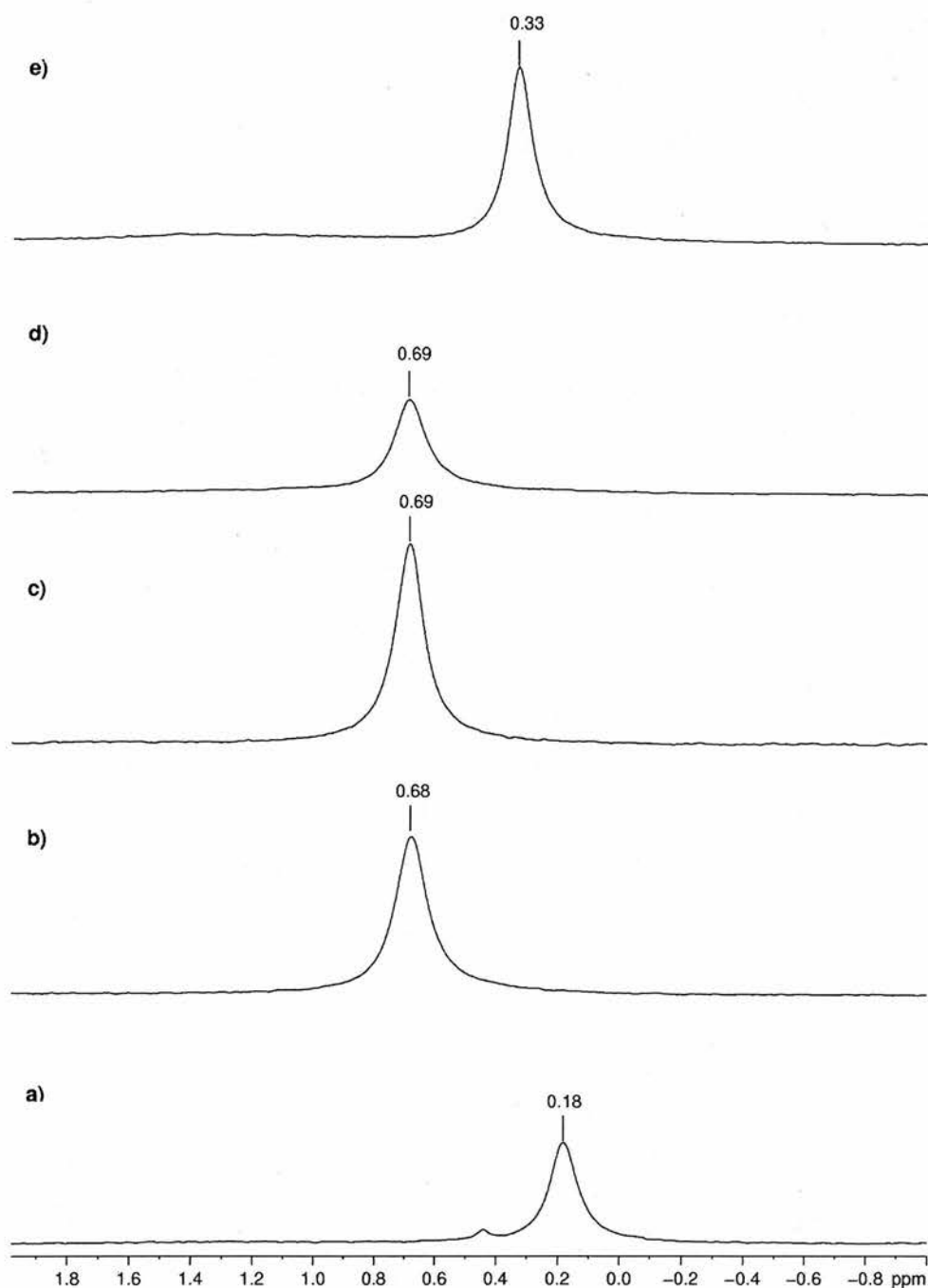


Figure 94. ^7Li NMR spectra for the different enolate anions. Conditions: -78°C , THF, LiHMDS. A capillary containing acetone- d_6 was used as a lock signal in each case. ^7Li chemical shifts are given with respect to 0.1M solution of Li_2SO_4 (as external standard, with a $\delta=0$ ppm)) in H_2O . a) LiHMDS (starting material), b) **138**, c) **137**, d) **24**, e) **136**.

Figure 95 shows the full scale of ^7Li NMR of the enolate of **136**. An additional broad signal at 1.4 ppm can be observed. Although the presence of this signal cannot be explained, it may also be of relevance in explaining the reduced enantiomeric excess observed on the formation of **139**.

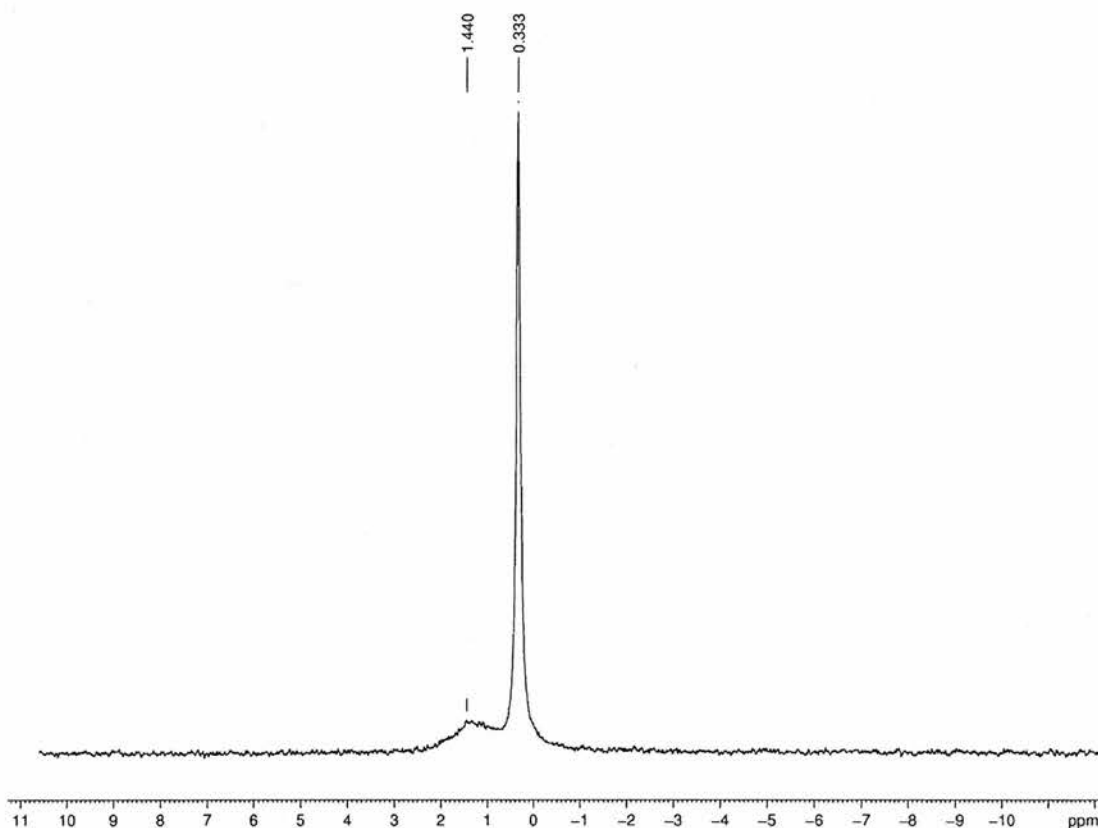


Figure 95. ^7Li NMR spectrum of **136**.

One possible rationalisation of these results is as follows: analogous oxygen-centred enolates are formed on treatment of quinolones **137**, **138** and **24** with lithium bis(trimethylsilyl)amide (see structure **146** as a representative example) (Figure 96). However, in the case of quinolone **136**, the corresponding enolate (**144**) is energetically disfavoured due to a steric interaction between the methyl and O-Li groups. An alternative structure (**145**) may therefore be formed (explaining the difference in the observed chemical shift) which results in a reduced level of selectivity for the corresponding hydroxylation reaction.



Figure 96. Interaction between the lithium enolate and the methyl groups in **24** and **136**. Steric effects are more likely to appear in the case of the lithium enolate **144**.

A second possible rationalisation of the observed differences in the ^7Li NMR, could be related to the formation of different lithium aggregates in solution. Literature precedent^{24, 53, 54, 55} has reported that lithium enolates of ketones can exist and react as molecular aggregates in solution. The studies also showed that these enolates are solvated and therefore for example can form cubic tetrameric aggregates in solution (in solvents such as tetrahydrofuran, dioxolane, dioxane). However, in our case, the lithium enolate derived from **136** could be differently ordered compared to the other analogues leading to a different level of selectivity on reaction with the oxaziridines **78**, **81** and **82**.

To conclude these studies it will be necessary to use computational molecular modelling to establish the transition state of the lithium enolate of the ketones with the Davis oxaziridines. Due to time constraints, these studies will be performed at a future date.

3.5. REFERENCES

- 1 Finn, M. G., *Chirality*, **2002**, *14*, 534-540.
- 2 Raban, M. and Mislow, K., *Tetrahedron Lett.*, **1965**, *48*, 4249-4253
- 3 Dale, J. A. and Mosher, H. S., *J. Am. Chem. Soc.*, **1968**, *90*, 3732-3738.
- 4 Dale, J. A., Dull, D. L., Mosher, H. S., *J. Org. Chem.*, **1969**, *34*, 2543-2549.
- 5 Aitken, R. A. and Kilenyi, S. N., *Asymmetric Synthesis*, **1992**, Blackie Academic & Professional, Glasgow.
- 6 McCreary, M. D., Lewis, D. W., Wernick, D. L., Whitesides, G. M., *J. Am. Chem. Soc.*, **1974**, *96*, 1038-1054.
- 7 Pirkle, W. H. and Sikkenga, D. L., *J. Org. Chem.*, **1977**, *42*, 1370-1374.
- 8 Pirkle, W. H. and Hoover, D. J., *Top. Stereochem.*, **1982**, *13*, 263-331.
- 9 Pirkle, W. H. and Finn, J. M., *J. Org. Chem.*, **1981**, *46*, 2935-2938.
- 10 Raban, M. and Mislow, K., *Tetrahedron Lett.*, **1966**, *33*, 3961-3966.
- 11 Jacobus, J., Raban, M., Mislow, K., *J. Org. Chem.*, **1968**, *33*, 1142-1145.
- 12 Jacobus, J. and Jones, T. B., *J. Am. Chem. Soc.*, **1970**, *92*, 4583-4585.
- 13 Eliel, E. L. and Wilen, S. H., *Stereochemistry of Organic Compounds*, **1994**, John Wiley & Sons, Inc., New York.
- 14 Dale, J. A. and Mosher, H. S., *J. Am. Chem. Soc.*, **1973**, *95*, 512-519.
- 15 Brittain, H. G., *J. Chem. Soc., Dalton Trans.*, **1982**, 2059-2064.

- 16 Schurig, V., *Asymmetric Synthesis*, **1983**, Vol 1, pp 59-86, Academic Press, New York.
- 17 Toyo'oka, T., *J. Biochem. Biophys. Methods*, **2002**, *54*, 25-56.
- 18 Roussel, C., Del Rio, A., Pierrot-Sanders J, Piras, P., Vanthuynne, N., *J. Chromatogr., A*, **2004**, *1037*, 311-328.
- 19 Davis, F. A. and Chen, B-C., *Chem. Rev.*, **1992**, *92*, 919-934.
- 20 Davis, F. A., McCauley, J. P., Chattopadhyay, S., Harakal, M. E., Towson, J. C., Watson, W. H., Tavanaiepour, I., *J. Am. Chem. Soc.*, **1987**, *109*, 3370-3377.
- 21 Davis, F. A., Reddy, R. T., Weismiller, M, C., *J. Am. Chem. Soc.*, **1989**, *111*, 5964-5965.
- 22 Davis, F. A., Reddy, R. T., Han, W., Carroll, P. J., *J. Am. Chem. Soc.*, **1992**, *114*, 1428-1437.
- 23 Davis, F. A. and Haque, M. S., *J. Org. Chem.*, **1986**, *51*, 4083-4085.
- 24 Davis, F. A., Sheppard, A, C., Chen, B-C., Haque, M. S., *J. Am. Chem. Soc.*, **1990**, *112*, 6679-6690.
- 25 Davis, F. A. and Weismiller, M. C., *J. Org. Chem.*, **1990**, *55*, 3715-3717.
- 26 Davis, F. A., Weismiller, M, C., Murphy, C, K., Reddy, R. T., Chen, B-C., *J. Org. Chem.*, **1992**, *57*, 7274-7285.
- 27 Davis, F. A., Kumar, A., Chen, B-C., *J. Org. Chem.*, **1991**, *56*, 1143-1145.
- 28 Davis, F. A. and Sheppard, A. C., *Tetrahedron*, **1989**, *45*, 5703-5742.

- 29 Specht, K. M., Nam, J., Ho, D. M., Berova, N., Kondru, R. K., Beratan, D. N., Wipf, P., Pascal, R. A., Kahne, D., *J. Am. Chem. Soc.*, **2001**, *123*, 8961-8966.
- 30 Harada, N., Nakanishi, K., Tatsuoka, S., *J. Am. Chem. Soc.*, **1969**, *91*, 5896-5898.
- 31 Lewis, R. A., Korpiun, O., Mislow, K., *J. Am. Chem. Soc.*, **1967**, *89*, 4786-4787.
- 32 Sullivan, G. R., Dale, J. A., Mosher, H. S., *J. Org. Chem.*, **1973**, *38*, 2143-2147.
- 33 Trost, B. M., Belletire, J. L., Godleski, S., McDougal, P. G., Balkovec, J. M., Baldwin, J. J., Christy, M. E., Ponticello, G. S., Varga, S. L., Springer, J. P., *J. Org. Chem.*, **1986**, *51*, 2370-2374.
- 34 Latypov, S. K., Seco, J. M., Quinoa, E., Riguera, R., *J. Am. Chem. Soc.*, **1998**, *120*, 877-882.
- 35 Williamson, R. T., Barrios-Sosa, A. C., Mitra, A., Seaton, P. J., Weibel, D. B., Schroeder, F. C., Meinwald, J., Koehn, F. E., *Org. Lett.*, **2003**, *5*, 1745-1748.
- 36 Bijvoet, J. M., Peerdeman, A. F., Van Bommel, A. J., *Nature*, **1951**, *168*, 271-272.
- 37 Lange, J., Burzlaff, H., Bringmann, G., Schupp, O., *Tetrahedron*, **1995**, *51*, 9361-9366.
- 38 Bringmann, G., Hartung, T., Krocher, O., Gulden, K. P., Lange, J., Burzlaff, H., *Tetrahedron*, **1994**, *50*, 2831-2840.
- 39 Seco, J. M., Latypov, S. K., Quinoa, E., Riguera, R., *J. Org. Chem.*, **1997**, *62*, 7569-7574.

- 40 Seco, J. M., Quinoa, E., Riguera, R., *Tetrahedron: Asymmetry*, **2001**, *12*, 2915-2925.
- 41 Chataigner, I., Lebreton, J., Durand, D., Guingant, A., Villieras, J., *Tetrahedron Lett.*, **1998**, *39*, 1759-1762.
- 42 Ohtani, I., Kusumi, T., Kashman, Y., Kakisawa, H., *J. Am. Chem. Soc.*, **1991**, *113*, 4092-4096.
- 43 Wang, S., McClue, S. J., Ferguson, J. R., Hull, J. D., Stokes, S., Parsons, S., Westwood, R., Fisher, P. M., *Tetrahedron: Asymmetry*, **2001**, *12*, 2891-2894.
- 44 Moncrief, J. W. and Sims, S. P., *J. Chem. Soc., Chem. Commun.*, **1969**, 914-915.
- 45 Phillips, J. B., Molyneux, R. J., Sturm, E., Boekelheide, V., *J. Am. Chem. Soc.*, **1967**, *89*, 1704-1709.
- 46 Ross, S. D., Finkelstein, M., Petersen, R. C., *J. Am. Chem. Soc.*, **1958**, *80*, 4327-4330.
- 47 Mitchell, R. H., Lai, Y-H., Williams, R. V., *J. Org. Chem.*, **1979**, *44*, 4733-4735.
- 48 McKillop, A. and Bromley, D., *J. Org. Chem.*, **1972**, *37*, 88-92.
- 49 Mosnaim, D. and Nonhebel, D. C., *Tetrahedron*, **1969**, *25*, 1591-1595.
- 50 Zhu, G-D., Schaefer, V., Boyd, S. A., Okasinski, G. F., *J. Org. Chem.*, **2002**, *67*, 943-948.
- 51 Straight, A. F., Cheung, A., Limouze, J., Chen, I., Westwood, N. J., Sellers, J.R., Mitchison, T. J., *Science*, **2003**, *299*, 1743-1747.

- 52 Gielen, M., Willem, R., Wrackmeyer, B., *Advanced Applications of NMR to Organometallic Chemistry*, **1996**, John Wiley & Sons, Ltd, England.
- 53 Jackman, L. M. and Lange, B. C., *Tetrahedron*, **1977**, 33, 2737-2769.
- 54 Jackman, L. M. and Szeverenyi, N. M., *J. Am. Chem. Soc.*, **1977**, 99, 4954-4962.
- 55 Davis, F. A., Ulatowski, T. G., Haque, M. S., *J. Org. Chem.*, **1987**, 52, 5288-5290.

CHAPTER 4

RESULTS AND DISCUSSION

SYNTHESIS OF (S)-(-)-BLEBBISTATIN (7) ANALOGUES

4.1. SPECIFICITY AND POTENCY OF (S)-(-)-BLEBBISTATIN (7)

The progress of drug discovery during the past century has been possible thanks to the collaboration between different disciplines such as chemistry, biology, pharmacology and clinical sciences.¹ Organic chemistry also plays an important role in the discovery and synthesis of novel compounds that aid research in the medical sciences. Therefore, as organic chemists, we can synthesise small molecules as both molecular tools for biological studies and drug leads.²

The small molecule (S)-(-)-blebbistatin (7) is a relatively *specific* inhibitor of muscle and non-muscle myosin II (see Chapter 1, Section 1.4.3.1).³ However, it is important that analogues are prepared to increase its *potency* and improve its *specificity* between the myosin II subclasses. Furthermore, a recent study investigating the inhibition of other myosin classes has shown that (S)-(-)-blebbistatin (7) does not inhibit myosins from classes I, V, X, and XV (see for more details Chapter 1, Section 1.4.3.2).⁴ The synthesis and testing of (S)-(-)-blebbistatin (7) analogues may enable inhibitors of these myosin classes to be identified.

The studies described here are designed to enable the synthesis of novel chemical structures based on the blebbistatin core through the use of conventional synthetic methods (solution phase) and new techniques (combinatorial chemistry and parallel synthesis).

4.2. INTRODUCTION OF DIVERSITY INTO THE (S)-(-)-BLEBBISTATIN (7) CORE STRUCTURE

In order to achieve the goals discussed in Section 4.1, the first step involved the development of an efficient route to synthesise (S)-(-)-blebbistatin (7) itself as described in Chapter 2, section 2.1.2.

The second goal was to determine which positions within the (S)-(-)-blebbistatin (7) core structure could be used to introduce structural diversity. (S)-(-)-Blebbistatin

(7) is not an ideal core structure for incorporating structural diversity, due to the lack of functional groups and also the presence of seven quaternary carbon atoms. However, our analysis identified that 6 sites and 1 ring size could potentially be modified (Figure 97).



Figure 97. Different sites on the (*S*)-(-)-blebbistatin (7) core structure to be modified; a) Hydroxyl group (R^1), b) *N*-phenyl ring (R^2), c) Aromatic ring (R^3), d) Carbonyl group (R^4), e) Oxidation state of carbonyl and amidine and f) Pyrrolidine ring size (n).

4.3. PREPARATION OF (*S*)-(-)-BLEBBISTATIN (7) ANALOGUES SUBSTITUTED IN THE AROMATIC RING (R^3)

This section is focused on the synthesis of small molecule analogues of (*S*)-(-)-blebbistatin (7) substituted in the aromatic ring (R^3). The substituents present on an aromatic ring (*e.g.* electron-donating (methyl group) or electron-withdrawing (halogen atom, nitro groups) can have significant effects on the biological activity of a molecule.⁵ Early examples of this were reported in the 1960s and 1970s, where the influence of the substituent on the activity was found to be mainly dependent of lipophilic, electronic and steric factors.^{6, 7, 8, & 9} Figure 98 summarises the analogues that have been prepared including an analogue with an unsubstituted aromatic ring, analogues with the position of the methyl group varied, and an analogue incorporating an electron withdrawing group (nitro).

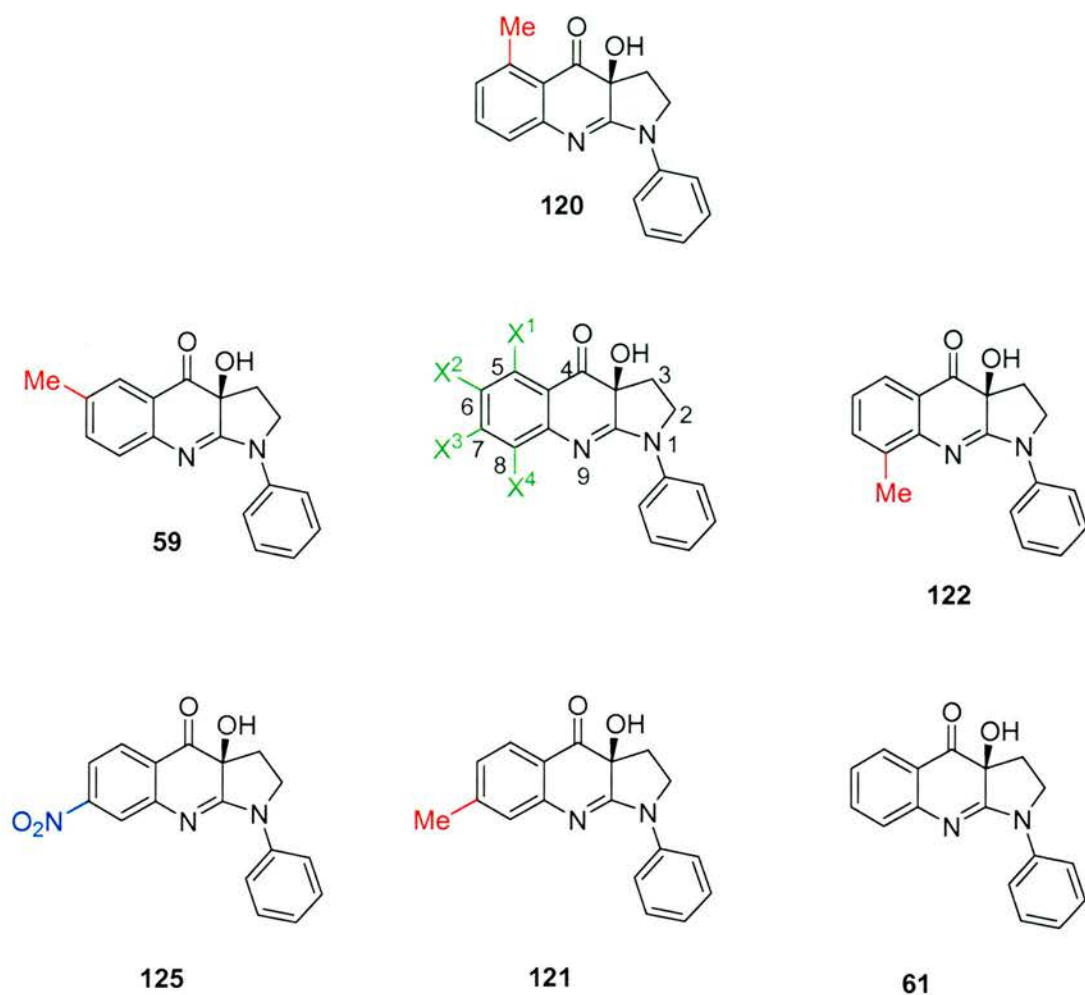


Figure 98. Analogues of (*S*)-(-)-blebbistatin (**7**) modified in one of the aromatic rings (R^3).

It is synthetically possible to vary the position of the substituents around the aromatic ring (R^3), because the starting anthranilate esters are relatively easy to prepare from commercially available anthranilic acids. The route followed for the synthesis of the methyl analogues of (*S*)-(-)-blebbistatin (**7**) was the same as described previously for the synthesis of (*S*)-(-)-blebbistatin (**7**) itself (Chapter 2, Section 2.1.2) (Figure 99).

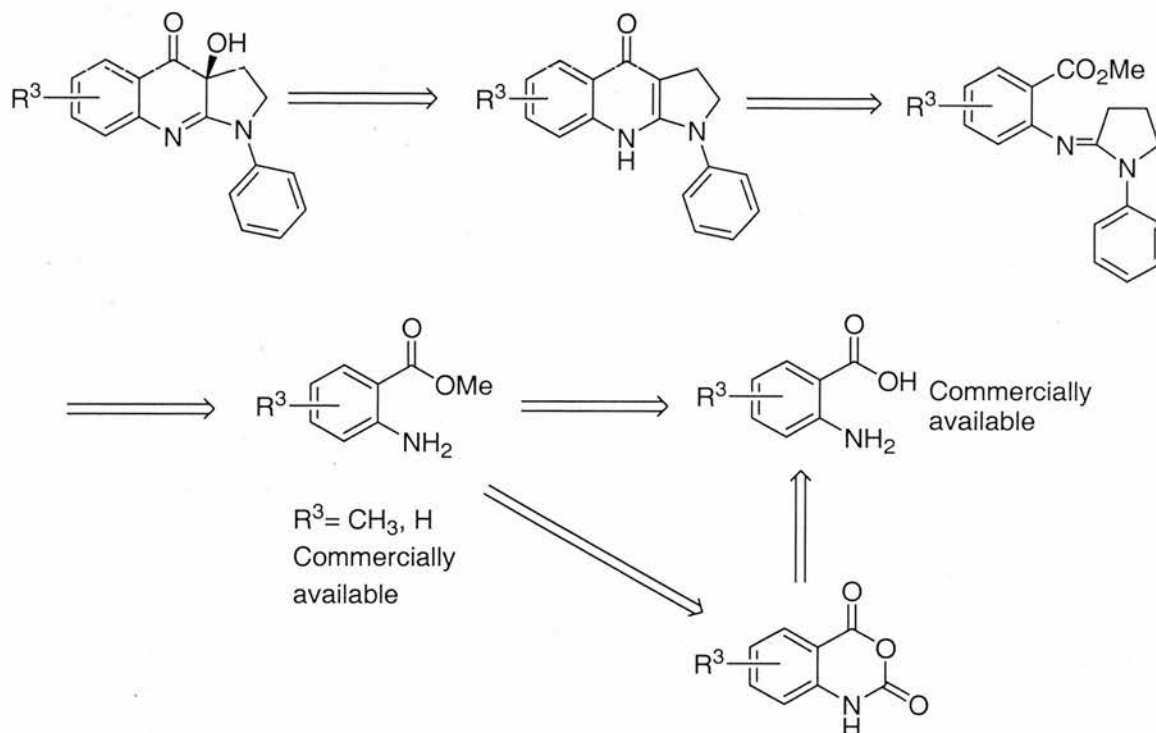


Figure 99. Retrosynthetic analysis of analogues of (*S*)-(-)-blebbistatin (**7**).

4.3.1. Synthesis of analogues with $R^3 = \text{Me}$

During the synthetic studies used to prepare these analogues, several interesting variations in the chemical transformations were observed across the series. The esterification of the commercially available acids was carried out for 2-amino-5-methyl benzoic acid (**26**), 2-amino-3-methyl benzoic acid (**147**) and 2-amino-4-methyl benzoic acid (**148**) in good yields (94%, 69%, and 84%, respectively). In addition, the methyl anthranilate (**33**) was commercially available and in the case of the methyl 6-methylantranilate (**149**), was previously prepared by Dr. Stephen Patterson in our laboratory. The coupling reaction between anthranilates and lactam **28** was carried out as described previously (Chapter 2, Section 2.1.3). The reaction afforded the corresponding amidines (Figure 100) in variable yields (from 14% to 41%). Table 7 summarises the results obtained.

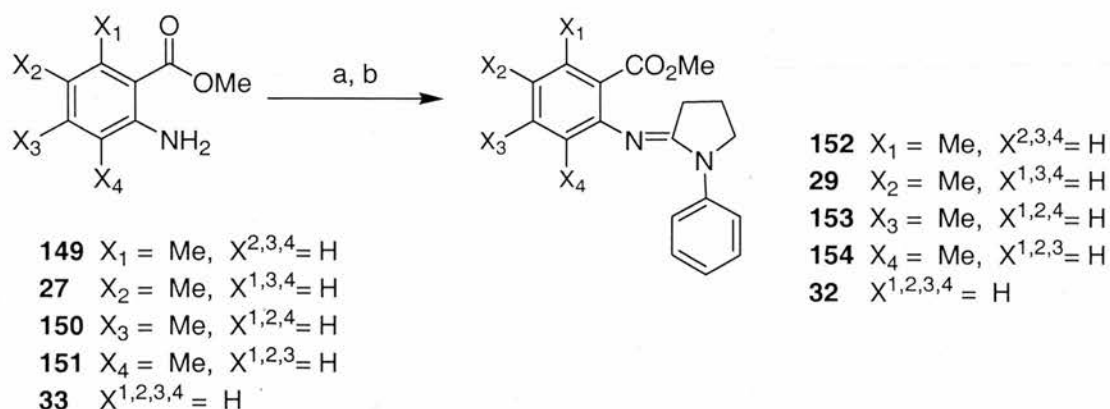


Figure 100. Synthesis of amidine analogues. Reagents and conditions: a) 1-phenyl-2-pyrrolidinone (**28**) (1.1 equiv), POCl_3 (1.0 equiv), DCM, RT, 3 hours, b) anthranilate esters (1.0 equiv), DCM, 40 °C, 16 hours.

Entry	Product	Time (h)	(ester) equiv ⁱ	POCl_3 equiv ⁱ	Lactam (28) equiv ⁱ	Yield (%)
1	152	16	1.0	1.0	1.1	28
2	29	16	1.0	1.0	1.1	41
3	153	16	1.0	1.0	1.1	24
4	154	16	1.0	1.0	1.1	14
5	32	16	1.0	1.0	1.1	26
6	154	72	1.0	1.0	1.1	52

Table 7. The table summarises the amidine forming coupling reactions for the different analogues. The amount of reagents are given in equivalentsⁱ and the time of the reaction in hours. Reagents and conditions: a) lactam **28**, POCl_3 , DCM, RT, 3 hours, b) anthranilate ester, DCM, 40 °C, 16 hours.

The position of the methyl group on the ring (R^3) does influence the yield of the coupling reaction. Electron-donating substituents in the *ortho* and *para* positions relative to the anthranilate nitrogen atom would be expected to increase the nucleophilicity of the aniline nitrogen atom and therefore, potentially increase the yield of the reaction. This is the case for anthranilate **27** which gives the best yield for the coupling reaction to form **29**. Surprisingly, formation of **154** occurred in significantly lower yield (14%), using the standard conditions. When the reaction was repeated but

run for 72 hours rather than 16 hours the yield increased considerably to 52% (entry 6). A steric effect due to the 3-methyl group presumably explains this observation (the aniline nitrogen is in this case double substituted in the *ortho* positions). When the methyl group is *meta* to the nitrogen functionality (anthranilates **149** and **150**) or when the unsubstituted anthranilate **33** is used, the yield for the coupling reactions is low (entries 1, 3 and 5).

The cyclisation of the amidines **152**, **29**, **153**, **154** and **32** to give the corresponding quinolones **136**, **24**, **137**, **138** and **31**, occurred in good yields (84-95%) for all the analogues (Figure 102). Interestingly the cyclisation of **154** required 12 hours at room temperature whereas **152**, **29**, **153** and **32**, were complete at 0 °C in 3 hours. However, a steric effect between the 3-methyl group and the N-metal group (N-Li) (**155a**) could explain this observation (Figure 101). Due to the presence of a single bond on the aniline nitrogen, rotation is possible resulting in the establishment of an equilibrium with the species **155b**. **155b** is more favoured due to the fact that the steric hindrance is reduced between the methyl and N-Li groups.

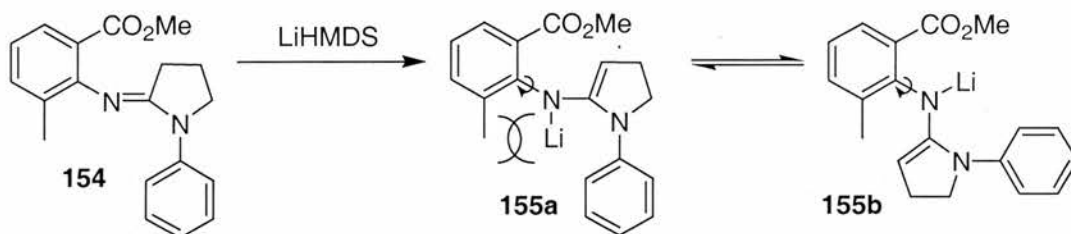


Figure 101. Steric effects during the formation of 3-methyl quinolone **154**.

Purification of the crude material was performed by flash column chromatography, eluting with neat ethyl acetate, due to the polarity of the quinolones **136**, **24**, **137**, **138** and **31**. It is worth noting that the samples were stable to any oxidative decomposition when they were stored under argon for long periods of time.

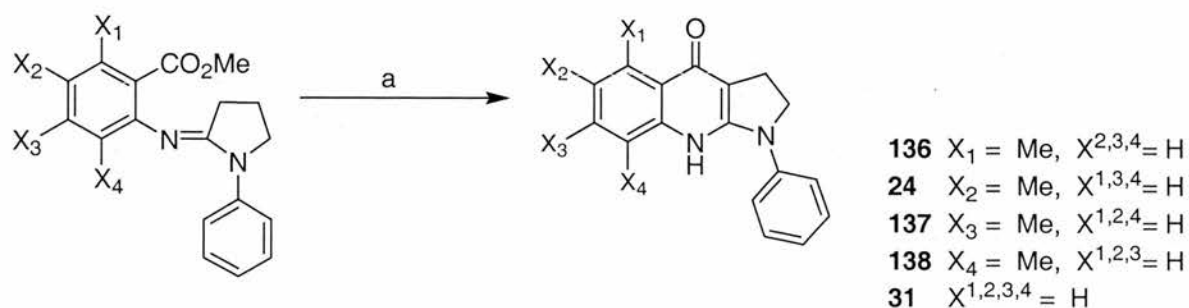


Figure 102. Synthesis of Quinolone analogues. Reagents and conditions: a) LiHMDS (2.5-3.0 equiv), THF, 0 °C-RT, 3.0-12 hours, 84-95%.

^1H NMR analysis of the quinolones **136**, **24**, **137**, **138** and **31** was carried out in d^8 -THF (Figure 103). However, ^{13}C NMR analysis proved challenging due the long relaxation times associated with several of the quaternary carbon atoms. Therefore the ^{13}C signals for quaternary carbons were either very weak or not observed. For example Figure 104 shows the ^{13}C NMR spectra for **138**. As can be seen the ^{13}C NMR signals for the quaternary carbons (C8a and C9a) were very weak after 5 hours of NMR data collection (number of scans 6000 and a delay of 1.5 seconds). Therefore, it was necessary to use alternative NMR techniques to ensure that weak peaks present in the ^{13}C spectrum, did not correspond to any minor impurities in the sample. The use of 2D NMR experiments such as ^1H - ^{13}C COSY spectra (HSQC: Heteronuclear Single Quantum Coherence, Figure 105) and long-range ^1H - ^{13}C COSY spectra (HMBC: Heteronuclear Multiple Bond Connectivity, Figure 106) proved helpful.

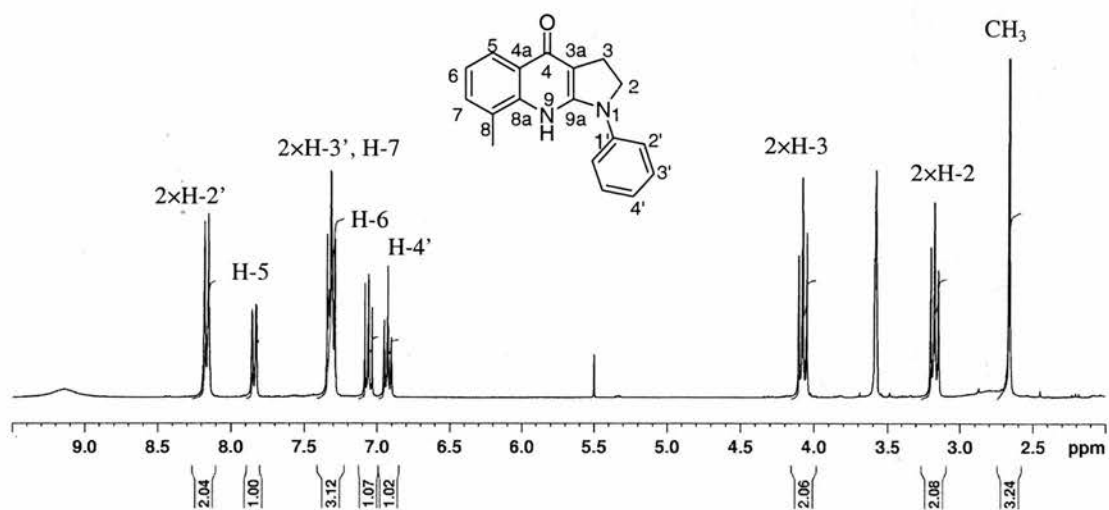


Figure 103. ^1H NMR of **138** in deuterated d^8 -THF (chemical shifts $\delta=3.57$ and 1.72 ppm (not shown)).

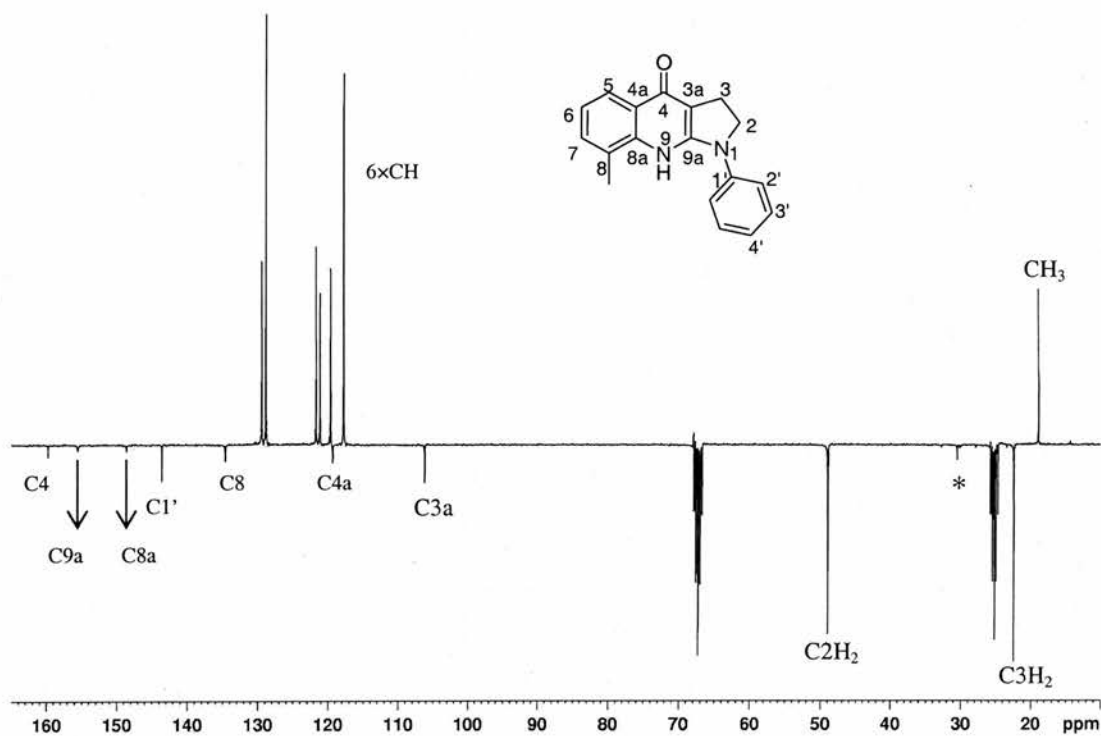


Figure 104. ^{13}C NMR of **138** in deuterated d^8 -THF (chemical shift $\delta=25.2$ and 67.2 ppm). *Signal corresponding to a minor impurity.

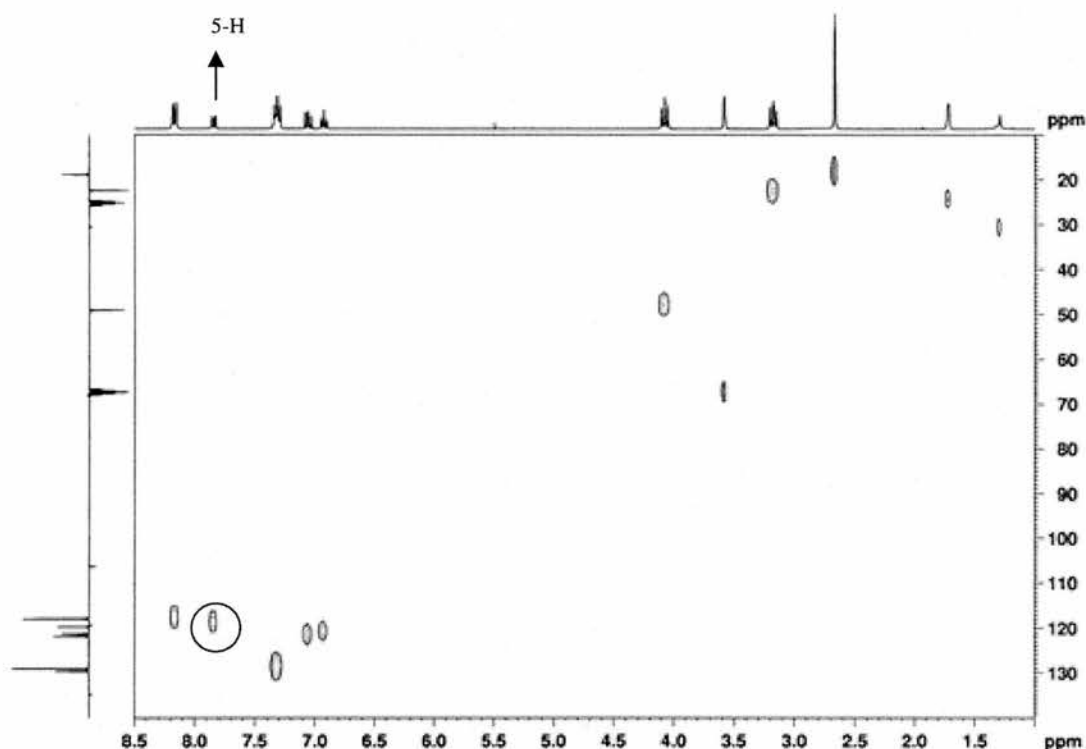


Figure 105. HSQC spectrum of **138**. ^1H chemical shifts (ppm) are on the (x)-axis and ^{13}C chemical shifts (ppm) are on the (y)-axis. This ^{13}C - ^1H HSQC spectrum is used to correlate an identified proton (*e.g.* 5-H) with the carbon to which is directly attached (*e.g.* 5-C).

Finally, the asymmetric hydroxylation of the quinolones gave the desired analogues of (*S*)-(-)-blebbistatin (**7**) in an analogous manner to that described in Chapter 3, Section 3.1.3. All the reactions were carried out at $-10\text{ }^\circ\text{C}$ with stirring for 16 hours. Davis oxaziridine **82** was used as the oxidising reagent in all of these reactions. The reactions afforded the desired compounds in good yields (63-87%) and variable enantiomeric excess. The results of these experiments have been discussed in detail in Chapter 3, Section 3.3. In addition, the biological activity of the different analogues **139**, **7**, **140**, **141** and **67** has been determined and is discussed in Chapter 5, Section 5.3.

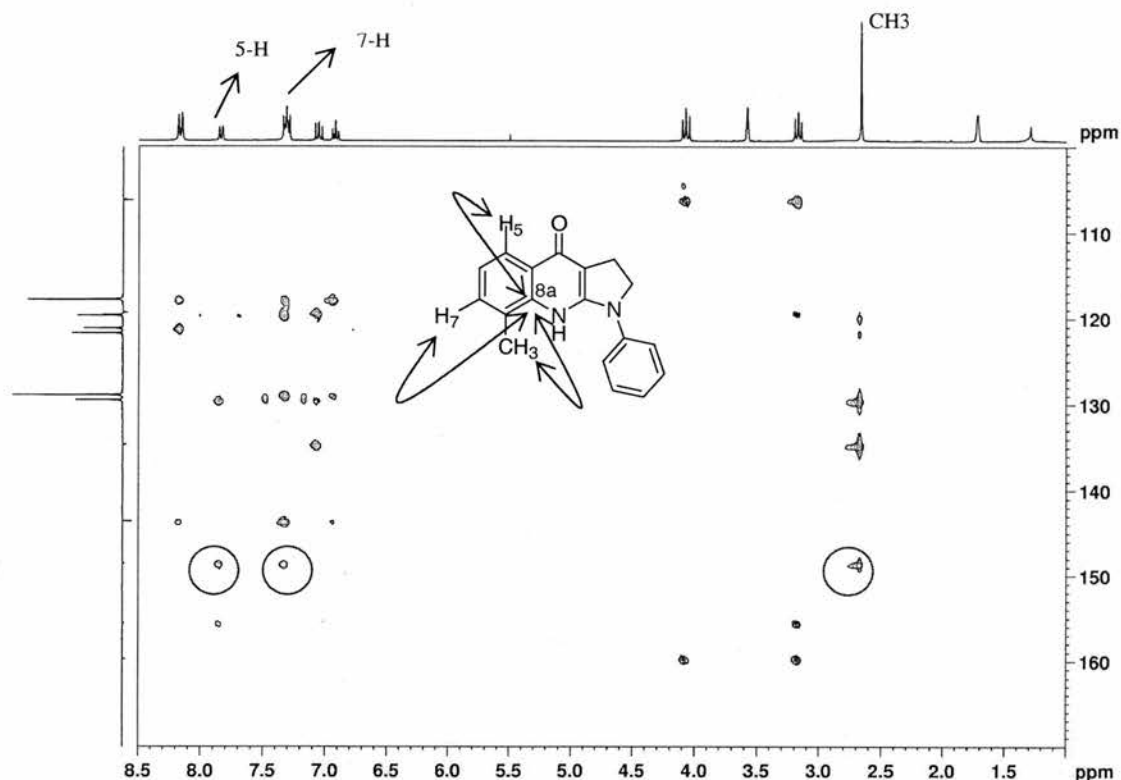


Figure 106. HMBC spectrum of **138**. ^1H chemical shifts are on the (x)-axis and ^{13}C chemical shifts are on the (y)-axis. This kind of spectrum is of great importance for the assignment of quaternary carbons as the proton is correlated to carbon atoms separated by two or three bonds. Here is shown the assignment of the quaternary carbon C-8a. This carbon is correlated by three bonds to two identified protons in the aromatic region (5-H and 7-H) centred at 7.84 and 7.27-7.36 ppm. In the same way the carbon is correlated to the methyl group (δ 2.65 ppm) by three bonds. Therefore the ^{13}C peak corresponding to C-8a will appear at 148.7 ppm, consistent with a weak signal in the ^{13}C NMR spectrum (Figure 104).

4.3.2. Preparation of an analogue of (*S*)-(-)-Blebbistatin (**7**) incorporating a nitro substituent in the aromatic ring (R^3)

This section is focused on the synthesis of an analogue of (*S*)-(-)-blebbistatin (**7**) with a nitro substituent at the C-7 position of the aromatic ring (R^3). A microscopy-based study¹⁰ recently identified a limitation in the usefulness of (\pm)-blebbistatin (**18**) in live-cell imaging experiments. These types of studies normally involve the irradiation of cells with light of a wavelength between 420-490 nm. It was found that (\pm)-blebbistatin (**18**) degrades when illuminated for long periods of time with filtered light (450-490 nm). The degradation of **18** afforded inactive products devoid of inhibitory activity. This degradation was proposed to occur *via* short-lived cytotoxic

intermediates which caused irreversible damage to the cells. A study of the UV-vis absorption spectrum of a sample of (\pm)-blebbistatin (**18**) was carried out in order to show the appearance of photodegradation products as a function of irradiation wavelength and time in phosphated-buffered saline (PBS) solution (Figure 107).¹⁰

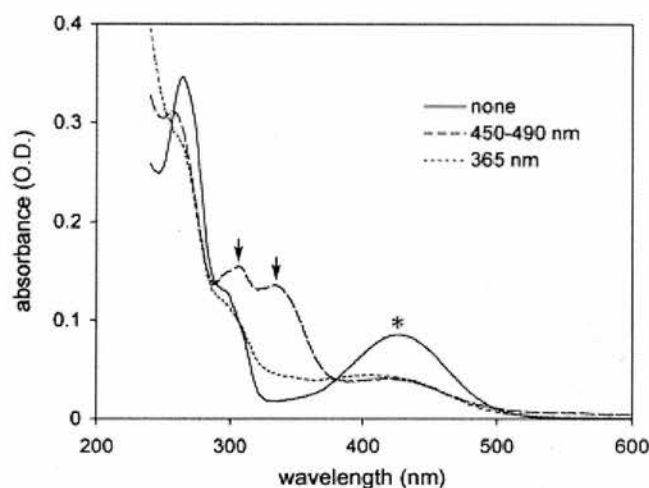


Figure 107. Absorption spectra of (\pm)-blebbistatin (**18**) and products formed following photodegradation. The UV-vis spectra were recorded using a 20 μ M solution of (\pm)-blebbistatin (**18**) in PBS and illumination for 1 hour with 365 or 450-490 nm light. The absorption spectra of blebbistatin without irradiation, showed strong absorbances at 265 nm and at 430 nm. The asterisk indicates that absorbance at 430 nm is decreased by illumination and the two arrows show the new peaks which appeared after illumination at 450-490 nm.¹⁰

It was also reported in the literature¹¹ that (\pm)-blebbistatin (**18**) is itself fluorescent, being a problem for its use in fluorescence microscopy techniques on live cells. This can be explained by the fact that when **18** is excited at 440 nm, light is subsequently emitted within the wavelength range (520-570 nm), which corresponds to the tag protein utilised in these experiments. To facilitate fluorescence imaging of live cells, the preparation of an analogue of (\pm)-blebbistatin (**18**) with optimised fluorescence emission properties and retained biological activity was envisaged.

It was proposed that the incorporation of a nitro group into the chromophore of **7** would modify its fluorescence properties and hence improve its photostability. It was envisaged that analogue **160** could therefore be used as a tool in biological experiments where (*S*)-(-)-blebbistatin (**7**) could not. It was hoped that the incorporation of the nitro functional group would not result in loss of biological activity. The biological testing of

(*S*)-(-)-blebbistatin (**7**) analogues had demonstrated that methyl substitution at C-7 could be tolerated (Chapter 5, Section 5.3). Therefore, a sample of (*S*)-(-)-7-nitroblebbistatin (**160**) was prepared utilising the synthetic methodology described in Chapter 2, section 2.1.2. (Figure 108).

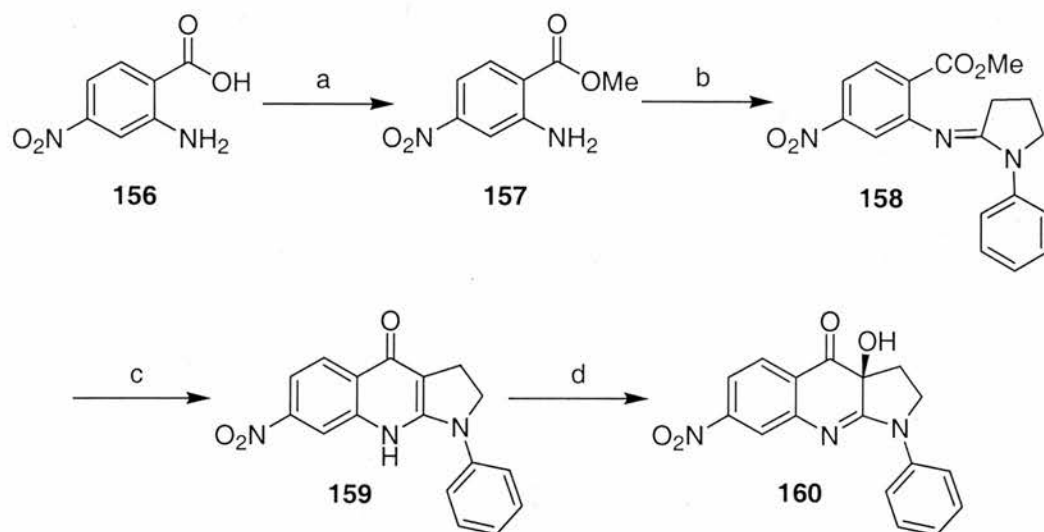


Figure 108. Preparation of a nitro containing analogue (**160**). Reagents and conditions: a) MeOH, H₂SO₄, 80°C, 96 hours, 81%; b) i) **28** (1.1 equiv), POCl₃ (1.0 equiv), DCM, RT, 3 hours; ii) **157** (1.0 equiv), DCM, 40°C, 72 hours, 22%; c) LiHMDS (2.5 equiv), THF, -78°C to 0°C, 96 hours, 44%; d) i) LiHMDS (1.2 equiv), THF, -78°C, 30 min; ii) **82** (3.1 equiv), THF, -10°C, 32 hours, 31%, 76% *ee*.

The synthetic route started with the synthesis of 2-amino-4-nitrobenzoic acid methyl ester (**157**) from commercially available 2-amino-4-nitrobenzoic acid (**156**). The nitro ester was then reacted to afford the desired amidine **158** in low yield. The coupling reaction was followed by TLC analysis, which showed no formation of **158** within 48 hours. This reaction was then left to reflux until the product was detected by TLC (72 hours). The cyclisation step was carried out over four days at 0 °C to give the nitroquinolone analogue **159** in low yield (44%). Finally the hydroxylation to give nitroblebbistatin analogue **160** was carried out in 31% yield. The time of the reaction and amount of the Davis reagent **82** were increased to 32 hours and 3.1 equivalents respectively. The enantiomeric excess of the reaction was measured by chiral HPLC giving a value of 76% *ee*. Interestingly, the order of elution of the two enantiomers from the chiral HPLC was different compared with (*S*)-(-)-blebbistatin (**7**) (see Experimental Section). In the case of **160**, the major enantiomer eluted second

($t_R = 11.22$ min). This result was supported by the fact that the sign of the optical rotation was negative value ($[\alpha]_D^{25} = -418$, in a concentration of 0.05 g/100mL in dichloromethane) consistent with the previous results for **7**. In addition, attempts to recrystallise the nitro analogue **160** afforded highly optically enriched **160** (>90% *ee*).

An optically enriched sample of **160** (76% *ee*) was then used in experiments to study its fluorescence properties. These experiments were carried out by Dr. Stephen Patterson in our laboratory and in the School of Physics. The UV-vis absorption spectra were recorded using a spectrophotometer and the measurements were recorded at a sample concentration of 10 mg L⁻¹, in HPLC grade methanol. The samples were excited at wavelengths of 420, 440, 460 and 488 nm in order to obtain fluorescence emission spectra.

From these experiments it was found that when **160** was excited at 440 nm, the fluorescence emission was significantly reduced compared to **7** (Figure 109). Therefore, nitro-blebbistatin analogue **160** may prove useful in fluorescence microscopy experiments.

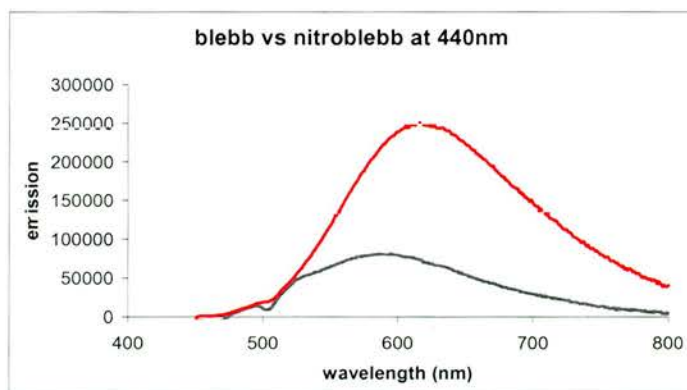


Figure 109. Fluorescence emission spectrum of (*S*)-(-)-blebbistatin (**7**) (red line) and its nitro-analogue **160** (black line) in the wavelength range 450-800 nm after excitation at 440 nm.

It was also found that **160** was stable when irradiated for 3 hours at wavelengths typically used for the fluorescence-based imaging of live cells (420-490 nm) (Figure 110B) whereas (*S*)-(-)-blebbistatin (**7**) over the same period of time, decomposed completely (Figure 110A), consistent with the literature reports.¹⁰

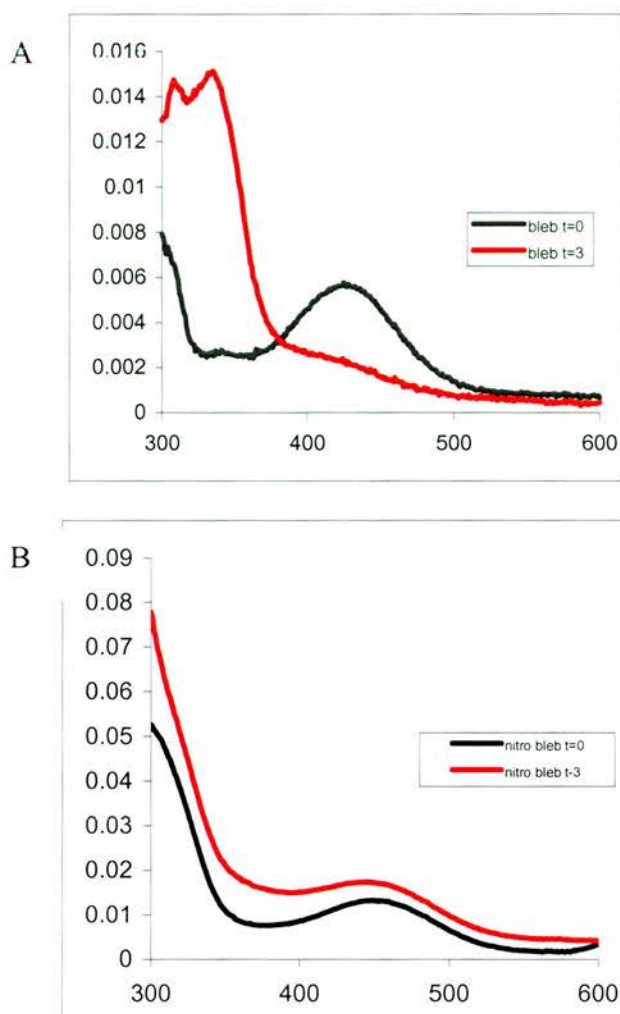


Figure 110. A) UV spectra of (*S*)-(-)-blebbistatin (**7**) in PBS (black line). The UV spectra of **7** after exposure to filtered light (436 and 510 nm) for 3 hours (red line). B) UV spectra of **160** in PBS (black line) and **160** after exposure to filtered light (436 and 510 nm) for 3 hours (red line).

In conclusion, it was found that the nitro analogue **160** can be considered as an important tool to be used in live-cell imaging experiments, where the use of (*S*)-(-)-blebbistatin (**7**) was limited. In addition, an optically enriched sample of **160** retains the biological activity against non-muscle myosin II ATPase, although its inhibitory activity was slightly lower than that of (*S*)-(-)-blebbistatin (**7**) (Chapter 5, Section 5.2).

4.3.3. Summary section

It is concluded that variations in the position of the methyl group around the aromatic ring (R^3) were possible. The synthesis of each analogue was achieved with an overall yield for the four step sequence of 16-28% except for the nitro analogue **160**,

which was prepared in an overall yield of 2.4%. Additionally the incorporation of a nitro functionality into the chromophore of **7** tunes its fluorescence properties, resulting in an important tool for the study of biological systems.

4.4. INTRODUCTION OF DIVERSITY AT THE QUATERNARY CARBON (3a) POSITION

Prior to this work nothing was known about the chemistry that could be carried out at the R¹ position of the blebbistatin core structure. In addition there have been no reports regarding the effect of substitution at this position on the biological activity. Therefore, the results in this section describe attempts to incorporate different functional groups at the C-3a position (Figure 111). The results from biological studies using these analogues are presented in Chapter 5.

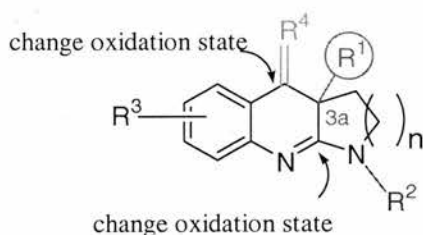


Figure 111. Sites of (*S*)-(-)-blebbistatin (**7**) to be modified.

4.4.1. Incorporation of Halogens at the R¹ position

The studies described in this section of the thesis involve the incorporation of halogens (fluorine, chlorine and bromine) at the C-3a position. The three target molecules are shown in Figure 112.

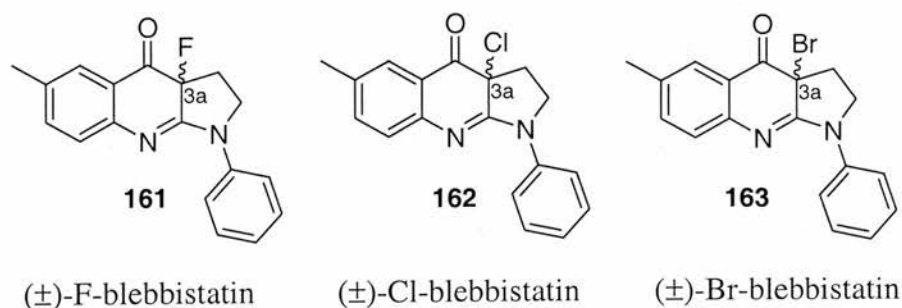


Figure 112. Structures of halogen-containing analogues of blebbistatin (**7**).

4.4.1.1. Synthesis of 3a-Chloro analogue (**162**)

The classic reagents to prepare an alkyl chloride from an alkyl alcohol include oxalyl chloride, thionyl chloride, phosphorous oxychloride, phosphorus trichloride and phosphorus pentachloride.^{12,13} Therefore, our initial approach to prepare the chloro analogue (**162**) used oxalyl chloride (Figure 113).

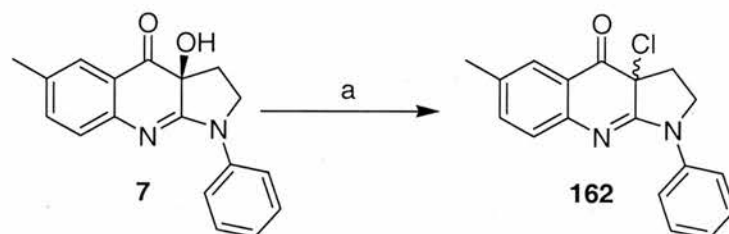


Figure 113. Synthesis of **162**. Reagents and conditions: a) Oxalyl chloride (5.0 equiv), DMAP (catalytic amount), Et₃N, DCM, RT, 2 hours, 62%.

Optically enriched (*S*)-(-)-blebbistatin (**7**) (86% *ee*) was treated with an excess of oxalyl chloride (5 equivalents) in the presence of base and a catalytic amount of DMAP. The 3a-chloro analogue (**162**) was isolated from the reaction after column chromatography in 62% yield. The mechanism of the reaction can be explained by nucleophilic substitution of the activated tertiary alcohol (as an ester) by the halide (chloride) ion (Figure 114). If the reaction were to proceed *via* a S_N2 mechanism, it would be expected to proceed with inversion of stereochemistry. The measurement of the optical rotation of **162** was therefore important in rationalising the reaction mechanism. The value for the specific rotation of **162** was zero ($[\alpha]_D^{25} = 0$, in a concentration of 0.1 g/100mL in dichloromethane), implying that the reaction occurs *via* an S_N1 mechanism. It is worth noting that the carbocation that is formed is tertiary and therefore relatively stable. However, the presence of the electron-withdrawing carbonyl and amidine groups would be expected to destabilise the carbocation.

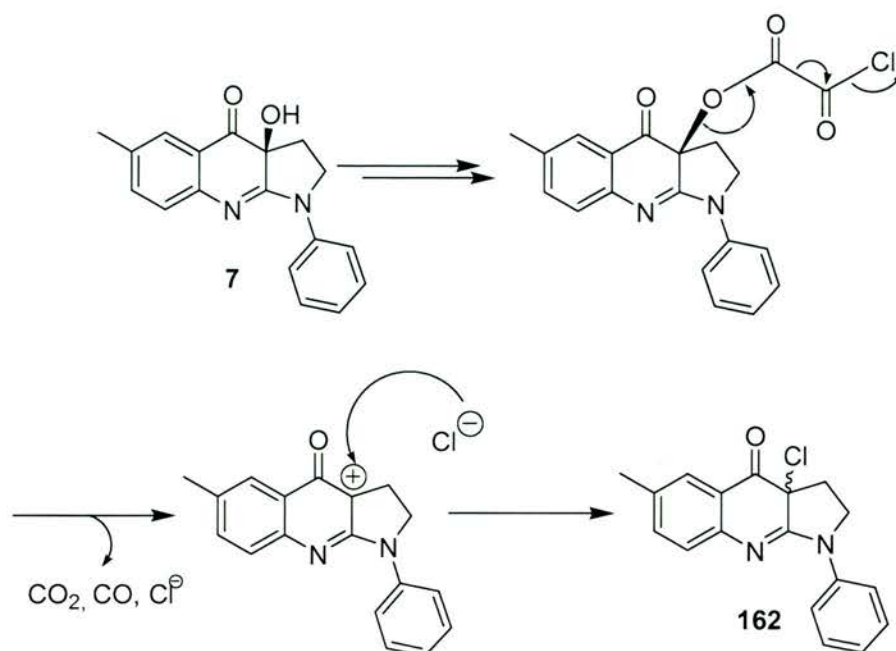


Figure 114. Proposed mechanism for the formation of **162** via an S_N1 mechanism.

1H NMR and MS analysis were consistent with the formation of **162**. The structure of this compound was also confirmed by X-ray crystallographic analysis (Figure 115).

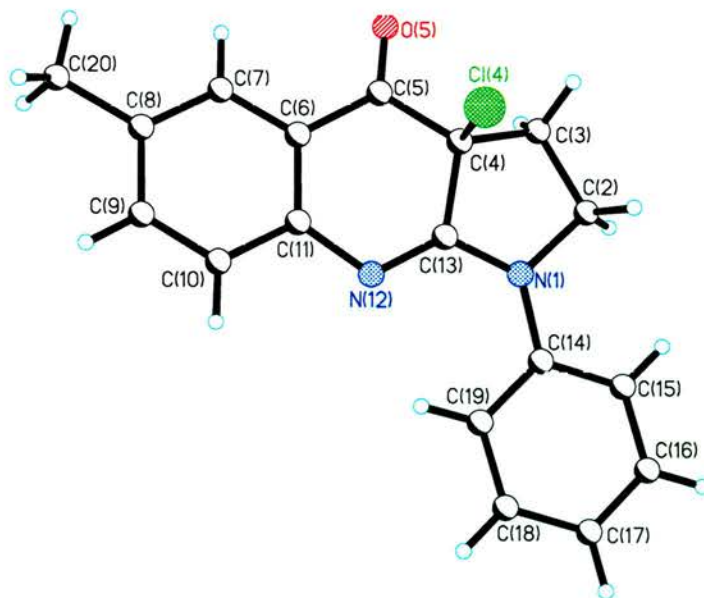


Figure 115. X-ray of 3a-chloro analogue **162**.

Interestingly, during our attempts to derivatise the tertiary alcohol functionality in (*S*)-(-)-blebbistatin (**7**) with Mosher's acid chloride¹⁴ (**103**) (Chapter 3, Section 3.2.1), **162** was isolated in 47% yield (Figure 116). This reaction was carried out by treating optically enriched (*S*)-(-)-blebbistatin (**7**) (86% *ee*) with Mosher's acid chloride (*R*)-(-)- α -methoxy- α -(trifluoromethyl)phenylacetylchloride) (**103**). The Mosher's reagent used in the reaction was either commercially available or synthesised from the (*S*)-(-) Mosher's acid **131**.¹⁵ A possible explanation could be that an ester derivative of (*S*)-(-)-blebbistatin (**7**) could have been formed during the reaction although the presence of HCl led to the nucleophilic substitution by chlorine (see mechanism shown in Figure 114) forming 3 α -chloro analogue (**162**). A ¹³C NMR spectrum of commercially available **103** did not show the presence of oxalyl chloride as an impurity.

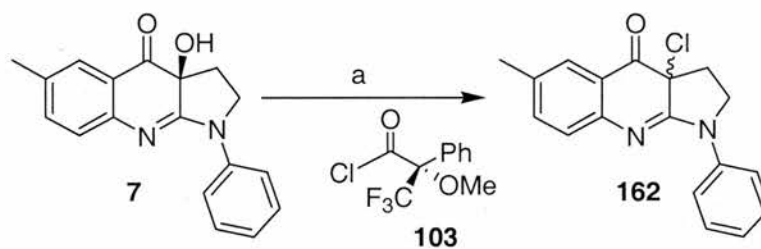


Figure 116. Synthesis of **162**. Reagents and conditions: a) DMAP (catalytic amount), Et₃N (25 equiv), (*R*)-(-)-Mosher acid chloride (**103**) (25 equiv), DCM, RT, 2 hours, 47%.

The synthesis of **162** was also achieved by following a literature procedure for the chlorination of quinolones of type **164** (Figure 117).¹⁶

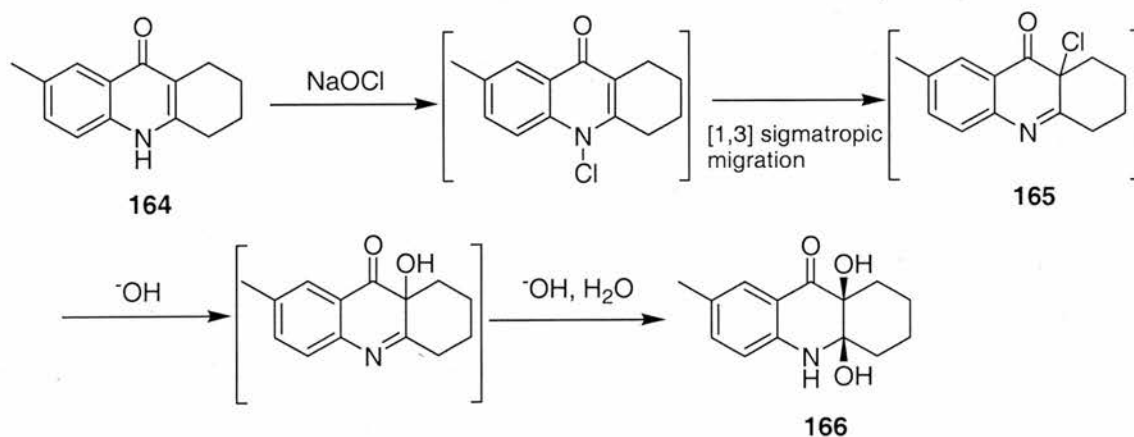


Figure 117. Proposed mechanism for the synthesis of the α -chloro ketone intermediate **165**.^{16, 17}

It was suggested that α -chloro ketone **165** is an intermediate formed during the oxidation of 7-methyl-1,2,3,4-tetrahydro-9(10*H*)-acridinone (**164**) to *cis*-4a,9a-dihydroxy-1,2,3,4,4a,9a-hexahydro-7-methyl-9(10*H*)-acridinone (**166**) on treatment with sodium hypochlorite.^{18,19} The isolation of the chloro analogue **165** was not achieved in their study.¹⁷

This reaction was originally considered of relevance to the synthesis of (\pm)-blebbistatin (**18**) itself. The preparation of the chloro analogue **162** from quinolone **24** followed by nucleophilic substitution of the Cl by OH (favoured by the neighbouring C=O group),¹⁷ could afford racemic (\pm)-blebbistatin (**18**) (Figure 118).

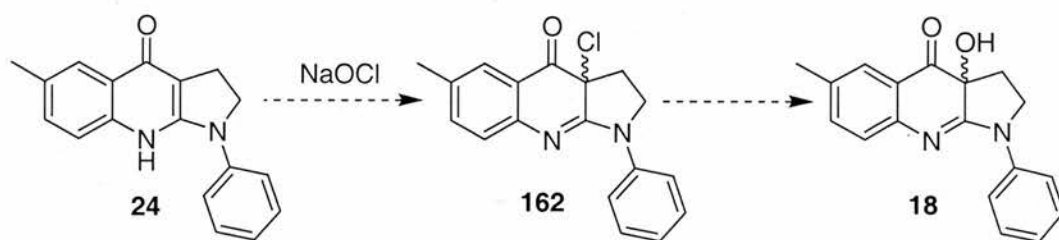


Figure 118. Proposed hydroxylation of quinolone **24** on route to (\pm)-blebbistatin (**18**).

It was decided then to attempt both the hydroxylation and chlorination of quinolone **24**. Therefore a solution of quinolone **24** was treated with sodium hypochlorite (NaOCl), at room temperature for 72 hours. TLC analysis of the reaction mixture indicated that the main component of the reaction was starting material **24**, although a new red spot was observed along with other small impurities. The red spot had an identical R_f value to authentic 3a-chloro blebbistatin (**162**). No spot which could correspond to (\pm)-blebbistatin (**18**) was observed when the crude reaction was purified by flash column chromatography. Compound **162** was finally obtained pure after two crystallisations with ethyl acetate/hexane, although the yield was low (21%). ¹H NMR and MS analysis confirmed the structure of **162** (Figure 119).

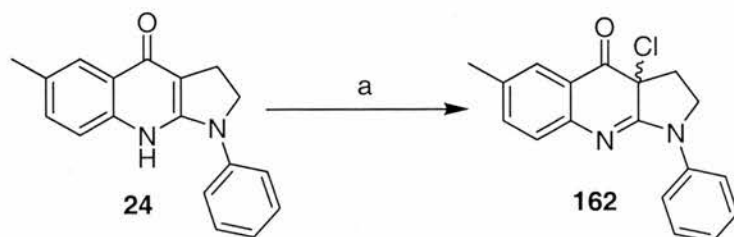


Figure 119. Synthesis of **162** via quinolone **24**. Reagents and conditions: a) NaOCl (24 equiv), THF, RT, 72 hours, 21%.

However, later attempts carried out by Dr. Stephen Patterson in our laboratory, led to the isolation of both, 3a-chloro blebbistatin (**162**) and (\pm)-blebbistatin (**18**) (Figure 120). The reaction was carried out with a solution of quinolone **24** in methanol and water which was treated with sodium hydroxide, followed by addition of the chlorinating reagent sodium dichloroisocyanurate (**167**). The reaction afforded **162** and **18** in 77 and 21% yield, respectively.

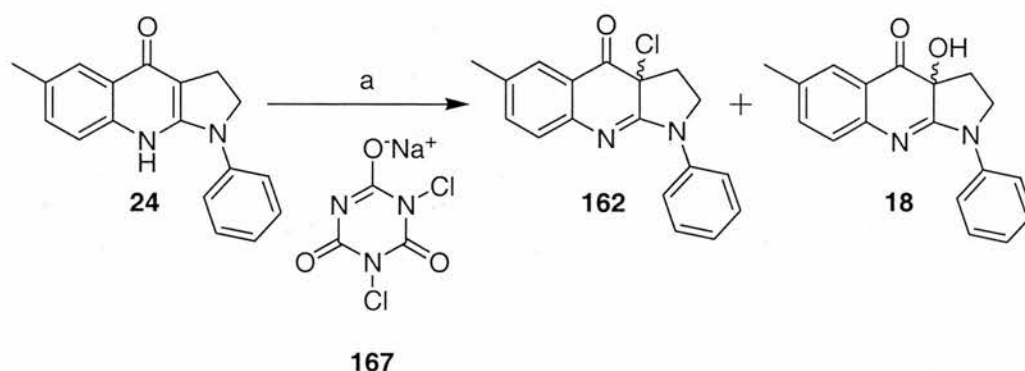


Figure 120. Synthesis of **162** and **18** from quinolone **24**. Reagents and conditions: a) **167** (0.5 equiv), 2 M NaOH, 2:1 MeOH/H₂O, RT, 40 min, 84% (**162**), 24% (**18**).

4.4.1.2. Synthesis of 3a-Fluoro analogue (**161**)

After successful incorporation of the chlorine atom, it was decided to continue the synthesis of new analogues with the incorporation of another halogen, fluorine.

The introduction of fluorine into organic molecules has been widely studied and can induce significant effects on the physical, chemical and biological properties of the molecules.^{20, 21} As the hydroxyl group of blebbistatin is incorporated by an electrophilic oxidising reagent, it was postulated that a fluorine atom could be introduced by an analogous electrophilic fluorinating reactant.

The most common electrophilic fluorinating reagents used in organic chemistry are perchloryl fluoride,²² O-F compounds such as trifluoromethyl hypofluorite,²³ xenon difluoride,²⁴ and fluorine itself.²⁵ However, selective fluorination can also be carried out with the more effective and user friendly²¹ reagent, Selectfluor™ (F-TEDA-BF₄) a commercially available *N*-fluoroammonium salt (**168**) (Figure 121).

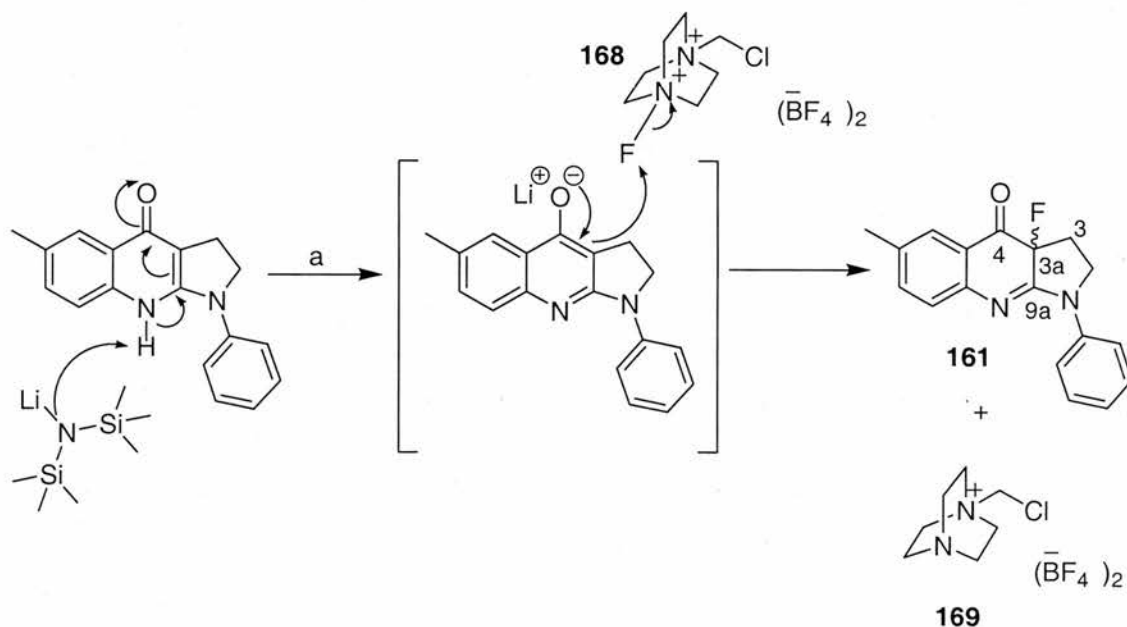


Figure 121. Synthesis of 3a-fluoroblebbistatin **161**. Reagents and conditions: a) i) LiHMDS (1.2equiv), Selectfluor™ (**168**) (2.0 equiv), THF, -78 °C, ii) RT, 24 hours, 96%.

The fluorination was found to be straightforward and was performed as follows (Figure 121). The reaction first involved the formation of the lithium enolate at -78 °C using lithium bis(trimethylsilyl)amide. Selectfluor™ was added after 30 minutes and the reaction mixture was warmed to room temperature. The reaction was then stirred for 24 hours. After purification by flash column chromatography, **161** was isolated in excellent yield (96%). ¹H NMR and ¹⁹F NMR analysis, in CDCl₃ confirmed the structure of **161**. The presence of fluorine in the molecule was detected by ¹⁹F NMR (doublet of doublets, coupling constants of $J=42$, $J=21$, $\delta_{\text{F}}=-149.56$ ppm). In the case of ¹H NMR, the diastereotopic protons gave complicated multiplets due to the fact that there is a coupling between the fluorine atom and the protons. The ¹³C NMR spectrum showed a coupling between carbon and fluorine for the following carbons 3-C ($^2J=24.9$ Hz), 3a-C ($^1J=174$ Hz), 9a-C ($^2J=17.1$ Hz) and 4-C ($^2J=19.9$ Hz). The measurement of the optical rotation **161** gave a value of zero, as expected. In addition, chiral HPLC analysis was carried out in order to determine the conditions for the separation of the two enantiomers corresponding to the racemic mixture of **161** (Figure 122).

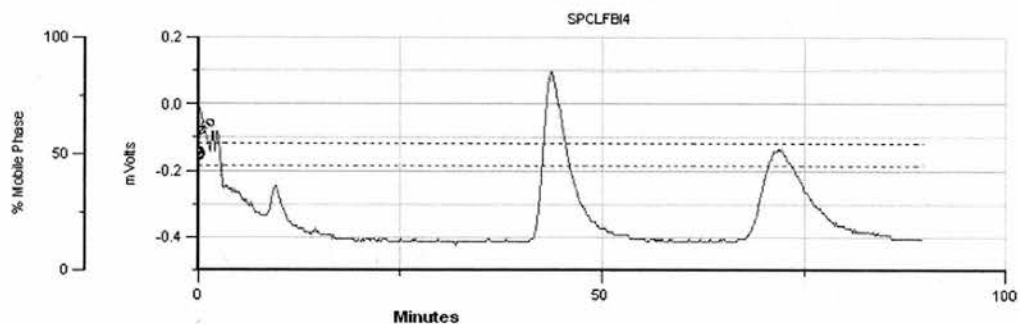


Figure 122. Chiral HPLC chromatography of 3a-fluoro analogue **161**. Conditions: Daicel Chiralpak AD-RH, Acetonitrile/Water 45:55, flow rate 0.9 mL min^{-1} , $\lambda=254 \text{ nm}$. A) Chromatogram of **161**, shows two peaks corresponding to a 1:1 mixture of enantiomers, first enantiomer $t_R=44 \text{ min}$. and second enantiomer $t_R=72 \text{ min}$.

It is interesting to note that when the ^1H NMR spectrum of **161** was recorded in CD_3OD , it showed the presence of a series of extra peaks in both the aliphatic and aromatic regions. Taking into account the possibility that nucleophiles can add to two different sites in the 3a-fluoro analogue (**161**), either the carbonyl group or the amidine functionality (Figure 123), the presence of CD_3OD as a solvent could give rise to the formation of adducts **170** or **171**.

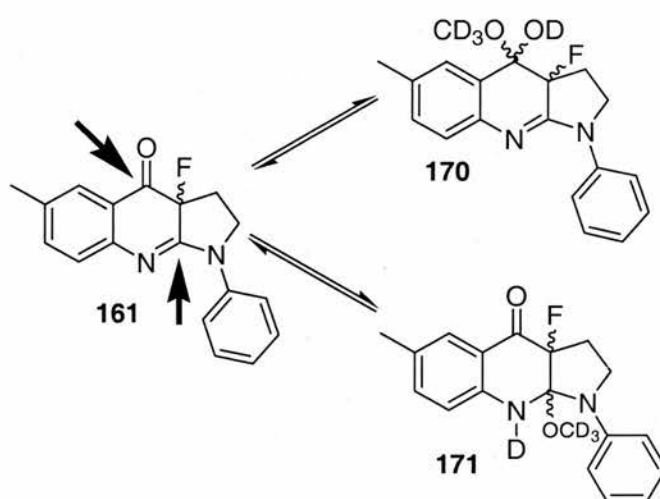


Figure 123. Proposed reversible addition of deuterated CD_3OD to 3a-fluoro analogue (**161**). **161** contains two electrophilic sites, the carbonyl and amidine carbons.

Figures 124-127 show the comparison of the ^1H NMR spectra of **161** in the aliphatic and aromatic regions, dissolved in CDCl_3 and CD_3OD . It is worth noting that the clearest change observed in the ^1H NMR in CD_3OD was observed in the aromatic region. Two set of signals corresponding to two compounds are clearly present. Interestingly there is a large change in chemical shift (0.3 ppm) for the proton corresponding to 7-H. This result was confirmed by ^1H - ^1H COSY analysis. This observation could suggest that addition of CD_3OD takes place at the carbonyl group, affecting mainly the aromatic proton located in the *para* position. Although it is still unclear as to the relative stereochemistry observed after addition of CD_3OD . Additionally, the ^{19}F NMR spectra showed two signals, one corresponding to the “starting material” with a chemical shift of -150.60 ppm and a new signal with a chemical shift of -167.20 ppm. The ratio between the two signals was 2.7:1, respectively.

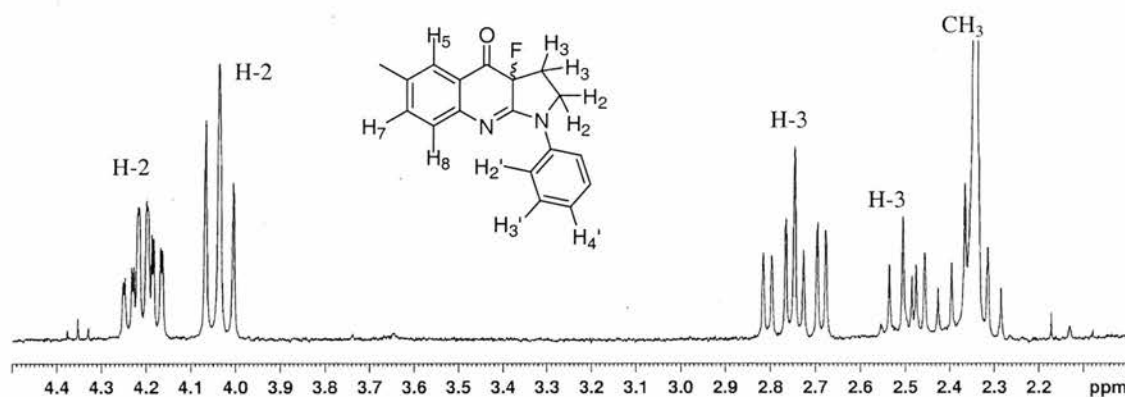


Figure 124. Aliphatic region of the ^1H NMR spectra of **161** in CDCl_3 .

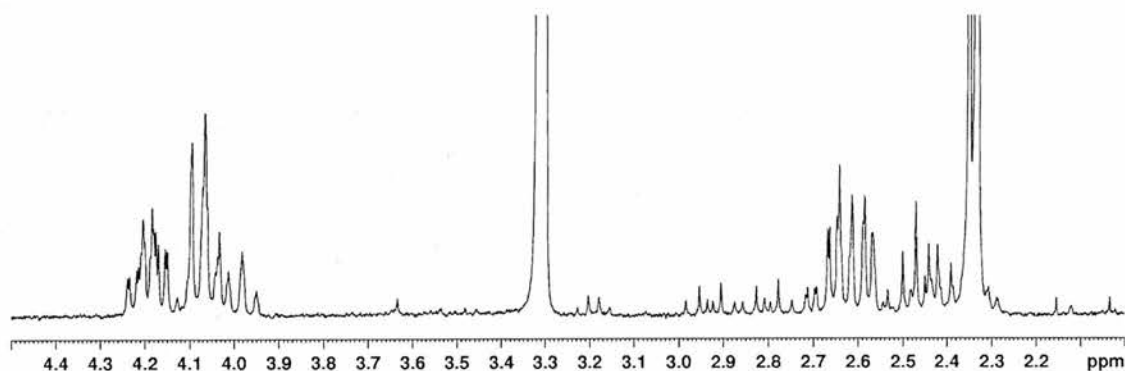


Figure 125. Aliphatic region of the ^1H NMR spectra of **161** in CD_3OD ($\delta = 3.31$ ppm).

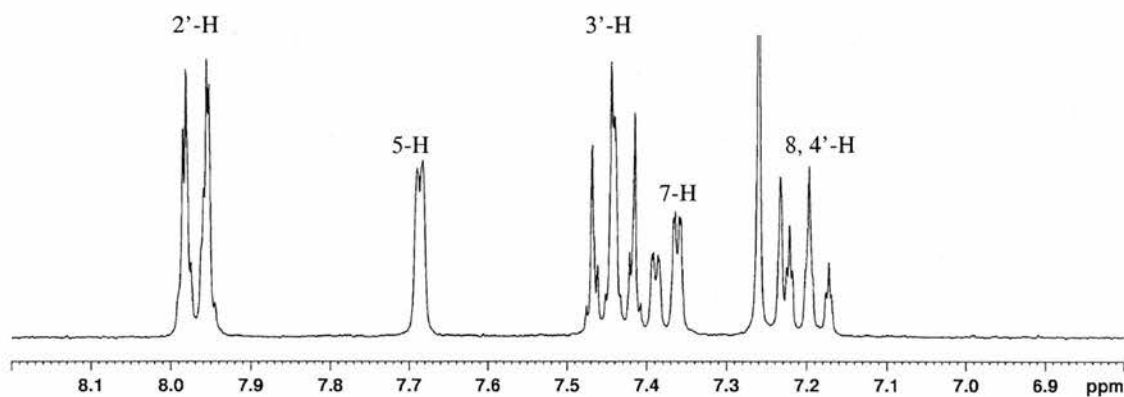


Figure 126. Aromatic region of the ^1H NMR spectra of **161** in CDCl_3 .

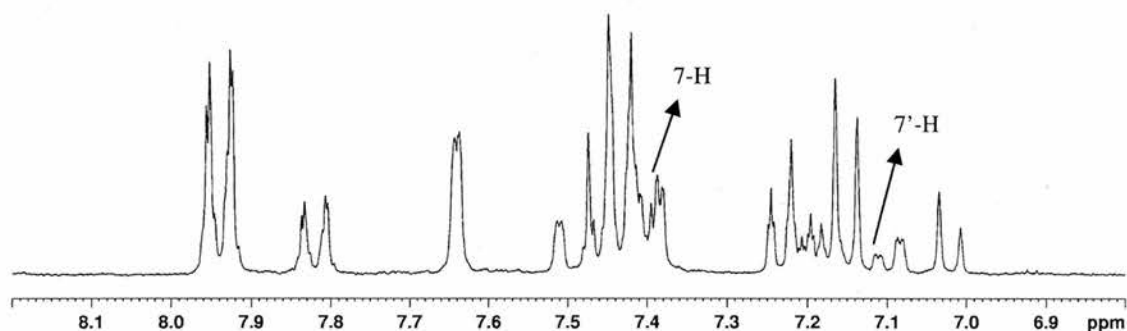


Figure 127. Aromatic region of the ^1H NMR spectra of **161** in CD_3OD .

The results of these studies were compared with the ^1H NMR spectra obtained for (*S*)-(-)-blebbistatin (**7**). It was found that when **7** was dissolved in CD_3OD and analysed by ^1H NMR, no analogous adducts were formed.

Although not carried out due to time constraints, preparation of chiral α -fluorocarbonyl compounds can be achieved by enantioselective electrophilic fluorination with the use of reagents derived from cinchona alkaloids.^{26, 27, & 28}

The asymmetric fluorination is carried out with commercially available reagents and can afford high chemical yields and high enantioselectivities. An example of this approach is the enantioselective fluorination of the oxindole **172** to afford (*S*)-(+)-BMS-204352 (MaxiPost) (a K^+ -channel opener) (**173**) (Figure 128) with two different fluorinating reagents.^{29, 30}

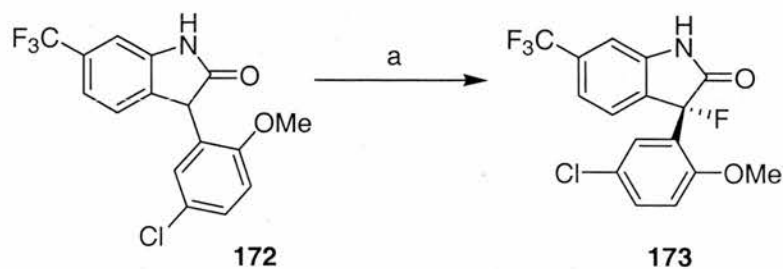


Figure 128. Asymmetric fluorination of the oxindole **172**. Reagents and conditions: a) F-2NaphtQN-BF₄ (**174**), DABCO (base), THF/CH₃CN/DCM (1/3/4), -78 °C, 96%, 88% *ee*, b) (DHQ)₂AQN /SelectfluorTM (**175**), DCM/CH₃CN (1/1), -80 °C, 16 hours, 94%, 84% *ee*.^{29, 30}

In one case the fluorinating reagent was the *N*-fluoroammonium salt of cinchona alkaloids, F-2NaphtQN-BF₄ (**174**). This reagent affords **173** in high enantioselectivities (88% *ee*) and in high yield (96%).³⁰ In addition the reaction was carried out using a combination of alkaloid and Selectfluor [(DHQ)₂AQN/SelectfluorTM (**175**)]³¹, affording **173** in high enantioselectivity (84% *ee*) and also high chemical yield (94%) (Figure 129).²⁹

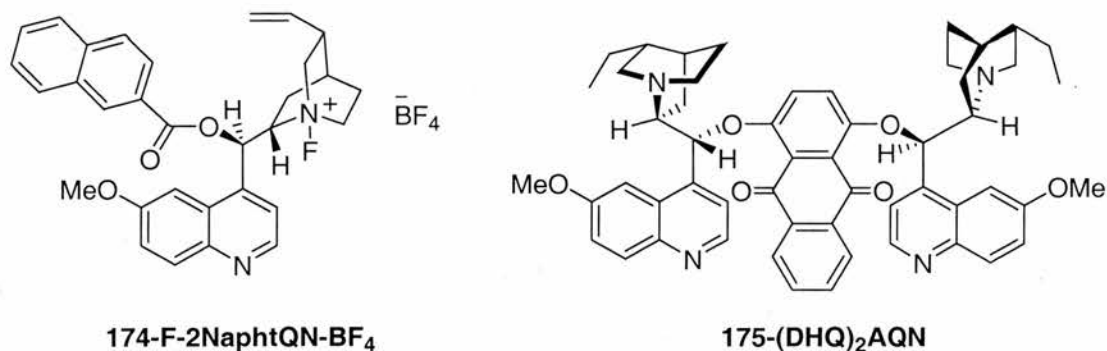


Figure 129. Fluorinating reagents.

4.4.1.3. Synthesis of 3a-Bromine analogue (**163**)

The next target molecule in this series was the bromine containing analogue **163**. It was envisaged that this analogue could be prepared by the use of oxalyl bromide in an analogous manner to the use of oxalyl chloride to prepare the chloro analogue (**162**).

Accordingly, optically enriched (*S*)-(-)-blebbistatin (**7**) was treated with an excess of oxalyl bromide (5 equivalents), DMAP and base in dichloromethane. The reaction mixture was stirred at room temperature for 16 hours. TLC analysis showed that starting material **7** was the main component of the reaction. ^1H NMR of the crude reaction mixture showed only the presence of unreacted starting material (Figure 130).

An attempt to synthesise the 3a-bromo analogue (**163**) was also made using PBr_3 (Figure 130).³² This reagent was added to a solution of **7** in chloroform at 0 °C. The reaction mixture was stirred at room temperature for 30 minutes and then refluxed for 2.5 hours. ^1H NMR analysis showed only the presence of unreacted starting material **7**.

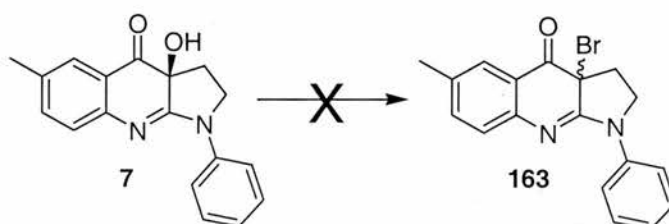


Figure 130. Attempted synthesis of 3a-bromo analogue **163**. Reagents and conditions: a) Oxalyl bromide (5.0 equiv), DMAP (catalytic amount), Et_3N , DCM, RT, 16 hours. b) PBr_3 (3.3 equiv), CHCl_3 , 60 °C, 2.5 hours.

To summarise, the 3a-chloro **162** and 3a-fluoro **161** analogues were prepared in moderate and excellent yields, respectively. Formation of a 3a-bromo derivative **163** proved unsuccessful. Due to time constraints an alternative approach using quinolone **24** and NaOBr was not performed.

4.4.2. Attempts to derivatise the Blebbistatin core structure at position 3a

4.4.2.1. Acylation of the tertiary alcohol

Given the fact that the molecule of (*S*)-(-)-blebbistatin (**7**) contains an alcohol functionality (position (**3a**)) it was of interest to chemically derivatise this position. A classical way to acylate an alcohol is by reacting with an acid chloride.

The acid chlorides used in this section contain a bromine atom (Figure 131). Additionally, incorporation of such a heavy atom into a molecule is advantageous when using X-ray crystallography to determine the absolute stereochemistry (Chapter 3, Section 3.2).³³ Therefore, it was decided to use *p*-bromo and *m*-bromo benzoyl chlorides as acylating reagents for this reaction.

The preparation of ester derivatives of **7** was expected to prove challenging, due to the presence of steric effects at the reaction centre. The synthesis of the ester derivatives was carried out in line with previous attempts to determine the absolute stereochemistry of (*S*)-(-)-blebbistatin (**7**) by formation of the Mosher's ester at the C-3a position (Chapter 3, Section 3.2.1).

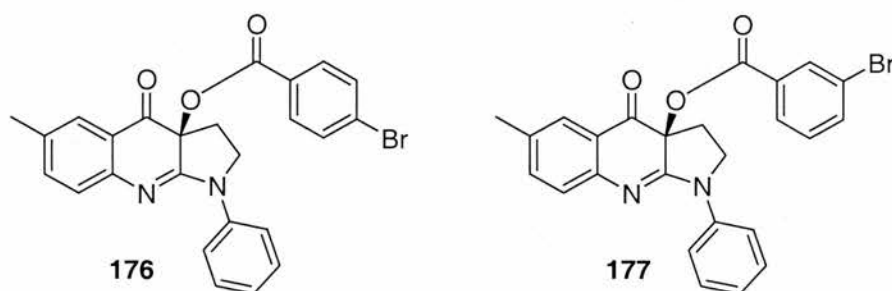


Figure 131. Ester analogues of (*S*)-(-)-blebbistatin (**7**).

The mechanism of the reaction consists of nucleophilic attack by DMAP (more nucleophilic than the alcohol) on the benzoyl chloride to form a highly electrophilic intermediate (due to the positive charge). This intermediate then reacts with the alcohol in the presence of an excess of base to give the ester. Due to the poor nucleophilicity of the tertiary alcohol, it was necessary to use a large excess (10 equivalents) of the corresponding benzoyl chlorides to drive the reaction to completion.

The reaction was carried out with highly optically enriched (*S*)-(-)-blebbistatin (**7**) (86% *ee*) in the presence of a catalytic amount of DMAP and excess of pyridine (Figure 132). 3-Bromo-benzoylchloride (**178**) was added to the solution and the reaction mixture was stirred at room temperature for 24 hours. The crude solid was purified by flash column chromatography on silica gel to afford **177** in excellent yield (97%).

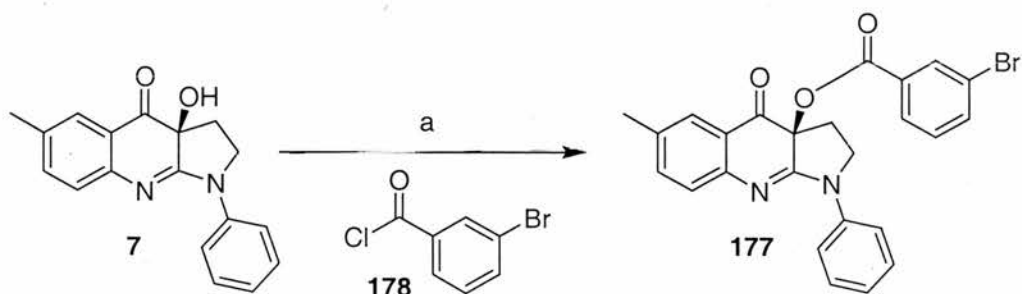


Figure 132. Synthesis of an ester analogue of blebbistatin **177**. Reagents and conditions: a) DMAP (0.50 equiv), py (4.0 equiv), **178** (10 equiv), DCM, RT, 24 hours, 97%.

The ^1H NMR of the ester derivative **177** showed a more complicated aromatic region, due to the presence of three aromatic rings. The MS analysis showed the presence of the two isotopes of bromine at m/z 474 [M^{79}] $^+$ and 476 [M^{81}] $^+$. Additionally the sign for the optical rotation was negative ($[\alpha]_{\text{D}}^{25} = -568$, in a concentration of 0.1 g/100mL in dichloromethane), which was consistent with **177** being in the same enantiomeric series as (–)-(*S*)-blebbistatin (**7**). However, attempts to recrystallise **177** from ethyl acetate/hexane to obtain an optically pure sample of **177** to enable absolute stereochemical assignment by X-ray analysis were unsuccessful.

Similarly, the preparation of **176** (Figure 133) from highly optically enriched (*S*)-(–)-blebbistatin (**7**) (86% *ee*) and 4-bromobenzoyl chloride (**179**) was carried out using the same procedure as for **177**. **176** was prepared in quantitative yield. The sign for the optical rotation was also negative ($[\alpha]_{\text{D}}^{25} = -607$, in a concentration of 0.1 g/100mL in dichloromethane), which was consistent with the sign of **7**. ^1H NMR analysis showed the presence of a new AA'XX' system in the aromatic region which is consistent with the presence of a substituent at the 4 position in an aromatic ring.

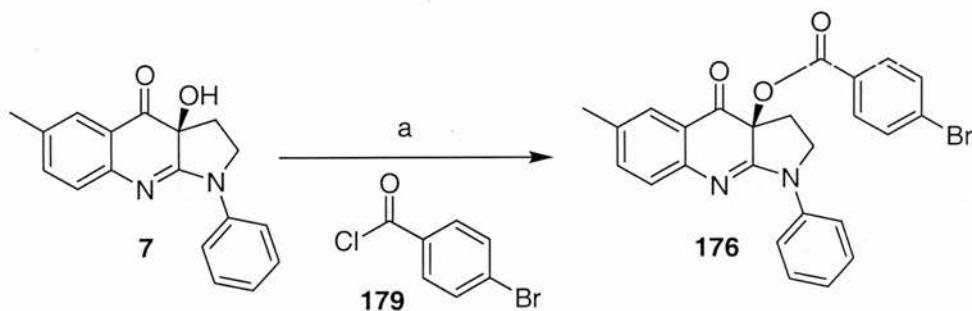


Figure 133. Synthesis of the ester analogue **176**. Reagents and conditions: a) DMAP (0.50 equiv), py (4.0 equiv), **179** (10 equiv), DCM, RT, 24 hours, 100%.

Several initial attempts to crystallise **176** did not yield sufficiently high quality crystals for X-ray analysis. Finally, **176** was recrystallised from ethyl acetate/hexane to afford high quality crystals which were analysed by X-ray crystallography. Furthermore, the structure and the absolute configuration were solved by the heavy-atom method.³⁴ The *absolute configuration* of **176** was confirmed as *S* (Figure 134). This result was consistent with the data presented in Chapter 3, Section 3.2.1.

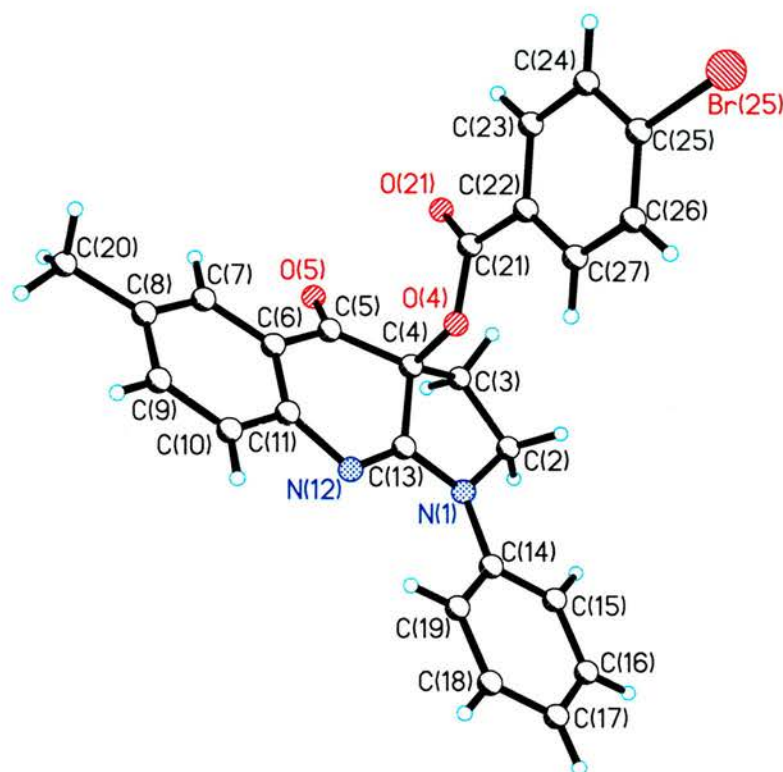


Figure 134. X-Ray crystal structure of **176**.

In order to confirm that no racemisation³⁵ had occurred during the reaction it was decided to hydrolyse a recrystallised sample of **176** back to **7** and to check the optical purity of **7** formed by this route. Therefore, it was important to confirm that the preparation of ester derivatives could be carried out without racemisation. It was envisaged that the preparation of optically pure analogues of **7**, from highly optically enriched samples, would not be possible in case of compounds that do not recrystallise. Therefore, an alternative route to optically pure analogues of **7** could be through the preparation of the ester derivatives, recrystallisation to obtain an optically pure sample and their subsequent hydrolysis without racemisation.

The hydrolysis of the ester was carried out under basic conditions using lithium hydroxide at room temperature for 3 hours (Figure 135). The crude solid was purified by flash column chromatography on silica gel affording (*S*)-(-)-blebbistatin (**7**) in a moderate yield (55%).

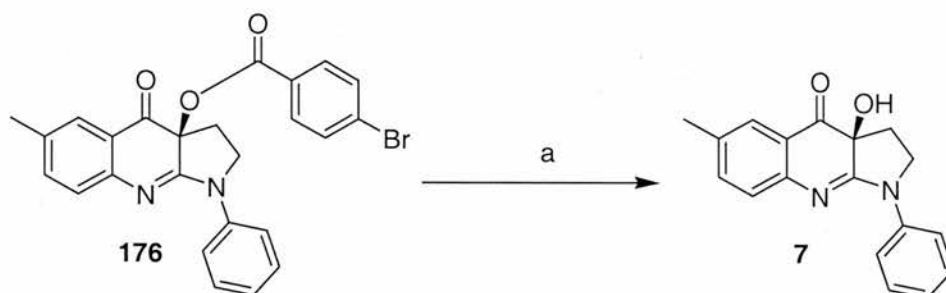


Figure 135. Hydrolysis of **176** under basic conditions. Reagents and conditions: a) LiOH (1.0 equiv), THF, RT, 3 hours, 55%.

Chiral HPLC analysis was used to confirm the assignment of the stereochemistry of **7** derived from **176** by comparison with authentic material of (*S*)-(-)-blebbistatin (**7**) (Figure 136). Samples of enantiomerically pure (*S*)-(-)-blebbistatin (**7**) and (*R*)-(+)-blebbistatin (**23**) were analysed as standards affording in each case a single peak (Figures 136A and 136B, respectively). **7** prepared from recrystallised **176** was also analysed and showed the presence of a single peak in the chromatogram (Figure 136C). The retention time for the pure enantiomer **7** and **7** prepared by hydrolysis of **176** were very similar (7.13 and 7.27 min). In contrast, the retention time for the pure enantiomer (*R*)-(+)-blebbistatin (**23**) was 10.12 min. When **7** prepared by hydrolysis of **176** was doped with enantiomerically pure (*R*)-(+)-blebbistatin (**23**), two peaks corresponding to each enantiomer were observed (Figure 136D). In the same way, when enantiomerically pure (*S*)-(-)-blebbistatin (**7**) was mixed with **7** prepared by hydrolysis of **176** only one peak was observed (Figure 136E). Finally, the last chromatogram showed the presence of two peaks when the three samples of **7**, **23** and hydrolysed **176** were mixed (Figure 136F). This result therefore confirmed that hydrolysed **176** was the same enantiomer as **7**, as judged by the retention time which was the same in both cases. Therefore, from these experiments it was found that a two step procedure had been developed in which enantiomerically enriched

(*S*)-(-)-blebbistatin (**7**) could be acylated on the 3a-OH group, purified by crystallisation to give optically pure **176** and then hydrolysed back to give optically pure **7**.

In summary, the acylation of the tertiary alcohol functionality in **7** with different bromobenzoyl chlorides was possible by using a large excess of the acid chloride due to the steric hindrance associated with the 3a tertiary alcohol. Furthermore the *absolute configuration* of (*S*)-(-)-blebbistatin (**7**) was established by X-ray analysis of a bromo containing derivative **176** and was found to be consistent with the results presented in Chapter 3, Section 3.2.1.

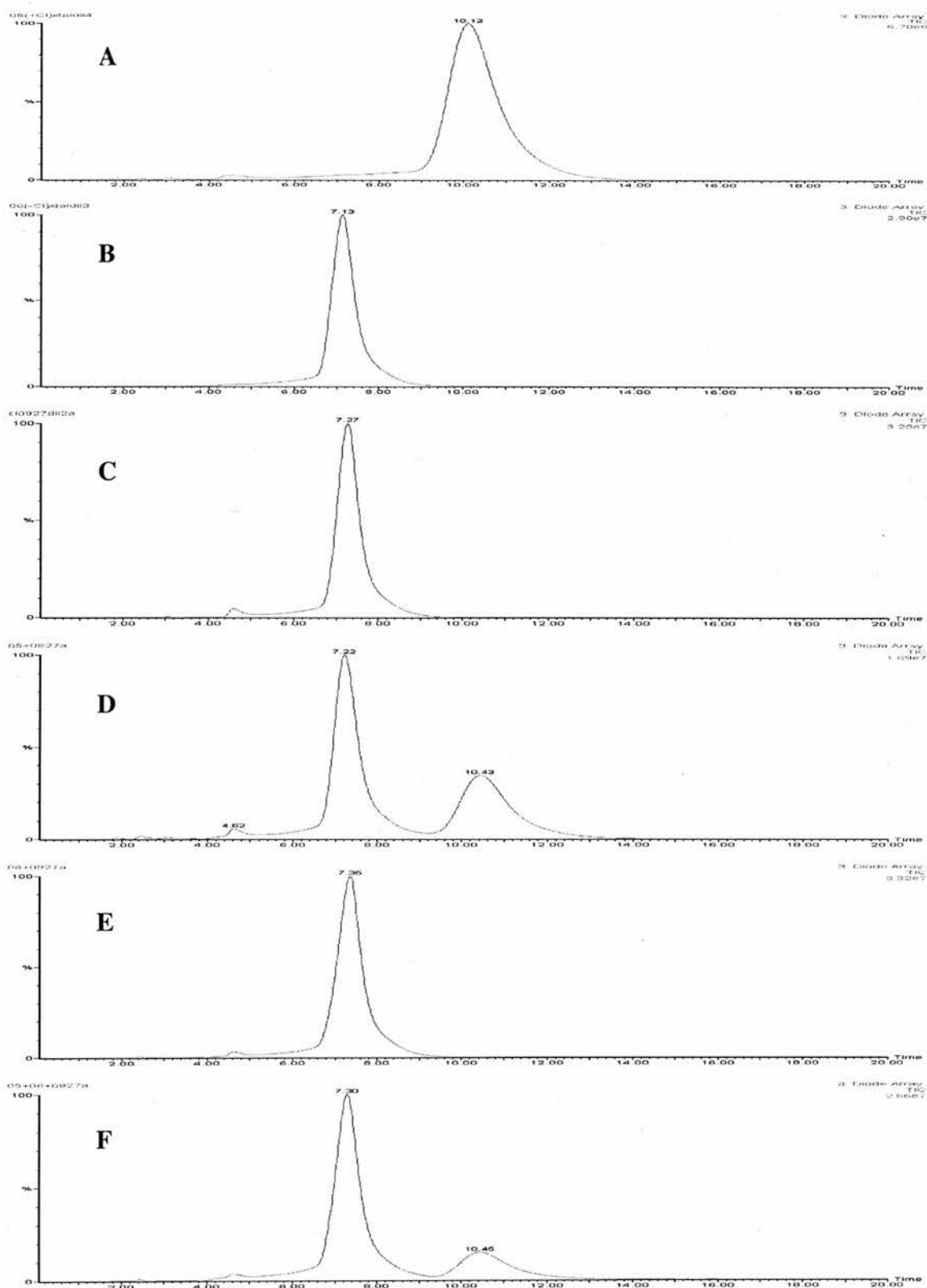


Figure 136. Chiral HPLC analysis of blebbistatin enantiomers from various synthetic routes. HPLC conditions: Daicel Chiralpak AD-RH, Acetonitrile/Water 50:50, flow rate 0.8 mL min^{-1} , $\lambda=254 \text{ nm}$. Chromatograms; A) optically pure enantiomer (+)-(R)-blebbistatin (**23**), $t_R=10.12$ min, B) optically pure enantiomer (-)-(S)-blebbistatin (**7**), $t_R=7.13$ min, C) **7** prepared by hydrolysis of **176**, $t_R=7.27$ min, D) A+C, $t_R=7.22$ min, $t_R=10.43$ min, E) B+C, $t_R=7.35$ min, F) A+B+C, $t_R=7.30$ min, $t_R=10.45$ min.

4.4.2.2. Alkylation of the 3a alcohol

A common reaction in organic chemistry is the methylation of the alcohol functionality.^{36,37} This section describes the methylation of the tertiary alcohol from enantiomerically enriched (*S*)-(-)-blebbistatin (**7**) using methyl iodide. The purpose of this reaction was to provide an alternative method of studying the importance of the OH group to the biological activity of (*S*)-(-)-blebbistatin (**7**) without adding significant steric bulk.

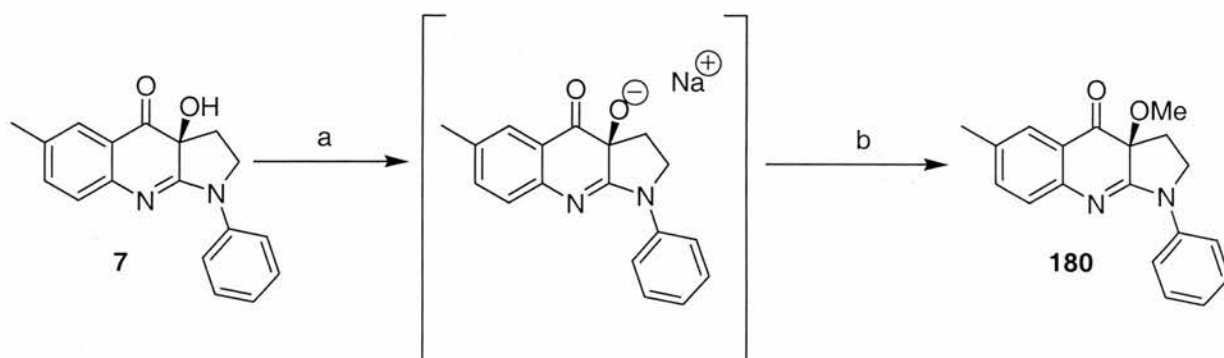


Figure 137. Synthesis of a methylated analogue of blebbistatin (**180**). Reagents and conditions: a) NaHMDS (1.5 equiv), THF, -78-0 °C, b) MeI (5.0 equiv), THF, 0 °C, 1 hour, RT, 16 hours, 91%.

The mechanism of the reaction involved deprotonation of the alcohol moiety in optically enriched **7** (86% *ee*) with NaHMDS at low temperature (Figure 137). The reaction was then warmed to 0 °C, and an excess (5 equivalents) of the methylating agent methyl iodide was added. An excess of methyl iodide was required to drive the reaction to completion. The reaction was then stirred at room temperature for 16 hours. TLC analysis showed the complete conversion of the starting material **7** to the desired product **180**. The reaction was quenched with saturated ammonium chloride solution and extracted with dichloromethane to afford **180** in excellent yield. ¹H NMR showed the presence of a clear singlet at 3.27 ppm corresponding to the CH₃ of the methoxy group. Furthermore ¹³C NMR, HSQC and HMBC analyses were also consistent with the assigned structure. The optical rotation for the compound was $[\alpha]_D^{25} = -462$ (concentration of 0.05 g/100 mL in dichloromethane).

4.4.3. Carbon-Carbon bond formation

One of the most challenging issues in organic chemistry is the creation of a carbon-carbon bond. It was therefore of interest to attempt to prepare analogues of **7** in which the 3a alcohol was replaced by a carbon chain (Figure 138).

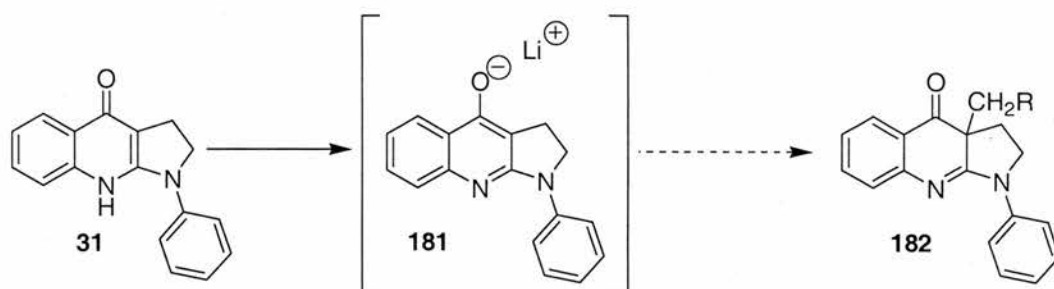


Figure 138. Proposed incorporation of a carbon-carbon bond *via* enolate **181**.

A common method of making carbon-carbon bonds is through the alkylation of an enolate. These types of reactions are complicated when the enolate is sterically encumbered as in **181**. Alkylation on the oxygen atom rather than on the carbon atom often occurs in such cases. Additionally, in our case, the heterocyclic core structure also contains a nitrogen atom that can be alkylated (Figure 139).

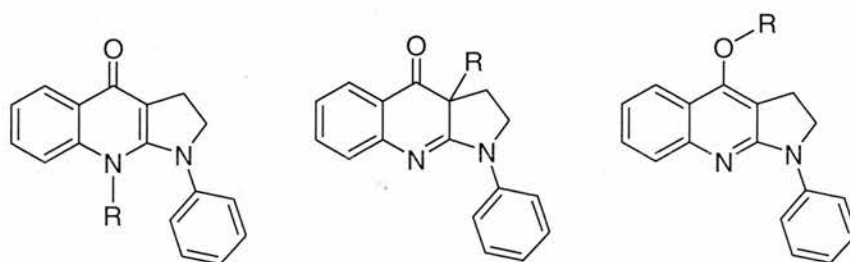


Figure 139. Different positions to alkylate the heterocyclic core structure.

In this section the alkylation step was attempted by the use of several reagents including methyltrifluoromethanesulfonate (**183**) and benzylbromide (**184**) (Figure 140).

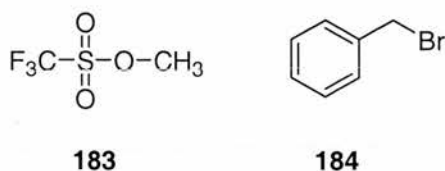


Figure 140. Alkylating reagents.

The first attempt to alkylate at the **3a** position on the heterocyclic core structure was carried out with methyl trifluoromethanesulfonate (**183**) as an alkylating reagent. This involved the formation of the lithium enolate **181** at $-78\text{ }^{\circ}\text{C}$ followed by addition of **183** (Figure 141). The reaction was stirred at $-20\text{ }^{\circ}\text{C}$ for 16 hours. The crude product was purified by flash column chromatography to afford the O-alkylated analogue **185** in 44% yield.

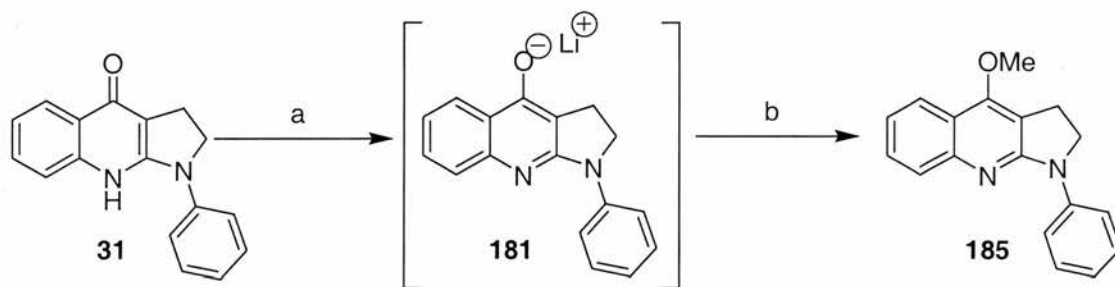


Figure 141. Synthesis of O-alkylated analogue **185**. Reagents and conditions: a) i) LiHMDS (1.2 equiv), THF, $-78\text{ }^{\circ}\text{C}$, 30 min, b) **183** (2.0 equiv), $-20\text{ }^{\circ}\text{C}$, 16 hours, 44%.

^1H NMR analysis confirmed the presence of **185** due to the presence of a singlet corresponding to the CH_3 of the methoxy group at δ 4.15 ppm. This result can be rationalised by the fact that **183** is a hard electrophile and therefore more likely to react at the oxygen atom (hard nucleophile).

Literature precedent³⁸ reported the formation of an O-alkylated product **188** when 7-chloro-4-hydroxy-3-(2-phthalimidoethyl)-2(1*H*)-quinolone (**186**) was treated with methyl toluene-*p*-sulphonate (**187**) in anhydrous medium at room temperature (Figure 142). Whereas when the reaction was heated to $50\text{--}60\text{ }^{\circ}\text{C}$ the N-**189** and O-**188** alkylated products were both present.

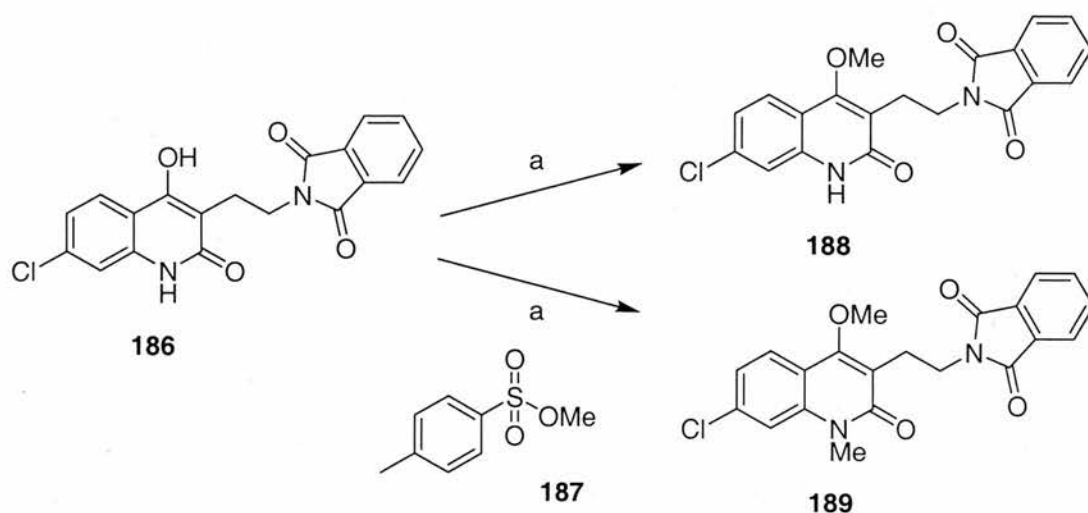


Figure 142. Selective alkylation of **186**. Reagents and conditions: a) K_2CO_3 (1.0 equiv), **187** (2.2 equiv), DMF, RT, 17 hours, 93%. Unselective alkylation of **186**. Reagents and conditions: a) K_2CO_3 (1.0 equiv), **187** (large excess), DMF, 50-60 °C, 17 hours, 32%.³⁸

A second attempt to alkylate the carbon at position **3a** was carried out with benzylbromide (**184**) (Figure 143). This involved the formation of the lithium enolate at -78 °C followed by addition of benzylbromide (**184**). The reaction was warmed to -20 °C and stirred for 16 hours. The reaction was followed by TLC which showed mainly the presence of unreacted starting material.

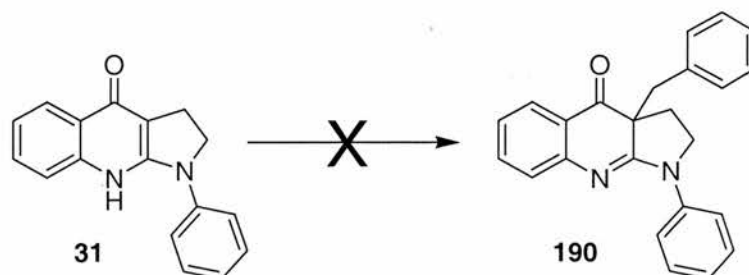


Figure 143. Attempted benzylation of carbon at **3a** position. Reagents and conditions: a) i) LiHMDS (1.2 equiv), THF, -78 °C, 30 min, ii) benzylbromide (**184**) (2.0 equiv), -20 °C, 16 hours.

Many methods described in the literature based on the use of magnesium methyl carbonate³⁹ or dialkyl carbonates⁴⁰ to prepare β -keto esters suggest that these reagents will not give the required level of control in the attempted C-acylation of **181**. Additionally, alternative reagents such as acyl halides or anhydrides⁴¹ are expected to

give a mixture of O-, C- and N- acylated products. It was then decided to use methyl cyanofornate, known as Mander's reagent (**191**)⁴¹ (Figure 144), a reagent that is known to prefer C-acylation of enolates in a regio-selective process to give the corresponding β -keto ester derivatives even in sterically demanding situations.

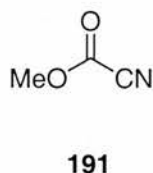


Figure 144. The acylating reagent Mander's reagent (**191**).

A literature example for the preparation of β -keto esters by acylation of preformed enolates is shown in Figure 145. The results from different acylations using methyl cyanofornate showed that when the substrates have the β -carbon of the enolate sterically hindered, the O-acylated products are obtained from the reaction. It was found that enolate **192** was converted by methyl cyanofornate (**191**) in a 1:4 mixture of **193** and **194** when the reaction was carried in THF. However when the solvent was changed to diethyl ether, the O-acylation was almost suppressed with the predominant formation of the β -keto ester **194**. The stereochemistry of the product was determined by comparison with authentic material.⁴²

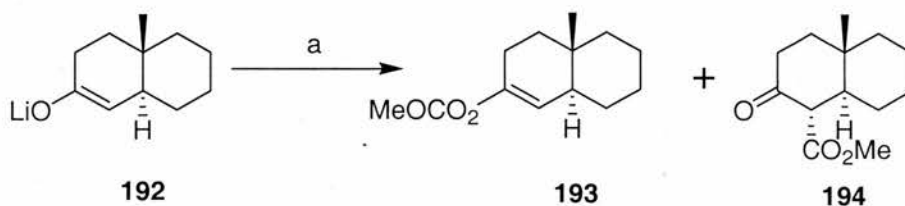


Figure 145. Preparation of β -keto esters by acylation of preformed enolates. Reagents and conditions: a) **191** (1.1 equiv), Et₂O, -78-0 °C, 20:1 (**194**:**193**).⁴²

In our case, the reaction commenced with the formation of the lithium enolate, reacting H-quinolone **31** with lithium bis(trimethylsilyl)amide at -78 °C (Figure 146). The lithium enolate was then reacted with Mander's reagent. The reaction was warmed at -10 °C and stirred for 16 hours. TLC analysis of the reaction mixture indicated mainly the presence of unreacted starting material. Purification by flash

chromatography enabled only the isolation of unreacted starting material **31**. Subsequently, ^1H NMR analysis showed only the presence of unreacted starting material **31**.

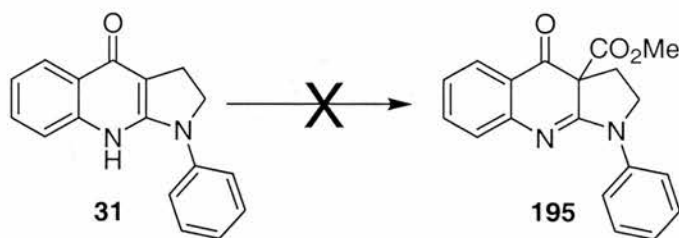


Figure 146. Attempted alkylation of carbon at **3a** position. Reagents and conditions: a) i) LiHMDS (1.2 equiv), THF, $-78\text{ }^\circ\text{C}$, 30 min, ii) Mander's reagent (**191**) (2.0 equiv), $-10\text{ }^\circ\text{C}$, 16 hours.

In summary, attempts to introduce a carbon-carbon bond at position **3a** by the use of alkylating and acylating reagents were unsuccessful. Formation of an O-alkylated product was achieved by using methyl trifluoromethyl sulfonate (**183**). No evidence for formation of the *N*-alkylated isomer was obtained. Due to time constraints it was not possible to study this reaction further. An alternative approach *via* 3a-chloro blebbistatin (**162**) was proposed based on literature precedent⁴³ in which an α -chloro ketone (**196**) (Figure 147) was stereoselectively methylated *via* halohydrin formation and rearrangement. Again, due to the time constraints this procedure was not investigated.

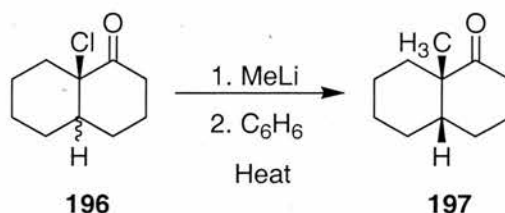


Figure 147. Literature example for the methylation of α -chloro ketones.⁴³

4.5. CHANGE IN THE OXIDATION STATE OF THE HETEROCYCLIC CORE STRUCTURE (7)

This section is focused on the reduction of the core structure of (*S*)-(-)-blebbistatin (**7**). The molecule contains two sites suitable for reduction, the carbonyl group and the amidine moiety. Furthermore, regarding the biological activity of (*S*)-(-)-

blebbistatin (**7**), it was considered of interest to explore whether these parts of the molecule were of importance for activity.

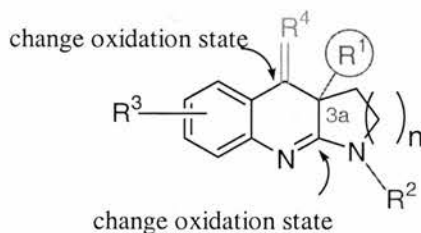


Figure 148. Functionalities to be reduced in the blebbistatin core structure.

A well known reagent used in the reduction of carbonyl groups is sodium borohydride (NaBH₄). Therefore, it was decided to attempt the reduction of (*S*)-(-)-blebbistatin (**7**) with this reagent. Optically enriched blebbistatin **7** (86% *ee*) was dissolved in methanol and treated with one equivalent of sodium borohydride. The reaction mixture was stirred at room temperature for 30 minutes. TLC analysis showed the presence of two new spots with similar R_f values. The crude ¹H NMR of the reaction showed a mixture of two compounds in a ratio of 1.5:1. Purification by flash column chromatography afforded two products **198** (37%) and **199** (50%), which are assigned as having the structures shown in Figure 149. It is interesting to note that the same result was obtained when the reaction was carried out with 0.5 equivalents of NaBH₄.

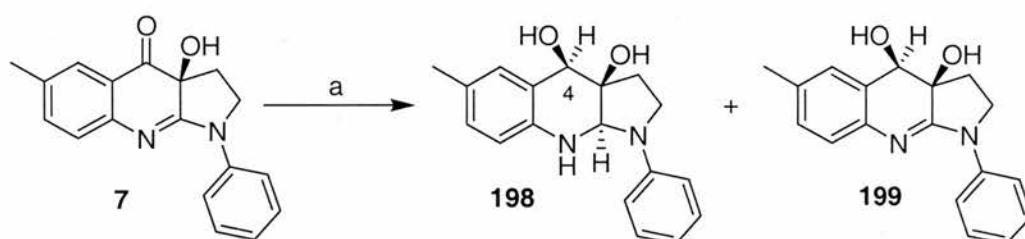


Figure 149. Reduction of the blebbistatin core structure (**7**) and proposed reaction products. Reagents and conditions: a) NaBH₄ (1.0 equiv), MeOH, RT, 30 min., 37% (**198**) and 50% (**199**).

However, the reduction of **7** can afford four more products, one diastereoisomer for **199** and another 3 diastereoisomers for **198** (Figure 150). Therefore, the following section discusses the reasons for the relative stereochemical assignments of the two structures **198** and **199**.

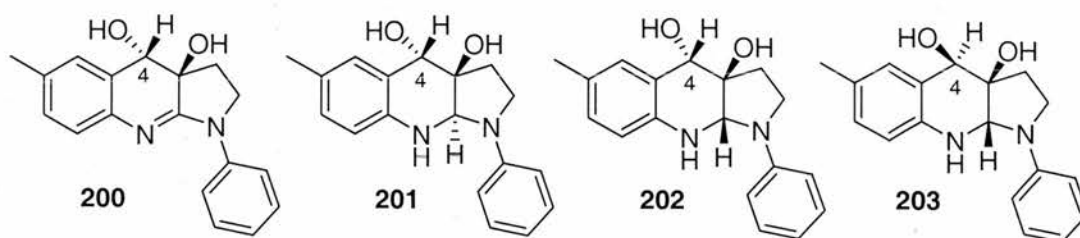


Figure 150. Possible additional products from the reduction of **7** with NaBH_4 .

The identity of **199** was established from the following evidence: the mass spectrum in ES^+ mode showed a peak corresponding to m/z 295 $[\text{M}+\text{H}]^+$. Although reduction at the amidine moiety to give **204** (Figure 151) would give the same mass, other evidence in support of this structure assignment for compound **199** were; i) the infrared spectrum, which showed no band for the carbonyl group ($\text{C}=\text{O}$ IR stretching band was 1694 cm^{-1} in **7**) but did show an IR band corresponding to the amidine moiety at 1593 cm^{-1} , ii) the ^{13}C NMR spectrum did not show the presence of the peak corresponding to the carbonyl group (δ 194.1 ppm in **7**) but instead showed the presence of a signal corresponding to the new 4C-H carbon at δ 74.9 ppm (C-4 in **199**, PENDANT indicates that this is a CH). In addition, the signal for the amidine in the ^{13}C NMR appeared at 163.4 ppm (164.7 ppm in **7**). ^1H NMR confirmed the presence of an additional proton at δ 4.78 ppm (H-4) in CDCl_3 .

It is worth noting that the blebbistatin core structure is characterised by a bright yellow colour. Due to the reduction of the carbonyl group **199** was colourless. One further experiment was carried out to clarify whether the amidine moiety was reduced instead of the carbonyl group in **7**. It was decided to oxidise **199** with the Dess-Martin periodinane oxidising reagent⁴⁴ (**205**) (Figure 151). A small amount of **199** was dissolved in a vial and the oxidising reagent was added to it. The solution in the vial turned yellow and TLC analysis showed a spot with the same R_f as (*S*)-(-)-blebbistatin (**7**).

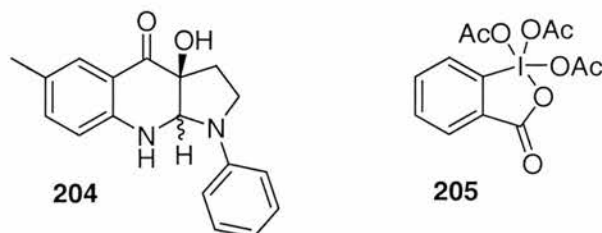


Figure 151. Proposed reduction at the amidine moiety (**204**) and Dess-Martin reagent (**205**).

Crystallisation of a sample of **199** from acetonitrile, afforded needles of sufficient quality for X-ray analysis (Figure 152). The studies enabled the relative stereochemistry of the diol **199** to be assigned. The result showed the *syn* diol diastereoisomer, where the two OH groups are on the same side of the molecular plane with the O5-C5-C4-O4 dihedral angle being 60 °C (*gauche* conformation). This arrangement was consistent with literature precedent stating that the reduction of carbonyl groups with sodium borohydride ordinarily leads to the formation of equatorial alcohols corresponding to axial attack of the hydride.^{45, 46}

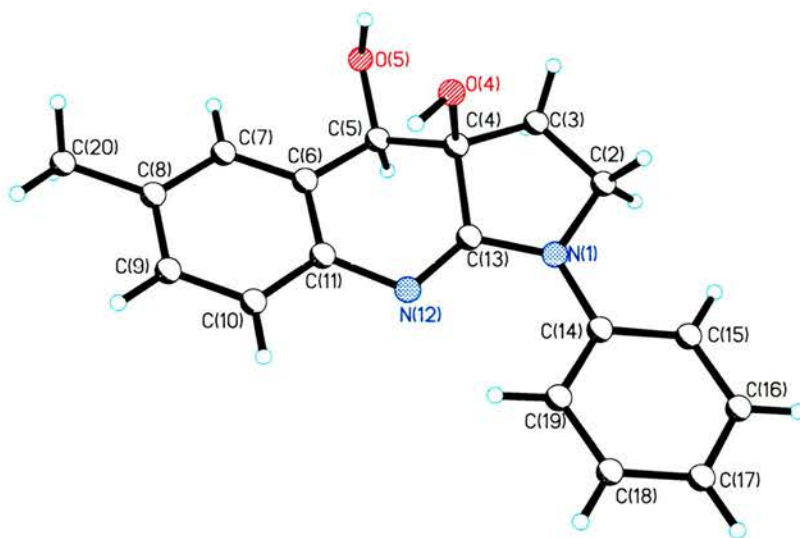


Figure 152. X-Ray crystal structure of **199**.

The structural assignment of the doubly reduced compound **198** was based on infrared spectrum, NMR and mass spectral analysis. Mass spectral analysis (ES⁺ mode) showed a peak corresponding to the mass (296) plus sodium m/z 319 [M+Na]⁺. IR analysis did not show the bands corresponding to either the carbonyl group or the amidine. The ¹³C NMR spectrum showed two peaks corresponding to the new stereogenic centres that have been formed at 71.6 ppm (C-4) and 72.9 ppm (C-9a), corresponding to CH by PENDANT. The ¹H NMR in CDCl₃ also confirmed the presence of two new singlets corresponding to one proton each at 4.55 ppm (H-4) and 5.07 ppm (H-9a).

For an additional way to prove the structure of **198**, it was decided to attempt the reduction of **199**. It was found that when the reaction was carried out with NaBH₄ under the same conditions described previously, **199** is reduced to **198** (Figure 153). TLC analysis of the crude reaction mixture showed the presence of a new compound with identical R_f to compound **198**. ¹H NMR analysis of the crude reaction mixture confirmed the presence of both starting material (**199**) and product (**198**) in a ratio of 1:2. Purification of the crude reaction mixture by flash column chromatography and subsequent analysis by ¹H NMR, confirmed the structure of the compound as **198**.

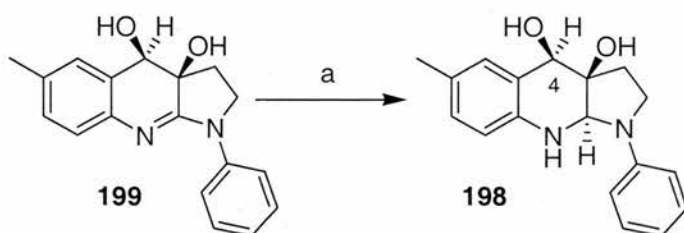


Figure 153. Reduction of **199** to **198** with NaBH₄. Reagents and conditions: a) NaBH₄ (1.0 equiv), MeOH, RT, 2.5 hours, 52%.

In conclusion, the reduction of (*S*)-(-)-blebbistatin (**7**) showed that one diastereoisomer (**199**) is formed on reduction of the carbonyl group and in addition **199** can be further reduced, to compound **198**. Unfortunately attempts to crystallise compound **198** to determine its stereochemistry were unsuccessful. In addition, NOESY experiments were carried out to study the distance in space between the protons H-9a and H-4, in order to determine the relative stereochemistry of **198**. In this case, the results from the NMR experiments were inconclusive and therefore it was not possible to deduce the stereochemistry of **198**. Therefore, following the proposed mechanism for the first reduction, it was postulated that the transferred hydride to the carbon of the N=C, could be also done from the bottom face, opposite to the OH groups. The structure and relative stereochemistry of the doubly reduced compound **198** was then suggested to be as drawn in Figure 154.

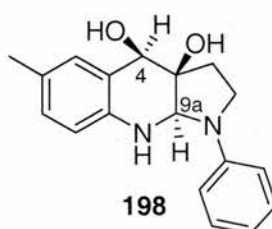


Figure 154. Proposed structure for the double reduced blebbistatin analogue (**198**).

During attempts to reduce the *para*-bromo phenyl analogue of blebbistatin (**135**) (Chapter 3, Section 3.2.1) with hydrogen using 10% Pd on charcoal, it was found that the core structure could also be reduced. H₂/Pd/C reducing agent is a chemoselective reducing agent which reduces easily alkenes and imines but the reduction of carbonyl groups by this reagent combination is considered more difficult. It was therefore decided to attempt the reduction of the core structure of (*S*)-(-)-blebbistatin (**7**) using H₂/Pd/C. Optically enriched blebbistatin (**7**) (86% *ee*) was dissolved in a mixture of MeOH and DMF with triethylamine in the presence of 10% Pd/C. Hydrogen gas was then added and the reaction mixture was stirred at room temperature for 48 hours. Purification by flash column chromatography afforded the reduced product **199** in 55% yield (Figure 155).

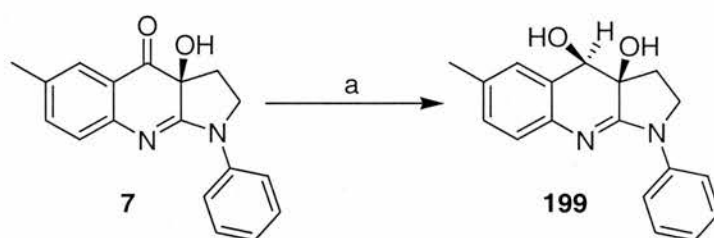


Figure 155. Reduction of the blebbistatin core structure (**7**). Reagents and conditions: a) 10% Pd/C (3.0 equiv), Et₃N, H₂ (balloon), 1:1 MeOH:DMF, RT, 48 hours, 55%.

¹H NMR analysis and ¹³C NMR of the product of this reaction showed that the carbonyl group was reduced during the reaction whereas the amidine moiety was not. Interestingly it was reported in the literature that the catalytic hydrogenation of aromatic ketones and aldehydes can afford methylene compounds *via* intermediary benzyl alcohols with the employment of 10% Pd/C.⁴⁷ Crystallisation of **199**, prepared by reduction of **7** using H₂/Pd/C, from acetonitrile, afforded the same result as the reduction with NaBH₄ (Figure 156). Interestingly, Figure 157 shows the formation of an intermolecular H-bonding between the oxygen (O4) from one molecule of **199** and the oxygen (O5) of another molecule of **199**.

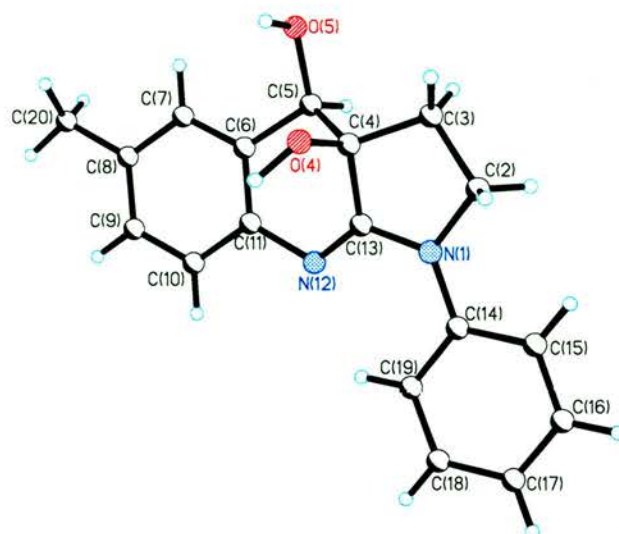


Figure 156. X-Ray of the reduced product **199** with $\text{H}_2/\text{Pd/C}$ (10%).

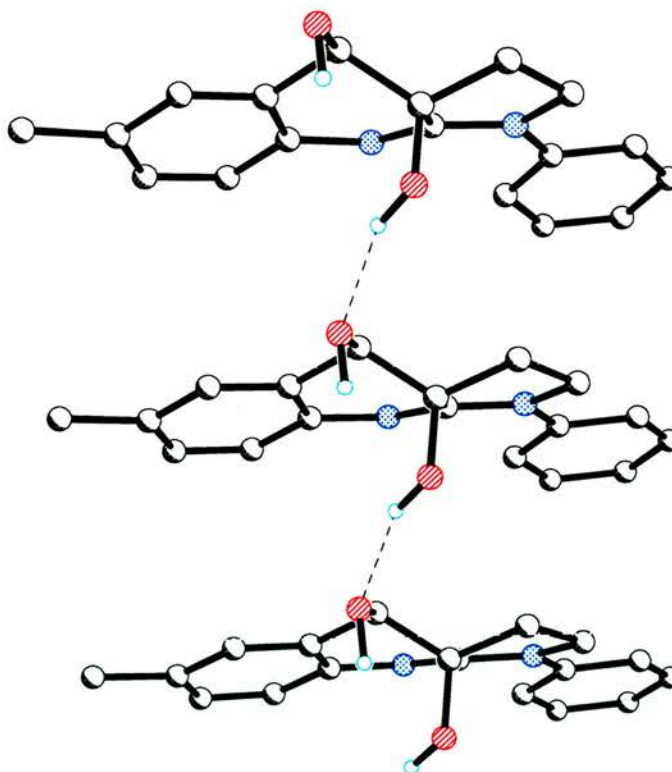


Figure 157. Intermolecular hydrogen bonding between the hydrogen atom (from the 4-Oxygen) and the 5-Oxygen in **199**.

4.6. INCORPORATION OF DIVERSITY AT THE *N*-PHENYL RING (R^2)

Exploration on the *N*-phenyl ring (R^2) started first with the preparation of the *para*-bromo containing analogue of blebbistatin (**135**) to assign the absolute stereochemistry of (*S*)-(-)-blebbistatin (**7**) (Chapter 3, Section 3.2.1). The synthesis of this compound proved that substitution at C-4' could be achieved (Figure 158). Initial attempts to prepare alkylated analogues (*N*-methyl and *N*-ethyl) from commercially available pyrrolidinones (**39** and **53**) failed as described previously (Chapter 2, Section 2.1.4.1). An alternative to this approach involved the incorporation of a methoxy group at the position C-4' of the *N*-phenyl ring (Figure 158). Subsequent removal of the *p*-methoxy phenyl group in a single mild deprotection step, would then afford an *N*-H analogue (**207**). Selective alkylation of the amidine functionality would then be required to prepare *N*-alkyl analogues of (*S*)-(-)-blebbistatin (**7**).

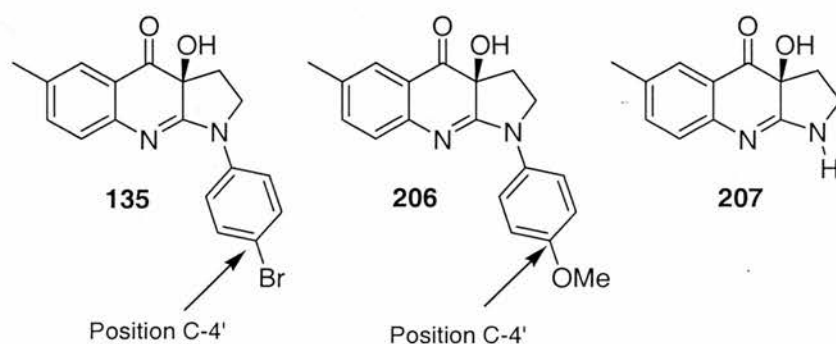


Figure 158. Different analogues derivatised at *N*-phenyl ring (R^2).

The synthesis of the *p*-anisyl analogue **206** followed the same synthetic route as described for (*S*)-(-)-blebbistatin (**7**) (Chapter 2, Section 2.1.2) (Figure 159), affording the desired compound (**206**) in an overall yield of 12.1% (4 steps) and high enantiomeric excess. The synthesis commenced with the preparation of the starting materials. A reaction carried out by Dr Patterson afforded the *p*-methoxy moiety lactam **210** from pyrrolidinone (**208**) and *p*-iodoanisole (**209**).

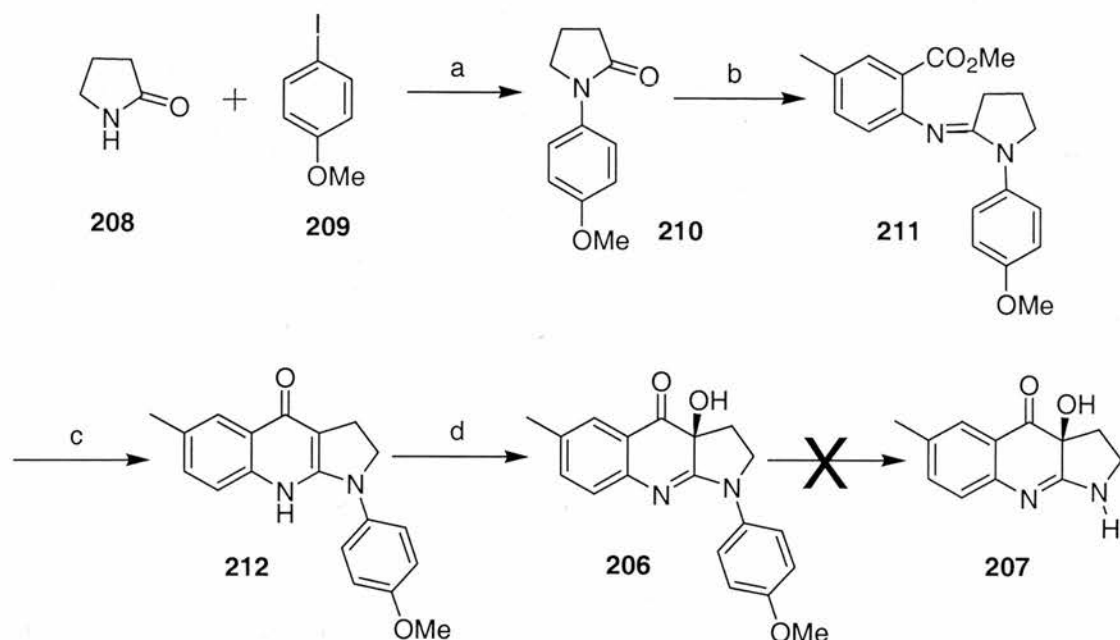


Figure 159. Preparation of *N*-phenyl-analogue **206**. Reagents and conditions: a) **208** (1.2 equiv), **209** (1.0 equiv), K_3PO_4 (2.0 equiv), CuI (0.10 equiv), *N,N'*-dimethylethylenediamine (0.20 equiv), PhMe, 70 °C, 16 hours, 88%, b) i) **210** (1.1 equiv), $POCl_3$ (1.0 equiv), DCM, RT, 3 hours; ii) **27** (1.0 equiv), 40 °C, 35 hours, 18%; c) LiHMDS (3.0 equiv), THF, -78 °C to 0 °C, 3 hours, 85%; d) i) LiHMDS (1.2 equiv), THF, -78 °C, 30 min; ii) **82** (2.4 equiv), THF, -10 °C, 16 hours, 90%, 82% *ee*, $[\alpha]_D^{25} = -460$ ($c = 0.08$ in $CHCl_3$); e) recrystallisation from MeCN >99% *ee*; f) CAN (5.0 equiv), MeCN:H₂O (1:1), 0 °C, 2 hours and RT, 16 hours.

The coupling step between the lactam analogue **210** and anthranilate **27** was carried out for 35 hours to afford the desired amidine moiety **211** in a low yield. The presence of an electron-donating group at the *para* position to the nitrogen led us to expect an improvement in the yield of this reaction compared to the *N*-phenyl lactam (**28**), but this was not observed with **211** being formed in only 18%. The cyclisation step was carried at 0 °C within three hours to give the quinolone analogue **212** in good yield (85%). Finally the blebbistatin analogue **206** was prepared in excellent yield (90%) using the Davis methodology. The enantiomeric excess of the crude reaction mixture was measured by chiral HPLC analysis (82% *ee*). Recrystallisation from acetonitrile gave crystals which when analysed by chiral HPLC showed that **206** had been prepared in greater than 99% *ee*. The deprotection of the *p*-anisyl moiety *via* oxidation with CAN has been previously reported in the literature.^{48,49} However, attempts to cleave the *p*-anisyl moiety (**206**), on a small scale (10–15 mg), to obtain **207**

proved unsuccessful. The oxidation was carried out in the presence of CAN in a mixture of 1:1 acetonitrile-water. The reaction was then cooled to 0 °C and stirred for 16 hours at room temperature. Purification by flash column chromatography afforded four fractions which were analysed by ^1H NMR and mass spectroscopy. One of the products did exhibit a peak in the mass spectrum corresponding to the mass of the desired product **207** (m/z (ES^+) 217). However ^1H NMR did not give enough information because of the small amount of compound isolated from the column. Due to time restrictions further investigation of the other three products and additional attempts to improve the synthesis were not undertaken, although it is still being considered as a first priority in future work to explore the chemistry of (*S*)-(-)-blebbistatin (**7**) in the R^2 position.

4.7. REFERENCES

- 1 Drews, J., *Science*, **2000**, 287, 1960-1964.
- 2 Baillie, T. A and McCoss, M., *Science*, **2004**, 303, 1810-1813.
- 3 Straight, A. F., Cheung, A., Limouze, J., Chen, I., Westwood, N. J., Sellers, J. R., Mitchison, T. J., *Science*, **2003**, 299, 1743-1747.
- 4 Limouze, J., Straight, A. F., Mitchison, T., Sellers, J. R., *J. Muscle. Res. Cell Motil.*, **2004**, 25, 337-341.
- 5 Patrick, G. L., *An Introduction to Medicinal Chemistry*, **2001**, Second Edition, Oxford University Press Inc., New York.
- 6 Maybridge MedChem., Technical notes for the Medicinal Chemist. Topliss Sets in Drug Design. Vol.2, pag 3.
- 7 Hansch, C and Fujita, T., *J. Am. Chem. Soc.*, **1964**, 86, 1616-1626.
- 8 Topliss, J. G., *J. Med. Chem.*, **1972**, 15, 1006-1011.
- 9 Topliss, J. G., *J. Med. Chem.*, **1977**, 20, 463-469.
- 10 Kolega, J., *Biochem. Biophys. Res. Commun.*, **2004**, 320, 1020-1025.
- 11 Sakamoto, T., Limouze, J., Combs, C. A., Straight, A. F., Sellers, J. R., *Biochemistry*, **2005**, 44, 584-588.
- 12 Smith, M. B. and March, J., *March's Advanced Organic Chemistry*, **2001**, Firth Edition, John Wiley & Sons, Inc., New York.

- 13 Carey, F. A. and Sundberg, R. J., *Advanced Organic Chemistry. Part B: Reactions and Synthesis*, **2001**, Fourth Edition, Kluwer Academic/Plenum Publishers, New York.
- 14 Dale, J. A., Dull, D. L., Mosher, H. S., *J. Org. Chem.*, **1969**, *34*, 2543-2549.
- 15 Ward, D. E., and Rhee, C. K., *Tetrahedron Lett.*, **1991**, *32*, 7165-7166.
- 16 Staskun, B., *J. Org. Chem.*, **1988**, *53*, 5287-5291.
- 17 Boeyens, J. C. A., Denner, L., Marais, J. L. C., Staskun, B., *S. Afr. J. Chem.*, **1988**, *41*, 63-67.
- 18 Marais, J. L. C., Pickl, W., Staskun, B., *J. Org. Chem.*, **1990**, *55*, 1969-1972.
- 19 Boeyens, J. C. A., Denner, L., Marais, J. L. C., Staskun, B., *S. Afr. J. Chem.*, **1986**, *39*, 221-223.
- 20 Banks, R. E., Smart, B. E., Tatlow, J. C., *Organofluorine Chemistry. Principles and Commercial Applications*, **1994**, Plenum, New York.
- 21 Banks, R. E., *J. Fluorine Chem.*, **1998**, *87*, 1-17.
- 22 Syvret, R. G., Perchloryl fluoride, in Paquette, L. A., et al. (Eds.), *Encyclopedia of Reagents for Organic Synthesis*, **1995**, Vol. 6, Wiley, New York.
- 23 Rozen, S., *Chem. Rev.*, **1996**, *96*, 1717-1736.
- 24 Tuis, M. A., *Tetrahedron*, **1995**, *51*, 6605-6634.
- 25 Rozen, S., *Synthetic Fluorine Chemistry*, **1992**, Wiley, New York.

- 26 Cahard, D., Audouard, C., Plaquevent, J. C., Roques, N., *Org. Lett.*, **2000**, *23*, 3699-3701.
- 27 Cahard, D., Audouard, C., Plaquevent, J. C., Toupet, L., Roques, N., *Tetrahedron Lett.*, **2001**, *42*, 1867-1869.
- 28 Zoute, L., Audouard, C., Plaquevent, J. C., Cahard, D., *Org. Biomol. Chem.*, **2003**, *11*, 1833-1834.
- 29 Shibata, N., Ishimaru, T., Suzuki, E., Kirk, K. L., *J. Org. Chem.*, **2003**, *68*, 2494-2497.
- 30 Ma, J-A. and Cahard, D., *Chem. Rev.*, **2004**, *104*, 6119-6146.
- 31 Shibata, N., Suzuki, E., Asahi, T., Shiro, M., *J. Am. Chem. Soc.*, **2001**, *123*, 7001-7009.
- 32 Takeuchi, K., Okazaki, T., Kitagawa, T., Ushino, T., Ueda, K., Endo, T., *J. Org. Chem.*, **2001**, *66*, 2034-2043.
- 33 Bijvoet, J. M., Peerdeman, A. F., Van Bommel, A. J., *Nature*, **1951**, *168*, 271-272.
- 34 Buchi, G., Francisco, M. A., Murray, W. V., *Tetrahedron Lett.*, **1983**, *24*, 2527-2530.
- 35 Trost, B. M., Belletire, J. L., Godleski, S., McDougal, P. G., Balkovec, J. M., Baldwin, J. J., Christy, M. E., Ponticello, G. S., Varga, S. L., Springer, J. P., *J. Org. Chem.*, **1986**, *51*, 2370-2374.
- 36 Larock, R. C., *Comprehensive Organic Transformations*, **1989**, VCH Publishers, Inc., New York.

- 37 Greene, T.W and Wuts, P. G. M., *Protective Groups in Organic Synthesis*, **1991**, Second Edition, John Wiley & Sons, Inc., New York.
- 38 Tanaka, T., Lijima, I., Miyazaki, M., Iwakuma, T., *J. Chem. Soc., Perkin Trans. 1*, **1974**, 1593-1596.
- 39 Pelletier, S. W., Chappell, R. L., Parthasarthy, P. C, Lewin, N., *J. Org. Chem.*, **1966**, *31*, 1747-1752.
- 40 Soloway, S. B. and Laforge, F. B., *J. Am. Chem. Soc.*, **1947**, *69*, 2677-2678.
- 41 Mander, L. N. and Sethi, S. P., *Tetrahedron Lett.*, **1983**, *24*, 5425-5428.
- 42 Crabtree, S. R., Chu, W. L. A., Mander, L. N., *Synlett.*, **1990**, *3*, 169-170.
- 43 Sisti, A, J. and Vitale, A. C., *J. Org. Chem.*, **1972**, *37*, 4090-4094.
- 44 Dess, D. B. and Martin, J. C., *J. Org. Chem.*, **1983**, *48*, 4156-4158.
- 45 Craig, J. C., Dinner, A., Mulligan, P. J., *J. Org. Chem.*, **1974**, *39*, 1669-1676.
- 46 Kornfeld, E. C., Fornefeld, E.J., Kline, G. B., Mann, M. J., Morrison, D. E., Jones, R. G., Woodward, R. B., *J. Am. Chem. Soc.*, **1956**, *78*, 3087-3114.
- 47 Sajiki, H., Hattori, K., Hirota, K., *J. Chem. Soc., Perkin Trans. 1*, **1998**, 4043-4044.
- 48 Kronenthal, D. R., Han, C. Y., Taylor, M. K., *J. Org. Chem.*, **1982**, *47*, 2765-2768.
- 49 Fukuyama, T., Frank, R. K., Jewell, C. F., *J. Am. Chem. Soc.*, **1980**, *102*, 2122-2123.

CHAPTER 5

RESULTS AND DISCUSSION

BIOLOGICAL INVESTIGATIONS ON BLEBBISTATIN

5.1. CRYSTAL STRUCTURE OF BLEBBISTATIN AND MYOSIN II

Since the completion of the laboratory work associated with this research project a crystal structure of the (*S*)-(-)-blebbistatin-myosin II complex has been published¹. This result is of great interest in order to confirm how (*S*)-(-)-blebbistatin (**7**) binds to the protein and therefore how it effects the protein activity.

As described previously in Chapter 1, Section 1.4.3.3, (*S*)-(-)-blebbistatin (**7**) was found to stabilise the ADP-Pi-myosin complex, with the consequent inhibition of phosphate release.² This observation was consistent with the crystal structure of (*S*)-(-)-blebbistatin (**7**) bound to the *MgADP-vanadate* complex (which mimics the ADP-Pi state³) of *Dictyostelium discoideum* myosin II.¹

The selectivity of the two enantiomers of blebbistatin (**7** and **23**) can be explained by the presence of hydrogen bonds between the protein and the hydroxyl group. In the case of the (*S*)-(-)-enantiomer (**7**) hydrogen bonds are formed from the OH group (on the top face of the molecule) to the main chain amide carbonyl oxygen of Leu262 and to the main chain amide hydrogen of Gly240 (Figure 160). In contrast, the binding of the (*R*)-(+)-enantiomer (**23**) is of lower affinity due to the absence of the equivalent hydrogen bonds.¹

It was also found that the binding of (*S*)-(-)-blebbistatin (**7**) to myosin was stabilised by hydrophobic interactions. For instance both the phenyl ring and tetrahydropyrrolo ring are surrounded by non-polar aliphatic and aromatic residues (Figure 160).

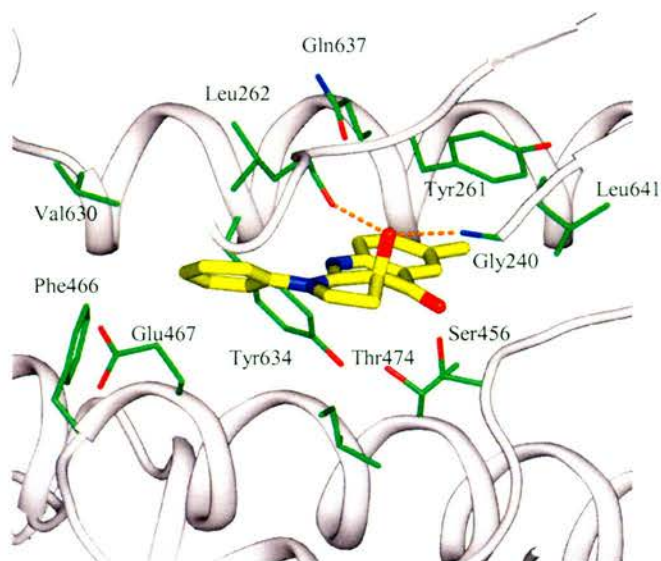


Figure 160. Interaction between (*S*)-(-)-blebbistatin (**7**) (yellow) and selected amino acids of myosin (green sticks). In red is shown the hydrogen bonds between the OH group of (*S*)-(-)-blebbistatin (**7**) and the amino acids, Leu262 and Gly240.¹

Finally, the specificity of (*S*)-(-)-blebbistatin (**7**) for different classes and subclasses of myosin can be explained by the presence or absence of similar residues in different myosins. Table 8 shows the variation of residues across the myosins as compared to the model myosin used in the crystallisation studies (*Dictyostelium discoideum II*). For instance, looking at the selected contact residue for (*S*)-(-)-blebbistatin (e.g. serine 456), it is interesting to note that the variation of this residue for another through the different subclasses resulted in a decrease of the inhibitory activity. A possible explanation could arise from the size of the residue involved in such interaction with the small molecule (e.g. alanine *versus* tyrosine and phenylalanine, where the phenyl ring would be in the way of the small molecule).

It has been observed that the best inhibition occurs for skeletal muscle myosin II, non-muscle myosin IIB, non-muscle myosin IIA and *D. discoideum* myosin II. In contrast, low or no inhibition was observed for smooth muscle myosin II, myosin I, myosin V and myosin X. Although the residues in smooth muscle myosin II are nearly identical to those in *D. discoideum* II (only substitution of Ser456 for Ala) (Table 8), the lack of inhibition was proposed to be a result of differences in the position of residues related to Leu262.¹

Myosin	Selected blebbistatin contact residues				IC ₅₀ (μM)
Dictyostelium II	Ser456	Thr474	Tyr634	Gln637	4.9
Nonmuscle IIA	Ala	Thr	Tyr	Gln	5.1
Nonmuscle IIB	Ala	Thr	Tyr	Ser	1.8
Skeletal II	Ala	Thr	Phe	Asn	0.5
Smooth II	Ala	Thr	Tyr	Gln	79.6
Ib	Tyr	Cys	Phe	Ser	>150
Va	Tyr	Ala	Phe	Ser	>150
X	Phe	Ala	Phe	Ser	>150

Table 8. Binding of (*S*)-(-)-blebbistatin (**7**) to selected amino acids on the different myosins.¹

The publication of the crystal structure of myosin bound to (*S*)-(-)-blebbistatin (**7**) is also of importance in order to understand which parts of (*S*)-(-)-blebbistatin (**7**) could be changed to increase its potency and also to alter its selectivity towards different myosins. The crystal structure shows that the appropriate sites (where there is space) to introduce diversity in the (*S*)-(-)-blebbistatin (**7**) core structure are around both the phenyl and tetrahydropyrrolo rings. It was envisaged that the biological activity of (*S*)-(-)-blebbistatin (**7**) could be improved by the introduction of a bromine atom at the *para* position of the phenyl ring (C4').

Therefore, (*S*)-(-)-bromo-blebbistatin (**135**) was sent to Rayment's research group to perform crystallographic studies. Rayment and co-workers were able to grow crystals of the (*S*)-(-)-bromoblebbistatin-myosin complex and obtained X-ray data (Figure 161). The data was solved and showed that the bromine at the *para* position on the phenyl ring was accommodated in the protein structure. The bromine atom forms hydrophobic interactions with the surrounding amino acids residues.

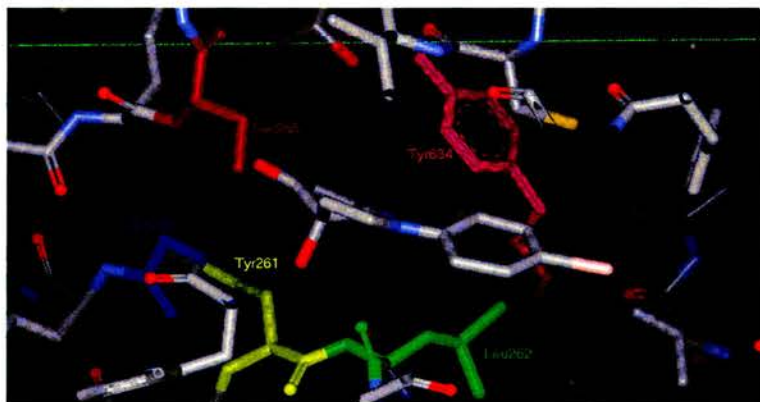


Figure 161. Crystal structure of the (*S*)-(-)-bromo-blebbistatin (**135**)-myosin complex.

(*S*)-(-)-Bromo-blebbistatin (**135**) was also sent to Prof. Seller's laboratory in order to test its biological activity against non-muscle myosin II. It was found that **135** was a more potent inhibitor than (*S*)-(-)-blebbistatin (**7**) itself (data not shown).

5.2. BIOLOGICAL ACTIVITY OF (*S*)-(-)-BLEBBISTATIN (**7**), (*R*)-(+)-BLEBBISTATIN (**23**) AND NITROBLEBBISTATIN (**160**)

As described in Chapter 1, section 1.5, one of the aims of the project was to prepare highly enriched enantiomers of blebbistatin (**18**) for biological testing. Therefore, samples of highly enriched (*S*)-(-)-blebbistatin (**7**) (>99% *ee*) and (*R*)-(+)-blebbistatin (**23**) (>99% *ee*) were sent to Prof. Sellers' laboratory in order to determine their biological activities. In addition an optically enriched sample of (*S*)-(-)-nitro blebbistatin (**160**) (76% *ee*) was also sent for biological testing.

The inhibitory activity of the three samples was tested against non-muscle myosin II. A NADH-coupled assay was carried out to measure the actin-activated ATPase activity. The assay works as follows (see also Figure 162):

- i) Myosin hydrolyses ATP to produce ADP and Pi.
- ii) Pyruvate kinase converts ADP and phosphoenolpyruvate (PEP) into ATP and pyruvate.
- iii) Lactate dehydrogenase reduces pyruvate to lactate. This converts the cofactor NADH into NAD⁺.

- iv) The production of NAD⁺ can be monitored by spectrophotometry. For every molecule of ATP hydrolysed by myosin, one molecule of NAD⁺ is produced.

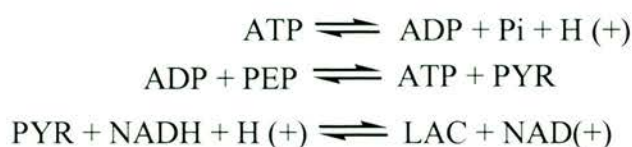


Figure 162. NADH-coupled assay.

The inhibition values are expressed as percentage inhibitions where the DMSO was used as a control (100% activity, 0% inhibition). The assay mixture contained 10 μM actin (without the actin, myosin ATPase activity would be very low, see for more details Chapter 1, Section 1.4.1) and 1 mM ATP.

The results from the assays are represented in the curves shown in Figure 163. The x-axis shows the concentration of the inhibitors (0.1 to 100 μM) and the y-axis shows the % of inhibition.

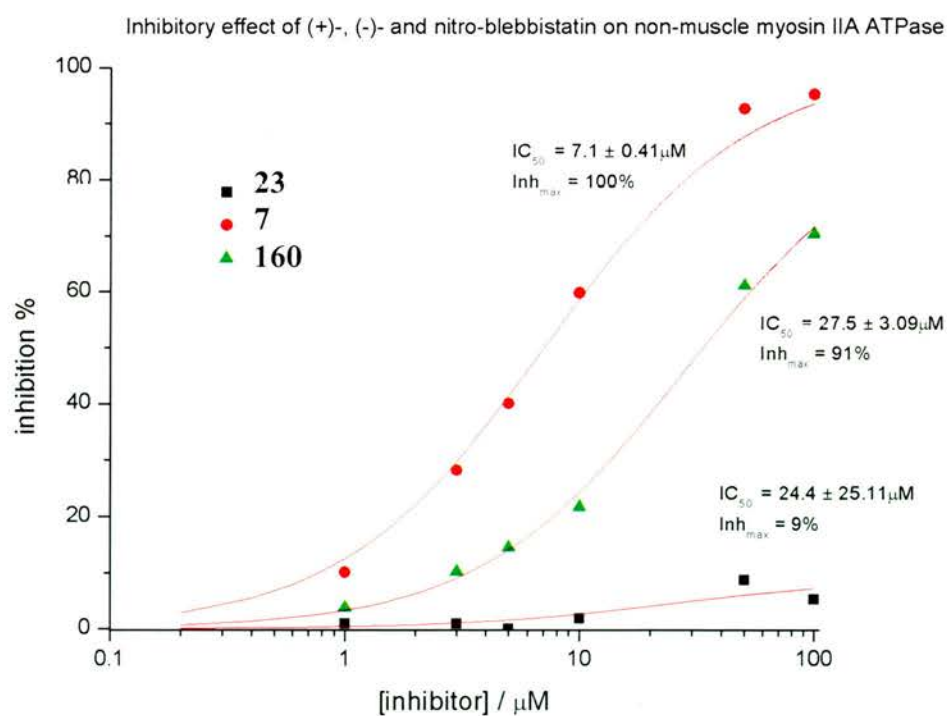


Figure 163. Inhibitory activity of (S)-(-)-blebbistatin (7), (R)-(+)-blebbistatin (23) and nitro blebbistatin (160).

As it can be observed, the (-)-enantiomer (**7**) showed a maximum of inhibition of 100% for a concentration of 100 μM whereas the (+)-enantiomer (**23**) gave only a 9% of inhibition at the same concentration, being consistent with results obtained by Straight *et al.*⁴ (Chapter 1, Section 1.4.3.1). The IC_{50} values were 7.1 μM for **7** and 24.4 μM for **23**. The nitro analogue **160** showed an inhibition of 91% at a concentration of 100 μM with an IC_{50} of 27.5 μM . It is worth noting that this inhibition value is lower than that observed for **7**. Despite this decrease in activity, this result was of great interest due to the fact that the nitro analogue **160** retained the inhibitory activity against non-muscle myosin II. Therefore, **160** can be used as molecular tool in certain biological assays where **7** is not suitable (Chapter 4, Section 4.3.2).

5.3. PRELIMINARY BIOLOGICAL TESTING OF BLEBBISTATIN ANALOGUES

The first batch of samples biologically tested was composed of optically enriched samples of the methyl analogues (**139**, **140**, **141**, **7**), H-blebbistatin (**67**), fluoro blebbistatin (**161**) and a reduced analogue (**213**) (Figure 164). The hydroxylation of the methyl analogues was carried out with both types of Davis oxaziridines **81** and **78**. The enantiomeric excess values obtained in the hydroxylation reactions are shown in Table 6, Chapter 3).

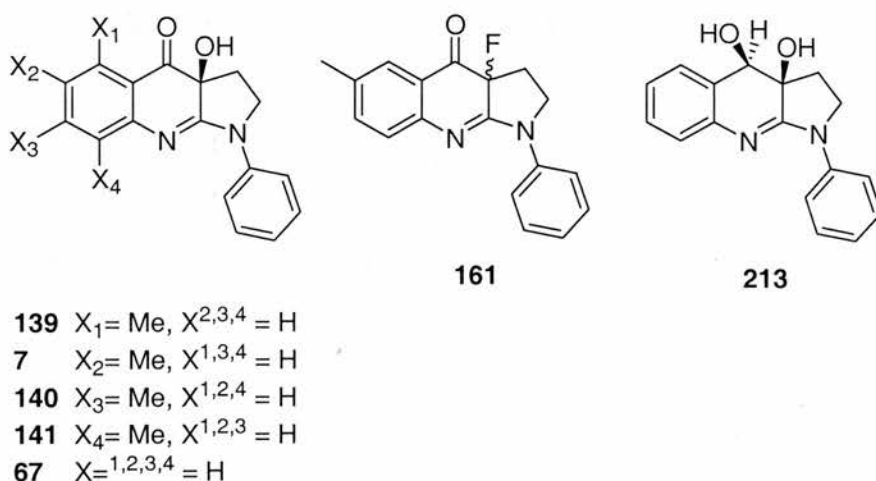


Figure 164. Different analogues sent in a first batch.

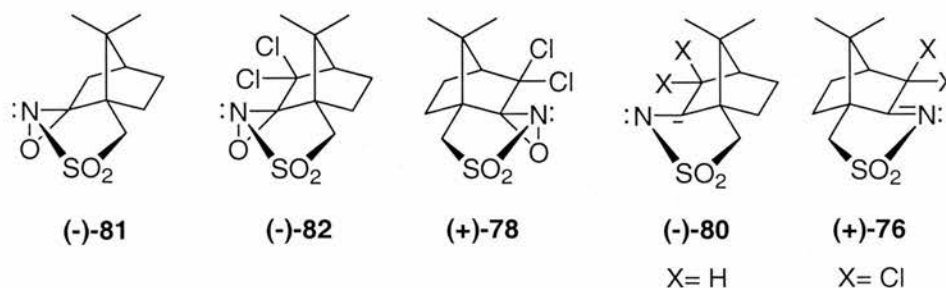


Figure 165. Davis oxaziridines used to prepare the different analogues of blebbistatin.

The NADH-coupled assay was carried out for all the samples in order to test their inhibition of myosin ATPase activity. Samples of racemic blebbistatin **18** and sulfonimines (+)-**76** and (-)-**80** were used as a controls.

Figure 166 shows the effect of the different analogues on the myosin ATPase activities of scallop striated muscle, cardiac muscle and skeletal muscle myosin II. The concentration used for testing the analogues was 100 μM . The concentration of actin in the assay was 10 μM .

The results showed a number of trends:

- Inhibition of skeletal muscle myosin ATPase: The highest inhibition values (>80%) were found for the analogues (+)-**139**, (-)-**139**, (+)-**23**, (-)-**7**, (+)-**67**, (-)-**67**, and fluoro-blebbistatin (**161**). Surprisingly, only small differences were found between the different enantiomers of these analogues. This can be explained due to the fact that the samples were not optically pure and also the concentrations used for testing in each case were very high. It is important to note that the inhibition of **141** was lower than the other methyl analogues. Therefore, substitution at C-8 reduces the inhibitory activity.
- Similar values of inhibition were observed for cardiac muscle myosin II. In this case, the (+)-enantiomers gave lower values than the (-)-enantiomers, as expected.

- The inhibition of scallop muscle myosin II showed that analogue **139** gave the highest inhibitory activity.
- The reduced analogue **213** was inactive against all three myosins. The reduction of the ketone functionality to the alcohol on (*S*)-(-)-blebbistatin (**7**) could change the shape of the inhibitor with the consequent loss in biological activity.

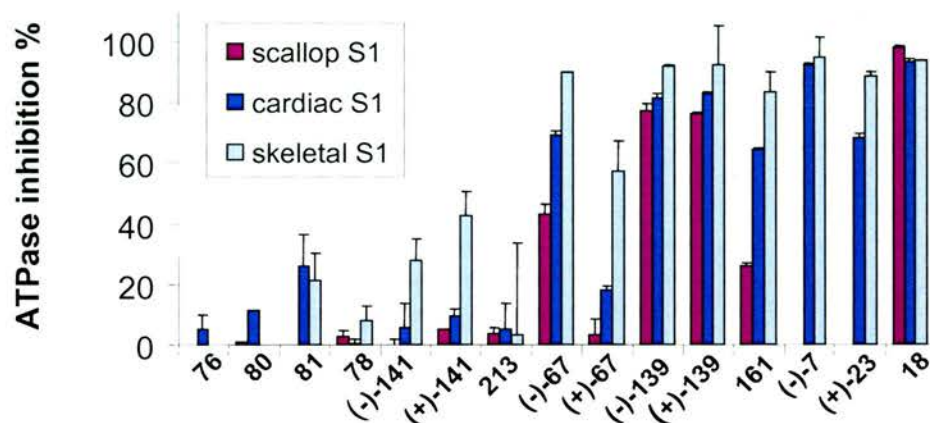


Figure 166. Effect of different compounds on the ATPase activity of scallop muscle, cardiac muscle and skeletal muscle myosin II.

In summary, the results were consistent with the results obtained by Straight *et al.*⁴ where racemic blebbistatin (**18**) inhibited the ATPase activity of scallop, cardiac and skeletal myosins II.

Differences were also found in the inhibitory activity of the analogues of (*S*)-(-)-blebbistatin (**7**) within the myosin II class. Figure 167 summarises the results obtained for the effect of the blebbistatin analogues on the ATPase activity of the three isoforms of non-muscle myosin II and smooth muscle myosin II. The concentration used for testing the analogues was 100 μM . The concentration of actin in the assay was 10 μM .

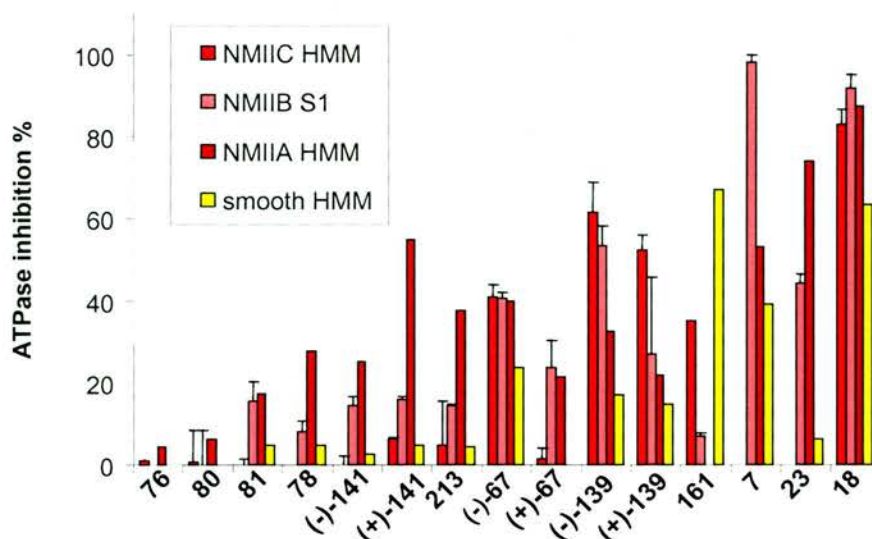


Figure 167. Effect of different compounds on the ATPase activity of non-muscle IIA, non-muscle IIB, non-muscle IIC and smooth muscle myosin II.

The results showed in Figure 167 can be summarised as follows:

- Inhibition of smooth muscle myosin was found for racemic blebbistatin (**18**) and the fluoro analogue (**161**) with values over 60%. However, lower inhibition was observed for (–)-enantiomer of **7** and (–)-enantiomer **141** (20-40%).
- In the case of non-muscle myosin IIA, the highest inhibition was observed for racemic blebbistatin (**18**) and (+)-**23** followed by inhibition with (–)-**7**, (+)-**141**. Lower values were found for (+)-**67**, (+)-**139** and (–)-**141**.
- Non-muscle myosin IIB was significantly inhibited by racemic blebbistatin (**18**), (–)-**7**, (–)-**139** and (–)-**67**. Interesting low inhibition was observed for **141**. This can be rationalised by the position of the methyl group at the C-8.
- In addition, non-muscle myosin IIC was inhibited by racemic blebbistatin (**18**), fluoro analogue (**161**), blebbistatin analogue **139** and (–)-**67**.

In summary, smooth muscle was mainly inhibited by fluoro analogue (**161**) and racemic blebbistatin (**18**). In the case of non-muscle myosin IIA the inhibition was

caused by racemic blebbistatin (**18**), and the (+)-enantiomers of **23** and **141**. In addition the highest values of inhibitory activity for non-muscle myosin IIB were found for racemic (**18**) and the (–)-enantiomers of **7** and **139**. Finally non-muscle myosin IIC was mainly inhibited by the two enantiomers of **139** and racemic **18**.

The results, although preliminary, provided important information in order to determine the specificity of the different analogues. Figure 168 shows a graph with promising examples of specificity of methyl analogues over the three isoforms of non-muscle myosin II. Non-muscle myosin IIC was inhibited by (+)-**139** to a greater extent than was observed for non-muscle myosin IIB and non-muscle myosin IIA. In contrast, non-muscle myosin IIA was significantly inhibited by (+)-**141**, over and above the inhibition levels observed for non-muscle myosin IIB and non-muscle myosin IIC. Interestingly the larger differentiation between isoforms is observed in the (+)-enantiomers.

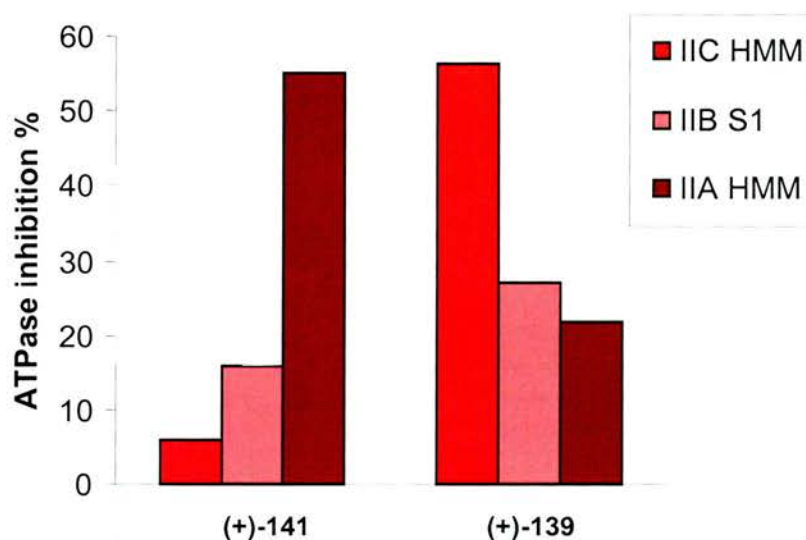


Figure 168. Specificity in (+)-139 and (+)-141.

The same set of compounds was also tested against two different classes of myosins, class V and class X. The concentration used for the analogues was of 100 μM . The concentration of actin was 10 μM . Interestingly out of the set of compounds, only the fluoro-blebbistatin analogue (**161**) (~60%) and reduced blebbistatin **213** (~20%) inhibited myosin X (Figure 169). Although there is not clear rationalisation for these two inhibitions, however, differences in the shape of the active site of myosin X,

compared with myosin II, could explain the inhibition of these compounds against this class of myosin.

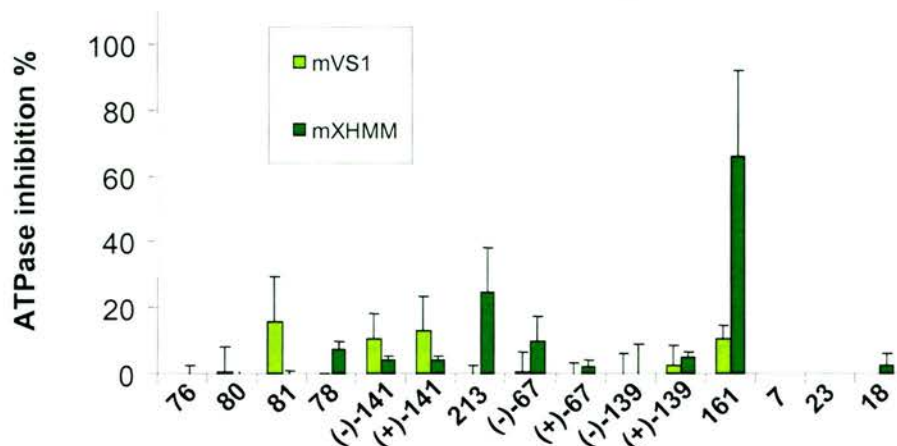


Figure 169. Effect of different compounds on the ATPase activity of myosin V and myosin X.

A new batch of compounds containing the methyl analogues **139** and **140** and **214** (see this structure in Figure 171) were assayed against skeletal muscle myosin II (Figure 170). **140** was prepared with three different Davis oxaziridines, affording enantiomeric excess of 28% for (-)-**81** (**140a**), 90% for (-)-**82** (**140b**) and 90% for (+)-**78** (Figure 165). In addition **139** was prepared with (-)-**82** and (+)-**78** (64-65% *ee*). The concentrations used for the analogues were 3 μ M and 100 μ M. Furthermore the concentration used for actin was of 10 μ M.

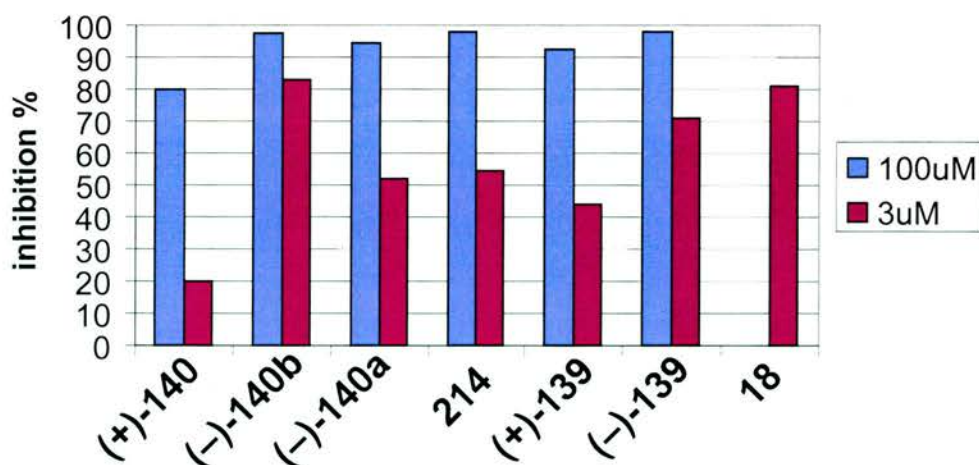


Figure 170. Effect of different compounds on the ATPase activity of skeletal muscle myosin II.

The results showed that at low concentration of inhibitor ($3\mu\text{M}$) the highest inhibitory activities were found for racemic blebbistatin (**18**) ($\sim 80\%$), (-)-**139** ($\sim 70\%$) and (-)-**140b** ($\sim 80\%$). In contrast, the inhibitory activity of bromo blebbistatin **214** (90% *ee*) was only 50% . The inhibitory activity for the (+)-enantiomers was lower as expected. However, when the concentration of the analogues was increased to $100\mu\text{M}$ the values of inhibition were similar for all the samples.

More recently, a final batch of analogues was sent to be tested against myosin II and different classes of myosin. Included in this batch were the methyl analogues (see Figure 164), fluoro-blebbistatin (**161**) and chloro-blebbistatin (**162**), ester derivative **176**, methoxy analogue of blebbistatin **180**, partially reduced blebbistatin **199** and *p*-methoxy-blebbistatin (**206**) (Figure 171). The samples were highly optically enriched ($>90\%$ *ee*).

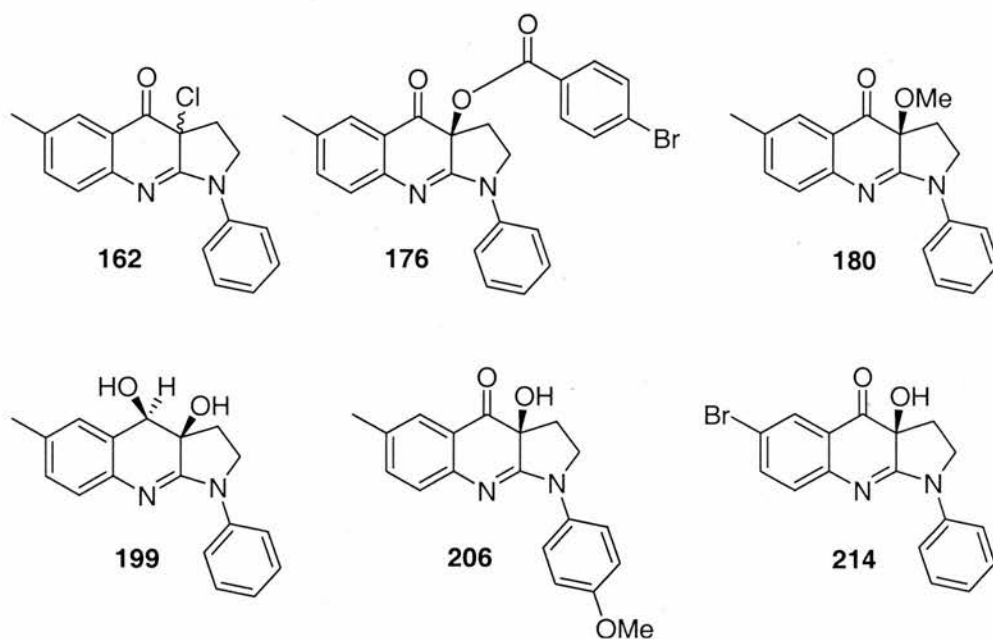


Figure 171. Structures of different analogues of **7**.

Unfortunately, the biological data for most of the compounds did not arrive in time to be included in this thesis. Nevertheless, the methoxy analogue of blebbistatin **180** was found to be inactive against myosin II (data not shown). Furthermore partially reduced blebbistatin **199** and doubly reduced blebbistatin **198** were also found to be inactive against myosin II (data not shown).

In summary, it was observed that blebbistatin and its analogues were specific for the myosin II class over other family members such as myosin V and X. The specificity within the myosin II class was also tested. The results showed fluoro blebbistatin (**161**) as a specific inhibitor of smooth muscle myosin. In addition, blebbistatin analogue **141** was found to only have inhibitory activity against skeletal and non-muscle myosin IIA. Furthermore, it is interesting to note that (+)-**141** was more potent than the (-)-enantiomer, contrary to expectations. In addition, promising specificity data was found for (+)-enantiomers of **141** and **139** within the non-muscle myosin II isoforms.

5.4. SECTION SUMMARY

In conclusion, although preliminary, the data found for the inhibitory activity of the different analogues, will be useful in order to enable the preparation of specific inhibitors within the same class and subclasses of myosins. Furthermore the lack of activity of methoxy blebbistatin analogue **180**, reduced blebbistatin **199** and fully reduced blebbistatin **198**, gave an idea of which functional groups are important in the blebbistatin core structure. However, both the carbonyl and OH group were necessary for the biological activity of (*S*)-(-)-blebbistatin (**7**). In addition, the crystal structure of blebbistatin also showed the parts of this molecule that can introduce diversity in order to synthesise compounds of increased potency (*e.g.* modifications in the R4 position and also the size of the tetrahydropyrrolo ring).

5.5. REFERENCES

- 1 Allingham, J. S., Smith, R., Rayment, I., *Nature Struct. Mol. Biol.*, **2005**, Advance online publication.
- 2 Kovacs, M., Toth, J., Hetenyi, C., Malnasi-Csizmadia, A., Sellers, J. R., *J. Biol. Chem.*, **2004**, 279, 35557-35563.
- 3 Smith, C. A. and Rayment, I., *Biochemistry*, **1996**, 35, 5404-5417.
- 4 Straight, A. F., Cheung, A., Limouze, J., Chen, I., Westwood, N. J., Sellers, J. R., Mitchison, T. J., *Science*, **2003**, 299, 1743-1747.

CHAPTER 6

CONCLUSIONS AND FUTURE WORK

CONCLUSIONS AND FUTURE WORK

CONCLUSIONS

In this thesis, the development of one efficient synthetic route to prepare the core structure of (-)-blebbistatin (**7**) has been presented. The incorporation of a hydroxy group has been achieved by asymmetric hydroxylation using Davis oxaziridines as the oxidising reagents. It has been found that this reaction gives high values of enantiomeric excess. In addition, the chemical structure of (-)-blebbistatin (**7**) has been confirmed by X-ray crystallographic analysis.

To determine the stereochemistry of **7**, a bromo containing analogue of blebbistatin (**135**) was prepared using the same synthetic route and analysed by X-ray diffraction. The absolute configuration of the crystallised bromo-blebbistatin analogue (**135**) was found to be *S*. Further comparison, by chiral HPLC, showed that a reduced sample of **135** back to **7** was identical to a sample of **7** prepared by the usual route. Therefore, this result led to the assignment of (-)-blebbistatin (**7**) as *S*.

In addition, the synthesis of a nitro-blebbistatin analogue (**160**) has been shown to be of great interest. Since this compound is a potent inhibitor of non-muscle myosin II and has modified fluorescence properties, it can replace (*S*)-(-)-blebbistatin (**7**) as a molecular tool in live-cell imaging experiments.

Our studies show that the core structure of (*S*)-(-)-blebbistatin (**7**) can be chemically modified, enabling the preparation of different analogues. Biological testing of some of these analogues has proved that both the carbonyl and hydroxy group must be present in the core structure of (*S*)-(-)-blebbistatin (**7**) for it to exhibit inhibitory activity.

FUTURE WORK

The use of (*S*)-(-)-blebbistatin (**7**), as a molecular tool, has had an impact on biomedical research in the last two years. A number of papers have reported the importance of this molecule to dissect biological processes. Therefore, this is of

importance for the development of new projects where synthetic chemistry has a key role for the optimisation and preparation of novel small molecule inhibitors. The recent publication of the crystal structure of the blebbistatin-myosin complex has helped to develop a better understanding of which parts of the molecule are available for introducing diversity with retention of biological activity.

Therefore, the identification of more potent and specific inhibitors of myosin II will be possible by the preparation of small focussed libraries of (*S*)-(-)-blebbistatin (**7**) (Figure 172). This approach can be carried out by the development of a solid supported synthesis of (*S*)-(-)-blebbistatin (**7**).

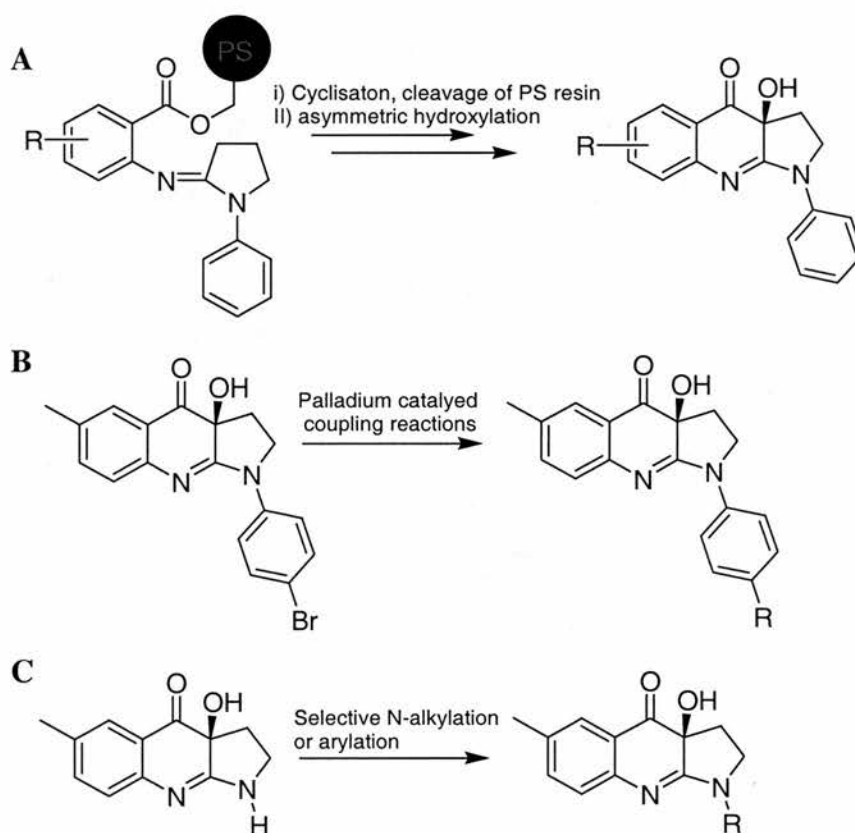


Figure 172. Design to prepare future libraries of compounds from (*S*)-(-)-blebbistatin (**7**).

Therefore, the preparation of these small libraries are based on several resin bound intermediates that will be reacted with lactam activated intermediates to afford the corresponding amidines (Figure 172A). Further cyclisation of the resulting amidines and subsequent treatment with either Davis reagent or with alternative electrophiles will lead to a large number of blebbistatin analogues. The preparation of

small focussed libraries can be also achieved by the incorporation of different substituents at the R^2 position where it is known not to disrupt the inhibitory activity (Figures 172B and 172C). These analogues will be screened, in order to discover novel bioactive compounds which will be more specific for myosin II compared to (*S*)-(-)-blebbistatin (**7**).

CHAPTER 7

EXPERIMENTAL

EXPERIMENTAL

7.1. General Methods

Chemicals and solvents were purchased from Acros, Aldrich, Fisher Chemicals, Fluka and Lancaster and were used as received unless otherwise stated. Air and moisture sensitive reactions were carried out under an inert atmosphere of dried argon and glassware was oven dried (145 °C).

Tetrahydrofuran (THF) was dried by heating under reflux with sodium/benzophenone under a nitrogen atmosphere and collected by distillation. Dichloromethane (DCM) was dried by heating under reflux over calcium hydride and distilled under an atmosphere of nitrogen. Anhydrous methanol (MeOH) was purchased from Aldrich.

Analytical thin-layer chromatography (TLC) was performed on pre-coated TLC plates SIL G-25 UV₂₅₄ (layer 0.25 mm silica gel with fluorescent indicator UV₂₅₄) (Aldrich). Developed plates were air dried and analysed under a UV lamp, Model UVGL-58 (Mineralight LAMP, Multiband UV_{254/365} nm) and where necessary, stained with a solution of ceric ammonium molybdate or iodine on silica to aid identification. Flash column chromatography was performed using silica gel (40-63 µm, Fluorochem).

Melting points were determined using an Electrothermal 9100 capillary melting point apparatus. Values are quoted to the nearest 0.5 °C and are uncorrected.

¹H Nuclear magnetic resonance (NMR) spectra were recorded on a Bruker Avance 300 (300.1 MHz), Bruker Avance 500 (499.9 MHz) or a Varian Gemini 2000 (300.0 MHz) spectrometer, using deuteriochloroform (or other indicated solvent) as reference or internal deuterium lock. ¹³C NMR spectra using the PENDANT sequence and internal deuterium lock were recorded on a Bruker Avance 300 (75.5 MHz) or a Bruker Avance 500 (125.7 MHz) spectrometer. All other ¹³C spectra were recorded on a Varian Gemini 2000 (75.5 MHz) spectrometer using composite pulse ¹H decoupling. ¹⁹F NMR spectra were recorded on a Bruker Avance 300 (282.3 MHz) spectrometer using ¹H decoupling and ¹H coupling. Deuterated solvent was used as the lock and the

residual protonated solvent as the internal reference. ^{31}P NMR spectra were recorded on a Bruker Avance 300 (121.5 MHz) or a Bruker Avance 500 (202.4 MHz) instrument using ^1H decoupling and internal deuterium lock. The chemical shift data for each signal are given as (δ) in units of parts per million (ppm) using the residual solvent as the internal reference in all cases (CDCl_3 δ_{H} 7.27 ppm, δ_{C} 77.0 ppm), ($[\text{D}_8]\text{THF}$ δ_{C} 25.2 ppm, 67.2 ppm), ($[\text{D}_6]\text{DMSO}$ δ_{H} 2.5 ppm, δ_{C} 39.5 ppm) and ($[\text{D}_4]\text{MeOD}$ δ_{H} 3.31; 4.79 ppm, δ_{C} 49 ppm). Coupling constants (J) are quoted in Hz and are recorded to the nearest 0.1 Hz. The multiplicity of each signal is indicated by the following abbreviations: s, singlet; d, doublet; dd, doublet of doublets; ddd, doublet of doublet of doublets; dt, doublet of triplets; t, triplet; q, quartet; ddq, doublet of doublet of quartets; m, multiplet and br, broad. Two-dimensional NMR spectroscopy such as ^1H - ^1H COSY spectra (Correlated Spectroscopy), ^1H - ^{13}C COSY spectra (HSQC: Heteronuclear Single Quantum Coherence) and long-range ^1H - ^{13}C COSY spectra (HMBC: Heteronuclear Multiple Bond Connectivity), were carried out to determine the correlation between ^1H and ^{13}C .

Fourier Transform Infrared (FT-IR) spectra were recorded as Nujol mulls for solids and dichloromethane solutions for liquids using a Perkin-Elmer Paragon series 1000 Fourier Transform spectrometer. Absorption maxima are reported in wavenumbers (cm^{-1}). Intensities of the maxima are quoted as strong (s), medium (m) and weak (w).

Low resolution and high-resolution (HR) mass spectral analysis (EI and CI) were recorded using a VG AUTOSPEC mass spectrometer or a Micromass GCT (Time-of-Flight), high performance, orthogonal acceleration spectrometer coupled to an Agilent Technologies 6890N GC system. Electrospray mass spectrometry (ESMS) was recorded on a high performance orthogonal acceleration reflecting TOF mass spectrometer, coupled to a Waters 2975 HPLC. Only major peaks are reported and intensities are quoted as percentages of the base peak.

Microanalysis for carbon, hydrogen and nitrogen were performed using EA 1110 CHNS CE Instruments, elemental analyser.

The enantiomeric excess (*ee*) of the samples was measured using two systems of chiral high performance liquid chromatography (HPLC):

a) HPLC system which includes a Waters 2996 photodiode array detector, Waters 2795 Alliance HT Separations Module, Micromass LCT, Thinkcenter IBM running MassLynx™ 4.0.Global. Separations were performed using a Daicel® Chiralpak AD-RH HPLC analytical chiral column (150 × 4.6 mm, 5 μm).

b) HPLC system which includes a Waters 2700 Sample Manager, Waters 600 Controller, Waters 2487 Dual λ Absorbance Detector, Thinkcenter COMPAQ deskpro EN running MassLynx™ version 3.5. Separations were performed using a Daicel® Chiralpak AD-RH HPLC analytical chiral column (150 × 4.6 mm, 5 μm).

Specific Optical Rotation measurements were performed using an Optical Activity AA-1000 automatic polarimeter (Optical Activity Ltd. Polarimeter millidegree-autoranging), operating at 589 nm using a 2 mL solution cell with a 20 cm path length. The concentration (*c*) is expressed in g/100 mL (equivalent to g/0.1 dm³). Specific rotations are denoted $[\alpha]_D^T$ and are given in units of 10⁻¹ deg cm² g⁻¹ (T= ambient temperature in °C).

UV absorption spectra were recorded on a Cary Varian model 300 absorption spectrophotometer, and time-integrated PL spectra were measured on a Jobin Yvon Fluoromax 2 fluorimeter. Measurements were recorded at a sample concentration of 10 mg L⁻¹, in HPLC grade methanol. The samples were excited at wavelengths of 420, 440, 460 and 488 nm, and the optical densities of the samples were similar and small (~0.2).

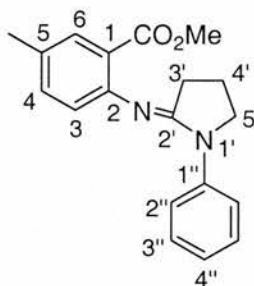
Ultra Violet irradiation was carried out in quartz apparatus using a 400 W medium pressure Hg lamp.

X-Ray Crystallography data were recorded on: a) Bruker SMART diffractometer with graphite-monochromated Mo-Kα radiation (λ= 0.71073 Å), sealed tube and CCD detector, b) Mer-Rigaku, mercury detector 007 with Mo-Kα radiation

($\lambda = 0.71073 \text{ \AA}$) generator (rotating anode), c) Cop-Saturn 92 detector 007, Cu-K α radiation with rotating.

7.2. Synthetic Route to (S)-(-)-Blebbistatin (7)

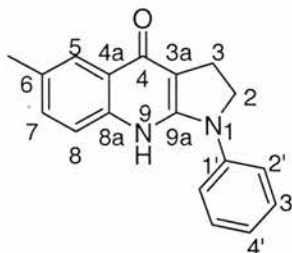
7.2.1. Preparation of methyl 5-methyl-2-(1-phenylpyrrolidin-2-ylideneamino)benzoate (29)



Phosphorus oxychloride (0.46 g, 0.30 mL, 3.0 mmol, 1.0 equiv) was added dropwise to a solution of 1-phenyl-2-pyrrolidinone (**28**) (0.54 g, 3.4 mmol, 1.1 equiv) in dry dichloromethane (3.0 mL) and the reaction mixture was stirred for 3 hours at room temperature. A solution of 2-amino-5-methyl-benzoic acid methyl ester (**27**) (0.50 g, 3.0 mmol, 1.0 equiv) in dry dichloromethane (12 mL) was then added and the mixture refluxed for 16 hours, then cooled and concentrated *in vacuo*. The resulting solid was dissolved in aqueous hydrochloric acid (0.30 M, 100 mL) and extracted with dichloromethane (3 \times 100 mL). The aqueous phase was then basified with aqueous sodium hydroxide solution (2.0 M, pH adjusted to 8) and extracted with ethyl acetate (3 \times 100 mL). The first organic extracts were concentrated *in vacuo* and the resulting solid was carried through the above procedure three more times. All ethyl acetate extracts were combined, dried (MgSO₄) and concentrated *in vacuo* to give the desired compound **29** (0.38 g, 1.2 mmol, 41%) as a white crystalline solid. An analytical sample of **29** was prepared by recrystallisation from ethyl acetate/hexane; mp 119-120 °C; ¹H NMR (300 MHz, CDCl₃): δ =1.98-2.09 (m (7 lines), 2 H; 4'-H), 2.32 (br s, 3 H; CH₃), 2.46 (t, ³J(H,H) = 7.8 Hz, 2 H; 3'-H), 3.82 (s, 3 H, OCH₃), 3.87 (t, ³J(H,H) = 6.9 Hz, 2 H; 5'-H), 6.72 (d, ³J(H,H) = 8.1 Hz, 1 H; Ar-3-H), 7.01-7.10 (m, ³J(H,H) = 7.4 Hz, 1 H; Ar-4''-H), 7.19 (ddq, ³J(H,H) = 8.1 Hz, ⁴J(H,H) = 2.2 Hz, ⁴J(H,H) = 0.6 Hz, 1 H; Ar-4-H), 7.35 (dd, ³J(H,H) = 8.7 Hz, ³J(H,H) = 7.4 Hz, 2 H; Ar-

3''-H), 7.65-7.68 (m, 1 H; Ar-6-H), 7.82 ppm (dd, $^3J(\text{H,H}) = 8.7$ Hz, $^4J(\text{H,H}) = 0.9$ Hz, 2 H; Ar-2''-H); ^{13}C NMR (75.5 MHz, CDCl_3): $\delta = 19.7$ (C4'), 20.5 (CH₃), 29.1 (C3'), 50.6 (C5'), 51.7 (OCH₃), 120.2 (C2''), 121.9 (C1), 122.9 (C4''), 123.0 (C3), 128.5 (C3''), 130.9 (C5), 131.0 (C6), 133.4 (C4), 141.4 (C1''), 150.5 (C2), 159.7 (C2'), 167.8 ppm (C=O); IR (CH_2Cl_2 thin film): $\nu_{\text{max}} = 1721$ (s) (C=O), 1652 (s) (C=N), 756 (m) (Ar-H), 692 cm^{-1} (m); LRMS (EI): m/z (%): 308 (85) [M]⁺, 307 (100) [M]⁺, 249 (10) [CO₂Me], 202 (45), 77 (14) [C₆H₅]; HRMS (EI): m/z calc'd for C₁₉H₂₀N₂O₂ [M]⁺: 308.1524; found: 308.1519; Anal. calc'd for C₁₉H₂₀N₂O₂: C, 74.00; H, 6.54; N, 9.08; found: C, 74.02; H, 6.55; N, 9.05.

7.2.2. Preparation of 6-methyl-1-phenyl-2,3,4,9-tetrahydro-1H-pyrrolo[2,3-b]quinolin-4-one (24)

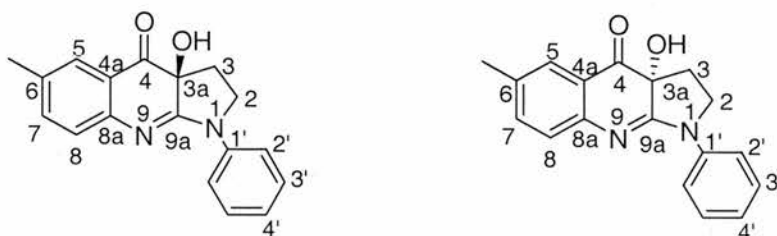


A solution of amidine **29** (0.20 g, 0.60 mmol, 1.0 equiv) in anhydrous THF (30 mL) was cooled to -78 °C and stirred for 15 minutes. Lithium bis(trimethylsilyl)amide (1.0 M in THF, 1.9 mL, 1.9 mmol, 3.0 equiv) was added dropwise to the reaction mixture, which was warmed to 0 °C over 3 hours and quenched at 0 °C with saturated aqueous ammonium chloride (5.0 mL). Further saturated aqueous ammonium chloride (150 mL) was added. The aqueous phase was extracted with dichloromethane (3×100 mL) and the combined organic extracts dried (MgSO_4) and concentrated *in vacuo* to give an orange solid. Purification by flash column chromatography on silica gel (eluting with 100% ethyl acetate), gave the desired compound **24** (0.16 g, 0.60 mmol, 90%) as an off-white solid; mp 189 - 190 °C; ^1H NMR (300 MHz, D_6 -DMSO): $\delta = 2.41$ (s, 3 H; CH₃), 3.17 (t, $^3J(\text{H,H}) = 8.0$ Hz, 2 H; 3-H), 4.06 (t, $^3J(\text{H,H}) = 8.0$ Hz, 2 H; 2-H), 6.96-7.02 (m, 1 H; Ar-4'-H), 7.31 (dd, $^3J(\text{H,H}) = 8.3$ Hz, $^4J(\text{H,H}) = 1.6$ Hz, 1 H; Ar-7-H), 7.34-7.41 (m, 2 H; Ar-3'-H), 7.50 (d, $^3J(\text{H,H}) = 8.3$ Hz, 1 H; Ar-8-H), 7.76 (br s, 1 H; Ar-5-H), 8.04-8.11 ppm (m, 2 H; Ar-2'-H); ^{13}C NMR (75.5 MHz, CDCl_3)*: $\delta = 21.1$ (CH₃), 24.0 (C3), 52.2 (C2), 104.1

(C3a), 119.6 (C2'), 120.9 (C4'), 123.3 (C4a), 123.6 (C5), 124.2 (C8) 129.4 (C3'), 130.9 (C7), 132.2 (C6), 138.6 (C1'), 140.4 (C8a), 154.9 (C9a), 163.0 ppm (C4); IR (Nujol): ν_{\max} =1571 (s), 1490 (m), 1460 (s), 1309 (s), 1272 (w), 818 (w), 753 (m) (Ar-H), 188 cm^{-1} (m); LRMS (EI): m/z (%): 276 (100) $[\text{M}]^+$, 57 (13); HRMS (EI): m/z calc'd for $\text{C}_{18}\text{H}_{16}\text{N}_2\text{O}_1$ $[\text{M}^+]$: 276.1263; found: 276.1259.

*The assignment of ^{13}C signals was made by using Pendant, HMBC and HSQC NMR analysis.

7.2.3. Preparation of *S*-3a-hydroxy-6-methyl-1-phenyl-2,3,3a,4-tetrahydro-1*H*-pyrrolo[2,3-*b*]quinolin-4-one (7) ((*S*)-(-)-blebbistatin) + *R*-3a-hydroxy-6-methyl-1-phenyl-2,3,3a,4-tetrahydro-1*H*-pyrrolo[2,3-*b*]quinolin-4-one (23) ((*R*)-(+)-blebbistatin)



Method 1a: Photodegradation of quinolone 24 in DMSO

A solution of quinolone **24** (0.12 g, 0.42 mmol) in DMSO (5 mL) was allowed to stand open to the air in direct sunlight for 40 days. The reaction was concentrated *in vacuo* to give a dark yellow oil which was purified by flash column chromatography eluting with 20% ethyl acetate/hexane to give (\pm)-blebbistatin (**18**) as a bright yellow solid (0.027 g, 0.092 mmol, 22%). Analytical data for (\pm)-blebbistatin (**18**) prepared by this method was identical to that for **7** (see method 3) except for $[\alpha]_{\text{D}}^{25} = 0$ ($c=0.1$ in dichloromethane).

Method 1b: Photodegradation of quinolone 24 in DMSO using a Mercury Lamp

A solution of quinolone **24** (0.028 g, 0.095 mmol) in DMSO (5.0 mL) was irradiated (mercury lamp (400 W) medium pressure, unfiltered) for 3 hours in a quartz

flask in air. The mixture was poured into water (50 mL) and extracted with diethyl ether (3 x 50 mL). The combined organic extracts were washed with water (3 x 50 mL), dried (MgSO_4) and concentrated *in vacuo* to give a dark yellow oil. The crude oil was purified by flash column chromatography eluting with 20% ethyl acetate/hexane to give (\pm)-blebbistatin (**18**) as a bright yellow solid (0.0080 g, 0.027 mmol, 29%). Analytical data for (\pm)-blebbistatin (**18**) prepared by this method were identical to that for **7** (see method 3) except for $[\alpha]_D^{25} = 0$ (c=0.1 in dichloromethane). Chiral HPLC analysis indicated that the compound was prepared as a racemic mixture (two peaks of equal integration).

Method 2: Photodegradation of quinolone **24** in THF using a Mercury Lamp

A solution of quinolone **24** (0.033 g, 0.12 mmol) in THF (5.0 mL) was irradiated (mercury lamp, 400 W, medium pressure, unfiltered) for 3 hours in a quartz flask under air. The mixture was poured into water (50 mL) and extracted with diethyl ether (3 x 50 mL). The combined organic extracts were washed with water (3 x 50 mL), dried (MgSO_4) and concentrated *in vacuo* to give a dark yellow oil. The crude oil was purified by flash column chromatography eluting with 20% ethyl acetate/hexane to give (\pm)-blebbistatin (**18**) as a bright yellow solid (0.009 g, 0.030 mmol, 26%). All the analytical data were identical to that for **7** (see method 3), except for $[\alpha]_D^{25} = 0$ (c=0.1 in dichloromethane) and chiral HPLC analysis (*ee*=0%).

Method 3: Asymmetric hydroxylation of **24**

a) Reagent: Dihalo oxaziridine **82**

A solution of quinolone **24** (0.20 g, 0.70 mmol, 1.0 equiv) in dry THF (17 mL) was added dropwise to lithium bis(trimethylsilyl)amide (1.0 M in THF, 0.90 mL, 0.90 mmol, 1.2 equiv) in dry THF (4.0 mL) at -78 °C under argon. The reaction was stirred for 30 minutes at -78 °C and a solution of dihalo oxaziridine **82** (0.50 g, 1.7 mmol, 2.4 equiv) in dry THF (10 mL) was added via a cannula. After 16 hours at -10 °C saturated aqueous ammonium iodide (5.0 mL, 10 equiv) and diethyl ether (5.0 mL) were added and the reaction mixture gradually warmed to room temperature. Saturated aqueous sodium thiosulfate (15 mL) was then added and the reaction mixture

extracted with diethyl ether (2×10 mL). The combined organic extracts were dried (MgSO_4) and concentrated *in vacuo* to give a yellow solid. The solid was partitioned between dichloromethane (100 mL) and aqueous hydrochloric acid solution (0.30 M, 100 mL). The aqueous phase was washed with dichloromethane (3×100 mL), basified with aqueous sodium hydroxide solution (2.0 M, pH adjusted to 8) and extracted with ethyl acetate (2×100 mL). The organic extracts were dried (MgSO_4) and concentrated *in vacuo* to give (*S*)-(-)-blebbistatin (**7**) (0.17 g, 0.6 mmol, 82%) as a bright yellow solid. The enantiomeric excess of **7** was 86% as determined by chiral-phase HPLC analysis; mp 192-193 °C; $[\alpha]_D^{25} = -461$ ($c=0.1$ in dichloromethane); ^1H NMR (300 MHz, CDCl_3): $\delta = 2.15\text{-}2.30$ (m, 1 H; 3-H), 2.32 (br s, 3 H; CH₃), 2.44 (dd, $^2J(\text{H,H}) = 13.8$ Hz, $^3J(\text{H,H}) = 5.4$ Hz, 1 H; 3-H), 3.79-3.88 (m, 1 H; 2-H), 3.96 (dt, $^2J(\text{H,H}) = 9.8$ Hz, $^3J(\text{H,H}) = 5.7$ Hz, 1 H; 2-H), 7.06 (d, $^3J(\text{H,H}) = 8.1$ Hz, 1 H; Ar-8-H), 7.14-7.24 (m, 2 H; Ar-4',7-H), 7.39-7.47 (m, 2 H; Ar-3'-H), 7.65 (br d, $^4J(\text{H,H}) = 1.9$ Hz, 1 H; Ar-5-H), 7.85-7.92 ppm (m, 2 H; Ar-2'-H); ^{13}C NMR (75.5 MHz, CDCl_3): $\delta = 20.6$ (CH₃), 29.0 (C₃), 48.3 (C₂), 77.4 (C_{3a}), 120.0 (C_{4a}), 120.4 (C_{2'}), 124.7 (C_{4'}), 125.8 (C₈), 127.1 (C₅), 128.8 (C_{3'}), 133.4 (C₆), 137.2 (C₇), 139.7 (C_{1'}), 148.1 (C_{8a}), 164.7 (C_{9a}), 194.1 ppm (C₄); IR (Nujol): $\nu_{\text{max}} = 1694$ (s) (C=O), 1593 (s), 1299 (m), 1108 (m), 755 (m) (Ar-H), 735 cm^{-1} (m); LRMS (CI^+): m/z (%): 293 (100) $[\text{M}+\text{H}]^+$, 277 (32); HRMS (EI): m/z calc'd for $\text{C}_{18}\text{H}_{16}\text{O}_2\text{N}_2$ $[\text{M}^+]$: 292.1213; found: 292.1216; Anal. calc'd for $\text{C}_{18}\text{H}_{16}\text{O}_2\text{N}_2$: C, 73.95; H, 5.52; N, 9.58: found: C, 74.04; H, 5.40; N, 9.69; HPLC (Daicel Chiralpak AD, acetonitrile/water 50:50, flow rate 0.8 mL min^{-1} , $\lambda = 254\text{ nm}$): major enantiomer: $t_R = 6.33\text{ min.}$, and minor enantiomer: $t_R = 8.60\text{ min.}$

An analytical sample of **7** was prepared by recrystallisation from acetonitrile; $[\alpha]_D^{25} = -530$ ($c=0.1$ in dichloromethane). Chiral HPLC analysis showed that after a single recrystallisation (*S*)-(-)-blebbistatin (**7**) was prepared with an *ee* of >99%. HPLC (Daicel Chiralpak AD, acetonitrile/water 50:50, flow rate 0.8 mL min^{-1} , $\lambda = 254\text{ nm}$): major enantiomer: $t_R = 6.22\text{ min.}$

b) Reagent: Dihalo oxaziridine **78**

A solution of quinolone **24** (0.35 g, 1.3 mmol, 1.0 equiv) in dry THF (13 mL) was added dropwise to lithium bis(trimethylsilyl)amide (1.0 M in THF, 1.6 mL, 1.6 mmol, 1.2 equiv) in dry THF (8.0 mL) at $-78\text{ }^\circ\text{C}$ under argon. The reaction was

stirred for 30 minutes at $-78\text{ }^{\circ}\text{C}$ and a solution of dihalo oxaziridine **78** (0.90 g, 3.1 mmol, 2.4 equiv) in dry THF (15 mL) was added via a cannula. After 16 hours at $-10\text{ }^{\circ}\text{C}$ saturated aqueous ammonium iodide (5.0 mL, 10 equiv) and diethyl ether (5.0 mL) were added and the reaction mixture gradually warmed to room temperature. Saturated aqueous sodium thiosulfate (15 mL) was then added and the reaction mixture extracted with diethyl ether ($2 \times 10\text{ mL}$). The combined organic extracts were dried (MgSO_4) and concentrated *in vacuo* to give a yellow solid. The solid was partitioned between dichloromethane (100 mL) and aqueous hydrochloric acid solution (0.30 M, 100 mL). The aqueous phase was washed with dichloromethane ($3 \times 100\text{ mL}$), basified with aqueous sodium hydroxide solution (2.0 M, pH adjusted to 8) and extracted with ethyl acetate ($2 \times 100\text{ mL}$). The organic extracts were dried (MgSO_4) and concentrated *in vacuo* to give (*R*)-(+)-blebbistatin (**23**) (0.29 g, 0.99 mmol, 76%) as a bright yellow solid. The enantiomeric excess of **23** was 86% as determined by chiral-phase HPLC analysis. $[\alpha]_{\text{D}}^{25} = +441$ ($c=0.1$ in dichloromethane). HPLC (Daicel Chiralpak AD, acetonitrile/water 50:50, flow rate 0.8 mL min^{-1} , $\lambda=254\text{ nm}$): minor enantiomer: $t_{\text{R}} = 6.33\text{ min.}$, and major enantiomer: $t_{\text{R}} = 8.60\text{ min.}$

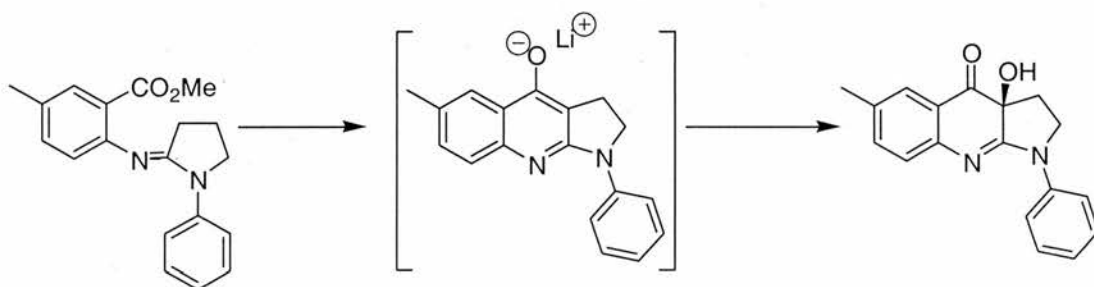
An analytical sample of **23** was prepared by recrystallisation from acetonitrile; $[\alpha]_{\text{D}}^{25} = +525$ ($c=0.2$ in dichloromethane). Chiral HPLC analysis showed that after a single recrystallisation (*R*)-(+)-blebbistatin (**23**) was prepared with an *ee* of $>99\%$. HPLC (acetonitrile/water 50:50, flow rate 0.8 mL min^{-1} , $\lambda=254\text{ nm}$): major enantiomer: $t_{\text{R}} = 8.73\text{ min.}$

c) Reagent: Dihydro oxaziridine **81**

A solution of quinolone **24** (0.040 g, 0.15 mmol, 1.0 equiv) in dry THF (10 mL) was added dropwise to lithium bis(trimethylsilyl)amide (1.0 M in THF, 0.18 mL, 0.18 mmol, 1.2 equiv) in dry THF (4.0 mL) at $-78\text{ }^{\circ}\text{C}$ under argon. The reaction was stirred for 30 minutes at $-78\text{ }^{\circ}\text{C}$ and a solution of dihydro oxaziridine **81** (0.080 g, 0.36 mmol, 2.4 equiv) in dry THF (5.0 mL) was added via a cannula. After 16 hours at $-10\text{ }^{\circ}\text{C}$ saturated aqueous ammonium iodide (5.0 mL, 10 equiv) and diethyl ether (5.0 mL) were added and the reaction mixture gradually warmed to room temperature. Saturated aqueous sodium thiosulfate (15 mL) was then added and the reaction mixture extracted with diethyl ether ($2 \times 10\text{ mL}$). The combined organic extracts were dried

(MgSO₄) and concentrated *in vacuo* to give a yellow solid. The solid was partitioned between dichloromethane (100 mL) and aqueous hydrochloric acid solution (0.30 M, 100 mL). The aqueous phase was washed with dichloromethane (3 × 100 mL), basified with aqueous sodium hydroxide solution (2.0 M, pH adjusted to 8) and extracted with ethyl acetate (2 × 100 mL). The organic extracts were dried (MgSO₄) and concentrated *in vacuo* to give (*S*)-(-)-blebbistatin (**7**) (0.031 g, 0.11 mmol, 73%) as a bright yellow solid. The enantiomeric excess of **7** was 42% as determined by chiral-phase HPLC analysis; $[\alpha]_D^{25} = -183$ (*c*=0.1 in dichloromethane). HPLC (Daicel Chiralpak AD, acetonitrile/water 50:50, flow rate 0.8 ml min⁻¹, $\lambda=254$ nm): major enantiomer: *t*_R = 6.07 min., and minor enantiomer: *t*_R = 8.57 min.

Method 4: Asymmetric hydroxylation of **24**: One pot reaction



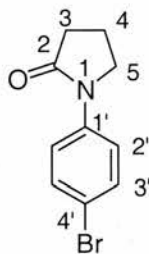
A solution of amidine **29** (0.0062 g, 0.020 mmol, 1.0 equiv) in anhydrous THF (1.0 mL) was cooled to -78 °C and stirred for 15 minutes. Lithium bis(trimethylsilyl)amide (1.0 M in THF, 0.022 mL, 0.022 mmol, 1.1 equiv) was added dropwise to the reaction mixture, which was warmed to 0 °C until no starting material was detected by TLC. A solution of dihydro oxaziridine **81** (0.0092 g, 0.040 mmol, 2.0 equiv) in dry THF (1.0 mL) was added via cannula at -78 °C. The reaction was then warmed to room temperature and quenched with saturated aqueous ammonium chloride (5.0 mL). Further saturated aqueous ammonium chloride (150 mL) was added. The aqueous phase was extracted with dichloromethane (3 × 100 mL) and the combined organic extracts dried (MgSO₄) and concentrated *in vacuo* to give a crude yellow solid. Purification by flash column chromatography on silica gel (eluting with 20% ethyl acetate/hexane), gave the desired compound **7** (0.0015 g, 0.0050 mmol, 25%) as a bright yellow solid. Analytical data for **7** prepared by this method were identical to that for **7** (see method 3).

7.3. Proof of absolute stereochemistry of (*S*)-(-)-Blebbistatin (**7**)

7.3.1. Attempted bromination of (*S*)-(-)-Blebbistatin (**7**)

A sample of optically enriched **7** (0.030 g, 0.10 mmol, 1.0 equiv) was dissolved in dry DMF (3.0 mL). A solution of *N*-bromosuccinimide (0.020 g, 0.10 mmol, 1.0 equiv) in dry DMF (3.0 mL) was added and the reaction stirred at room temperature for 24 hours. The reaction mixture was poured into water (50 mL) and extracted with diethyl ether (3 × 50 mL). The combined organic extracts were washed with water (3 × 50 mL), dried (MgSO₄) and concentrated *in vacuo* to afford a mixture of compounds from which it proved difficult to obtain a pure sample of a single compound.

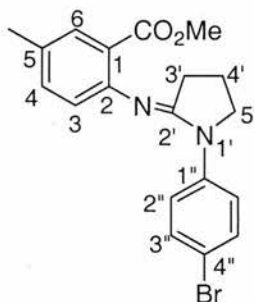
7.3.2. Preparation of 1-(4-bromophenyl)-2-pyrrolidinone (**132**)¹



1-Phenyl-2-pyrrolidinone (**29**) (5.0 g, 31 mmol, 1.0 equiv) and *N*-bromosuccinimide (5.3 g, 31 mmol, 1.0 equiv) were dissolved in anhydrous dimethylformamide (40 mL). The reaction mixture was left to stir at room temperature for two days. The mixture was poured into water (50 mL) and extracted with diethyl ether (3 × 50 mL). The organic extracts were washed with water (3 × 50 mL), dried (MgSO₄) and concentrated *in vacuo* to give a white solid (6.95 g). The crude solid was purified by recrystallisation from hexane/ethyl acetate to afford **132** (3.64 g, 15.2 mmol, 50%) as white needles; mp 99-100 °C (lit 97.5 °C);¹ ¹H NMR (300 MHz, CDCl₃): δ = 2.11-2.23 (m, 2 H; 4-H), 2.58-2.65 (m, 2 H; 3-H), 3.81-3.87 (m, 2 H; 5-H), 7.44-7.49 (m, AA' part of the AA'BB' system, 2 H; Ar-3'-H), 7.51-7.56 ppm (m, BB' part of the AA'BB' system, 2 H; Ar-2'-H); ¹³C NMR (75.5 MHz, CDCl₃): δ = 17.8 (C4), 32.6 (C3), 48.5 (C5), 117.1 (C4'), 121.2 (C3'), 131.7 (C2'), 138.4 (C1'), 174.2 ppm (C2); IR (Nujol): ν_{max}=1684 (s) (C=O), 1582 (m), 1309 (m), 1224 (m), 1065 (w), 828 cm⁻¹ (s);

LRMS (ES^+): m/z (%): 296 (28), 262 (100) $[(\text{M}+23)^+ (^{79}\text{Br})]$, 264 (96) $[(\text{M}+23)^+ (^{81}\text{Br})]$; HRMS (ES^+): m/z calc'd for $\text{C}_{10}\text{H}_{10}\text{NONa}^{79}\text{Br} [\text{M}+23]^+$: 261.9843; found: 261.9850 and calc'd for $\text{C}_{10}\text{H}_{10}\text{NONa}^{81}\text{Br} [\text{M}+23]^+$: 263.9823; found: 263.9835; Anal. calc'd for $\text{C}_{10}\text{H}_{10}\text{NOBr}$: C, 50.02; H, 4.20; N, 5.83; found: C, 49.72; H, 3.98; N, 5.66.

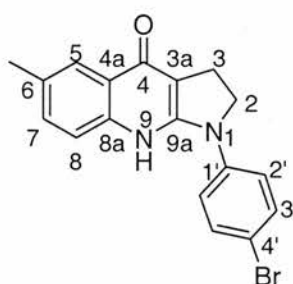
7.3.3. Preparation of methyl 2-[1-(4-bromophenyl)-pyrrolidin-2-ylideneamino]-5-methyl-benzoate (**133**)



Phosphorus oxychloride (0.81 g, 5.3 mmol, 0.90 equiv) was added dropwise to a solution of 1-(4-bromophenyl)-2-pyrrolidinone (**132**) (1.3 g, 5.3 mmol, 0.90 equiv) in dry dichloromethane (8.0 mL) and the reaction mixture was stirred for 3 hours at room temperature. A solution of the anthranilate **27** (0.98 g, 5.9 mmol, 1.0 equiv) in dry dichloromethane (15 mL) was then added and the mixture refluxed for 16 hours, then cooled and concentrated *in vacuo*. The resulting solid was dissolved in aqueous hydrochloric acid (0.30 M, 100 mL) and extracted with dichloromethane (3×100 mL). The aqueous phase was then basified with aqueous sodium hydroxide solution (2.0 M, pH adjusted to 8) and extracted with ethyl acetate (3×100 mL). The first organic extracts were concentrated *in vacuo* and the resulting solid was carried through the above procedure three more times. All ethyl acetate extracts were combined, dried (MgSO_4) and concentrated *in vacuo* to give the desired compound **133** (0.54 g, 1.4 mmol, 26%) as a pale-yellow oil; ^1H NMR (300 MHz, CDCl_3): δ =1.98-2.09 (m (6 lines), 2 H; 4'-H), 2.32 (br s, 3 H; CH₃), 2.45 (t, $^3J(\text{H},\text{H}) = 7.8$ Hz, 2 H; 3'-H), 3.80 (s, 3 H; OCH₃), 3.81-3.86 (m, 2 H; 5'-H), 6.70 (d, $^3J(\text{H},\text{H}) = 8.1$ Hz, 1 H; Ar-3-H), 7.19 (ddd, $^3J(\text{H},\text{H}) = 8.1$ Hz, $^4J(\text{H},\text{H}) = 2.1$ Hz, $^4J(\text{H},\text{H}) = 0.6$ Hz, 1 H; Ar-4-H), 7.41-7.46 (m, AA' part of the AA'XX' system, 2 H; Ar-3''-H), 7.67 (d, $^3J(\text{H},\text{H}) = 2.0$ Hz, 1 H; Ar-6-H), 7.71-7.77 ppm (m, XX' part of the AA'XX' system, 2 H; Ar-2''-H); ^{13}C NMR (75.5 MHz, CDCl_3): δ =20.0 (C4'), 21.0 (CH₃), 29.5 (C3'), 50.6 (C5'), 52.1 (OCH₃),

115.9 (C4''), 121.6 (C1), 122.1 (C2''), 123.3 (C3), 131.5 (C5), 131.7 (C3''), 131.8 (C6), 134.0 (C4), 140.9 (C1''), 150.6 (C2), 160.2 (C2'), 168.0 ppm (C=O); IR (Nujol): ν_{\max} = 1719 (m) (C=O), 1668 (m) (C=N), 1582 (m), 1197 (m), 1078 (m), 1003 (m), 826 cm^{-1} (m); LRMS (Cl^+): m/z (%): 389 (82) [(M+H)⁺ (⁸¹Br)], 387 (100) [(M+H)⁺ (⁷⁹Br)], 308 (15) [M-Br]⁺; HRMS (Cl^+): m/z calc'd $\text{C}_{19}\text{H}_{20}\text{N}_2\text{O}_2$ ⁷⁹Br [M + H]⁺: 387.0708; found: 387.0697 and calc'd $\text{C}_{19}\text{H}_{20}\text{N}_2\text{O}_2$ ⁸¹Br [M + H]⁺: 389.0688; found: 389.0703.

7.3.4. Preparation of 1-(4-bromophenyl)-6-methyl-2,3,4,9-tetrahydro-1H-pyrrolo[2,3-b]quinolin-4-one (**134**)

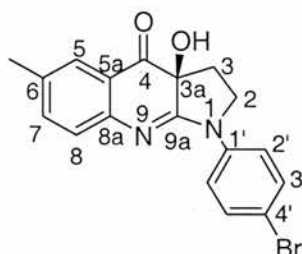


A solution of **133** (0.47 g, 1.2 mmol, 1.0 equiv) in anhydrous THF (45 mL) was cooled to $-78\text{ }^\circ\text{C}$ and stirred for 15 minutes. Lithium bis(trimethylsilyl)amide (1.0 M in THF, 3.7 mL, 3.7 mmol, 3.0 equiv) was added dropwise to the reaction mixture, which was warmed to $0\text{ }^\circ\text{C}$ over 3 hours and quenched at $0\text{ }^\circ\text{C}$ with saturated aqueous ammonium chloride (5.0 mL). Further saturated aqueous ammonium chloride (150 mL) was added. The aqueous phase was extracted with dichloromethane ($3 \times 100\text{ mL}$) and the combined organic extracts dried (MgSO_4), and concentrated *in vacuo*. Purification by flash column chromatography on silica gel (eluting with 100% ethyl acetate), gave the desired compound **134** (0.26 g, 0.70 mmol, 62%) as a brown solid; mp $187\text{--}188\text{ }^\circ\text{C}$; ^1H NMR (300 MHz, $\text{D}_6\text{-DMSO}$): δ = 2.41 (s, 3 H; CH₃), 3.16 (t, $^3J(\text{H,H}) = 8.1\text{ Hz}$, 2 H; 3-H), 4.02 (t, $^3J(\text{H,H}) = 8.1\text{ Hz}$, 2 H; 2-H), 7.32 (dd, $^3J(\text{H,H}) = 8.4\text{ Hz}$, $^4J(\text{H,H}) = 2.0\text{ Hz}$, 1 H; Ar-7-H), 7.49-7.54 (m, included AA' part of the AA'XX' system, 3 H; Ar-3',8-H), 7.77 (br s, 1 H; Ar-5-H), 8.04-8.09 ppm (m, XX' part of the AA'XX' system, 2 H; Ar-2'-H); ^{13}C NMR (75.5 MHz, $\text{D}_6\text{-DMSO}$)*: δ = 21.0 (CH₃), 22.0 (C3), 48.0 (C2), 106.3 (C3a), 112.0 (C4'), 118.7 (C4a), 119.0 (C2'), 120.5 (C5), 126.2 (C3''), 130.4 (C7), 131.0 (C6), 131.1 (C8), 141.4 (C1'), 146.2 (C8a), 153.9 (C9a), 159.1 ppm (C4); IR (Nujol): ν_{\max} = 1628 (m), 1572 (m), 1312 (m), 1054 (w), 1002 (w), 818 (w), 727

cm^{-1} (w) (Ar-H); LRMS (EI): m/z (%): 356 (85) [$\text{M}^+(\text{}^{81}\text{Br})$], 354 (100) [$\text{M}^+(\text{}^{79}\text{Br})$], 273 (12); HRMS (EI): m/z calc'd for $\text{C}_{18}\text{H}_{15}\text{N}_2\text{O}^{79}\text{Br}$ [M] $^+$: 354.0368; found: 354.0364.

*The assignment of ^{13}C signals was made by using Pendant, HMBC and HSQC NMR analysis.

7.3.5. Preparation of S-1-(4-bromophenyl)-3a-hydroxy-6-methyl-2,3,3a,4-tetrahydro-1H-pyrrolo[2,3-b]quinolin-4-one (135)

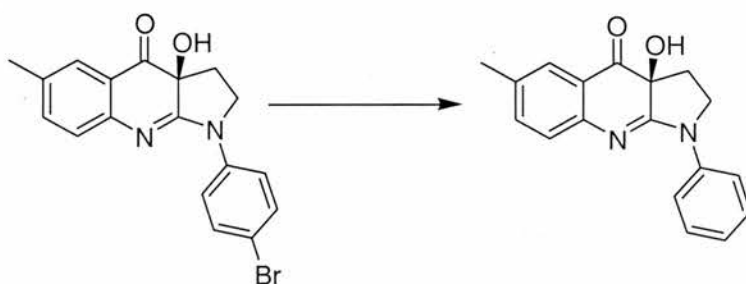


A solution of **134** (0.22 g, 0.62 mmol, 1.0 equiv) in dry THF (15 mL) was added dropwise to lithium bis(trimethylsilyl)amide (1.0 M in THF, 0.74 mL, 0.74 mmol, 1.2 equiv) in dry THF (4.0 mL) at $-78\text{ }^\circ\text{C}$ under argon. The reaction was stirred for 30 minutes at $-78\text{ }^\circ\text{C}$ and a solution of dihalo oxaziridine **82** (0.45 g, 1.5 mmol, 2.4 equiv) in dry THF (10 mL) was added via a cannula. After 16 hours at $-10\text{ }^\circ\text{C}$ saturated aqueous ammonium iodide (5.0 mL, 10 equiv) and diethyl ether (5.0 mL) were added and the reaction mixture gradually warmed to room temperature. Saturated aqueous sodium thiosulfate (15 mL) was then added and the reaction mixture extracted with diethyl ether ($2 \times 10\text{ mL}$). The combined organic extracts were dried (MgSO_4) and concentrated *in vacuo* to give a yellow solid. The solid was partitioned between dichloromethane (100 mL) and aqueous hydrochloric acid solution (0.30 M, 100 mL). The aqueous phase was washed with dichloromethane ($3 \times 100\text{ mL}$), basified with aqueous sodium hydroxide solution (2.0 M, pH adjusted to 8) and extracted with ethyl acetate ($2 \times 100\text{ mL}$). The ethyl acetate extracts were dried (MgSO_4) and concentrated *in vacuo* to give the desired compound **135** (0.16 g, 0.43 mmol, 69%) as a red solid. The enantiomeric excess of **135** was 88% as determined by chiral-phase HPLC analysis; mp $183\text{--}184\text{ }^\circ\text{C}$; $[\alpha]_{\text{D}}^{25} = -281$ ($c=0.1$ in dichloromethane); ^1H NMR (300 MHz, CDCl_3): $\delta = 2.22\text{--}2.29$ (m, 1 H; 3-H), 2.32 (s, 3 H; CH_3), 2.41-2.49 (m, 1 H; 3-H), 3.78-3.86 (m, 1 H; 2-H), 3.95-4.06 (m, 1 H; 2-H), 7.10 (d, $^3J(\text{H,H}) = 8.1\text{ Hz}$, 1 H; Ar-8-H), 7.25 (ddd,

$^3J(\text{H,H}) = 8.2$ Hz, $^4J(\text{H,H}) = 2.2$ Hz, $^4J(\text{H,H}) = 0.6$ Hz, 1 H; Ar-7-H), 7.47-7.54 (m, AA' part of the AA'XX' system, 2 H; Ar-3'-H), 7.62-7.65 (m, 1 H; Ar-5-H), 7.77-7.82 ppm (m, XX' part of the AA'XX' system, 2 H; Ar-2'-H); ^{13}C NMR (75.5 MHz, $\text{D}_8\text{-THF}$): $\delta = 20.6$ (C3), 29.5 (C3), 48.2 (C2), 73.8 (C3a), 116.3 (C4'), 121.8 (C2'), 122.2 (C4a), 126.9 (C8), 127.3 (C5), 132.1 (C3'), 133.6 (C6), 136.6 (C7), 141.3 (C1'), 149.8 (C8a), 166.3 (C9a), 194.8 ppm (C4); IR (Nujol): $\nu_{\text{max}} = 3304$ (br) (O-H), 1673 (s) (C=O), 1615 (s) (C=N), 1588 (w), 1490 (w), 1297 (m), 1258 (m), 1102 (w), 835 (w), 801 cm^{-1} (w); LRMS (CI^+): m/z (%): 373 (90) $[(\text{M}+\text{H})^+ (^{81}\text{Br})]$, 371 (100) $[(\text{M}+\text{H})^+ (^{79}\text{Br})]$, 355 (45), 344 (14), 292 (50) $[\text{M}-\text{Br}]^+$, 274 (9); HRMS (CI^+): m/z calc'd $\text{C}_{18}\text{H}_{16}\text{N}_2\text{O}_2^{79}\text{Br}$ $[\text{M} + \text{H}]^+$: 371.0395; found: 371.0395; Anal. calc'd for $\text{C}_{18}\text{H}_{15}\text{BrN}_2\text{O}_2$: C, 58.24; H, 4.07; N, 7.55; found: C, 58.21; H, 3.87; N, 7.63; HPLC (Daicel Chiralpak AD, acetonitrile/water 50:50, flow rate 0.8 mL min^{-1} , $\lambda = 254$ nm): major enantiomer: $t_{\text{R}} = 29.12$ min., and minor enantiomer: $t_{\text{R}} = 59.25$ min.

An analytical sample of **135** was prepared by recrystallisation from MeCN; $[\alpha]_{\text{D}}^{25} = -526$ ($c = 0.1$ in dichloromethane). Chiral HPLC analysis showed that after a single recrystallisation, **135** was prepared with an *ee* of >99%. HPLC (acetonitrile/water 50:50, flow rate 0.8 mL min^{-1} , $\lambda = 254$ nm): major enantiomer: $t_{\text{R}} = 29.18$ min.

7.3.6. Reduction of 1-(4-bromophenyl)-3a-hydroxy-6-methyl-2,3,3a,4-tetrahydro-1H-pyrrolo[2,3-b]quinolin-4-one (**135**)

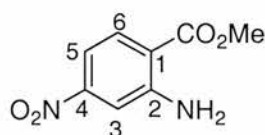


To a solution of **135** (0.015 g, 0.040 mmol, 1.0 equiv) in a 1:1 mixture of methanol and dimethyl formamide (6.0 mL) were added triethylamine (0.015 g) and 1% Pd/C (0.015 g) under argon. This suspension was then degassed under vacuum. Hydrogen was then introduced and the suspension was stirred at room temperature under hydrogen for 24 hours. The solid material was filtered off and washed with methanol (2.0 mL). The filtrate was concentrated *in vacuo* and the residue was purified

by flash column chromatography on silica gel (eluting with 20% ethyl acetate/hexane), to give the desired compound (*S*)-(-)-blebbistatin (**7**) (0.012 g, 0.040 mmol, 100%(quant)) as bright yellow solid. ^1H NMR and MS agrees with the authentic material of **7**.

7.4. Preparation of (*S*)-(-)-Blebbistatin (**7**) analogues substituted at the aromatic ring (R^3)

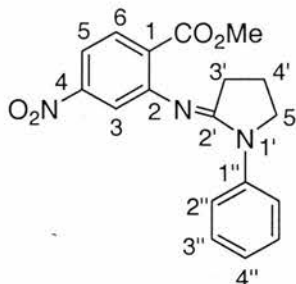
7.4.1. Preparation of 2-amino-4-nitro-benzoic acid methyl ester (**157**)



A literature method² for preparing benzoic acid methyl esters was adapted as follows:

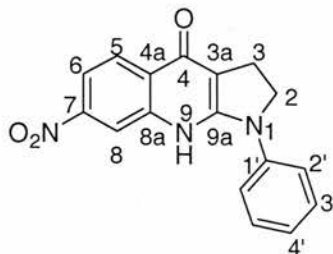
2-Amino-4-nitro benzoic acid (**156**) (0.45 g, 2.5 mmol, 1.0 equiv) was dissolved in methanol (50 mL) and H_2SO_4 (conc., 2.0 mL) was added. The reaction mixture was refluxed for four days, cooled and concentrated *in vacuo*. The resulting solid was dissolved in aqueous sodium hydroxide solution (2.0 M, 100 mL) and extracted with ethyl acetate (3×100 mL). The organic extracts were combined, dried (MgSO_4), and concentrated *in vacuo* to give a solid. The solid was purified by flash column chromatography on silica gel (eluting with 10% ethyl acetate/hexane), to give the desired compound **157** (0.39 g, 2.0 mmol, 81%) as a red solid; mp 153-154 °C; ^1H NMR (300 MHz, CDCl_3): δ =3.91 (s, 3 H; OCH_3), 7.39 (dd, $^3J(\text{H,H}) = 8.8$ Hz, $^4J(\text{H,H}) = 2.3$ Hz, 1 H; Ar-5-H), 7.50 (dd, $^4J(\text{H,H}) = 2.3$ Hz, $^4J(\text{H,H}) = 0.4$, 1 H; Ar-3-H), 8.00 ppm (dd, $^3J(\text{H,H}) = 8.8$ Hz, $^4J(\text{H,H}) = 0.4$ Hz, 1 H; Ar-6-H); ^{13}C NMR (75.5 MHz, CDCl_3): δ =52.2 (CH_3), 110.0 (C_5), 111.1 (C_3), 114.9 (C_1), 132.8 (C_6), 132.9 (C_2), 150.6 ($\text{C}-\text{NO}_2$), 167.3 ppm ($\text{C}=\text{O}$); IR (Nujol): ν_{max} =3487 (m) (N-H), 3378 (m) (N-H), 1701 (m) (C=O), 1519 (m), 1251 (m), 730 cm^{-1} (m) (Ar-H); LRMS (Cl^+): m/z (%): 197 (100) $[\text{M}+\text{H}]^+$, 165 (14), 135 (17); HRMS (Cl^+): m/z calc'd for $\text{C}_8\text{H}_9\text{N}_2\text{O}_4$ $[\text{M}+\text{H}]^+$: 197.0562; found: 197.0568.

7.4.2. Preparation of methyl 4-nitro-2-(1-phenylpyrrolidin-2-ylideneamino)benzoate (**158**)



Phosphorus oxychloride (0.62 g, 0.38 mL, 4.1 mmol, 1.0 equiv) was added dropwise to a solution of 1-phenyl-2-pyrrolidinone (**28**) (0.72 g, 4.5 mmol, 1.1 equiv) in dry dichloromethane (10 mL) and the reaction mixture was stirred for 3 hours at room temperature. A solution of 2-Amino-4-nitro-benzoic acid methyl ester (**157**) (0.80 g, 4.1 mmol, 1.0 equiv) in dry dichloromethane (20 mL) was then added and the mixture refluxed for 72 hours, then cooled and concentrated *in vacuo*. The resulting solid was dissolved in aqueous hydrochloric acid (0.30 M, 100 mL) and extracted with dichloromethane (3 × 100 mL). The aqueous phase was then basified with aqueous sodium hydroxide solution (2.0 M, pH adjusted to 8) and extracted with ethyl acetate (3 × 100 mL). The first organic extracts were concentrated *in vacuo* and the resulting solid was carried through the above procedure three more times. All ethyl acetate extracts were combined, dried (MgSO₄) and concentrated *in vacuo* to give the desired compound **158** (0.30 g, 0.90 mmol, 22%) as a crystalline yellow solid; mp 111-112 °C; ¹H NMR (300 MHz, CDCl₃): δ =2.03-2.15 (m, 2 H; 4'-H), 2.52 (t, ³J(H,H) = 7.8 Hz, 2 H; 3'-H), 3.86 (s, 3 H; OCH₃), 3.91 (t, ³J(H,H) = 6.9 Hz, 2 H; 5'-H), 7.06-7.13 (m, 1 H; Ar-4''-H), 7.32-7.39 (m, 2 H; Ar-3''-H), 7.66 (d, ³J(H,H) = 2.3 Hz, 1 H; Ar-3-H), 7.71-7.81 (m, 3 H; Ar-2'',5-H), 7.92 ppm (d, ³J(H,H) = 8.6 Hz, 1 H; Ar-6-H); ¹³C NMR (75.5 MHz, CDCl₃): δ =19.6 (C_{4'}), 29.5 (C_{3'}), 50.9 (C_{5'}), 52.2 (OCH₃), 115.7 (C₅), 118.0 (C₃), 120.8 (C_{2''}), 123.7 (C_{4''}), 128.2 (C₁), 128.5 (C_{3''}), 131.5 (C₆), 140.6 (C_{1'}), 150.0 (C₄), 153.9 (C₂), 160.2 (C_{2'}), 166.1 ppm (C=O); IR (Nujol): ν_{max}=1726 (s) (C=O), 1653 (s) (C=N), 1588 (m), 1306 (w), 1238 (w), 1198 (w), 762 cm⁻¹ (w) (Ar-H); LRMS (CI⁺): *m/z* (%): 368 (10), 340 (100) [M+H]⁺, 310 (9); HRMS (CI⁺): *m/z* calc'd for C₁₈H₁₈N₃O₄ [M+H]⁺: 340.1297; found: 340.1294.

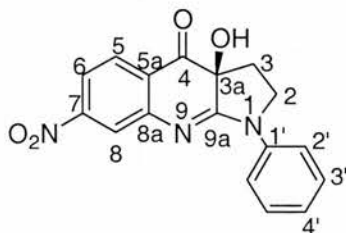
7.4.3. Preparation of 7-nitro-1-phenyl-1,2,3,9-tetrahydro-4H-pyrrolo[2,3-b]quinolin-4-one (159)



A solution of **158** (0.25 g, 0.74 mmol, 1.0 equiv) in anhydrous THF (15 mL) was cooled to $-78\text{ }^{\circ}\text{C}$ and stirred for 15 minutes. Lithium bis(trimethylsilyl)amide (1.0 M in THF, 0.74 mL, 0.74 mmol, 1.0 equiv) was added dropwise to the reaction mixture, which was warmed to $0\text{ }^{\circ}\text{C}$ and stirred for 16 hours. Additional base (0.39 mL, 0.5 equiv) was added every 24 hours. After 4 days the reaction was quenched by addition of saturated aqueous ammonium chloride (5.0 mL) and the reaction allowed to warm to room temperature. Further saturated aqueous ammonium chloride (150 mL) was added, the aqueous phase was extracted with dichloromethane ($3 \times 100\text{ mL}$) and the combined organic extracts dried (MgSO_4) and concentrated *in vacuo*. Purification by flash column chromatography on silica gel (eluting with 100% ethyl acetate), gave the desired compound **159** (0.099 g, 0.32 mmol, 44%) as an orange solid; mp $270\text{--}271\text{ }^{\circ}\text{C}$ (decomp.); $^1\text{H NMR}$ (300 MHz, $\text{D}_4\text{-MeOD}$): δ = 4.15 (t, $^3J(\text{H,H}) = 8.3\text{ Hz}$, 2 H; 3-H), 5.14 (t, $^3J(\text{H,H}) = 8.3\text{ Hz}$, 2 H; 2-H), 8.21 (t, $^3J(\text{H,H}) = 7.5\text{ Hz}$, 1 H; Ar-4''-H), 8.40-8.47 (m, 2 H; Ar-3''-H), 8.59-8.66 (m, 2 H; Ar-2''-H), 8.96 (dd, $^3J(\text{H,H}) = 8.9\text{ Hz}$, $^4J(\text{H,H}) = 2.3\text{ Hz}$, 1 H; Ar-6-H), 9.18 (d, $^3J(\text{H,H}) = 8.9\text{ Hz}$, 1 H; Ar-5-H), 9.33 ppm (d, $^4J(\text{H,H}) = 2.3\text{ Hz}$, 1 H; Ar-8-H); $^{13}\text{C NMR}$: (75.5 MHz, $\text{D}_8\text{-THF}$): δ = 22.5 (C3), 49.4 (C2), 110.4 (C3a), 115.7 (C6), 118.7 (C2'), 122.1 (C8), 122.4 (C4'), 123.2 (C5), 124.0 (C4a), 129.0 (C3'), 142.6 (C1'), 148.8 (C8a), 149.2 (C7), 154.6 (C9a), 162.1 (C4); IR (Nujol): ν_{max} = 1628 (m), 1575 (m), 1542 (m), 1335 (m), 1295 (m), 750 (w) (Ar-H), 727 cm^{-1} (m) (Ar-H); LRMS (ES^+): m/z (%): 308 (100) [$\text{M}+\text{H}$] $^+$; HRMS (ES^+): m/z calc'd for $\text{C}_{17}\text{H}_{14}\text{N}_3\text{O}_3$ [$\text{M}+\text{H}$] $^+$: 308.1035; found: 308.1036.

*The assignment of ^{13}C signals was made by using Pendant, HMBC and HSQC NMR analysis.

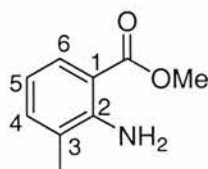
7.4.4. Preparation of *S*-3a-hydroxy-7-nitro-1-phenyl-1,2,3,3a-tetrahydro-4*H*-pyrrolo[2,3-*b*]quinolin-4-one (**160**)



A solution of **159** (0.032 g, 0.10 mmol, 1.0 equiv) in dry THF (6.0 mL) was added dropwise to lithium bis(trimethylsilyl)amide (1.0 M in THF, 0.12 mL, 0.12 mmol, 1.2 equiv) in dry THF (2.0 mL) at $-78\text{ }^{\circ}\text{C}$ under argon. The reaction was stirred for 30 minutes at $-78\text{ }^{\circ}\text{C}$ and a solution of dihalo oxaziridine **82** (0.093 g, 0.31 mmol, 3.1 equiv) in dry THF (6.0 mL) was added via a cannula. After 32 hours at $-10\text{ }^{\circ}\text{C}$ saturated aqueous ammonium iodide (5.0 mL, 10 equiv) and diethyl ether (5.0 mL) were added and the reaction mixture gradually warmed to room temperature. Saturated aqueous sodium thiosulfate (15 mL) was then added and the reaction mixture extracted with diethyl ether ($2 \times 10\text{ mL}$). The combined organic extracts were dried (MgSO_4) and concentrated *in vacuo* to give a orange solid. The solid was partitioned between dichloromethane (100 mL) and aqueous hydrochloric acid solution (0.30 M, 100 mL). The aqueous phase was washed with dichloromethane ($3 \times 100\text{ mL}$), basified with aqueous sodium hydroxide solution (2.0 M, pH adjusted to 8) and extracted with ethyl acetate ($2 \times 100\text{ mL}$). The organic extracts were dried (MgSO_4) and concentrated *in vacuo* to give a red solid. The solid was purified by flash column chromatography on silica gel (eluting with 20% ethyl acetate/hexane), to give the desired product **160** (0.010 g, 0.032mmol, 31%) as a red solid. The enantiomeric excess of **160** prepared by this route was 76% as determined by chiral-phase HPLC analysis; mp $187\text{-}188\text{ }^{\circ}\text{C}$. $[\alpha]_{\text{D}}^{25} = -418$ ($c=0.05$ in dichloromethane); $^1\text{H NMR}$ (300 MHz, $\text{D}_8\text{-THF}$): $\delta = 2.29\text{-}2.42$ (m, 2 H; 3-H), 3.98-4.07 (m, 1 H; 2-H), 4.17-4.27 (m, 1 H; 2-H), 7.10-7.18 (m, 1 H; Ar-4'-H), 7.35-7.44 (m, 2 H; Ar-3'-H), 7.80 (dd, $^3J(\text{H,H}) = 8.4\text{ Hz}$, $^4J(\text{H,H}) = 2.2\text{ Hz}$, 1 H; Ar-6-H), 7.94 (dd, $^3J(\text{H,H}) = 8.4\text{ Hz}$, $^5J(\text{H,H}) = 0.3\text{ Hz}$, 1 H; Ar-5-H), 7.99 (dd, $^4J(\text{H,H}) = 2.2\text{ Hz}$, $^5J(\text{H,H}) = 0.3\text{ Hz}$, 1 H; Ar-8-H), 8.09-8.14 ppm (m, 2 H; Ar-2'-H); $^{13}\text{C NMR}$ (75.5 MHz, $\text{D}_8\text{-THF}$): $\delta = 29.31$ (C3), 49.0 (C2), 75.0 (C3a), 117.3 (C6), 121.1 (C2'), 121.3 (C8), 125.0 (C4'), 126.7 (C4a), 128.3 (C5), 129.3 (C3'), 141.4 (C1'), 153.0

(C8a), 154.2 (C7), 167.8 (C9a), 193.0 ppm (C4); IR (Nujol): ν_{\max} = 1707 (s) (C=O), 1625 (m) (C=N), 1578 (m), 1256 (m), 739 (m) (Ar-H), 721 cm^{-1} (w) (Ar-H); LRMS (ES⁺): m/z (%): 413 (10), 356 (95) [M+MeOH]⁺, 324 (100) [M+H]⁺; HRMS (ES⁺): m/z calc'd for C₁₇H₁₄N₃O₄ [M+H]⁺: 324.0984; found: 324.0987. HPLC (Daicel Chiralpak AD, acetonitrile/water 50:50, flow rate 0.5 mL min⁻¹, λ =254 nm): minor enantiomer: t_R = 9.73 min., and major enantiomer: t_R = 11.22 min.

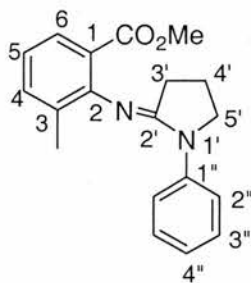
7.4.5. Preparation of methyl 2-amino-3-methyl-benzoate (**151**)³



A literature method² for preparing benzoic acid methyl esters was adapted as follows:

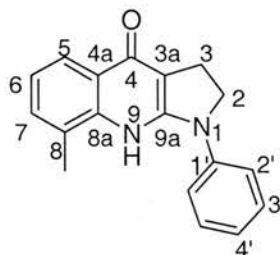
A solution of commercially available 2-amino-3-methylbenzoic acid (**147**) (2.4 g, 16 mmol, 1.0 equiv) in methanol (40 mL) and concentrated H₂SO₄ (2.5 mL) was refluxed for 48 hours. The reaction mixture was cooled and concentrated *in vacuo*. The resulting solid was dissolved in aqueous sodium bicarbonate (100 mL, pH adjusted to 8) and extracted with ethyl acetate (3 × 100 mL). The combined organic extracts were dried (MgSO₄) and concentrated *in vacuo*. Purification by flash column chromatography on silica gel (eluting with 10% ethyl acetate/hexane) gave the desired compound **151** (1.8 g, 11 mmol, 69%) as a brown oil (lit.³ oil, no more data available); ¹H NMR (300 MHz, CDCl₃): δ = 2.16 (s, 3 H; CH₃), 3.87 (s, 3 H; OCH₃), 6.58 (dd, ³*J*(H,H) = 8.1 Hz, ³*J*(H,H) = 7.2 Hz, 1 H; Ar-5-H), 7.19 (ddq, ³*J*(H,H) = 7.2 Hz, ⁴*J*(H,H) = 1.6 Hz, ⁴*J*(H,H) = 0.8 Hz, 1 H; Ar-4-H), 7.79 ppm (ddq, ³*J*(H,H) = 8.1 Hz, ⁴*J*(H,H) = 1.6 Hz, ⁴*J*(H,H) = 0.5 Hz, 1 H; Ar-6-H); ¹³C NMR (75.5 MHz, CDCl₃): δ = 17.2 (CH₃), 51.2 (OCH₃), 110.0 (C1), 115.4 (C6), 122.8 (C3), 129.0 (C5), 134.6 (C4), 148.8 (C2), 168.9 ppm (C=O); IR (Nujol): ν_{\max} = 3505 (s) (N-H), 3366 (s) (N-H), 1697 (s) (C=O), 1614 (m), 1569 (m), 1248 (s), 750 cm^{-1} (m) (Ar-H); LRMS (EI⁺): m/z (%): 165 (100) [M]⁺, 105 (98), 133 (50); HRMS (EI⁺): m/z calc'd for C₉H₁₁NO₂ [M]⁺: 165.0790; found: 165.0791.

7.4.6. Preparation of methyl 3-methyl-2-(1-phenylpyrrolidin-2-ylideneamino)benzoate (**154**)



Phosphorus oxychloride (0.63 g, 0.38 mL, 4.1 mmol, 1.0 equiv) was added dropwise to a solution of 1-phenyl-2-pyrrolidinone (**28**) (0.73 g, 4.5 mmol, 1.1 equiv) in dry dichloromethane (5.0 mL) and the reaction mixture was stirred for 3 hours at room temperature. A solution of methyl 3-methylantranilate (**151**) (0.68 g, 4.1 mmol, 1.0 equiv) in dry dichloromethane (15 mL) was then added and the mixture refluxed for 72 hours, then cooled and concentrated *in vacuo*. The resulting solid was dissolved in aqueous hydrochloric acid (0.30 M, 100 mL) and extracted with dichloromethane (3 × 100 mL). The aqueous phase was then basified with aqueous sodium hydroxide solution (2.0 M, pH adjusted to 8) and extracted with ethyl acetate (3 × 100 mL). The first organic extracts were concentrated *in vacuo* and the resulting solid was carried through the above procedure three more times. All ethyl acetate extracts were combined, dried (MgSO₄) and concentrated *in vacuo* to give the desired compound **154** (0.65 g, 2.1 mmol, 52%) as a white crystalline solid; mp 95-96 °C; ¹H NMR (300 MHz, CDCl₃): δ=1.98-2.10 (m, 2 H; 4'-H), 2.10-2.25 (m, 4 H; 3'-H, CH₃), 2.52-2.67 (m, 1 H; 3'-H), 3.78 (s, 3 H; OCH₃), 3.89 (t, ³J(H,H) = 6.8 Hz, 2 H; 5'-H), 6.91-6.97 (m (3 lines), ³J(H,H) = 7.7 Hz, 1 H; Ar-5-H), 7.07 (tt, ³J(H,H) = 7.4 Hz, ⁴J(H,H) = 1.2 Hz, 1 H; Ar-4''-H), 7.29-7.34 (m, 1 H; Ar-4-H), 7.34-7.41 (m, 2 H; Ar-3''-H), 7.70 (ddq, ³J(H,H) = 7.9 Hz, ⁴J(H,H) = 1.6 Hz, ⁴J(H,H) = 0.5 Hz, 1 H; Ar-6-H), 7.83-7.90 ppm (m, 2 H; Ar-2''-H); ¹³C NMR (75.5 MHz, CDCl₃): δ =18.2 (CH₃), 19.3 (C4'), 29.4 (C3'), 50.2 (C5'), 51.3 (OCH₃), 119.8 (C2''), 120.9 (C5), 121.2 (C1), 122.4 (C4''), 128.1 (C6), 128.2 (C3''), 130.0 (C3), 133.4 (C4), 141.3 (C1''), 151.3 (C2), 158.9 (C2'), 167.5 ppm (C=O); IR (Nujol): ν_{max}=1720 (s) (C=O), 1654 (s) (C=N), 1587 (m), 747 (m) (Ar-H), 722 cm⁻¹ (m); LRMS (ES⁺): m/z (%): 309 (100) [M+H]⁺; HRMS (ES⁺): m/z calc'd for C₁₉H₂₁N₂O₂ [M+H]⁺: 309.1603; found: 309.1610.

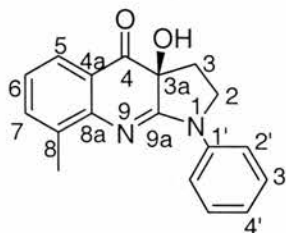
7.4.7. Preparation of 8-methyl-1-phenyl-2,3,4,9-tetrahydro-1H-pyrrolo[2,3-b]quinolin-4-one (138)



A solution of amidine **154** (0.50 g, 1.6 mmol, 1.0 equiv) in anhydrous THF (50 mL) was cooled to $-78\text{ }^{\circ}\text{C}$ and stirred for 15 minutes. Lithium bis(trimethylsilyl)amide (1.0 M in THF, 4.9 mL, 4.9 mmol, 3.0 equiv) was added dropwise to the reaction mixture, which was warmed to room temperature over 12 hours and quenched at room temperature with saturated aqueous ammonium chloride (5.0 mL). Further saturated aqueous ammonium chloride (150 mL) was added. The aqueous phase was extracted with dichloromethane ($3 \times 100\text{ mL}$) and the combined organic extracts dried (MgSO_4) and concentrated *in vacuo* to give an orange solid. Purification by flash column chromatography on silica gel (eluting with 50% ethyl acetate/hexane), gave the desired compound **138** (0.42 g, 1.5 mmol, 95%) as an off-white solid; mp $231\text{--}232\text{ }^{\circ}\text{C}$; $^1\text{H NMR}$ (500 MHz, $\text{D}_8\text{-THF}$): $\delta=2.65$ (s, 3 H; $\underline{\text{C}}\underline{\text{H}}_3$), 3.16 (t, $^3J(\text{H,H}) = 8.1\text{ Hz}$, 2 H; 3- $\underline{\text{H}}$), 4.07 (t, $^3J(\text{H,H}) = 8.1\text{ Hz}$, 2 H; 2- $\underline{\text{H}}$), 6.89-6.96 (m, 1 H; Ar-4'- $\underline{\text{H}}$), 7.05 (dd, $^3J(\text{H,H}) = 8.1\text{ Hz}$, $^3J(\text{H,H}) = 7.0\text{ Hz}$, 1 H; Ar-6- $\underline{\text{H}}$), 7.27-7.36 (m, 3 H; Ar-3',7- $\underline{\text{H}}$), 7.84 (br dd, $^3J(\text{H,H}) = 8.1\text{ Hz}$, $^4J(\text{H,H}) = 0.8\text{ Hz}$, 1 H; Ar-5- $\underline{\text{H}}$), 8.12-8.19 ppm (m, 2 H; Ar-2'- $\underline{\text{H}}$); $^{13}\text{C NMR}$ (125.7 MHz, $\text{D}_8\text{-THF}$)*: $\delta=18.8$ ($\underline{\text{C}}\underline{\text{H}}_3$), 22.4 ($\underline{\text{C}}\underline{\text{3}}$), 48.8 ($\underline{\text{C}}\underline{\text{2}}$), 106.1 ($\underline{\text{C}}\underline{\text{3a}}$), 117.7 ($\underline{\text{C}}\underline{\text{2'}}$), 119.2 ($\underline{\text{C}}\underline{\text{4a}}$), 119.6 ($\underline{\text{C}}\underline{\text{5}}$), 121.1 ($\underline{\text{C}}\underline{\text{4'}}$), 121.6 ($\underline{\text{C}}\underline{\text{6}}$), 128.8 ($\underline{\text{C}}\underline{\text{3'}}$), 129.4 ($\underline{\text{C}}\underline{\text{7}}$), 134.3 ($\underline{\text{C}}\underline{\text{8}}$), 143.5 ($\underline{\text{C}}\underline{\text{1'}}$), 148.7 ($\underline{\text{C}}\underline{\text{8a}}$), 155.2 ($\underline{\text{C}}\underline{\text{9a}}$), 160.0 ppm ($\underline{\text{C}}\underline{\text{4}}$); IR (Nujol): $\nu_{\text{max}}=1566$ (s), 1539 (m), 1307 (s), 1075 (w), 750 (m) (Ar-H), 722 (m), 693 cm^{-1} (m); LRMS (ES^+): m/z (%): 277 (100) $[\text{M}+\text{H}]^+$; HRMS (ES^+): m/z calc'd for $\text{C}_{18}\text{H}_{17}\text{N}_2\text{O}$ $[\text{M}+\text{H}]^+$: 277.1341; found: 277.1336.

*The assignment of ^{13}C signals was made by using Pendant, HMBC and HSQC NMR analysis.

7.4.8. Preparation of *S*-3a-hydroxy-8-methyl-1-phenyl-2,3,3a,4-tetrahydro-1*H*-pyrrolo[2,3-*b*]quinolin-4-one (**141**)



a) Reagent: Dihalo oxaziridine **82**

A solution of quinolone **138** (0.20 g, 0.72 mmol, 1.0 equiv) in dry THF (28 mL) was added dropwise to lithium bis(trimethylsilyl)amide (1.0 M in THF, 0.87 mL, 0.87 mmol, 1.2 equiv) in dry THF (5.0 mL) at $-78\text{ }^{\circ}\text{C}$ under argon. The reaction was stirred for 30 minutes at $-78\text{ }^{\circ}\text{C}$ and a solution of dihalo oxaziridine **82** (0.52 g, 1.7 mmol, 2.4 equiv) in dry THF (10 mL) was added via a cannula. After 16 hours at $-10\text{ }^{\circ}\text{C}$ saturated aqueous ammonium iodide (5.0 mL, 10 equiv) and diethyl ether (5.0 mL) were added and the reaction mixture gradually warmed to room temperature. Saturated aqueous sodium thiosulfate (15 mL) was then added and the reaction mixture extracted with diethyl ether ($2 \times 10\text{ mL}$). The combined organic extracts were dried (MgSO_4) and concentrated *in vacuo* to give a yellow solid. The solid was partitioned between dichloromethane (100 mL) and aqueous hydrochloric acid solution (0.30 M, 100 mL). The aqueous phase was washed with dichloromethane ($3 \times 100\text{ mL}$), basified with aqueous sodium hydroxide solution (2.0 M, pH adjusted to 8) and extracted with ethyl acetate ($2 \times 100\text{ mL}$). The organic extracts were dried (MgSO_4) and concentrated *in vacuo* to give **141** (0.13 g, 0.45 mmol, 63%) as a bright yellow solid. The enantiomeric excess of **141** was 86% as determined by chiral-phase HPLC analysis; mp $214\text{--}215\text{ }^{\circ}\text{C}$; $[\alpha]_{\text{D}}^{25} = -420$ ($c=0.1$ in dichloromethane); $^1\text{H NMR}$ (500 MHz, $\text{D}_8\text{-THF}$): $\delta = 2.21\text{--}2.35$ (m, 2 H; 3-H), 2.45 (s, 3 H; CH₃), 3.94-3.99 (m (3 lines), 1 H; 2-H), 4.13 (dt, $^2J(\text{H,H}) = 9.6\text{ Hz}$, $^3J(\text{H,H}) = 6.0\text{ Hz}$, 1 H; 2-H), 6.90-6.94 (m (3 lines), $^3J(\text{H,H}) = 7.5\text{ Hz}$, 1 H; Ar-6-H), 7.05-7.09 (m (3 lines), $^3J(\text{H,H}) = 7.3\text{ Hz}$, 1 H; Ar-4'-H), 7.33-7.39 (m, 3 H; Ar-3',7-H), 7.62-7.65 (m, 1 H; Ar-5-H), 8.16-8.20 ppm (m, 2 H; Ar-2'-H); $^{13}\text{C NMR}$ (125.7 MHz, $\text{D}_8\text{-THF}$): $\delta = 18.3$ (CH₃), 29.6 (C₃), 48.1 (C₂), 73.4 (C_{3a}), 119.9 (C_{2'}), 122.0 (C_{4a}), 123.1 (C₆), 123.8 (C_{4'}), 124.9 (C₅), 129.1 (C_{3'}), 134.3 (C₈),

136.9 (C7), 142.0 (C1'), 150.5 (C8a), 165.6 (C9a), 195.2 ppm (C4); IR (Nujol): ν_{\max} =3329 (s), 1670 (s), 1618 (s), 1590 (s), 1297 (m), 754 cm^{-1} (m) (Ar-H); LRMS (ES⁺): m/z (%): 293 (100) [M+H]⁺; HRMS (ES⁺): m/z calc'd for C₁₈H₁₇N₂O₂ [M+H]⁺: 293.1290; found: 293.1300; An analytical sample of **141** was prepared by recrystallisation from acetonitrile; Anal. calc'd for C₁₈H₁₆N₂O₂: C, 73.95; H, 5.52; N, 9.58; found: C, 73.62; H, 5.58; N, 9.60; HPLC (Daicel Chiralpak AD, acetonitrile/water 50:50, flow rate 0.8 mL min⁻¹, λ =254 nm): major enantiomer: t_R = 16.67 min., and minor enantiomer: t_R = 52.30 min. Chiral HPLC analysis showed that after a single recrystallisation, **141** was prepared with an *ee* of >99%.

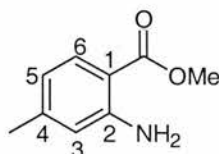
b) Reagent: Dihalo oxaziridine **78**

A solution of quinolone **138** (0.085 g, 0.31 mmol, 1.0 equiv) in dry THF (15 mL) was added dropwise to lithium bis(trimethylsilyl)amide (1.0 M in THF, 0.37 mL, 0.37 mmol, 1.2 equiv) in dry THF (5.0 mL) at -78 °C under argon. The reaction was stirred for 30 minutes at -78 °C and a solution of dihalo oxaziridine **78** (0.21 g, 0.74 mmol, 2.4 equiv) in dry THF (10 mL) was added via a cannula. After 16 hours at -10 °C saturated aqueous ammonium iodide (5.0 mL, 10 equiv) and diethyl ether (5.0 mL) were added and the reaction mixture gradually warmed to room temperature. Saturated aqueous sodium thiosulfate (15 mL) was then added and the reaction mixture extracted with diethyl ether (2 × 10 mL). The combined organic extracts were dried (MgSO₄) and concentrated *in vacuo* to give a yellow solid. The solid was partitioned between dichloromethane (100 mL) and aqueous hydrochloric acid solution (0.30 M, 100 mL). The aqueous phase was washed with dichloromethane (3 × 100 mL), basified with aqueous sodium hydroxide solution (2.0 M, pH adjusted to 8) and extracted with ethyl acetate (2 × 100 mL). The organic extracts were dried (MgSO₄) and concentrated *in vacuo* to give **141** (0.069 g, 0.24 mmol, 77%) as a bright yellow solid. The enantiomeric excess of **141** was 88% as determined by chiral-phase HPLC analysis; $[\alpha]_D^{25}$ = +400 (c=0.1 in dichloromethane). HPLC (Daicel Chiralpak AD, acetonitrile/water 50:50, flow rate 0.8 mL min⁻¹, λ =254 nm): minor enantiomer: t_R = 16.17 min., and major enantiomer: t_R = 48.65 min.

c) Reagent: Dihydro oxaziridine **81**

A solution of quinolone **138** (0.054 g, 0.19 mmol, 1.0 equiv) in dry THF (10 mL) was added dropwise to lithium bis(trimethylsilyl)amide (1.0 M in THF, 0.23 mL, 0.23 mmol, 1.2 equiv) in dry THF (2.0 mL) at -78 °C under argon. The reaction was stirred for 30 minutes at -78 °C and a solution of dihydro oxaziridine **81** (0.10 g, 0.46 mmol, 2.4 equiv) in dry THF (5.0 mL) was added via a cannula. After 16 hours at -10 °C saturated aqueous ammonium iodide (5.0 mL, 10 equiv) and diethyl ether (5.0 mL) were added and the reaction mixture gradually warmed to room temperature. Saturated aqueous sodium thiosulfate (15 mL) was then added and the reaction mixture extracted with diethyl ether (2 × 10 mL). The combined organic extracts were dried (MgSO₄) and concentrated *in vacuo* to give a yellow solid. The solid was partitioned between dichloromethane (100 mL) and aqueous hydrochloric acid solution (0.30 M, 100 mL). The aqueous phase was washed with dichloromethane (3 × 100 mL), basified with aqueous sodium hydroxide solution (2.0 M, pH adjusted to 8) and extracted with ethyl acetate (2 × 100 mL). The organic extracts were dried (MgSO₄) and concentrated *in vacuo* to give **141** (0.018 g, 0.062 mmol, 33%) as a bright yellow solid. The enantiomeric excess of **141** was 40% as determined by chiral-phase HPLC analysis; HPLC* (Daicel Chiralpak AD, acetonitrile/water 50:50, flow rate 1.0 mL min⁻¹, λ=254 nm): major enantiomer: t_R= 13.85 min., and minor enantiomer: t_R= 40.00 min.

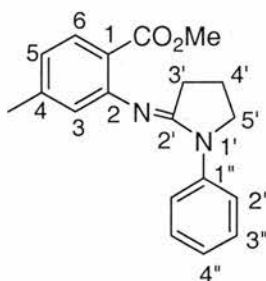
*HPLC analysis was developed in a different machine from a) and b) procedures.

7.4.9. Preparation of methyl 2-amino-4-methyl-benzoate (150**)³**

A literature method² for preparing benzoic acid methyl esters was adapted as follows:

A solution of commercially available 2-amino-4-methylbenzoic acid (**148**) (0.67 g, 4.4 mmol, 1.0 equiv) in methanol (50 mL) and concentrated H₂SO₄ (2.0 mL) was refluxed for 48 hours. The reaction mixture was cooled and concentrated *in vacuo*. The resulting solid was dissolved in aqueous sodium bicarbonate (100 mL, pH adjusted to 8) and extracted with ethyl acetate (3 × 100 mL). The combined organic extracts were dried (MgSO₄) and concentrated *in vacuo*. Purification by flash column chromatography on silica gel (eluting with 10% ethyl acetate/hexane) gave the desired compound **150** (0.61 g, 3.7 mmol, 84%) as a brown solid; mp 35-36°C (lit.³ 35 °C); ¹H NMR (300 MHz, CDCl₃): δ=2.26 (s, 3 H; CH₃), 3.85 (s, 3 H; OCH₃), 6.43-6.49 (m, 2 H; Ar-3,5-H), 7.74 ppm (d, ³J(H,H) = 8.7 Hz, 1 H; Ar-6-H); ¹³C NMR (75.5 MHz, CDCl₃): δ =21.5 (CH₃), 51.3 (OCH₃), 108.2 (C1), 116.7 (C3), 117.7 (C5), 131.0 (C6), 144.8 (C4), 150.4 (C2), 168.5 ppm (C=O).

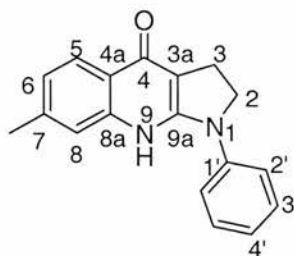
7.4.10. Preparation of methyl 4-methyl-2-(1-phenylpyrrolidin-2-ylideneamino)benzoate (**153**)



Phosphorus oxychloride (1.4 g, 0.84 mL, 9.1 mmol, 1.0 equiv) was added dropwise to a solution of 1-phenyl-2-pyrrolidinone (**28**) (1.6 g, 10 mmol, 1.1 equiv) in dry dichloromethane (10 mL) and the reaction mixture was stirred for 3 hours at room temperature. A solution of methyl 4-methylantranilate (**150**) (1.5 g, 9.1 mmol, 1.0 equiv) in dry dichloromethane (25 mL) was then added and the mixture refluxed for 16 hours, then cooled and concentrated *in vacuo*. The resulting solid was dissolved in aqueous hydrochloric acid (0.30 M, 100 mL) and extracted with dichloromethane (3 × 100 mL). The aqueous phase was then basified with aqueous sodium hydroxide solution (2.0 M, pH adjusted to 8) and extracted with ethyl acetate (3 × 100 mL). The first organic extracts were concentrated *in vacuo* and the resulting solid was carried through the above procedure three more times. All ethyl acetate extracts were

combined, dried (MgSO_4) and concentrated *in vacuo* to give the desired compound **153** (0.66 g, 2.1 mmol, 24%) as an either a waxy solid or brown oil depending on ambient temperature; ^1H NMR (300 MHz, CDCl_3): δ = 1.97-2.08 [m (7 lines), 2 H; 4'-H], 2.32 (br s, 3 H; CH_3), 2.47 (t, $^3J(\text{H,H}) = 7.8$ Hz, 2 H; 3'-H), 3.80 (s, 3 H; OCH_3), 3.86 (t, $^3J(\text{H,H}) = 6.9$ Hz, 2 H; 5'-H), 6.66 (br s, 1 H; Ar-3-H), 6.83 (ddq, $^3J(\text{H,H}) = 8.0$ Hz, $^4J(\text{H,H}) = 1.6$ Hz, $^4J(\text{H,H}) = 0.5$ Hz, 1 H; Ar-5-H), 7.02-7.09 (m, 1 H; Ar-4''-H), 7.31-7.40 (m, 2 H; Ar-3''-H), 7.80 (d, $^3J(\text{H,H}) = 8.0$ Hz, 1 H; Ar-6-H), 7.82-7.87 ppm (m, 2 H; Ar-2''-H); ^{13}C NMR (75.5 MHz, CDCl_3): δ = 19.5 ($\text{C}4'$), 21.3 (CCH_3), 29.0 ($\text{C}3'$), 50.3 ($\text{C}5'$), 51.4 (OCH_3), 118.9 ($\text{C}1$), 120.0 ($\text{C}2''$), 122.4 ($\text{C}5$), 122.7 ($\text{C}4''$), 123.5 ($\text{C}3$), 128.3 ($\text{C}3''$), 130.9 ($\text{C}6$), 141.2 ($\text{C}1''$), 143.2 ($\text{C}4$), 153.1 ($\text{C}2$), 159.2 ($\text{C}2'$), 167.2 ppm ($\text{C}=\text{O}$); IR (Nujol): ν_{max} = 1690 (s) ($\text{C}=\text{O}$), 1602 (s) ($\text{C}=\text{N}$), 1529 (m), 779 (m), 750 (m) (Ar-H), 693 cm^{-1} (m); LRMS (ES^+): m/z (%): 309 (100) [$\text{M}+\text{H}$] $^+$, 277 (24) [$\text{M}-\text{MeOH}$] $^+$; HRMS (ES^+): m/z calc'd for $\text{C}_{19}\text{H}_{21}\text{N}_2\text{O}_2$ [$\text{M}+\text{H}$] $^+$: 309.1603; found: 309.1597.

7.4.11. Preparation of 7-methyl-1-phenyl-2,3,4,9-tetrahydro-1*H*-pyrrolo[2,3-*b*]quinolin-4-one (**137**)

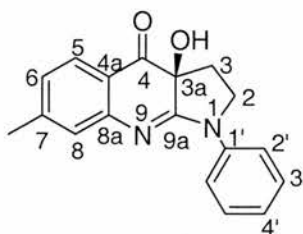


A solution of amidine **153** (0.58 g, 1.9 mmol, 1.0 equiv) in anhydrous THF (55 mL) was cooled to -78 $^{\circ}\text{C}$ and stirred for 15 minutes. Lithium bis(trimethylsilyl)amide (1.0 M in THF, 5.7 mL, 5.7 mmol, 3.0 equiv) was added dropwise to the reaction mixture, which was warmed to 0 $^{\circ}\text{C}$ over 3 hours and quenched at 0 $^{\circ}\text{C}$ with saturated aqueous ammonium chloride (5.0 mL). Further saturated aqueous ammonium chloride (150 mL) was added. The aqueous phase was extracted with dichloromethane (3×100 mL) and the combined organic extracts dried (MgSO_4) and concentrated *in vacuo* to give an orange solid. Purification by flash column chromatography on silica gel (eluting with 100% ethyl acetate), gave the desired compound **137** (0.51 g, 1.8 mmol, 95%) as an off-white solid; mp 186 - 187 $^{\circ}\text{C}$;

^1H NMR (500 MHz, $\text{D}_8\text{-THF}$): δ =2.41 (s, 3 H; $\underline{\text{CH}_3}$), 3.16 (t, $^3J(\text{H,H}) = 8.2$ Hz, 2 H; 3- $\underline{\text{H}}$), 4.01 (t, $^3J(\text{H,H}) = 8.2$ Hz, 2 H; 2- $\underline{\text{H}}$), 6.90-6.97 (m, 1 H; Ar-4'- $\underline{\text{H}}$), 7.00 (ddq, $^3J(\text{H,H}) = 8.2$ Hz, $^4J(\text{H,H}) = 1.3$ Hz, $^4J(\text{H,H}) = 0.3$ Hz, 1 H; Ar-6- $\underline{\text{H}}$), 7.25-7.34 (m, 2 H; Ar-3'- $\underline{\text{H}}$), 7.41 (br s, 1 H; Ar-8- $\underline{\text{H}}$), 7.92 (d, $^3J(\text{H,H}) = 8.2$ Hz, 1 H; Ar-5- $\underline{\text{H}}$), 7.96-8.05 ppm (m, 2 H; Ar-2'- $\underline{\text{H}}$); ^{13}C NMR (75.5 MHz, $\text{D}_8\text{-THF}$)*: δ =21.5 ($\underline{\text{CH}_3}$), 22.8 ($\underline{\text{C}3}$), 49.8 ($\underline{\text{C}2}$), 105.5 ($\underline{\text{C}3\text{a}}$), 117.7 ($\underline{\text{C}4\text{a}}$), 118.8 ($\underline{\text{C}2'}$), 121.8 ($\underline{\text{C}4'}$), 122.2 ($\underline{\text{C}5}$), 124.0 ($\underline{\text{C}6}$), 128.0 ($\underline{\text{C}8}$), 129.0 ($\underline{\text{C}3'}$), 139.0 ($\underline{\text{C}7}$), 143.3 ($\underline{\text{C}1'}$), 144.0 ($\underline{\text{C}8\text{a}}$), 149.2 ($\underline{\text{C}9\text{a}}$), 160.6 ppm ($\underline{\text{C}4}$); IR (Nujol): ν_{max} =1630 (m), 1578 (s), 1308 (w), 750 (m) (Ar-H), 722 (m), 688 cm^{-1} (w); LRMS (Cl^+): m/z (%): 305 (11), 277 (99) [$\text{M}+\text{H}$] $^+$; HRMS (Cl^+): m/z calc'd for $\text{C}_{18}\text{H}_{17}\text{N}_2\text{O}$ [$\text{M}+\text{H}$] $^+$: 277.1341; found: 277.1342.

*The assignment of ^{13}C signals was made by using Pendant, HMBC and HSQC NMR analysis.

7.4.12. Preparation of *S*-3a-hydroxy-7-methyl-1-phenyl-2,3,3a,4-tetrahydro-1*H*-pyrrolo[2,3-*b*]quinolin-4-one (140)



a) Reagent: Dihalo oxaziridine **82**

A solution of quinolone **137** (0.050 g, 0.18 mmol, 1.0 equiv) in dry THF (10 mL) was added dropwise to lithium bis(trimethylsilyl)amide (1.0 M in THF, 0.22 mL, 0.22 mmol, 1.2 equiv) in dry THF (5.0 mL) at -78 °C under argon. The reaction was stirred for 30 minutes at -78 °C and a solution of dihalo oxaziridine **82** (0.13 g, 0.44 mmol, 2.4 equiv) in dry THF (10 mL) was added via a cannula. After 16 hours at -10 °C saturated aqueous ammonium iodide (5.0 mL, 10 equiv) and diethyl ether (5.0 mL) were added and the reaction mixture gradually warmed to room temperature. Saturated aqueous sodium thiosulfate (10 mL) was then added and the reaction mixture extracted with diethyl ether (2×10 mL). The combined organic

extracts were dried (MgSO_4) and concentrated *in vacuo* to give a yellow solid. The solid was partitioned between dichloromethane (100 mL) and aqueous hydrochloric acid solution (0.30 M, 100 mL). The aqueous phase was washed with dichloromethane (3×100 mL), basified with aqueous sodium hydroxide solution (2.0 M, pH adjusted to 8) and extracted with ethyl acetate (2×100 mL). The organic extracts were dried (MgSO_4) and concentrated *in vacuo* to give **140** (0.045 g, 0.15 mmol, 83%) as a bright yellow solid. The enantiomeric excess of **140** was 90% as determined by chiral-phase HPLC analysis; mp 223-224 °C; $[\alpha]_{\text{D}}^{25} = -354$ ($c=0.1$ in dichloromethane); ^1H NMR (300 MHz, D_8 -THF): $\delta = 2.16$ - 2.32 (m, 2 H; 3-H), 2.33 (s, 3 H; CH₃), 3.89-3.97 (m, 1 H; 2-H), 4.12 (dt, $^2J(\text{H,H}) = 9.7$ Hz, $^3J(\text{H,H}) = 6.2$ Hz, 1 H; 2-H), 6.84 (ddq, $^3J(\text{H,H}) = 7.8$ Hz, $^4J(\text{H,H}) = 1.6$ Hz, $^4J(\text{H,H}) = 0.6$ Hz, 1 H; Ar-6-H), 7.05-7.10 (m, 2 H; Ar-4',8-H), 7.30-7.38 (m, 2 H; Ar-3'-H), 7.66 (d, $^3J(\text{H,H}) = 7.8$ Hz, 1 H; Ar-5-H), 8.10-8.16 ppm (m, 2 H; Ar-2'-H); ^{13}C NMR (75.5 MHz, D_8 -THF): $\delta = 21.6$ (CH₃), 29.6 (C₃), 48.3 (C₂), 74.0 (C_{3a}), 120.2 (C_{2'}), 120.5 (C_{4a}), 123.9 (C_{4'}), 124.5 (C₆), 127.2 (C₅), 127.4 (C₈), 129.0 (C_{3'}), 142.0 (C_{1'}), 146.7 (C₇), 152.7 (C_{8a}), 167.0 (C_{9a}), 194.3 ppm (C₄); IR (Nujol): $\nu_{\text{max}} = 1664$ (m), 1593 (m), 1300 (w), 1264 (w), 752 (m) (Ar-H), 722 cm^{-1} (w); LRMS (ES^+): m/z (%): 293 (100) $[\text{M}+\text{H}]^+$; HRMS (ES^+): m/z calc'd for $\text{C}_{18}\text{H}_{17}\text{N}_2\text{O}_2$ $[\text{M}+\text{H}]^+$: 293.1290; found: 293.1296; Anal. calc'd for $\text{C}_{18}\text{H}_{16}\text{N}_2\text{O}_2$: C, 73.95; H, 5.52; N, 9.58; found: C, 73.90; H, 5.56; N, 9.69; HPLC (Daicel Chiralpak AD, acetonitrile/water 50:50, flow rate 1.0 mL min^{-1} , $\lambda = 254$ nm): major enantiomer: $t_{\text{R}} = 9.39$ min., and minor enantiomer: $t_{\text{R}} = 12.42$ min.

An analytical sample of **140** was prepared by recrystallisation from acetonitrile; $[\alpha]_{\text{D}}^{25} = -450$ ($c=0.1$ in dichloromethane); Chiral HPLC analysis showed that after a single recrystallisation **140** was prepared with an *ee* of >99%.

b) Reagent: Dihalo oxaziridine **78**

A solution of quinolone **137** (0.050 g, 0.18 mmol, 1.0 equiv) in dry THF (10 mL) was added dropwise to lithium bis(trimethylsilyl)amide (1.0 M in THF, 0.22 mL, 0.22 mmol, 1.2 equiv) in dry THF (5.0 mL) at -78 °C under argon. The reaction was stirred for 30 minutes at -78 °C and a solution of dihalo oxaziridine **78** (0.13 g, 0.44 mmol, 2.4 equiv) in dry THF (10 mL) was added via a cannula. After 16 hours at -10 °C saturated aqueous ammonium iodide (5.0 mL, 10 equiv) and diethyl

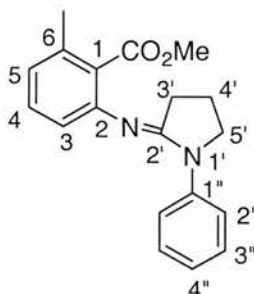
ether (5.0 mL) were added and the reaction mixture gradually warmed to room temperature. Saturated aqueous sodium thiosulfate (10 mL) was then added and the reaction mixture extracted with diethyl ether (2×10 mL). The combined organic extracts were dried (MgSO_4) and concentrated *in vacuo* to give a yellow solid. The solid was partitioned between dichloromethane (100 mL) and aqueous hydrochloric acid solution (0.30 M, 100 mL). The aqueous phase was washed with dichloromethane (3×100 mL), basified with aqueous sodium hydroxide solution (2.0 M, pH adjusted to 8) and extracted with ethyl acetate (2×100 mL). The organic extracts were dried (MgSO_4) and concentrated *in vacuo* to give **140** (0.034 g, 0.12 mmol, 67%) as a bright yellow solid. The enantiomeric excess of **140** was 90% as determined by chiral-phase HPLC analysis; HPLC (Daicel Chiralpak AD, acetonitrile/water 50:50, flow rate 1.0 mL min^{-1} , $\lambda=254 \text{ nm}$): minor enantiomer: $t_{\text{R}}=9.78 \text{ min.}$, and major enantiomer: $t_{\text{R}}=12.65 \text{ min.}$

c) Reagent: Dihydro oxaziridine **81**

A solution of quinolone **137** (0.050 g, 0.18 mmol, 1.0 equiv) in dry THF (10 mL) was added dropwise to lithium bis(trimethylsilyl)amide (1.0 M in THF, 0.22 mL, 0.22 mmol, 1.2 equiv) in dry THF (5.0 mL) at $-78 \text{ }^\circ\text{C}$ under argon. The reaction was stirred for 30 minutes at $-78 \text{ }^\circ\text{C}$ and a solution of dihydro oxaziridine **81** (0.13 g, 0.44 mmol, 2.4 equiv) in dry THF (10 mL) was added via a cannula. After 16 hours at $-10 \text{ }^\circ\text{C}$ saturated aqueous ammonium iodide (5.0 mL, 10 equiv) and diethyl ether (5.0 mL) were added and the reaction mixture gradually warmed to room temperature. Saturated aqueous sodium thiosulfate (10 mL) was then added and the reaction mixture extracted with diethyl ether (2×10 mL). The combined organic extracts were dried (MgSO_4) and concentrated *in vacuo* to give a yellow solid. The solid was partitioned between dichloromethane (100 mL) and aqueous hydrochloric acid solution (0.30 M, 100 mL). The aqueous phase was washed with dichloromethane (3×100 mL), basified with aqueous sodium hydroxide solution (2.0 M, pH adjusted to 8) and extracted with ethyl acetate (2×100 mL). The organic extracts were dried (MgSO_4) and concentrated *in vacuo* to give **140** (0.037 g, 0.13 mmol, 72%) as a bright yellow solid. The enantiomeric excess of **140** was 28% as determined by chiral-phase HPLC analysis; $[\alpha]_{\text{D}}^{25} = -120$ ($c=0.1$ in dichloromethane). HPLC (Daicel Chiralpak AD,

acetonitrile/water 50:50, flow rate 0.9 mL min⁻¹, $\lambda=254$ nm): major enantiomer: $t_R=11.53$ min., and minor enantiomer: $t_R=15.74$ min.

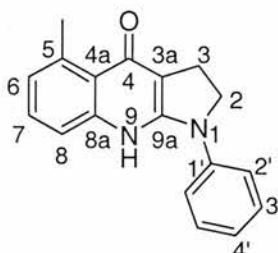
7.4.13. Preparation of methyl 6-methyl-2-(1-phenylpyrrolidin-2-ylideneamino)benzoate (**152**)



Phosphorus oxychloride (0.55 g, 0.33 mL, 3.6 mmol, 1.0 equiv) was added dropwise to a solution of 1-phenyl-2-pyrrolidinone (**28**) (0.64 g, 3.9 mmol, 1.1 equiv) in dry dichloromethane (8.0 mL) and the reaction mixture was stirred for 3 hours at room temperature. A solution of methyl 6-methylantranilate (**149**) (0.59 g, 3.6 mmol, 1.0 equiv) in dry dichloromethane (15 mL) was then added and the mixture refluxed for 16 hours, then cooled and concentrated *in vacuo*. The resulting solid was dissolved in aqueous hydrochloric acid (0.30 M, 100 mL) and extracted with dichloromethane (3 × 100 mL). The aqueous phase was then basified with aqueous sodium hydroxide solution (2.0 M, pH adjusted to 8) and extracted with ethyl acetate (3 × 100 mL). The first organic extracts were concentrated *in vacuo* and the resulting solid was carried through the above procedure three more times. All ethyl acetate extracts were combined, dried (MgSO₄) and concentrated *in vacuo* to give the desired compound **152** (0.32 g, 1.0 mmol, 28%) as a white solid; mp 97-98 °C; ¹H NMR (300 MHz, CDCl₃): δ = 1.96-2.08 (m, 2 H; 4'-H), 2.34 (s, 3 H; CH₃), 2.59 (t, ³J(H,H) = 7.8 Hz, 2 H; 3'-H), 3.79-3.86 (m, 5 H; 5'-H, OCH₃), 6.62-6.68 (m, 1 H; Ar-5-H), 6.82-6.88 (m, 1 H; Ar-3-H), 7.03-7.10 (m, 1 H; Ar-4''-H), 7.14-7.21 (m (3 lines), ³J(H,H) = 7.8 Hz, 1 H; Ar-4-H), 7.31-7.39 (m, 2 H; Ar-3''-H), 7.76-7.83 ppm (m, 2 H; Ar-2''-H); ¹³C NMR (75.5 MHz, CDCl₃): δ = 19.4 (CH₃), 19.8 (C4'), 29.3 (C3'), 50.5 (C5'), 51.8 (OCH₃), 118.7 (C5), 120.0 (C2''), 123.0 (C4''), 123.7 (C3), 127.5 (C1), 128.5 (C3''), 129.7 (C4), 135.3 (C6), 141.2 (C1''), 149.4 (C2), 161.0 (C2'), 170.2 ppm (C=O); IR (Nujol): ν_{\max} = 1718 (s) (C=O), 1647 (s) (C=N), 1587 (m), 761 (m) (Ar-H), 722 (m), 692 cm⁻¹

(m); LRMS (ES⁺): m/z (%): 309 (100) [M+H]⁺; HRMS (ES⁺): m/z calc'd for C₁₉H₂₁N₂O₂ [M+H]⁺: 309.1603; found: 309.1610.

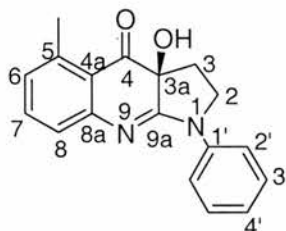
7.4.14. Preparation of 5-methyl-1-phenyl-2,3,4,9-tetrahydro-1H-pyrrolo[2,3-b]quinolin-4-one (**136**)



A solution of amidine **152** (0.060 g, 0.19 mmol, 1.0 equiv) in anhydrous THF (10 mL) was cooled to -78 °C and stirred for 15 minutes. Lithium bis(trimethylsilyl)amide (1.0 M in THF, 0.57 mL, 0.57 mmol, 3.0 equiv) was added dropwise to the reaction mixture, which was warmed to 0 °C over 3 hours and quenched at 0 °C with saturated aqueous ammonium chloride (5.0 mL). Further saturated aqueous ammonium chloride (150 mL) was added. The aqueous phase was extracted with dichloromethane (3×100 mL) and the combined organic extracts dried (MgSO₄) and concentrated *in vacuo* to give an orange solid. Purification by flash column chromatography on silica gel (eluting with 80% ethyl acetate/hexane), gave the desired compound **136** (0.044 g, 0.16 mmol, 84%) as an off-white solid; mp 240-241 °C (decomp.); ¹H NMR (300 MHz, D₈-THF): δ =2.85 (s, 3 H; CH₃), 3.16 (t, ³ J (H,H) = 8.3 Hz, 2 H; 3-H), 4.02 (t, ³ J (H,H) = 8.3 Hz, 2 H; 2-H), 6.85-6.90 (m, 1 H; Ar-6-H), 6.91-6.97 (m, 1 H; Ar-4'-H), 7.21 (dd, ³ J (H,H) = 8.2 Hz, ³ J (H,H) = 7.2 Hz, 1 H; Ar-7-H), 7.26-7.34 (m, 2 H; Ar-3'-H), 7.41-7.46 (m, 1 H; Ar-8-H), 7.93-8.00 ppm (m, 2 H; Ar-2'-H); ¹³C NMR (75.5 MHz, D₈-THF)*: δ =23.0 (C3), 24.4 (CH3), 49.9 (C2), 106.6 (C3a), 118.7 (C2'), 118.9 (C4a), 121.9 (C4'), 124.5 (C8), 125.6 (C6), 128.4 (C7), 129.0 (C3'), 135.7 (C5), 143.3 (C1'), 149.0 (C8a), 156.1 (C9a), 158.0 ppm (C4); IR (Nujol): ν_{max} =1614 (m), 1570 (s), 1310 (s), 754 (m) (Ar-H), 722 cm⁻¹(m); LRMS (ES⁺): m/z (%): 277 (100) [M+H]⁺; HRMS (ES⁺): m/z calc'd for C₁₈H₁₇N₂O [M+H]⁺: 277.1341; found: 277.1336.

*The assignment of ¹³C signals was made by using pendant, HMBC and HSQC NMR analysis.

7.4.15. Preparation of *S*-3a-hydroxy-5-methyl-1-phenyl-2,3,3a,4-tetrahydro-1*H*-pyrrolo[2,3-*b*]quinolin-4-one (**139**)



a) Reagent: Dihalo oxaziridine **82**

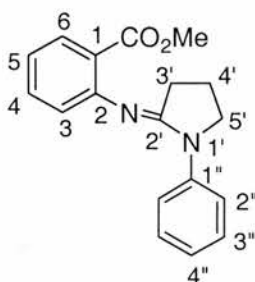
A solution of quinolone **136** (0.022 g, 0.080 mmol, 1.0 equiv) in dry THF (10 mL) was added dropwise to lithium bis(trimethylsilyl)amide (1.0 M in THF, 0.095 mL, 0.095 mmol, 1.2 equiv) in dry THF (2.0 mL) at $-78\text{ }^{\circ}\text{C}$ under argon. The reaction was stirred for 30 minutes at $-78\text{ }^{\circ}\text{C}$ and a solution of dihalo oxaziridine **82** (0.060 g, 0.19 mmol, 2.4 equiv) in dry THF (4.0 mL) was added via a cannula. After 16 hours at $-10\text{ }^{\circ}\text{C}$ saturated aqueous ammonium iodide (5.0 mL, 10 equiv) and diethyl ether (5.0 mL) were added and the reaction mixture gradually warmed to room temperature. Saturated aqueous sodium thiosulfate (5.0 mL) was then added and the reaction mixture extracted with diethyl ether ($2 \times 10\text{ mL}$). The combined organic extracts were dried (MgSO_4) and concentrated *in vacuo* to give a yellow solid. The solid was partitioned between dichloromethane (100 mL) and aqueous hydrochloric acid solution (0.30 M, 100 mL). The aqueous phase was washed with dichloromethane ($3 \times 100\text{ mL}$), basified with aqueous sodium hydroxide solution (2.0 M, pH adjusted to 8) and extracted with ethyl acetate ($2 \times 100\text{ mL}$). The organic extracts were dried (MgSO_4) and concentrated *in vacuo* to give **139** (0.020 g, 0.070 mmol, 87%) as a bright yellow solid. The enantiomeric excess of **139** was 64% as determined by chiral-phase HPLC analysis; mp $227\text{--}228\text{ }^{\circ}\text{C}$; $[\alpha]_{\text{D}}^{25} = -310$ ($c=0.1$ in dichloromethane); ^1H NMR (300 MHz, $\text{D}_8\text{-THF}$): $\delta = 2.19\text{--}2.37$ (m, 2 H; 3-H), 2.53 (s, 3 H; CH₃), 3.90-3.98 (m (7 lines), 1 H; 2-H), 4.11 (dt, $^2J(\text{H,H}) = 9.6\text{ Hz}$, $^3J(\text{H,H}) = 6.4\text{ Hz}$, 1 H; 2-H), 6.82 (ddq, $^3J(\text{H,H}) = 7.5\text{ Hz}$, $^4J(\text{H,H}) = 1.2\text{ Hz}$, $^4J(\text{H,H}) = 0.6\text{ Hz}$, 1 H; Ar-6-H), 7.02-7.11 (m, 2 H; Ar-4',7-H), 7.25-7.29 (m (2 lines), $^3J(\text{H,H}) = 7.6\text{ Hz}$, 1 H; Ar-8-H), 7.30-7.38 (m, 2 H; Ar-3'-H), 8.08-8.14 ppm (m, 2 H; Ar-2'-H); ^{13}C NMR (75.5 MHz, $\text{D}_8\text{-THF}$): $\delta = 21.5$ (CH₃), 29.6 (C₃), 48.4 (C₂), 75.0 (C_{3a}), 120.1 (C_{2'}), 121.1 (C_{4a}), 123.9 (C_{4'}), 125.2

(C7), 127.0 (C6), 129.04 (C3'), 134.3 (C8), 141.4 (C5), 142.0 (C1'), 153.3 (C8a), 166.0 (C9a), 197.0 ppm (C4); IR (Nujol): ν_{\max} =1686 (m), 1618 (m), 1590 (m), 1313 (w), 1262 (w), 723 cm^{-1} (m) (Ar-H); LRMS (ES⁺): m/z (%): 293 (100) [M+H]⁺; HRMS (ES⁺): m/z calc'd for C₁₈H₁₇N₂O₂ [M+H]⁺: 293.1290; found: 293.1288; Anal. calc'd for C₁₈H₁₆N₂O₂: C, 73.95; H, 5.52; N, 9.58; found: C, 73.75; H, 5.54; N, 9.67. HPLC (Daicel Chiralpak AD, acetonitrile/water 50:50, flow rate 0.8 mL min⁻¹, λ =254 nm): major enantiomer: t_R = 6.05 min., and minor enantiomer: t_R = 8.02 min.

An analytical sample of **139** was prepared by recrystallisation from acetonitrile; $[\alpha]_D^{25}$ = -450 (c=0.07 in dichloromethane); Chiral HPLC analysis showed that after a single recrystallisation **139** was prepared with an *ee* of 98.9%.

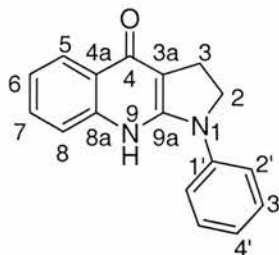
b) Reagent: Dihalo oxaziridine **78**

A solution of quinolone **136** (0.022 g, 0.080 mmol, 1.0 equiv) in dry THF (10 mL) was added dropwise to lithium bis(trimethylsilyl)amide (1.0 M in THF, 0.095 mL, 0.095 mmol, 1.2 equiv) in dry THF (2.0 mL) at -78 °C under argon. The reaction was stirred for 30 minutes at -78 °C and a solution of dihalo oxaziridine **78** (0.060 g, 0.19 mmol, 2.4 equiv) in dry THF (4.0 mL) was added via a cannula. After 16 hours at -10 °C saturated aqueous ammonium iodide (5.0 mL, 10 equiv) and diethyl ether (5.0 mL) were added and the reaction mixture gradually warmed to room temperature. Saturated aqueous sodium thiosulfate (5.0 mL) was then added and the reaction mixture extracted with diethyl ether (2 × 10 mL). The combined organic extracts were dried (MgSO₄) and concentrated *in vacuo* to give a yellow solid. The solid was partitioned between dichloromethane (100 mL) and aqueous hydrochloric acid solution (0.30 M, 100 mL). The aqueous phase was washed with dichloromethane (3 × 100 mL), basified with aqueous sodium hydroxide solution (2.0 M, pH adjusted to 8) and extracted with ethyl acetate (2 × 100 mL). The organic extracts were dried (MgSO₄) and concentrated *in vacuo* to give **139** (0.020 g, 0.070 mmol, 87%) as a bright yellow solid. The enantiomeric excess of **139** was 65% as determined by chiral-phase HPLC analysis; $[\alpha]_D^{25}$ = +336 (c=0.1 in dichloromethane). HPLC (Daicel Chiralpak AD, acetonitrile/water 50:50, flow rate 0.8 mL min⁻¹, λ =254 nm): minor enantiomer: t_R = 6.00 min., and major enantiomer: t_R = 8.17 min.

7.4.16. Preparation of methyl 2-(1-phenylpyrrolidin-2-ylideneamino)benzoate (**32**)

Phosphorus oxychloride (0.80 g, 0.50 mL, 5.3 mmol, 1.0 equiv) was added dropwise to a solution of 1-phenyl-2-pyrrolidinone (**28**) (0.94 g, 5.8 mmol, 1.1 equiv) in dry dichloromethane (6.0 mL) and the reaction mixture was stirred for 3 hours at room temperature. A solution of anthranilate **33** (0.80 g, 0.68 mL, 5.3 mmol, 1.0 equiv) in dry dichloromethane (15 mL) was then added and the mixture refluxed for 16 hours, then cooled and concentrated *in vacuo*. The resulting solid was dissolved in aqueous hydrochloric acid (0.30 M, 100 mL) and extracted with dichloromethane (3 × 100 mL). The aqueous phase was then basified with aqueous sodium hydroxide solution (2.0 M, pH adjusted to 8) and extracted with ethyl acetate (3 × 100 mL). The first organic extracts were concentrated *in vacuo* and the resulting solid was carried through the above procedure three more times. All ethyl acetate extracts were combined, dried (MgSO₄) and concentrated *in vacuo* to give the desired compound **32** (0.40 g, 1.4 mmol, 26%) as a white crystalline solid; mp 127-128 °C; ¹H NMR (300 MHz, CDCl₃): δ = 1.99-2.11 (m, 2 H; 4'-H), 2.48 (t, ³J(H,H) = 7.9 Hz, 2 H; 3'-H), 3.83 (s, 3 H; OCH₃), 3.88 (t, ³J(H,H) = 6.9 Hz, 2 H; 5'-H), 6.82 (dd, ³J(H,H) = 8.0 Hz, ⁴J(H,H) = 1.0 Hz, 1 H; Ar-3-H), 6.98-7.10 (m, 2 H; Ar-4'',5-H), 7.31-7.41 (m, 3 H; Ar-3'',4-H), 7.77-7.89 ppm (m, 3 H; Ar-2'',6-H); ¹³C NMR (75.5 MHz, CDCl₃): δ = 19.6 (C4'), 29.1 (C3'), 50.5 (C5'), 51.6 (OCH₃), 120.2 (C2''), 121.5 (C5), 122.1 (C1), 122.9 (C4''), 123.1 (C3), 128.4 (C3''), 130.7 (C6), 132.5 (C4), 141.2 (C1''), 153.0 (C2), 159.4 (C2'), 167.5 ppm (C=O); IR (Nujol): ν_{max} = 1721 (s) (C=O), 1654 (s) (C=N), 1591 (m), 756 (m) (Ar-H), 692 cm⁻¹ (m); LRMS (ES⁺): *m/z* (%): 295 (100) [M+H]⁺, 263 (22) [M-OMe]⁺; HRMS (ES⁺): *m/z* calc'd for C₁₈H₁₉N₂O₂ [M+H]⁺: 295.1447; found: 295.1449.

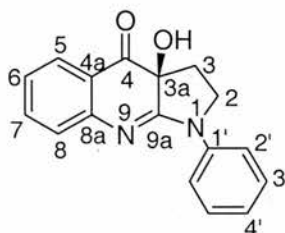
7.4.17. Preparation of 1-phenyl-2,3,4,9-tetrahydro-1H-pyrrolo[2,3-b]quinolin-4-one (31)



A solution of amidine **32** (0.50 g, 1.7 mmol, 1.0 equiv) in anhydrous THF (70 mL) was cooled to $-78\text{ }^{\circ}\text{C}$ and stirred for 15 minutes. Lithium bis(trimethylsilyl)amide (1.0 M in THF, 4.2 mL, 4.2 mmol, 2.5 equiv) was added dropwise to the reaction mixture, which was warmed to $0\text{ }^{\circ}\text{C}$ over 3 hours and quenched at $0\text{ }^{\circ}\text{C}$ with saturated aqueous ammonium chloride (5.0 mL). Further saturated aqueous ammonium chloride (150 mL) was added. The aqueous phase was extracted with dichloromethane ($3 \times 100\text{ mL}$) and the combined organic extracts dried (MgSO_4) and concentrated *in vacuo* to give an orange solid. Purification by flash column chromatography on silica gel (eluting with 100% ethyl acetate), gave the desired compound **31** (0.42 g, 1.6 mmol, 95%) as an off-white solid; mp $189\text{--}190\text{ }^{\circ}\text{C}$; ^1H NMR (300 MHz, $\text{D}_8\text{-THF}$): $\delta=3.19$ (t, $^3J(\text{H,H}) = 8.2\text{ Hz}$, 2 H; 3-H), 4.07 (t, $^3J(\text{H,H}) = 8.2\text{ Hz}$, 2 H; 2-H), 6.91-6.98 (m, 1 H; Ar-4'-H), 7.11-7.18 (m (7 lines), $^3J(\text{H,H}) = 6.9\text{ Hz}$, 1 H; Ar-6-H), 7.27-7.34 (m, 2 H; Ar-3'-H), 7.36-7.43 (m (7 lines), $^3J(\text{H,H}) = 6.9\text{ Hz}$, 1 H; Ar-7-H), 7.58-7.64 (m, 1 H; Ar-8-H), 8.00 (dd, $^3J(\text{H,H}) = 8.2\text{ Hz}$, $^4J(\text{H,H}) = 1.3\text{ Hz}$, 1 H; Ar-5-H), 8.02-8.08 ppm (m, 2 H; Ar-2'-H); ^{13}C NMR (75.5 MHz, $\text{D}_8\text{-THF}$)*: $\delta=22.6$ (C3), 49.5 (C2), 106.4 (C3a), 118.6 (C2'), 119.6 (C4a), 121.8 (C4'), 122.0 (C8,6), 126.6 (C5), 128.9 (C3',7), 143.3 (C1'), 148.4 (C8a), 157.7 (C9a), 159.5 ppm (C4); IR (Nujol): $\nu_{\text{max}}=1630$ (s), 1575 (s), 1297 (w), 756 (m) (Ar-H), 722 (m), 695 cm^{-1} (m); LRMS (ES^+): m/z (%): 263 (100) [$\text{M}+\text{H}$] $^+$; HRMS (ES^+): m/z calc'd for $\text{C}_{17}\text{H}_{15}\text{N}_2\text{O}$ [$\text{M}+\text{H}$] $^+$: 263.1184; found: 263.1180.

*The assignment of ^{13}C signals was made by using pendant, HMBC and HSQC NMR analysis.

7.4.18. Preparation of *S*-3a-hydroxy-1-phenyl-2,3,3a,4-tetrahydro-1*H*-pyrrolo[2,3-*b*]quinolin-4-one (**67**)



Method 1

a) Reagent: Dihalo oxaziridine **82**

A solution of quinolone **31** (0.050 g, 0.19 mmol, 1.0 equiv) in dry THF (10 mL) was added dropwise to lithium bis(trimethylsilyl)amide (1.0 M in THF, 0.23 mL, 0.23 mmol, 1.2 equiv) in dry THF (2.0 mL) at $-78\text{ }^{\circ}\text{C}$ under argon. The reaction was stirred for 30 minutes at $-78\text{ }^{\circ}\text{C}$ and a solution of dihalo oxaziridine **82** (0.14 g, 0.46 mmol, 2.4 equiv) in dry THF (6.0 mL) was added via a cannula. After 16 hours at $-10\text{ }^{\circ}\text{C}$ saturated aqueous ammonium iodide (5.0 mL, 10 equiv) and diethyl ether (5.0 mL) were added and the reaction mixture gradually warmed to room temperature. Saturated aqueous sodium thiosulfate (15 mL) was then added and the reaction mixture extracted with diethyl ether ($2 \times 10\text{ mL}$). The combined organic extracts were dried (MgSO_4) and concentrated *in vacuo* to give a yellow solid. The solid was partitioned between dichloromethane (100 mL) and aqueous hydrochloric acid solution (0.30 M, 100 mL). The aqueous phase was washed with dichloromethane ($3 \times 100\text{ mL}$), basified with aqueous sodium hydroxide solution (2.0 M, pH adjusted to 8) and extracted with ethyl acetate ($2 \times 100\text{ mL}$). The organic extracts were dried (MgSO_4) and concentrated *in vacuo* to give **67** (0.040 g, 0.15 mmol, 78%) as a bright yellow solid. The enantiomeric excess of **67** was 86% as determined by chiral-phase HPLC analysis; mp $203\text{--}204\text{ }^{\circ}\text{C}$; $[\alpha]_{\text{D}}^{25} = -414$ ($c=0.1$ in dichloromethane); $^1\text{H NMR}$ (300 MHz, CDCl_3): $\delta=2.21\text{--}2.34$ (m, 1 H; 3-H), 2.41-2.50 (m, 1 H; 3-H), 3.83-3.92 (m, 1 H; 2-H), 4.03 (dt, $^2J(\text{H,H}) = 9.8\text{ Hz}$, $^3J(\text{H,H}) = 5.8\text{ Hz}$, 1 H; 2-H), 7.05 (dt, $^3J(\text{H,H}) = 7.5\text{ Hz}$, $^4J(\text{H,H}) = 1.1\text{ Hz}$, 1 H; Ar-6-H), 7.16-7.23 (m, 2 H; Ar-4',8-H), 7.37-7.47 (m, 3 H; Ar-3',5-H), 7.83-7.87 (m, 1 H; Ar-7-H), 7.88-7.93 ppm (m, 2 H; Ar-2'-H); $^{13}\text{C NMR}$ (75.5 MHz, $\text{D}_8\text{-THF}$): $\delta=29.6$ (C3), 48.3 (C2), 74.0 (C3a), 120.3 (C2'), 122.44 (C4a), 123.5 (C6),

124.0 (C4'), 127.0 (C8), 127.1 (C7), 129.0 (C3'), 135.7 (C5), 141.9 (C1'), 152.6 (C8a), 166.7 (C9a), 194.8 ppm (C4); IR (Nujol): ν_{\max} =1698 (m), 1618 (m), 1593 (m), 1294 (w), 723 cm^{-1} (m) (Ar-H); LRMS (ES⁺): m/z (%): 279 (100) [M+H]⁺; HRMS (ES⁺): m/z calc'd for C₁₇H₁₅N₂O₂ [M+H]⁺: 279.1134; found: 279.1141; Anal. calc'd for C₁₇H₁₄N₂O₂: C, 73.37; H, 5.07; N, 10.07; found: C, 73.26; H, 4.84; N, 10.28; HPLC (Daicel Chiralpak AD, acetonitrile/water 50:50, flow rate 0.9 mL min⁻¹, λ =254 nm): major enantiomer: t_R = 7.72 min., and minor enantiomer: t_R = 11.07 min.

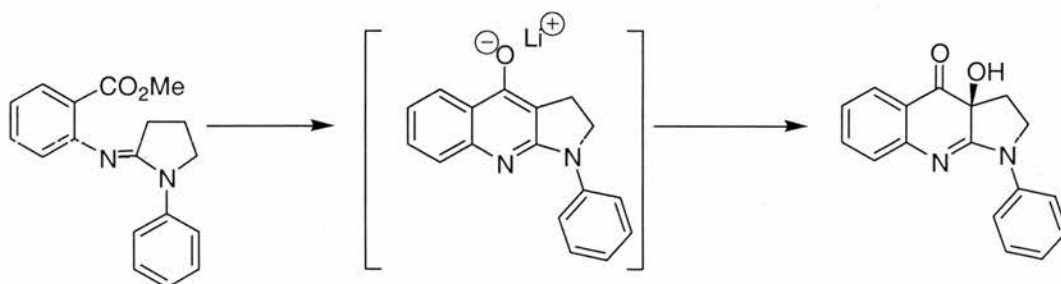
An analytical sample of **67** was prepared by recrystallisation from acetonitrile; $[\alpha]_D^{25}$ = -460 (c=0.1 in dichloromethane); Chiral HPLC analysis showed that after a single recrystallisation, **67** was prepared with an *ee* of >99%.

b) Reagent: Dihalo oxaziridine **78**

A solution of quinolone **31** (0.10 g, 0.38 mmol, 1.0 equiv) in dry THF (10 mL) was added dropwise to lithium bis(trimethylsilyl)amide (1.0 M in THF, 0.46 mL, 0.46 mmol, 1.2 equiv) in dry THF (4.0 mL) at -78 °C under argon. The reaction was stirred for 30 minutes at -78 °C and a solution of dihalo oxaziridine **78** (0.27 g, 0.91 mmol, 2.4 equiv) in dry THF (7.0 mL) was added via a cannula. After 16 hours at -10 °C saturated aqueous ammonium iodide (5.0 mL, 10 equiv) and diethyl ether (5.0 mL) were added and the reaction mixture gradually warmed to room temperature. Saturated aqueous sodium thiosulfate (15 mL) was then added and the reaction mixture extracted with diethyl ether (2 × 10 mL). The combined organic extracts were dried (MgSO₄) and concentrated *in vacuo* to give a yellow solid. The solid was partitioned between dichloromethane (100 mL) and aqueous hydrochloric acid solution (0.30 M, 100 mL). The aqueous phase was washed with dichloromethane (3 × 100 mL), basified with aqueous sodium hydroxide solution (2.0 M, pH adjusted to 8) and extracted with ethyl acetate (2 × 100 mL). The organic extracts were dried (MgSO₄) and concentrated *in vacuo* to give **67** (0.079 g, 0.28 mmol, 74%) as a bright yellow solid. The enantiomeric excess of **67** was 85% as determined by chiral-phase HPLC analysis; $[\alpha]_D^{25}$ = +410 (c=0.1 in dichloromethane). HPLC (Daicel Chiralpak AD, acetonitrile/water 50:50, flow rate 0.9 mL min⁻¹, λ =254 nm): minor enantiomer: t_R = 7.85 min., and major enantiomer: t_R = 11.15 min.

c) Reagent: Dihydro oxaziridine **81**

A solution of quinolone **31** (0.075 g, 0.29 mmol, 1.0 equiv) in dry THF (10 mL) was added dropwise to lithium bis(trimethylsilyl)amide (1.0 M in THF, 0.35 mL, 0.35 mmol, 1.2 equiv) in dry THF (3.0 mL) at -78 °C under argon. The reaction was stirred for 30 minutes at -78 °C and a solution of dihydro oxaziridine **81** (0.16 g, 0.70 mmol, 2.4 equiv) in dry THF (5.0 mL) was added via a cannula. After 16 hours at -10 °C saturated aqueous ammonium iodide (5.0 mL, 10 equiv) and diethyl ether (5.0 mL) were added and the reaction mixture gradually warmed to room temperature. Saturated aqueous sodium thiosulfate (15 mL) was then added and the reaction mixture extracted with diethyl ether (2 × 10 mL). The combined organic extracts were dried (MgSO₄) and concentrated *in vacuo* to give a yellow solid. The solid was partitioned between dichloromethane (100 mL) and aqueous hydrochloric acid solution (0.30 M, 100 mL). The aqueous phase was washed with dichloromethane (3 × 100 mL), basified with aqueous sodium hydroxide solution (2.0 M, pH adjusted to 8) and extracted with ethyl acetate (2 × 100 mL). The organic extracts were dried (MgSO₄) and concentrated *in vacuo* to give **67** (0.054 g, 0.19 mmol, 65%) as a bright yellow solid. The enantiomeric excess of **67** was 55% as determined by chiral-phase HPLC analysis; $[\alpha]_D^{25} = -153$ (c=0.1 in dichloromethane). HPLC (Daicel Chiralpak AD, acetonitrile/water 30:70, flow rate 0.8 mL min⁻¹, $\lambda=254$ nm): major enantiomer: $t_R = 17.78$ min., and minor enantiomer: $t_R = 26.75$ min.

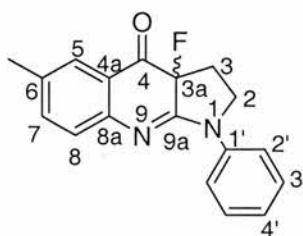
Method 2: One pot reaction

A solution of amidine **32** (0.24 g, 0.82 mmol, 1.0 equiv) in anhydrous THF (39 mL) was cooled to -78 °C and stirred for 15 minutes. Lithium bis(trimethylsilyl)amide (1.0 M in THF, 2.4 mL, 2.4 mmol, 3.0 equiv) was added

dropwise to the reaction mixture, which was warmed to 0 °C until no starting material was detected by TLC. A solution of dihydro oxaziridine **81** (0.34 g, 1.6 mmol, 2.0 equiv) in dry THF (20 mL) was added via cannula at -78 °C. The reaction was then warmed to room temperature and quenched with saturated aqueous ammonium chloride (5.0 mL). Further saturated aqueous ammonium chloride (150 mL) was added. The aqueous phase was extracted with dichloromethane (3 × 100 mL) and the combined organic extracts dried (MgSO₄) and concentrated *in vacuo* to give a crude yellow solid. Purification by flash column chromatography on silica gel (eluting with 20% ethyl acetate/hexane), gave the desired compound **67** (0.041 g, 0.15 mmol, 18%) as a bright yellow solid; $[\alpha]_D^{25} = -107$ (c=0.1 in dichloromethane). An analytical sample of **67** was prepared by recrystallisation from ethyl acetate/hexane to give crystals suitable for X-ray analysis. Analytical data for **67** prepared by this method were identical to that for **67** carried out in method 1.

7.5. Preparation of (S)-(-)-Blebbistatin (7) analogues substituted at the R¹ position

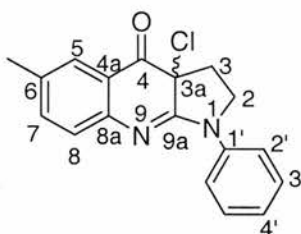
7.5.1. Preparation of 3a-fluoro-6-methyl-1-phenyl-2,3,3a,4-tetrahydro-1H-pyrrolo[2,3-b]quinolin -4-one (161)



A solution of quinolone **24** (0.070 g, 0.25 mmol, 1.0 equiv) in dry THF (15 mL) was added dropwise to lithium bis(trimethylsilyl)amide (1.0 M in THF, 0.30 mL, 0.30 mmol, 1.2 equiv) in dry THF (3.0 mL) at -78 °C under argon. The reaction was stirred for 30 minutes at -78 °C and SelectfluorTM (1-chloromethyl-4-fluoro-1,4-diazoniabicyclo[2.2.2]) (**168**) (0.18 g, 0.50 mmol, 2.0 equiv) was added. After 24 hours at room temperature the reaction mixture was quenched by the addition of saturated aqueous ammonium chloride (5.0 mL). The aqueous phase was extracted with dichloromethane (3 x 100mL) and the combined organic extracts dried (MgSO₄), and

concentrated *in vacuo* to give the desired compound **161** (0.072 g, 0.24 mmol, 96%) as a red solid; mp 128-129 °C; ^1H NMR (300 MHz, CDCl_3): δ = 2.28-2.53 (m, 4 H; 3- $\underline{\text{H}}$, $\underline{\text{CH}_3}$), 2.67-2.82 (m, 1 H; 3- $\underline{\text{H}}$), 4.00-4.07 (m, 1 H; 2- $\underline{\text{H}}$), 4.15-4.25 (m, 1 H; 2- $\underline{\text{H}}$), 7.16-7.23 (m, 1 H; Ar-4'- $\underline{\text{H}}$), 7.25-7.27 (m, 1 H; Ar-8- $\underline{\text{H}}$), 7.38 (ddq, $^3J(\text{H,H}) = 8.1$ Hz, $^4J(\text{H,H}) = 2.2$ Hz, $^4J(\text{H,H}) = 0.6$ Hz, 1 H; Ar-7- $\underline{\text{H}}$), 7.40-7.48 (m, 2 H; Ar-3'- $\underline{\text{H}}$), 7.67-7.70 (m, 1 H; Ar-5- $\underline{\text{H}}$), 7.94-8.00 ppm (m, 2 H; Ar-2'- $\underline{\text{H}}$); ^{19}F NMR (^1H , ^{19}F) (282.3 MHz, CDCl_3): $\delta_{\text{F}} = -149.6$ ppm (dd, $^3J(\text{H,F}) = 41.9$ Hz, $^3J(\text{H,F}) = 20.9$ Hz, 3- $\underline{\text{H}}$); ^{19}F NMR (^1H) (282.3 MHz, CDCl_3): $\delta_{\text{F}} = -149.6$ ppm; ^{13}C NMR (75.5 MHz, CDCl_3): δ = 20.6 ($\underline{\text{CH}_3}$), 26.7 (d, $^2J(\text{C,F}) = 24.9$ Hz, $\underline{\text{C}_3}$), 47.5 ($\underline{\text{C}_2}$), 88.3 (d, $^1J(\text{C,F}) = 174$ Hz, $\underline{\text{C}_{3a}}$), 120.0 ($\underline{\text{C}_{2'}}$), 120.6 ($\underline{\text{C}_{4a}}$), 124.6 ($\underline{\text{C}_{4'}}$), 126.7 ($\underline{\text{C}_8}$), 127.4 ($\underline{\text{C}_5}$), 128.9 ($\underline{\text{C}_{3'}}$), 133.8 ($\underline{\text{C}_6}$), 137.9 ($\underline{\text{C}_7}$), 139.8 ($\underline{\text{C}_{1'}}$), 149.1 ($\underline{\text{C}_{8a}}$), 159.5 (d, $^2J(\text{C,F}) = 17.1$ Hz, $\underline{\text{C}_{9a}}$), 189.7 ppm (d, $^2J(\text{C,F}) = 19.9$ Hz, $\underline{\text{C}_4}$); IR (Nujol): $\nu_{\text{max}} = 1702$ (s) (C=O), 1623 (s) (C=N), 1595 (s), 1298 (s), 1089 (m), 757 (m) (Ar-H), 722 (m), 690 cm^{-1} (m); LRMS (ES^+): m/z (%): 327 (94) [$\text{M} + \text{MeOH}$] $^+$, 295 (100) [$\text{M} + \text{H}$] $^+$; HRMS (ES^+): m/z calc'd for $\text{C}_{18}\text{H}_{16}\text{N}_2\text{OF}$ [$\text{M} + \text{H}$] $^+$: 295.1247; found: 295.1244.

7.5.2. Preparation of 3a-chloro-6-methyl-1-phenyl-2,3,3a,4-tetrahydro-1H-pyrrolo[2,3-b]quinolin-4-one (162)



Method 1

To an optically enriched **7** (0.010 g, 0.034 mmol, 1.0 equiv) in dry dichloromethane (5.0 mL) were added catalytic amount of DMAP, triethylamine (2 drops) and oxalyl chloride (0.021 g, 0.17 mmol, 5.0 equiv). The reaction mixture was stirred for 2 hours at room temperature and concentrated *in vacuo*. Purification by flash column chromatography on silica gel (eluting with 10% ethyl acetate/hexane) gave the desired compound **162** (0.0066 g, 0.021 mmol, 62%) as a red crystalline solid. An analytical sample of **162** was prepared by recrystallisation from ethyl acetate/hexane;

mp 180-181 °C; $[\alpha]_D^{25} = 0$ (c=0.1 in dichloromethane); δ_H (300 MHz, $CDCl_3$): $\delta = 2.36$ (s, 3 H; $\underline{CH_3}$), 2.55-2.68 (m, 1 H; 3- \underline{H}), 2.77 (dd, $^2J(H,H) = 14.5$ Hz, $^3J(H,H) = 5.4$ Hz, 1 H; 3- \underline{H}), 4.02-4.11 (m, 1 H; 2- \underline{H}), 4.27 (dt, $^2J(H,H) = 10.0$ Hz, $^3J(H,H) = 5.4$ Hz, 1 H; 2- \underline{H}), 7.17-7.24 (m (3 lines), $^3J(H,H) = 7.3$ Hz, 1 H; Ar-4'- \underline{H}), 7.26-7.31 (m, 1 H; Ar-8- \underline{H}), 7.36-7.41 (m, 1 H; Ar-7- \underline{H}), 7.41-7.49 (m, 2 H; Ar-3'- \underline{H}), 7.72 (br d, $^4J(H,H) = 1.6$ Hz, 1 H; Ar-5- \underline{H}), 7.91-7.98 ppm (m, 2 H; Ar-2'- \underline{H}); ^{13}C NMR (75.5 MHz, $CDCl_3$): $\delta = 20.7$ ($\underline{CH_3}$), 29.7 ($\underline{C3}$), 47.8 ($\underline{C2}$), 61.5 ($\underline{C3a}$), 120.0 ($\underline{C4a}$), 120.3, ($\underline{C2'}$), 124.9 ($\underline{C4'}$), 126.4 ($\underline{C8}$), 127.3 ($\underline{C5}$), 129.1 ($\underline{C3'}$), 134.2 ($\underline{C6}$), 137.6 ($\underline{C7}$), 139.9 ($\underline{C1'}$), 148.0 ($\underline{C8a}$), 161.7 ($\underline{C9a}$), 191.0 ppm ($\underline{C4}$); IR (Nujol): $\nu_{max} = 1694$ (s) (C=O), 1618 (s), 1595 (s), 1295 (s), 831 (m), 757 (m) (Ar-H), 722 cm^{-1} (m); LRMS (ES^+): m/z (%): 313 (35) [(M+H) $^+$ (^{37}Cl)], 311 (100) [(M+H) $^+$ (^{35}Cl)]; HRMS (ES^+): m/z calc'd for $C_{18}H_{16}N_2O^{35}Cl$ [(M+H) $^+$]: 311.0951; found: 311.0951; Anal. calc'd for $C_{18}H_{15}N_2OCl$: C, 69.57; H, 4.86; N, 9.01; found: C, 69.89; H, 4.54; N, 9.01.

Method 2

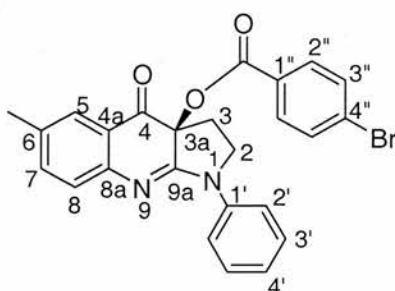
To an optically enriched **7** (0.010 g, 0.034 mmol, 1.0 equiv) in dry dichloromethane (5.0 mL) were added catalytic amount of DMAP, triethylamine (0.086 g, 0.12 mL, 0.85 mmol, 25 equiv) and Mosher's acid chloride (*R*)-(-) (**103**) (0.22 g, 0.85 mmol, 25 equiv). The reaction mixture was stirred for 2 hours at room temperature and concentrated *in vacuo*. The crude solid was dissolved in saturated aqueous sodium bicarbonate (pH adjusted to 8) and extracted with dichloromethane (2 × 100 mL). The organic extracts were combined, dried ($MgSO_4$) and concentrated *in vacuo* to give a red solid. Purification by flash column chromatography on silica gel (eluting with 10% ethyl acetate/hexane) afforded red crystals **162** (0.0050 g, 0.016 mmol, 47%) suitable for X-ray analysis (see Chapter 4, Section 4.4.1.1.).

Method 3

To a solution of quinolone **24** (0.20 g, 0.72 mmol, 1.0 equiv) in dry THF (45 mL) was added dropwise a solution of NaOCl (1.3 g, 1.1 mL, 17 mmol, 24 equiv) in dry THF (10 mL). The reaction mixture was stirred for 72 hours at room temperature and quenched with saturated aqueous ammonium chloride (5.0 mL). Further saturated aqueous ammonium chloride (150 mL) was added. The aqueous phase was extracted

with dichloromethane (3×100 mL) and the combined organic extracts dried (MgSO_4) and concentrated *in vacuo*. Purification by flash column chromatography on silica gel (eluting with 10% ethyl acetate/hexane) gave a red solid (0.13 g) which was recrystallised two times from hexane/ethyl acetate to give the desired compound **162** (0.045 g, 0.15 mmol, 21%) as red crystals. ^1H NMR analysis confirmed the presence of **162**.

7.5.3. Preparation of *S*-3a-(4-bromobenzoyloxy)-1-phenyl-2,3,3a,4-tetrahydro-1*H*-pyrrolo[2,3-*b*]quinolin-4-one (**176**)

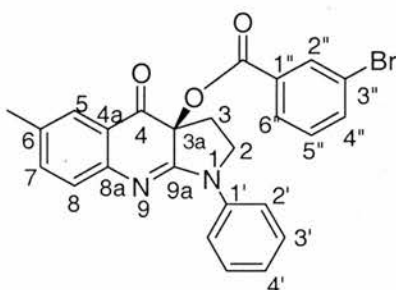


An optically enriched sample of **7** (0.090 g, 0.31 mmol, 1.0 equiv) was dissolved in dichloromethane (28 mL) and a catalytic amount of DMAP (0.020 g, 0.16 mmol, 0.50 equiv), dry pyridine (0.10 g, 1.2 mmol, 4.0 equiv) and 4-bromobenzoyl chloride (**179**) (0.70 g, 3.1 mmol, 10 equiv) were added. The reaction mixture was stirred for 24 hours at room temperature, quenched with saturated aqueous ammonium chloride (5.0 mL) and then poured into water (50 mL, pH adjusted to 8) and extracted with dichloromethane (3×50 mL). The combined organic extracts were dried (MgSO_4) and concentrated *in vacuo*. The solid was purified by flash column chromatography on silica gel (eluting with 10% ethyl acetate/hexane), to give the title compound **176** (0.15 g, 0.31 mmol, 100%) as a red solid. An analytical sample of this compound was prepared by recrystallisation from ethyl acetate/hexane; mp 161-162 °C; $[\alpha]_{\text{D}}^{25} = -607$ ($c=0.1$ in dichloromethane)*; ^1H NMR (300 MHz, CDCl_3): $\delta = 2.30$ (s, 3 H; CH_3), 2.69-2.89 (m, 2 H; 3- H), 4.01-4.09 (m (7 lines), 1 H; 2- H), 4.22 (dt, $^2J(\text{H,H}) = 9.5$ Hz, $^3J(\text{H,H}) = 6.5$ Hz, 1 H; 2- H), 7.16-7.23 (m, 2 H; Ar-4',8- H), 7.30 (ddq, $^3J(\text{H,H}) = 8.1$ Hz, $^4J(\text{H,H}) = 2.2$ Hz, $^4J(\text{H,H}) = 0.6$ Hz, 1 H; Ar-7- H), 7.40-7.50 (m, included AA' part of the AA'XX' system, 4 H; Ar-3'',3'- H), 7.55-7.58 (m, 1 H; Ar-5- H), 7.67-7.73 (m, XX' part of the AA'XX' system, 2 H; Ar-2'- H), 7.94-8.00 ppm (m, 2 H; Ar-2'- H);

^{13}C NMR (75.5 MHz, CDCl_3): δ =20.6 ($\underline{\text{C}}\text{H}_3$), 26.0 ($\underline{\text{C}}3$), 48.1 ($\underline{\text{C}}2$), 79.8 ($\underline{\text{C}}3\text{a}$), 120.1 ($\underline{\text{C}}2'$), 122.2 ($\underline{\text{C}}4''$), 124.5 ($\underline{\text{C}}4'$), 125.9 ($\underline{\text{C}}8$), 127.1 ($\underline{\text{C}}5$), 127.6 ($\underline{\text{C}}1''$), 128.9 ($\underline{\text{C}}4\text{a}$), 129.0 ($\underline{\text{C}}3'$), 131.4 ($\underline{\text{C}}2''$), 131.7($\underline{\text{C}}3''$), 133.6 ($\underline{\text{C}}6$), 136.8 ($\underline{\text{C}}7$), 140.0 ($\underline{\text{C}}1'$), 148.3 ($\underline{\text{C}}8\text{a}$), 160.3 ($\underline{\text{C}}9\text{a}$), 164.1 ($\underline{\text{C}}=\text{O}$), 192.3 ppm ($\underline{\text{C}}4$); IR (Nujol): ν_{max} =1734 (m) ($\text{C}=\text{O}$), 1591 (m), 1262 (m), 1089 (m), 1003 (m), 752 (m), 727 cm^{-1} (w) (Ar-H); LRMS (Cl^+): m/z (%): 277 (66) [$\text{M}-\text{C}_7\text{H}_4\text{O}_2^{81}\text{Br}$] $^+$, 275 (100) [$\text{M}-\text{C}_7\text{H}_4\text{O}_2^{79}\text{Br}$] $^+$, 201 (40) [$\text{C}_7\text{H}_4\text{O}_2^{79}\text{Br}$] $^+$, 203 (40) [$\text{C}_7\text{H}_4\text{O}_2^{81}\text{Br}$] $^+$; HRMS (Cl^+): m/z : calc'd for $\text{C}_{25}\text{H}_{20}\text{N}_2\text{O}_3^{79}\text{Br}$ [$\text{M}+\text{H}$] $^+$: 475.0657; found: 475.0661; Anal. calc'd for $\text{C}_{25}\text{H}_{19}\text{BrN}_2\text{O}_3$: C, 63.17; H, 4.03; N, 5.89; found: C, 63.37; H, 3.96; N, 5.59.

*The optical rotation measurement was carried out using non crystallised material.

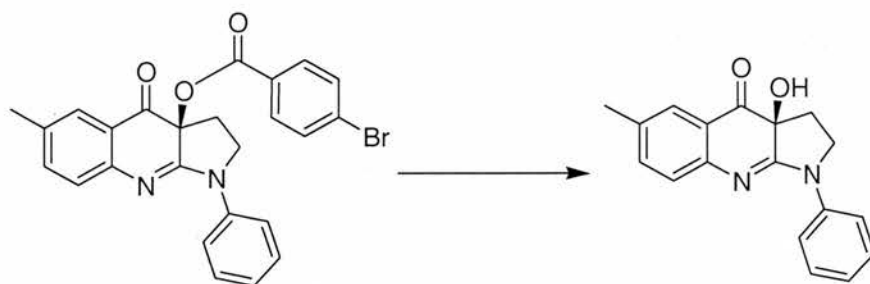
7.5.4. Preparation of *S*-3a-(3-bromobenzoyloxy)-1-phenyl-2,3,3a,4-tetrahydro-1*H*-pyrrolo[2,3-*b*]quinolin-4-one (177)



An optically enriched sample of **7** (0.090 g, 0.30 mmol, 1.0 equiv) was dissolved in dichloromethane (28 mL) and a catalytic amount of DMAP (0.020 g, 0.20 mmol, 0.50 equiv), dry pyridine (0.10 g, 1.2 mmol, 4.0 equiv) and 3-bromobenzoyl chloride (**178**) (0.70 g, 3.1 mmol, 10 equiv) were added. The reaction mixture was stirred for 24 hours at room temperature, quenched with saturated aqueous ammonium chloride (5.0 mL) and then poured into water (50 mL, pH adjusted to 8) and extracted with dichloromethane (3 \times 50 mL). The combined organic extracts were dried (MgSO_4) and concentrated *in vacuo*. The solid was purified by flash column chromatography on silica gel (eluting with 10% ethyl acetate/hexane), to give the title compound **177** (0.14 g, 0.30 mmol, 97%) as a red solid; mp 128-129 $^\circ\text{C}$; $[\alpha]_{\text{D}}^{25} = -568$ ($c=0.1$ in dichloromethane); ^1H NMR (300 MHz, CDCl_3): δ =2.32 (s, 3 H; $\underline{\text{C}}\text{H}_3$), 2.70-2.91 (m, 2 H; 3- $\underline{\text{H}}$), 4.01-4.11 (m (7 lines), 1 H; 2- $\underline{\text{H}}$), 4.22 (dt, $^2J(\text{H},\text{H}) = 9.5$ Hz, $^3J(\text{H},\text{H}) = 6.5$

Hz, 1 H; 2-H), 7.17-7.24 (m, 3 H; Ar-8,4',5''-H), 7.32 (ddq, $^3J(\text{H,H}) = 8.1 \text{ Hz}$, $^4J(\text{H,H}) = 2.2 \text{ Hz}$, $^4J(\text{H,H}) = 0.6 \text{ Hz}$, 1 H; Ar-7-H), 7.42-7.49 (m, 2 H; Ar-3'-H), 7.57-7.60 (m, 1 H; Ar-5-H), 7.64 (ddd, $^3J(\text{H,H}) = 8.0 \text{ Hz}$, $^4J(\text{H,H}) = 2.0 \text{ Hz}$, $^4J(\text{H,H}) = 1.0 \text{ Hz}$, 1 H; Ar-4''-H), 7.79 (ddd, $^3J(\text{H,H}) = 8.0 \text{ Hz}$, $^4J(\text{H,H}) = 2.0 \text{ Hz}$, $^4J(\text{H,H}) = 1.0 \text{ Hz}$, 1 H; Ar-6''-H), 7.96-8.01 ppm (m, 3 H; Ar-2',2''-H); ^{13}C NMR (75.5 MHz, CDCl_3): $\delta = 20.6$ (CH₃), 26.2 (C3), 48.1 (C2), 79.9 (C3a), 120.2 (C2'), 122.2 (C-Br), 122.4 (C1''), 124.6 (C4'), 125.9 (C8), 127.1 (C5), 128.5 (C6''), 129.0 (C3'), 130.0 (C5''), 130.6 (C4a), 132.8 (C2''), 133.6 (C6), 136.5 (C4''), 136.8 (C7), 139.9 (C1'), 148.2 (C8a), 160.2 (C9a), 163.5 (C=O), 192.2 ppm (C4); IR (Nujol): $\nu_{\text{max}} = 1734$ (m) (C=O), 1593 (m), 1253 (m), 1054 (m), 740 (m), 710 (m) (Ar-H), 681 cm^{-1} (w); LRMS (EI): m/z (%): 476 (30) [M^+ (^{81}Br)], 474 (32) [M^+ (^{79}Br)], 274 (100) [$\text{M}-\text{C}_7\text{H}_4\text{O}_2$ (^{79}Br) $^+$], 276 (58) [$\text{M}-\text{C}_7\text{H}_4\text{O}_2$ (^{81}Br) $^+$], 200 (64), 202 (63), 187 (63), 185 (64), 156 (40), 149 (48), 154 (38); HRMS (EI): m/z : calc'd for $\text{C}_{25}\text{H}_{19}\text{N}_2\text{O}_3$ (^{79}Br) [M] $^+$: 474.0579: found: 474.0580 and calc'd for $\text{C}_{25}\text{H}_{19}\text{N}_2\text{O}_3$ (^{81}Br) [M] $^+$: 476.0559: found: 476.0564.

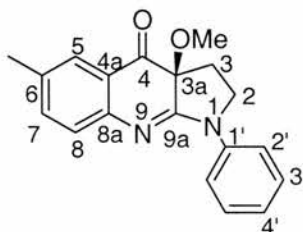
7.5.5. Basic hydrolysis of *S*-3a-(4-bromobenzoyloxy)-1-phenyl-2,3,3a,4-tetrahydro-1*H*-pyrrolo[2,3-*b*]quinolin-4-one (176)



Lithium hydroxide (0.0033 g, 0.040 mL, 0.080 mmol, 1.0 equiv) was added dropwise to a solution of **176** (0.038 g, 0.080 mmol, 1.0 equiv) in THF (5.0 mL). The reaction mixture was stirred for 3 hours at room temperature and quenched with saturated aqueous ammonium chloride (5.0 mL). Further saturated aqueous ammonium chloride (150 mL) was added. The aqueous phase was extracted with ethyl acetate (3 \times 100 mL) and the combined organic extracts dried (MgSO_4) and concentrated *in vacuo*. Purification by flash column chromatography on silica gel (eluting with 15% ethyl acetate/hexane) gave (*S*)-(-)-Blebbistatin (**7**) (0.013 g, 0.044 mmol, 55%) as a

bright yellow solid **7**, identical ^1H NMR with a sample prepared as in Section 7.2.3. HPLC; acetonitrile/water 50:50, flow rate 0.8 mL min^{-1} , $\lambda=254\text{ nm}$.

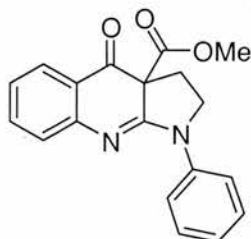
7.5.6. Preparation of *S*-3a-methoxy-6-methyl-1-phenyl-2,3,3a,4-tetrahydro-1*H*-pyrrolo[2,3-*b*]quinolin-4-one (**180**)



A solution of optically enriched **7** (0.020 g, 0.068 mmol, 1.0 equiv) in anhydrous THF (6.0 mL) was cooled to $-78\text{ }^\circ\text{C}$ and stirred for 15 minutes. Sodium bis(trimethylsilyl)amide (1.0 M in THF, 0.10 mL, 0.10 mmol, 1.5 equiv) was added dropwise to the reaction mixture which was warmed to $0\text{ }^\circ\text{C}$. A solution of iodomethane (0.048 g, 0.021 mL, 0.34 mmol, 5.0 equiv) was then added and the reaction mixture was stirred for 1 hour at $0\text{ }^\circ\text{C}$. After 16 hours at room temperature the reaction was quenched with saturated aqueous ammonium chloride (7.0 mL). Further saturated aqueous ammonium chloride (150 mL) was added. The aqueous phase was extracted with dichloromethane ($3 \times 50\text{ mL}$) and the combined organic extracts dried (MgSO_4) and concentrated *in vacuo* to afford **180** (0.019 g, 0.062 mmol, 91%) as a bright yellow solid; mp $220\text{--}221\text{ }^\circ\text{C}$; $[\alpha]_{\text{D}}^{25} = -462$ ($c=0.05$ in dichloromethane); ^1H NMR (300 MHz, CDCl_3): $\delta = 2.09\text{--}2.23$ (m, 1 H; 3-H), 2.34 (br s, 3 H; CH₃), 2.62 (dd, $^2J(\text{H,H}) = 14.3\text{ Hz}$, $^3J(\text{H,H}) = 5.3\text{ Hz}$, 1 H; 3-H), 3.27 (s, 3 H; OCH₃), 3.89-3.99 (m, 1 H; 2-H), 4.09 (dt, $^2J(\text{H,H}) = 9.8\text{ Hz}$, $^3J(\text{H,H}) = 5.7\text{ Hz}$, 1 H; 2-H), 7.12-7.19 (m, 1 H; Ar-4'-H), 7.24 (d, $^3J(\text{H,H}) = 8.1\text{ Hz}$, 1 H; Ar-8-H), 7.35 (ddq, $^3J(\text{H,H}) = 8.1\text{ Hz}$, $^4J(\text{H,H}) = 2.2\text{ Hz}$, $^4J(\text{H,H}) = 0.6\text{ Hz}$, 1 H; Ar-7-H), 7.38-7.46 (m, 2 H; Ar-3'-H), 7.64-7.66 (m, 1 H; Ar-5-H), 7.95-8.01 ppm (m, 2 H; Ar-2'-H); ^{13}C NMR (75.5 MHz, $\text{D}_8\text{-THF}$): $\delta = 20.6$ (CH₃), 30.5 (C₃), 48.2 (C₂), 52.7 (OCH₃), 79.1 (C_{3a}), 120.3 (C_{2'}), 122.5 (C_{4a}), 124.0 (C_{4'}), 126.7 (C₈), 127.0 (C₅), 129.1 (C_{3'}), 133.5 (C₆), 137.0 (C₇), 141.85 (C_{1'}), 150.5 (C_{8a}), 163.7 (C_{9a}), 193.7 ppm (C₄); IR (Nujol): $\nu_{\text{max}} = 1690$ (m), 1618 (m), 1592 (m), 1295 (w), 1038 (w), 832 (m), 760 (m) (Ar-H), 722 cm^{-1} (m);

LRMS (ES⁺): *m/z* (%): 307 (100) [M+H]⁺; HRMS (ES⁺): *m/z* calc'd for C₁₉H₁₉N₂O₂ [M+H]⁺: 307.1447; found: 307.1444.

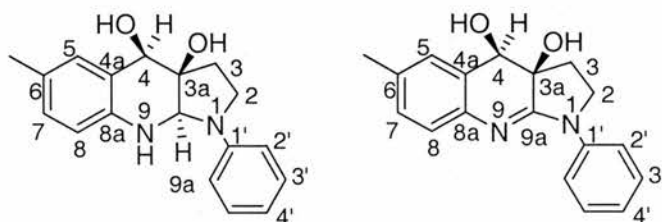
7.5.7. Attempted preparation of methyl 4-oxo-1-phenyl-2,3,3a,4-tetrahydro-1*H*-pyrrolo[2,3-*b*]-quinoline-3a-carboxylate (**195**)



A solution of quinolone **31** (0.050 g, 0.20 mmol, 1.0 equiv) in dry THF (7.0 mL) was added dropwise to lithium bis(trimethylsilyl)amide (1.0 M in THF, 0.24 mL, 0.24 mmol, 1.2 equiv) in dry THF (3.0 mL) at -78 °C under argon. The reaction was stirred for 30 minutes at -78 °C and a solution of methyl cyanoformate (**191**) (0.032 g, 0.030 mL, 0.40 mmol, 2.0 equiv) was added via a cannula. After 48 hours at -10 °C the reaction was quenched with saturated aqueous ammonium chloride (5.0 mL). Further saturated aqueous ammonium chloride (150 mL) was added. The aqueous phase was extracted with dichloromethane (3 × 100 mL) and the combined organic extracts dried (MgSO₄) and concentrated *in vacuo*. ¹H NMR of the crude mixture confirmed that only unreacted starting material was present.

7.6. Preparation of (*S*)-(-)-Blebbistatin (**7**) analogues substituted at the R⁴ position

7.6.1. Preparation of (3a*S*, 4*R*, 9a*S*)-6-methyl-1-phenyl-2,3,3a,4,9,9a-hexahydro-1*H*-pyrrolo[2,3-*b*]quinoline-3a,4-diol (**198**) and (3a*S*, 4*R*)-6-methyl-1-phenyl-2,3,3a,4-tetrahydro-1*H*-pyrrolo[2,3-*b*]quinoline-3a,4-diol (**199**)



Method 1

Sodium borohydride (0.011 g, 0.30 mmol, 1.0 equiv) was added dropwise to a solution of **7** (0.090 g, 0.30 mmol, 1.0 equiv) in dry methanol (35 mL). The reaction was stirred for 30 minutes at room temperature and quenched with saturated aqueous ammonium chloride (5.0 mL). Further saturated aqueous ammonium chloride (150 mL) was added. The aqueous phase was extracted with dichloromethane (3 × 100 mL) and the combined organic extracts dried (MgSO₄) and concentrated *in vacuo* to give a light yellow crude solid. Purification by flash column chromatography on silica gel (eluting with 15% ethyl acetate/hexane and 20% ethyl acetate), gave the desired product **198** (0.032 g, 0.11 mmol, 37%) as a yellow deliquescent solid and the diol **199** (0.043 g, 0.15 mmol, 50%) as a white solid.

a) Compound **198**: $[\alpha]_{\text{D}}^{25} = -407$ (c=0.5 in dichloromethane); ¹H NMR (300 MHz, CDCl₃): $\delta = 1.82\text{--}2.08$ (m, 2 H; 3-H), 2.24 (s, 3 H; CH₃), 3.26-3.37 (m, 1 H; 2-H), 3.45-3.60 (m, 1 H; 2-H), 4.55 (s, 1 H; 4-H), 5.07 (s, 1 H; 9a-H), 6.36 (d, ³*J*(H,H) = 8.1 Hz, 1 H; Ar-8-H), 6.66-6.74 (m, 2 H; Ar-2'-H), 6.75-6.84 (m, 1 H; Ar-4'-H), 6.93 (dd, ³*J*(H,H) = 8.1 Hz, ⁴*J*(H,H) = 1.5 Hz, 1 H; Ar-7-H), 7.01 (br s, 1 H; Ar-5-H), 7.26-7.33 ppm (m, 2 H; Ar-3'-H); ¹³C NMR (75.5 MHz, CDCl₃): $\delta = 20.3$ (CH₃), 32.7 (C₃), 44.9 (C₂), 71.6 (C₄), 72.9 (C_{9a}), 79.7 (C_{3a}), 112.3 (C_{2'}), 113.9 (C_{4'}), 117.4 (C₈), 119.6 (C_{4a}), 126.9 (C₆), 129.7 (C₅), 130.4 (C₇), 131.1 (C_{3'}), 138.4 (C_{8a}), 146.2 ppm (C_{1'}); IR (Nujol): $\nu_{\text{max}} = 3400$ (s), 1599 (s), 1263 (w), 1154 (w), 813 (w), 745 cm⁻¹ (s) (Ar-H); LRMS (ES⁺): *m/z* (%): 615 (16), 597 (29), 575 (20), 319 (100) [M+Na], 158 (12); HRMS (ES⁺): *m/z* calc'd for C₁₈H₂₀N₂O₂ [M+Na]: 319.1422; found: 319.1418.

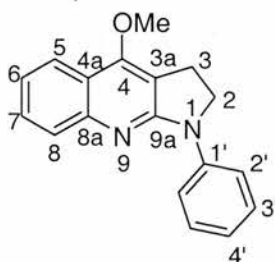
b) Compound **199**: mp 212-213 °C; $[\alpha]_{\text{D}}^{25} = -75$ (c=0.1 in dichloromethane); ¹H NMR (300 MHz, D₈-THF): $\delta = 2.08\text{--}2.21$ (m, 1 H; 3-H), 2.28 (s, 3 H; CH₃), 2.33-2.41 (m, 1 H; 3-H), 3.81-3.92 (m, 1 H; 2-H), 3.96-4.07 (m, 1 H; 2-H), 4.25 (d, ²*J*(H,H) = 9.2 Hz, 1 H; 4-H), 4.50 (s, 1 H; 3a-OH), 4.62 (d, ²*J*(H,H) = 9.2 Hz, 1 H; 4-OH), 6.88-7.02 (m, 3 H; Ar-4',7,8-H), 7.26-7.36 (m, 3 H; Ar-3',5-H), 8.08-8.14 ppm (m, 2 H; Ar-2'-H); ¹³C NMR (75.5 MHz, D₈-THF): $\delta = 21.0$ (CH₃), 34.5 (C₃), 48.2 (C₂), 74.9 (C₄), 75.0 (C_{3a}), 119.6 (C_{2'}), 122.8 (C_{4'}), 124.7 (C₈), 126.0 (C₅), 128.4 (C₇), 128.7 (C_{3'}), 129.5 (C_{4a}), 132.8 (C₆), 142.5 (C_{1'}), 143.7 (C_{8a}), 163.4 ppm (C_{9a}); IR (Nujol): $\nu_{\text{max}} = 3379$ (s), 1628 (m), 1593 (m), 1304 (w), 1155 (w), 758 cm⁻¹ (w) (Ar-H); LRMS (ES⁺):

m/z (%): 295 (100) $[M+H]^+$; HRMS (ES⁺): m/z calc'd for C₁₈H₁₉N₂O₂ $[M+H]^+$: 295.1447; found: 295.1451; An analytical sample of the diol **199** was prepared by recrystallisation from acetonitrile; Anal. calc'd for C₁₈H₁₈N₂O₂: C, 73.45; H, 6.16; N, 9.52; found: C, 73.58; H, 6.19; N, 9.88.

Method 2

To a solution of optically enriched **7** (0.020 g, 0.070 mmol, 1.0 equiv) in a 1:1 mixture of methanol and DMF (8.0 mL) were added triethylamine (0.020 g) and 10% Pd/C (0.022 g, 0.21 mmol, 3.0 equiv) under argon. This suspension was degassed under vacuum. Hydrogen was then introduced and the reaction was stirred at room temperature under hydrogen for 48 hours. The solid material was filtered off and washed with methanol. The filtrate was concentrated and the residue was purified by flash column chromatography on silica gel (eluting with 20% ethyl acetate/hexane), to give the desired compound **199** (0.011 g, 0.038 mmol, 55%) as a white solid. An analytical sample of **199** was prepared by recrystallisation from acetonitrile. ¹H NMR and ¹³C NMR were consistent with data from Method 1.

7.6.2. Preparation of 4-methoxy-1-phenyl-2,3-dihydro-1H-pyrrolo[2,3-b]quinoline (185)

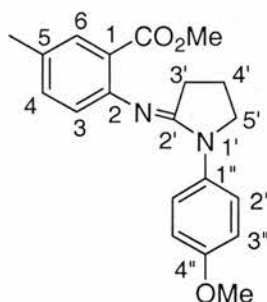


A solution of quinolone **31** (0.050 g, 0.20 mmol, 1.0 equiv) in dry THF (8.0 mL) was added dropwise to lithium bis(trimethylsilyl)amide (1.0 M in THF, 0.24 mL, 0.24 mmol, 1.2 equiv) in dry THF (2.0 mL) at -78 °C under argon. The reaction was stirred for 30 minutes at -78 °C and a solution of methyl triflate (**183**) (0.062 g, 0.040 mL, 0.40 mmol, 2.0 equiv) was added via a cannula. After 16 hours at -20 °C the reaction was quenched with saturated aqueous ammonium chloride (5.0 mL). Further saturated aqueous ammonium chloride (150 mL) was added. The aqueous phase was

extracted with dichloromethane (3 × 100 mL) and the combined organic extracts dried (MgSO₄) and concentrated *in vacuo*. Purification by flash column chromatography on silica gel (eluting with 30% ethyl acetate/hexane) gave the desired compound **185** (0.024 g, 0.087 mmol, 44%) as a light yellow solid; mp 144-145 °C; ¹H NMR (300 MHz, CDCl₃): δ=3.45 (t, ³J(H,H) = 8.0 Hz, 2 H; 3-H), 4.07 (t, ³J(H,H) = 8.0 Hz, 2 H; 2-H), 4.15 (s, 3 H; OCH₃), 7.02-7.10 (m, 1 H; Ar-4'-H), 7.19-7.27 (m (7 lines), ³J(H,H) = 6.9 Hz, 1 H; Ar-6-H), 7.37-7.45 (m, 2 H; Ar-3'-H), 7.46-7.55 (m (7 lines), ³J(H,H) = 6.9 Hz, 1 H; Ar-7-H), 7.75 (dd, ³J(H,H) = 8.3 Hz, ⁴J(H,H) = 0.6 Hz, 1 H; Ar-8-H), 7.92-8.04 ppm (m, 3 H; Ar-2',5-H); ¹³C NMR (75.5 MHz, CDCl₃): δ=24.1 (C₃), 48.6 (C₂), 58.9 (OCH₃), 108.1 (C_{3a}), 118.3 (C_{2'}), 119.8 (C_{4a}), 121.5 (C_{4'}), 121.9 (C₆), 122.4 (C₈), 126.6 (C₇), 128.7 (C_{3'}), 129.1 (C₅), 141.8 (C_{1'}), 148.4 (C_{8a}), 157.0 (C₄), 160.2 ppm (C_{9a}); IR (Nujol): ν_{max}= 1624 (m), 1595 (m), 1307 (m), 1112 (w), 753 cm⁻¹ (m) (Ar-H); LRMS (ES⁺): *m/z* (%): 299 (20), 277 (100) [M+H]⁺; HRMS (ES⁺): *m/z* calc'd for C₁₈H₁₇N₂O [M+H]⁺: 277.1341; found: 277.1335.

7.7. Preparation of (S)-(-)-Blebbistatin (7) analogues substituted at the R² position

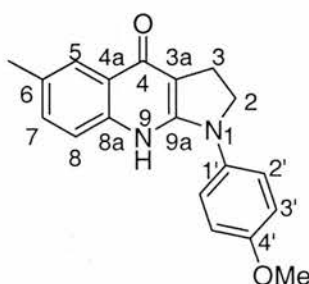
7.7.1. Preparation of methyl 5-methyl-2-[1-(4-methoxyphenyl)pyrrolidin-2-ylideneamino]benzoate (211)



Phosphorus oxychloride (1.3 g, 0.77 mL, 8.2 mmol, 1.0 equiv) was added dropwise to a solution of 1-(4-methoxy-phenyl)-2-pyrrolidinone (**210**) (1.7 g, 9.0 mmol, 1.1 equiv) in dry dichloromethane (10 mL) and the reaction was stirred for 3 hours at room temperature. A solution of anthranilate **27** (1.4 g, 8.2 mmol, 1.0 equiv) in dry dichloromethane (60 mL) was then added and the reaction refluxed for 35 hours. The reaction mixture was cooled and concentrated *in vacuo*. The resulting solid was dissolved in aqueous hydrochloric acid (0.30 M, 100 mL) and extracted with

dichloromethane (3×100 mL). The aqueous phase was then basified with aqueous sodium hydroxide solution (2.0 M, pH adjusted to 8) and extracted with ethyl acetate (3×100 mL). The first organic extracts were concentrated *in vacuo* and the resulting solid was carried through the above procedure three more times. All ethyl acetate extracts were combined, dried (MgSO_4) and concentrated *in vacuo* to give the desired compound **211** (0.50 g, 1.5 mmol, 18%) as a yellow thick oil; ^1H NMR (300 MHz, CDCl_3): δ = 1.91-2.03 (m, 2 H; 4'-H), 2.28 (s, 3 H; CH_3), 2.40 (t, $^3J(\text{H,H}) = 7.8$ Hz, 2 H; 3'-H), 3.73 (s, 3 H; 4''- OCH_3), 3.76 (t, $^3J(\text{H,H}) = 6.9$ Hz, 2 H; 5'-H), 3.80 (s, 3 H; OCH_3), 6.69 (d, $^3J(\text{H,H}) = 8.1$ Hz, 1 H; Ar-3-H), 6.84-6.91 (m, AA' part of the AA'XX' system, 2 H; Ar-3''-H), 7.14 (ddq, $^3J(\text{H,H}) = 8.1$ Hz, $^4J(\text{H,H}) = 2.2$ Hz, $^4J(\text{H,H}) = 0.6$ Hz, 1 H; Ar-4-H), 7.62-7.65 (m, 1 H; Ar-6-H), 7.65-7.71 ppm (m, XX' part of the AA'XX' system, 2 H; Ar-2''-H); ^{13}C NMR (75.5 MHz, CDCl_3): δ = 19.4 ($\text{C}4'$), 20.2 (CH_3), 28.6 ($\text{C}3'$), 50.7 ($\text{C}5'$), 51.3 (4''- OCH_3), 55.0 (OCH_3), 113.5 ($\text{C}3''$), 121.8 ($\text{C}1$), 122.0 ($\text{C}2''$), 123.0 ($\text{C}3$), 130.4 ($\text{C}5$), 130.6 ($\text{C}6$), 133.1 ($\text{C}4$), 134.5 ($\text{C}1''$), 150.6 ($\text{C}2$), 155.2 ($\text{C}4''$), 159.5 ($\text{C}2'$), 167.4 ppm ($\text{C}=\text{O}$); IR (Nujol): ν_{max} = 1680 (s), 1668 (s), 1600 (m), 1239 (m), 1094 (m), 833 (m), 725 cm^{-1} (m) (Ar-H); LRMS (ES^+): m/z (%): 339 (100) $[\text{M}+\text{H}]^+$; HRMS (ES^+): m/z calc'd for $\text{C}_{20}\text{H}_{23}\text{N}_2\text{O}_3$ $[\text{M}+\text{H}]^+$: 339.1709; found: 339.1702.

7.7.2. Preparation of 1-(4-methoxyphenyl)-6-methyl-2,3,4,9-tetrahydro-1H-pyrrolo[2,3-b]quinolin-4-one (212)

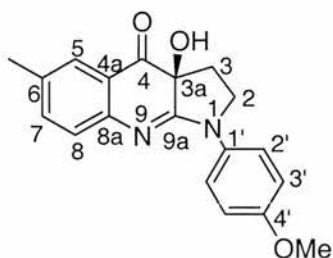


A solution of amidine **211** (0.39 g, 1.2 mmol, 1.0 equiv) in anhydrous THF (40 mL) was cooled to -78 $^{\circ}\text{C}$ and stirred for 15 minutes. Lithium bis(trimethylsilyl)amide (1.0 M in THF, 3.5 mL, 3.5 mmol, 3.0 equiv) was added dropwise to the reaction mixture, which was warmed to 0 $^{\circ}\text{C}$ over 3 hours and quenched at 0 $^{\circ}\text{C}$ with saturated aqueous ammonium chloride (5.0 mL). Further saturated aqueous

ammonium chloride (150 mL) was added. The aqueous phase was extracted with dichloromethane (3×100 mL) and the combined organic extracts dried (MgSO_4) and concentrated *in vacuo* to give a brown solid. Purification by flash column chromatography on silica gel (eluting with 100% ethyl acetate), gave the desired compound **212** (0.31 g, 1.0 mmol, 85%) as a yellow solid; mp 252-253 °C; ^1H NMR (300 MHz, D_8 -THF): δ =2.40 (s, 3 H; CH_3), 3.16 (t, $^3J(\text{H,H}) = 8.2$ Hz, 2 H; 3- $\underline{\text{H}}$), 3.74 (s, 3 H; 4'- OCH_3), 4.00 (t, $^3J(\text{H,H}) = 8.2$ Hz, 2 H; 2- $\underline{\text{H}}$), 6.84-6.92 (m, AA' part of the AA'XX' system, 2 H; Ar-3'- $\underline{\text{H}}$), 7.21 (dd, $^3J(\text{H,H}) = 8.4$ Hz, $^4J(\text{H,H}) = 1.9$ Hz, 1 H; Ar-7- $\underline{\text{H}}$), 7.46 (d, $^3J(\text{H,H}) = 8.4$ Hz, 1 H; Ar-8- $\underline{\text{H}}$), 7.79 (br s, 1 H; Ar-5- $\underline{\text{H}}$), 7.85-7.94 ppm (m, XX' part of the AA'XX' system, 2 H; Ar-2'- $\underline{\text{H}}$); ^{13}C NMR (75.5 MHz, D_8 -THF)*: δ =21.3 (CH_3), 22.5 (C3), 49.9 (C2), 55.0 (4'- OCH_3), 105.6 (C3a), 113.9 ($\text{C3}'$), 120.0 ($\text{C2}'$, C4a), 121.4 (C5), 125.4 (C8), 130.3 (C7), 130.8 (C6), 136.4 ($\text{C1}'$), 146.9 (C8a), 155.0 ($\text{C4}'$), 157.9 (C9a), 159.3 ppm (C4); IR (Nujol): ν_{max} =1629 (m), 1577 (m), 1241 (w), 1169 (w), 828 (m), 722 cm^{-1} (w) (Ar-H); LRMS (CI^+): m/z (%): 335 (10), 307 (100) $[\text{M}+\text{H}]^+$, 292 (19); HRMS (CI^+): m/z calc'd for $\text{C}_{19}\text{H}_{19}\text{N}_2\text{O}_2$ $[\text{M}+\text{H}]^+$: 307.1447; found: 307.1442.

*The assignment of ^{13}C signals was made by using Pendant, HMBC and HSQC NMR analysis.

7.7.3. Preparation of *S*-3a-hydroxy-1-(4-methoxyphenyl)-6-methyl-2,3,3a,4-tetrahydro-1*H*-pyrrolo[2,3-*b*]quinolin-4-one (206)

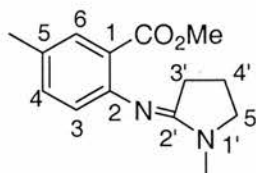


A solution of quinolone **212** (0.25 g, 0.82 mmol, 1.0 equiv) in dry THF (60 mL) was added dropwise to lithium bis(trimethylsilyl)amide (1.0 M in THF, 0.98 mL, 0.98 mmol, 1.2 equiv) in dry THF (5.0 mL) at -78 °C under argon. The reaction mixture was stirred for 30 minutes at -78 °C and a solution of dihalo oxaziridine **82** (0.59 g, 1.9 mmol, 2.4 equiv) in dry THF (10 mL) was added via a cannula. After 16

hours at $-10\text{ }^{\circ}\text{C}$ saturated aqueous ammonium iodide (5.0 mL, 10 equiv) and diethyl ether (5.0 mL) were added and the reaction gradually warmed to room temperature. Saturated aqueous sodium thiosulfate (15 mL) was then added and the reaction extracted with diethyl ether ($2 \times 10\text{ mL}$). The combined organic extracts were dried (MgSO_4) and concentrated *in vacuo* to give a yellow solid. The solid was partitioned between dichloromethane (100 mL) and aqueous hydrochloric acid solution (0.30 M, 100 mL). The aqueous phase was washed with dichloromethane ($3 \times 100\text{ mL}$), basified with aqueous sodium hydroxide solution (2.0 M, pH adjusted to 8) and extracted with ethyl acetate ($2 \times 100\text{ mL}$). The organic extracts were dried (MgSO_4) and concentrated *in vacuo* to give **206** (0.24 g, 0.74 mmol, 90%) as a bright yellow solid. The enantiomeric excess of **206** was 82% as determined by chiral-phase HPLC analysis; mp $217\text{--}218\text{ }^{\circ}\text{C}$; $[\alpha]_{\text{D}}^{25} = -460$ ($c=0.08$ in chloroform); $^1\text{H NMR}$ (300 MHz, $\text{D}_8\text{-THF}$): $\delta = 2.16\text{--}2.30$ (m, 5 H; 3-H, CH_3), 3.76 (s, 3 H; 4'- OCH_3), 3.81-3.92 (m, 1 H; 2-H), 4.01-4.15 (m, 1 H; 2-H), 5.82 (s, 1 H; OH), 6.86-6.94 (m, AA' part of the AA'XX' system, 2 H; Ar-3'-H), 7.08 (d, $^3J(\text{H,H}) = 8.1\text{ Hz}$, 1 H; Ar-8-H), 7.25 (dd, $^3J(\text{H,H}) = 8.1\text{ Hz}$, $^4J(\text{H,H}) = 2.2\text{ Hz}$, 1 H; Ar-7-H), 7.56 (br s, 1 H; Ar-5-H), 7.97-8.04 ppm (m, XX' part of the AA'XX' system, 2 H; Ar-2'-H); $^{13}\text{C NMR}$ (75.5 MHz, $\text{D}_8\text{-THF}$): $\delta = 20.5$ (CH_3), 29.8 (C_3), 48.5 (C_2), 55.3 ($\text{C}_4\text{'-OCH}_3$), 73.9 ($\text{C}_{3\text{a}}$), 114.1 ($\text{C}_{3\text{'}}$), 121.6 ($\text{C}_{2\text{'}}$), 122.1 ($\text{C}_{4\text{a}}$), 126.6 (C_8), 127.1 (C_5), 132.6 (C_6), 135.2 ($\text{C}_{1\text{'}}$), 136.5 (C_7), 150.7 ($\text{C}_{8\text{a}}$), 156.8 ($\text{C}_{4\text{'}}$), 165.9 ($\text{C}_{9\text{a}}$), 195.0 ppm (C_4); IR (Nujol): $\nu_{\text{max}} = 1690$ (m), 1623 (m), 1596 (m), 1293 (w), 831 (w), 735 cm^{-1} (w) (Ar-H); LRMS (CI^+): m/z (%): 323 (94) $[\text{M}+\text{H}]^+$, 322 (100) $[\text{M}^+]$, 305 (52), 266 (18); HRMS (CI^+): m/z calc'd for $\text{C}_{19}\text{H}_{19}\text{N}_2\text{O}_3$ $[\text{M}+\text{H}]^+$: 323.1396; found: 323.1396; Anal. calc'd for $\text{C}_{19}\text{H}_{18}\text{N}_2\text{O}_3$: C, 70.79; H, 5.63; N, 8.69; found: C, 70.62; H, 5.92; N, 8.77; HPLC (Daicel Chiralpak AD, acetonitrile/water 50:50, flow rate 0.8 mL min^{-1} , $\lambda = 254\text{ nm}$): major enantiomer: $t_{\text{R}} = 6.13\text{ min.}$, and minor enantiomer: $t_{\text{R}} = 8.43\text{ min.}$

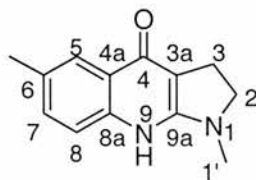
An analytical sample of **206** was prepared by recrystallisation from acetonitrile; $[\alpha]_{\text{D}}^{25} = -513$ ($c=0.1$ in chloroform); Chiral HPLC analysis showed that after a single recrystallisation, **206** was prepared with an *ee* of $>99\%$.

7.7.4. Preparation of methyl 5-methyl-2-(1-methylpyrrolidin-2-ylideneamino)benzoate (**54**)



Phosphorus oxychloride (0.74 g, 0.45 mL, 4.8 mmol, 1.0 equiv) was added dropwise to a solution of 1-methyl-2-pyrrolidinone (**39**) (0.53 g, 5.3 mmol, 1.1 equiv) in dry dichloromethane (5.0 mL) and the reaction was stirred for 3 hours at room temperature. A solution of anthranilate **27** (0.80 g, 4.8 mmol, 1.0 equiv) in dry dichloromethane (17 mL) was then added and the reaction refluxed for 16 hours. The reaction mixture was cooled and concentrated *in vacuo*. The resulting solid was dissolved in aqueous hydrochloric acid (0.30 M, 100 mL) and extracted with dichloromethane (3 × 100 mL). The aqueous phase was then basified with aqueous sodium hydroxide solution (2.0 M, pH adjusted to 8) and extracted with ethyl acetate (3 × 100 mL). The first organic extracts were concentrated *in vacuo* and the resulting solid was carried through the above procedure one more time. All ethyl acetate extracts were combined, dried (MgSO₄) and concentrated *in vacuo* to give the desired compound **54** (0.94 g, 3.8 mmol, 79%) as a brown thick oil; ¹H NMR (300 MHz, CDCl₃): δ = 1.64–1.76 (m, 2 H; 4'-H), 2.02 (t, ³J(H,H) = 7.8 Hz, 2 H; 3'-H), 2.09 (s, 3 H; CH₃), 2.78 (s, 3 H; N-CH₃), 3.17 (t, ³J(H,H) = 6.9 Hz, 2 H; 5'-H), 3.59 (s, 3 H; OCH₃), 6.54 (d, ³J(H,H) = 8.1 Hz, 1 H; Ar-3-H), 6.96 (ddq, ³J(H,H) = 8.1 Hz, ⁴J(H,H) = 2.2 Hz, ⁴J(H,H) = 0.6 Hz, 1 H; Ar-4-H), 7.40–7.42 ppm (m, 1 H; Ar-6-H); ¹³C NMR (75.5 MHz, CDCl₃): δ = 19.1 (C4'), 20.0 (CH₃), 27.1 (C3'), 30.8 (N-CH₃), 50.8 (C5'), 50.9 (OCH₃), 122.0 (C1), 123.8 (C3), 129.9 (C5), 130.2 (C6), 132.7 (C4), 150.9 (C2), 161.8 (C2'), 167.1 ppm (C=O); IR (Nujol): ν_{max} = 1728 (s) (C=O), 1667 (s) (C=N), 1289 (s), 1200 (s), 1080 (m), 834 (m), 722 cm⁻¹ (m); LRMS (ES⁺): *m/z* (%): 247 (100) [M+H]⁺, 215 (20) [M-OMe]⁺; HRMS (ES⁺): *m/z* calc'd for C₁₄H₁₉N₂O₂ [M+H]⁺: 247.1447; found: 247.1447.

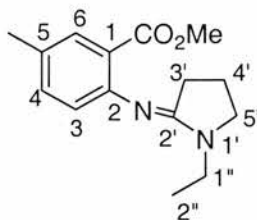
7.7.5. Attempted preparation of 1,6-dimethyl-2,3,4,9-tetrahydro-1*H*-pyrrolo[2,3-*b*]quinolin-4-one (62)



A solution of amidine **54** (0.25 g, 1.0 mmol, 1.0 equiv) in anhydrous THF (30 mL) was cooled to $-78\text{ }^{\circ}\text{C}$ and stirred for 15 minutes. Lithium bis(trimethylsilyl)amide (1.0 M in THF, 2.0 mL, 2.0 mmol, 2.0 equiv) was added dropwise to the reaction mixture which was warmed to $-40\text{ }^{\circ}\text{C}$ for 16 hours and quenched at $-40\text{ }^{\circ}\text{C}$ with saturated aqueous ammonium chloride (5.0 mL). Further saturated aqueous ammonium chloride (150 mL) was added. The aqueous phase was extracted with dichloromethane ($3 \times 100\text{ mL}$) and the combined organic extracts dried (MgSO_4) and concentrated *in vacuo* to give a brown oil. Purification by flash column chromatography on silica gel (eluting with 100% ethyl acetate) yielded three fractions:

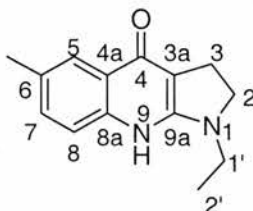
- fraction 1 (0.037 g) was a yellow oil, m/z (%) (ES^+): 475 (100) $[\text{M}+\text{H}]^+$, HRMS (ES^+): m/z calc'd for $\text{C}_{27}\text{H}_{31}\text{N}_4\text{O}_4$ $[\text{M}+\text{H}]^+$: 475.2345; found: 475.2332.
- fraction 2 (0.045 g) was a brown oil, m/z (%): 475 (100) $[\text{M}+\text{H}]^+$, 497 (24), 473 (14).
- fraction 3 was a brown oil, ^1H NMR and mass spectrum consistent with unreacted starting material **54**.

7.7.6. Preparation of methyl 5-methyl-2-(1-ethylpyrrolidin-2-ylideneamino)benzoate (**55**)



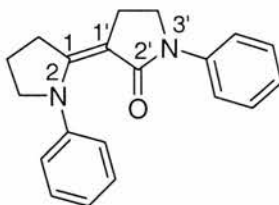
Phosphorus oxychloride (0.74 g, 0.45 mL, 4.8 mmol, 1.0 equiv) was added dropwise to a solution of 1-ethyl-2-pyrrolidinone (**53**) (0.60 g, 5.3 mmol, 1.1 equiv) in dry dichloromethane (5.0 mL) and the reaction was stirred for 3 hours at room temperature. A solution of anthranilate **27** (0.80 g, 4.8 mmol, 1.0 equiv) in dry dichloromethane (17 mL) was then added and the reaction refluxed for 16 hours. The reaction mixture was cooled concentrated *in vacuo*. The resulting solid was dissolved in aqueous hydrochloric acid (0.30 M, 100 mL) and extracted with dichloromethane (3 × 100 mL). The aqueous phase was then basified with aqueous sodium hydroxide solution (2.0 M, pH adjusted to 8) and extracted with ethyl acetate (3 × 100 mL). The first organic extracts were concentrated *in vacuo* and the resulting solid was carried through the above procedure one more time. All ethyl acetate extracts were combined, dried (MgSO₄) and concentrated *in vacuo* to give the desired compound **55** (0.40 g, 1.5 mmol, 31%) as a brown thick oil; ¹H NMR (300 MHz, CDCl₃): δ = 1.07 (t, ³J(H,H) = 7.2 Hz, 3 H; 2''-H), 1.69-1.82 (m, 2 H; 4'-H), 2.08 (t, ³J(H,H) = 7.8 Hz, 2 H; 3'-H), 2.15 (s, 3 H; CH₃), 3.24 (t, ³J(H,H) = 6.9 Hz, 2 H; 5'-H), 3.33 (q, ³J(H,H) = 7.2 Hz, 2 H; 1'-H), 3.65 (s, 3 H; OCH₃), 6.58 (d, ³J(H,H) = 8.0 Hz, 1 H; Ar-3-H), 7.01 (dd, ³J(H,H) = 8.0 Hz, ⁴J(H,H) = 1.8 Hz, 1 H; Ar-4-H), 7.45 ppm (br d, ⁴J(H,H) = 1.8 Hz, 1 H; Ar-6-H); ¹³C NMR (75.5 MHz, CDCl₃): δ = 11.5 (C2''), 19.4 (C4'), 20.1 (CH₃), 27.5 (C3'), 38.1 (C1''), 48.0 (C5'), 51.1 (OCH₃), 122.3 (C1), 123.9 (C3), 130.0 (C5), 130.4 (C6), 132.8 (C4), 151.1 (C2), 160.9 (C2'), 167.5 ppm (C=O); IR (Nujol): ν_{max}=1727 (s) (C=O), 1663 (s) (C=N), 1286 (s), 1198 (s), 1080 (m), 834 (m), 788 (m), 738 cm⁻¹ (m); LRMS (ES⁺): *m/z* (%): 261 (100) [M+H]⁺, 229 (10) [M-OMe]⁺; HRMS (ES⁺): *m/z* calc'd for C₁₅H₂₁N₂O₂ [M+H]⁺: 261.1603; found: 261.1594.

7.7.7. Attempted synthesis of 1-ethyl-6-methyl-2,3,4,9-tetrahydro-1*H*-pyrrolo[2,3-*b*]quinolin-4-one (63)



A solution of amidine **55** (0.15 g, 0.58 mmol, 1.0 equiv) in anhydrous THF (20 mL) was cooled to $-78\text{ }^{\circ}\text{C}$ and stirred for 15 minutes. Lithium bis(trimethylsilyl)amide (1.0 M in THF, 1.2 mL, 1.2 mmol, 2.0 equiv) was added dropwise to the reaction mixture which was warmed to $-40\text{ }^{\circ}\text{C}$ for 16 hours and quenched at $-40\text{ }^{\circ}\text{C}$ with saturated aqueous ammonium chloride (5.0 mL). Further saturated aqueous ammonium chloride (150 mL) was added. The aqueous phase was extracted with dichloromethane ($3 \times 100\text{ mL}$) and the combined organic extracts dried (MgSO_4) and concentrated *in vacuo* to afford a mixture of compounds from which it proved difficult to obtain a pure sample of a single compound.

7.7.8. Isolation of 1,1-diphenyl-[2,3]bipyrrolidinyliden-2-one (**52**)⁴⁵



Phosphorus oxychloride (2.6 mL, 4.2 g, 27 mmol, 11 equiv) was added dropwise to a solution of 1-phenyl-2-pyrrolidinone (**28**) (0.40 g, 2.5 mmol, 1.0 equiv) in dry dichloromethane (10 mL) and the reaction was stirred for 48 hours at room temperature. A solution of anthranilate **27** (0.25 g, 1.5 mmol, 0.60 equiv) in dry dichloromethane (1.0 mL) and a solution of diisopropylethylamine (4.3 mL, 3.2 g, 25 mmol, 10 equiv) were then added and the reaction refluxed for 16 hours. The reaction mixture was cooled, diluted with aqueous hydrochloric acid (0.30 M, 100 mL) and extracted with dichloromethane ($3 \times 100\text{ mL}$). The aqueous phase was then basified with aqueous

sodium hydroxide solution (2.0 M, pH adjusted to 8) and extracted with ethyl acetate (3 × 100 mL). The combined organic extracts were then dried (MgSO₄) and concentrated *in vacuo* to afford a crude brown solid. Purification by flash column chromatography on silica gel (eluting with 20% ethyl acetate/hexane) gave **52** (0.076 g, 0.25 mmol, 10%) as a white crystalline solid; mp 129-130 °C (lit.^{4,5} 129 °C); ¹H NMR (300 MHz, CDCl₃): δ = 2.01-2.15 (m, 4 H; 2 × CH₂), 3.37 (t, ³J(H,H) = 7.6 Hz, 2 H; CH₂), 3.59 (t, ³J(H,H) = 7.0 Hz, 2 H; CH₂), 3.76 (t, ³J(H,H) = 7.0 Hz, 2 H; CH₂), 7.00-7.18 (m, 4 H; Ar-H), 7.28-7.38 (m, 4 H; Ar-H), 7.59-7.65 ppm (m, 2 H; Ar-H); LRMS (Cl⁺): *m/z* (%): 305 (100) [M+H]⁺.

7.8. REFERENCES

- 1 Smith; L. And Merits, I., *Kgl. Fysiograf. Sällskap Lund, Förh.* **1953**, 23, 88-91.
[*Chem. Abstr.* **1955**, 15857 g]
- 2 Cai, S. X., Zhou, Z-L., Huang, J-C., Whittemore, E. R., Egbuwoku, Z. O., Lu, Y., Hawkinson, J. E., Woodward, R. M., Weber, E., Keana, J. F. W., *J. Med. Chem.*, **1996**, 39, 3248-3255.
- 3 Niculescu-Duvaz, I., Ionescu, M., Cambanis, A., Vitan, M., Feyns, V., *J. Med. Chem.*, **1968**, 11, 500-503.
- 4 Buchel, K. H., Bocz, A. K., Korte, F., *Chem. Ber.*, **1966**, 99, 724-735.
- 5 Eilingsfeld, H., Seefelder, M., Weidinger, H., *Angew. Chem.*, **1960**, 22, 836-845.

APPENDIX

APPENDIX

1. CRYSTALLOGRAPHIC DATA

1.1. X-Ray data of methyl 5-methyl-2-(1-phenylpyrrolidin-2-ylideneamino)benzoate (29)

Crystal data and structure refinement for clnw15.

Identification code	clnw15	
Empirical formula	C ₁₉ H ₂₀ N ₂ O ₂	
Formula weight	308.37	
Temperature	93(2) K	
Wavelength	0.71073 Å	
Crystal system	Orthorhombic	
Space group	P2(1)2(1)2(1)	
Unit cell dimensions	a = 10.4659(16) Å	α = 90°.
	b = 11.374(2) Å	β = 90°.
	c = 13.026(3) Å	γ = 90°.
Volume	1550.6(5) Å ³	
Z	4	
Density (calculated)	1.321 Mg/m ³	
Absorption coefficient	0.086 mm ⁻¹	
F(000)	656	
Crystal size	0.3000 x 0.3000 x 0.1000 mm ³	
Theta range for data collection	2.50 to 25.35°.	
Index ranges	-10 ≤ h ≤ 12, -13 ≤ k ≤ 8, -14 ≤ l ≤ 15	
Reflections collected	9513	
Independent reflections	2769 [R(int) = 0.0183]	
Completeness to theta = 25.35°	97.4 %	
Absorption correction	MULTISCAN	
Max. and min. transmission	1.0000 and 0.6025	
Refinement method	Full-matrix least-squares on F ²	
Data / restraints / parameters	2769 / 0 / 211	
Goodness-of-fit on F ²	1.033	
Final R indices [I > 2σ(I)]	R1 = 0.0252, wR2 = 0.0646	
R indices (all data)	R1 = 0.0259, wR2 = 0.0649	
Absolute structure parameter	1.2(8)	

Extinction coefficient	0.017(4)
Largest diff. peak and hole	0.132 and -0.146 e.Å ⁻³

1.2. X-Ray data of *S*-3a-hydroxy-6-methyl-1-phenyl-2,3,3a,4-tetrahydro-1*H*-pyrrolo[2,3-*b*]quinolin-4-one (7) ((*S*)-(-)-blebbistatin)

Crystal data and structure refinement for clnw14.

Identification code	clnw14	
Empirical formula	C18 H16 N2 O2	
Formula weight	292.33	
Temperature	93(2) K	
Wavelength	1.54178 Å	
Crystal system	Monoclinic	
Space group	P2(1)	
Unit cell dimensions	a = 5.8412(5) Å	α = 90°.
	b = 19.9242(16) Å	β = 94.228(6)°.
	c = 6.1298(5) Å	γ = 90°.
Volume	711.45(10) Å ³	
Z	2	
Density (calculated)	1.365 Mg/m ³	
Absorption coefficient	0.726 mm ⁻¹	
F(000)	308	
Crystal size	0.15 x 0.15 x 0.15 mm ³	
Theta range for data collection	7.24 to 70.46°.	
Index ranges	-6 ≤ h ≤ 7, -24 ≤ k ≤ 23, -7 ≤ l ≤ 7	
Reflections collected	6343	
Independent reflections	2046 [R(int) = 0.0254]	
Completeness to theta = 70.46°	85.0 %	
Absorption correction	MULTISCAN	
Max. and min. transmission	1.0000 and 0.505259	
Refinement method	Full-matrix least-squares on F ²	
Data / restraints / parameters	2046 / 2 / 204	
Goodness-of-fit on F ²	1.063	
Final R indices [I > 2σ(I)]	R1 = 0.0577, wR2 = 0.1437	
R indices (all data)	R1 = 0.0578, wR2 = 0.1438	
Absolute structure parameter	0.1(3)	
Largest diff. peak and hole	0.302 and -0.397 e.Å ⁻³	

1.3. X-Ray data of *S*-1-(4-bromophenyl)-3a-hydroxy-6-methyl-2,3,3a,4-tetrahydro-1*H*-pyrrolo[2,3-*b*]quinolin-4-one (135)

Crystal data and structure refinement for clnw13.

Identification code	clnw13	
Empirical formula	C ₁₈ H ₁₅ Br N ₂ O ₂	
Formula weight	371.23	
Temperature	93(2) K	
Wavelength	0.71073 Å	
Crystal system	Orthorhombic	
Space group	P2(1)2(1)2(1)	
Unit cell dimensions	a = 5.6627(11) Å	α = 90°.
	b = 11.588(2) Å	β = 90°.
	c = 23.364(5) Å	γ = 90°.
Volume	1533.1(5) Å ³	
Z	4	
Density (calculated)	1.608 Mg/m ³	
Absorption coefficient	2.693 mm ⁻¹	
F(000)	752	
Crystal size	0.2000 x 0.0100 x 0.0100 mm ³	
Theta range for data collection	2.48 to 26.37°.	
Index ranges	-5 ≤ h ≤ 6, -14 ≤ k ≤ 14, -29 ≤ l ≤ 29	
Reflections collected	17140	
Independent reflections	2899 [R(int) = 0.1326]	
Completeness to theta = 26.37°	92.9 %	
Absorption correction	MULTISCAN	
Max. and min. transmission	1.0000 and 0.2554	
Refinement method	Full-matrix least-squares on F ²	
Data / restraints / parameters	2899 / 1 / 213	
Goodness-of-fit on F ²	1.059	
Final R indices [I > 2σ(I)]	R1 = 0.0766, wR2 = 0.1552	
R indices (all data)	R1 = 0.1095, wR2 = 0.1725	
Absolute structure parameter	-0.01(2)	
Largest diff. peak and hole	0.848 and -0.752 e.Å ⁻³	

1.4. X-Ray data of *S*-3a-hydroxy-1-phenyl-2,3,3a,4-tetrahydro-1*H*-pyrrolo[2,3-*b*]quinolin-4-one (67)

Crystal data and structure refinement for clnw1 (yellow crystal).

Identification code	clnw1	
Empirical formula	C ₁₇ H ₁₄ N ₂ O ₂	
Formula weight	278.30	
Temperature	125(2) K	
Wavelength	0.71073 Å	
Crystal system	Orthorhombic	
Space group	P2(1)2(1)2(1)	
Unit cell dimensions	a = 4.9441(10) Å	α = 90°.
	b = 12.336(3) Å	β = 90°.
	c = 21.448(4) Å	γ = 90°.
Volume	1308.1(5) Å ³	
Z	4	
Density (calculated)	1.413 Mg/m ³	
Absorption coefficient	0.094 mm ⁻¹	
F(000)	584	
Crystal size	.18 x .08 x .05 mm ³	
Theta range for data collection	1.90 to 23.25°.	
Index ranges	-5 ≤ h ≤ 5, -13 ≤ k ≤ 12, -23 ≤ l ≤ 23	
Reflections collected	6931	
Independent reflections	1832 [R(int) = 0.1223]	
Completeness to theta = 23.25°	98.7 %	
Absorption correction	Sadabs	
Max. and min. transmission	1.00000 and 0.610493	
Refinement method	Full-matrix least-squares on F ²	
Data / restraints / parameters	1832 / 1 / 195	
Goodness-of-fit on F ²	0.610	
Final R indices [I > 2σ(I)]	R1 = 0.0429, wR2 = 0.1044	
R indices (all data)	R1 = 0.0684, wR2 = 0.1234	
Absolute structure parameter	2(3)	
Extinction coefficient	0.033(5)	
Largest diff. peak and hole	0.195 and -0.184 e.Å ⁻³	

Crystal data and structure refinement for clnw3 (green crystal).

Identification code	clnw3	
Empirical formula	C17 H14 N2 O2	
Formula weight	278.30	
Temperature	125(2) K	
Wavelength	0.71073 Å	
Crystal system	Triclinic	
Space group	P1	
Unit cell dimensions	a = 5.86(4) Å	$\alpha = 94.68(5)^\circ$.
	b = 6.01(4) Å	$\beta = 91.72(6)^\circ$.
	c = 9.52(6) Å	$\gamma = 96.95(4)^\circ$.
Volume	331(4) Å ³	
Z	1	
Density (calculated)	1.395 Mg/m ³	
Absorption coefficient	0.093 mm ⁻¹	
F(000)	146	
Crystal size	.2 x .1 x .1 mm ³	
Theta range for data collection	2.15 to 23.80°.	
Index ranges	-6<=h<=6, -6<=k<=6, -8<=l<=10	
Reflections collected	1552	
Independent reflections	1296 [R(int) = 0.0826]	
Completeness to theta = 23.80°	92.4 %	
Absorption correction	MULTISCAN	
Max. and min. transmission	1.00000 and 0.450656	
Refinement method	Full-matrix least-squares on F ²	
Data / restraints / parameters	1296 / 4 / 195	
Goodness-of-fit on F ²	1.008	
Final R indices [I>2sigma(I)]	R1 = 0.0387, wR2 = 0.0789	
R indices (all data)	R1 = 0.0476, wR2 = 0.0829	
Absolute structure parameter	0.1(19)	
Extinction coefficient	0.20(2)	
Largest diff. peak and hole	0.218 and -0.203 e.Å ⁻³	

1.5. X-Ray data of 3a-chloro-6-methyl-1-phenyl-2,3,3a,4-tetrahydro-1H-pyrrolo[2,3-b]quinolin-4-one (162)

Crystal data and structure refinement for clnw5.

Identification code	clnw5	
Empirical formula	C ₁₈ H ₁₅ Cl N ₂ O	
Formula weight	310.77	
Temperature	125(2) K	
Wavelength	0.71073 Å	
Crystal system	Orthorhombic	
Space group	Pbca	
Unit cell dimensions	a = 12.444(3) Å	α = 90°.
	b = 10.136(2) Å	β = 90°.
	c = 22.962(5) Å	γ = 90°.
Volume	2896.2(11) Å ³	
Z	8	
Density (calculated)	1.425 Mg/m ³	
Absorption coefficient	0.267 mm ⁻¹	
F(000)	1296	
Crystal size	.1 x .1 x .02 mm ³	
Theta range for data collection	2.41 to 25.39°.	
Index ranges	-13 ≤ h ≤ 14, -12 ≤ k ≤ 12, -27 ≤ l ≤ 25	
Reflections collected	15873	
Independent reflections	2613 [R(int) = 0.0954]	
Completeness to theta = 25.39°	97.9 %	
Absorption correction	Multiscan	
Max. and min. transmission	1.00000 and 0.661650	
Refinement method	Full-matrix least-squares on F ²	
Data / restraints / parameters	2613 / 0 / 201	
Goodness-of-fit on F ²	0.892	
Final R indices [I > 2σ(I)]	R1 = 0.0406, wR2 = 0.0755	
R indices (all data)	R1 = 0.0791, wR2 = 0.0839	
Extinction coefficient	0.00051(12)	
Largest diff. peak and hole	0.248 and -0.212 e.Å ⁻³	

1.6. X-Ray data of *S*-3a-(4-bromobenzoyloxy)-1-phenyl-2,3,3a,4-tetrahydro-1*H*-pyrrolo[2,3-*b*]quinolin-4-one (176)

Crystal data and structure refinement for CLNW17.

Identification code	clnw17	
Empirical formula	C ₂₅ H ₁₉ Br N ₂ O ₃	
Formula weight	475.33	
Temperature	93(2) K	
Wavelength	0.71073 Å	
Crystal system	Monoclinic	
Space group	P2(1)	
Unit cell dimensions	a = 10.784(3) Å	α = 90°.
	b = 6.7081(18) Å	β = 103.914(7)°.
	c = 14.814(4) Å	γ = 90°.
Volume	1040.2(5) Å ³	
Z	2	
Density (calculated)	1.518 Mg/m ³	
Absorption coefficient	2.007 mm ⁻¹	
F(000)	484	
Crystal size	0.2000 x 0.0500 x 0.0500 mm ³	
Theta range for data collection	3.03 to 25.34°.	
Index ranges	-12 ≤ h ≤ 12, -8 ≤ k ≤ 6, -14 ≤ l ≤ 17	
Reflections collected	6300	
Independent reflections	3178 [R(int) = 0.0207]	
Completeness to theta = 25.34°	97.3 %	
Absorption correction	Multiscan	
Max. and min. transmission	1.0000 and 0.6601	
Refinement method	Full-matrix least-squares on F ²	
Data / restraints / parameters	3178 / 1 / 282	
Goodness-of-fit on F ²	1.027	
Final R indices [I > 2σ(I)]	R1 = 0.0251, wR2 = 0.0581	
R indices (all data)	R1 = 0.0272, wR2 = 0.0592	
Absolute structure parameter	0.000(6)	
Largest diff. peak and hole	0.406 and -0.289 e.Å ⁻³	

1.7. X-Ray data of (3*aS*, 4*R*)-6-methyl-1-phenyl-2,3,3*a*,4-tetrahydro-1*H*-pyrrolo[2,3-*b*]quinoline-3*a*,4-diol (199)

a) Crystal data and structure refinement for clnw19 (reduction with NaBH₄).

Identification code	clnw19	
Empirical formula	C ₁₈ H ₁₈ N ₂ O ₂	
Formula weight	294.34	
Temperature	93(2) K	
Wavelength	0.71073 Å	
Crystal system	Orthorhombic	
Space group	P2(1)2(1)2(1)	
Unit cell dimensions	a = 5.1364(9) Å	α = 90°.
	b = 13.782(3) Å	β = 90°.
	c = 20.038(5) Å	γ = 90°.
Volume	1418.5(5) Å ³	
Z	4	
Density (calculated)	1.378 Mg/m ³	
Absorption coefficient	0.091 mm ⁻¹	
F(000)	624	
Crystal size	0.2000 x 0.0200 x 0.0200 mm ³	
Theta range for data collection	1.79 to 25.32°.	
Index ranges	-6 ≤ h ≤ 4, -16 ≤ k ≤ 16, -16 ≤ l ≤ 23	
Reflections collected	8761	
Independent reflections	2528 [R(int) = 0.0262]	
Completeness to theta = 25.32°	98.4 %	
Absorption correction	Multiscan	
Max. and min. transmission	1.0000 and 0.4523	
Refinement method	Full-matrix least-squares on F ²	
Data / restraints / parameters	2528 / 2 / 210	
Goodness-of-fit on F ²	1.071	
Final R indices [I > 2σ(I)]	R1 = 0.0340, wR2 = 0.0798	
R indices (all data)	R1 = 0.0377, wR2 = 0.0821	
Absolute structure parameter	-0.7(12)	
Extinction coefficient	0.0062(15)	
Largest diff. peak and hole	0.166 and -0.184 e.Å ⁻³	

b) Crystal data and structure refinement for CLNW20 (reduction with H₂/Pd/C).

Identification code	clnw20	
Empirical formula	C ₁₈ H ₁₈ N ₂ O ₂	
Formula weight	294.34	
Temperature	173(2) K	
Wavelength	1.54178 Å	
Crystal system	Orthorhombic	
Space group	P2(1)2(1)2(1)	
Unit cell dimensions	a = 5.14430(10) Å	α = 90°.
	b = 13.8150(3) Å	β = 90°.
	c = 20.1361(5) Å	γ = 90°.
Volume	1431.04(5) Å ³	
Z	4	
Density (calculated)	1.366 Mg/m ³	
Absorption coefficient	0.722 mm ⁻¹	
F(000)	624	
Crystal size	0.200 x 0.030 x 0.030 mm ³	
Theta range for data collection	3.88 to 67.60°.	
Index ranges	-5<=h<=5, -16<=k<=16, -24<=l<=23	
Reflections collected	18158	
Independent reflections	2417 [R(int) = 0.0733]	
Completeness to theta = 67.60°	94.7 %	
Absorption correction	Multiscan	
Max. and min. transmission	1.0000 and 0.2882	
Refinement method	Full-matrix least-squares on F ²	
Data / restraints / parameters	2417 / 2 / 209	
Goodness-of-fit on F ²	1.029	
Final R indices [I>2sigma(I)]	R1 = 0.0377, wR2 = 0.0880	
R indices (all data)	R1 = 0.0413, wR2 = 0.0900	
Absolute structure parameter	0.0(3)	
Largest diff. peak and hole	0.141 and -0.161 e.Å ⁻³	

2. LC-MASS ANALYSIS

2.1. LC-MASS for (\pm)-3a-hydroxy-6-methyl-1-phenyl-2,3,3a,4-tetrahydro-1H-pyrrolo[2,3-b]quinolin-4-one (**18**) ((\pm)-blebbistatin)

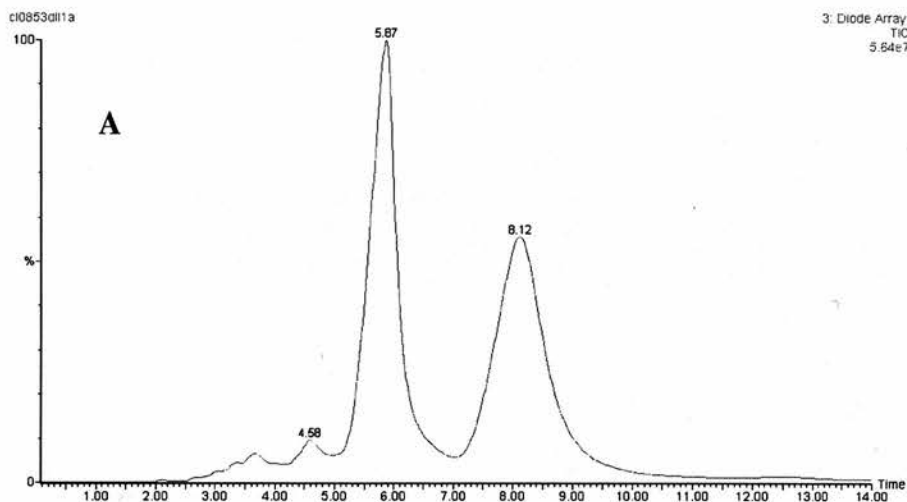
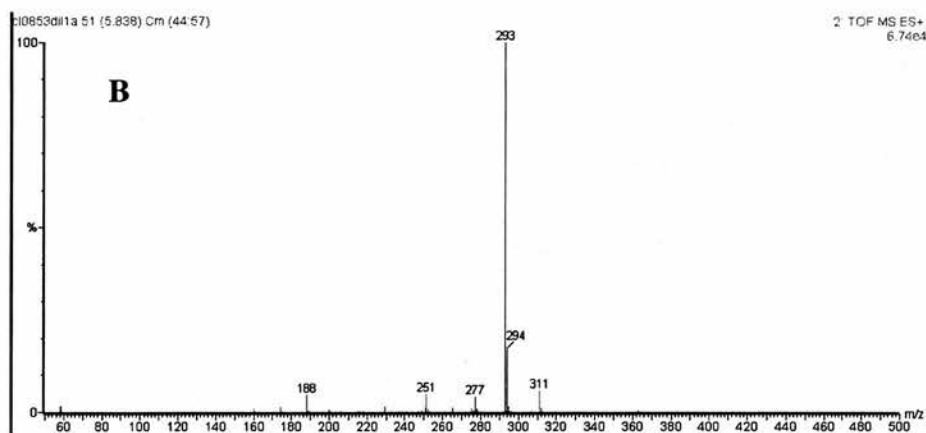


Figure 1. Chiral HPLC analysis. Conditions: Daicel Chiralpak AD-RH, Acetonitrile/Water 50:50, flow rate 0.8 mL min⁻¹, $\lambda=254$ nm. A) Chromatogram of the purified product **18**: first enantiomer $t_R=5.87$ min., $\lambda_{max}=249$ nm and second enantiomer $t_R=8.12$ min., $\lambda_{max}=249$ nm.



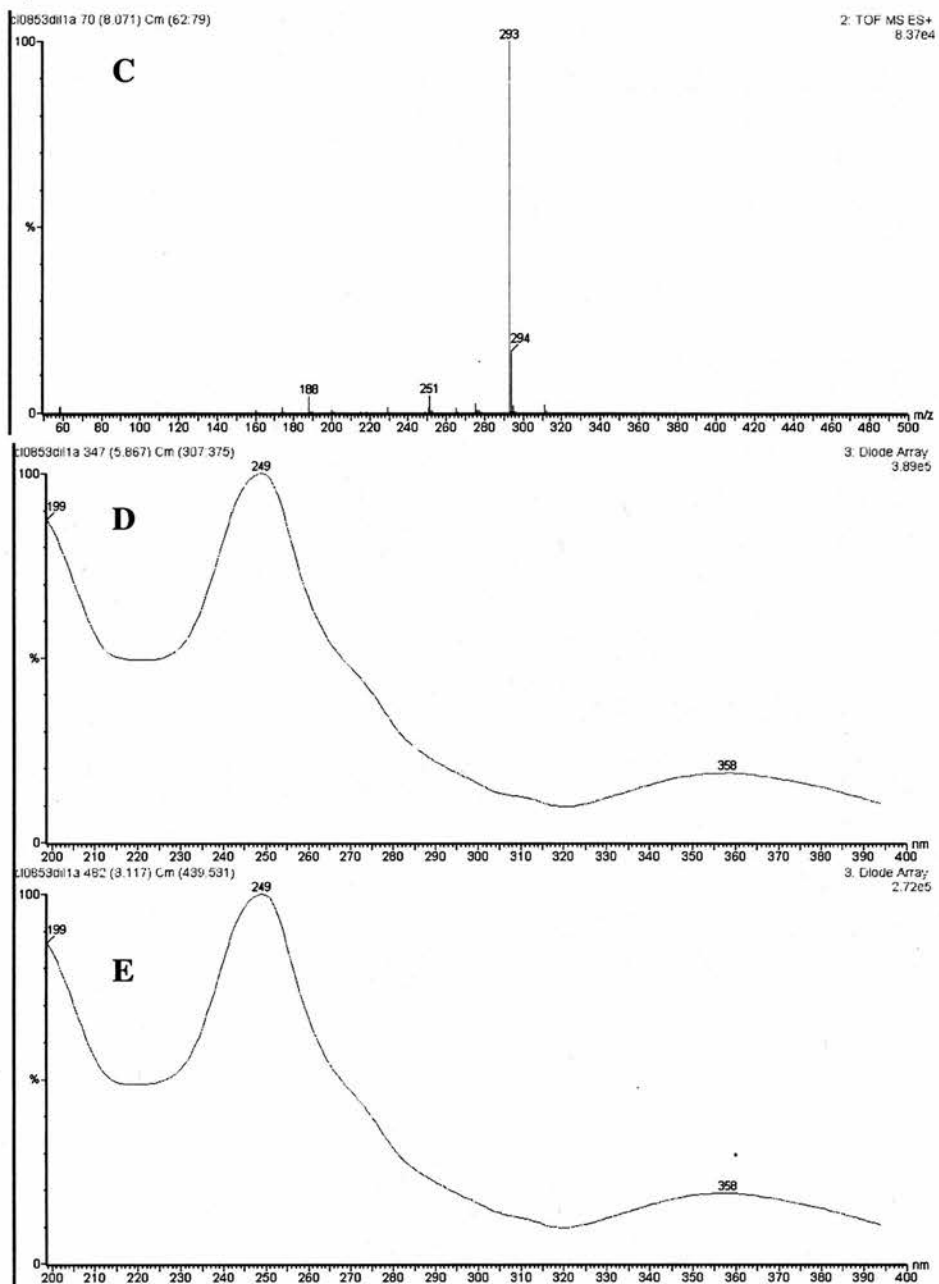


Figure 2. A) UV chromatogram of racemic blebbistatin (**18**). B) ESMS (+ve) of peak $t_R=5.87$ min. $[M+H]^+=293$. C) ESMS (+ve) of peak $t_R=8.12$ min. $[M+H]^+=293$. D) UV-vis spectra of peak $t_R=5.87$ min. max=249 nm. E) UV-vis spectra of peak $t_R=8.12$ min. max=249 nm.

2.2. LC-MASS for *S*-3a-hydroxy-6-methyl-1-phenyl-2,3,3a,4-tetrahydro-1*H*-pyrrolo[2,3-*b*]quinolin-4-one (7) ((*S*)-(-)-blebbistatin)

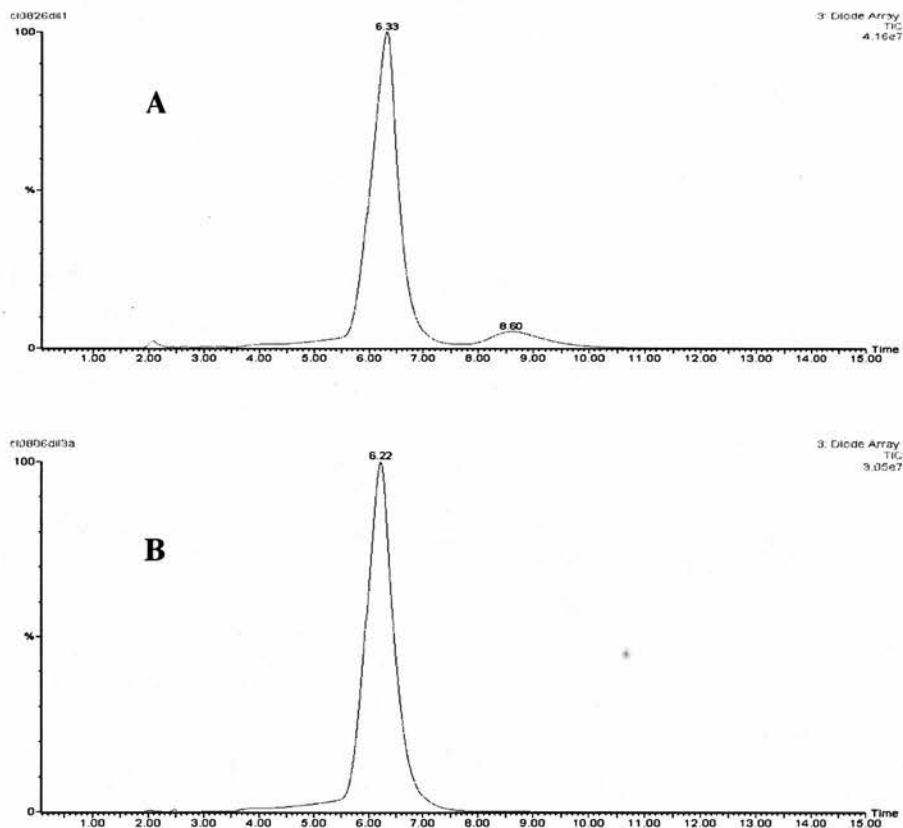
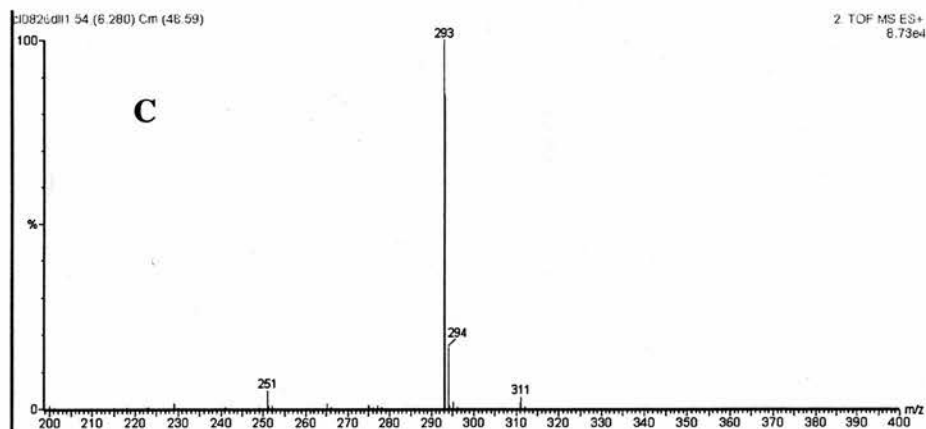


Figure 3. Chiral HPLC analysis. Conditions: Daicel Chiralpak AD-RH, Acetonitrile/Water 50:50, flow rate 0.8 mL min⁻¹, $\lambda=254$ nm. A) Chromatogram of the crude mixture of 7: major enantiomer $t_R=6.33$ min., $\lambda_{max}=249$ nm. and minor enantiomer $t_R=8.60$ min., $\lambda_{max}=249$ nm., B) Chromatogram of crystallised 7: major enantiomer $t_R=6.22$ min., $\lambda_{max}=249$ nm.



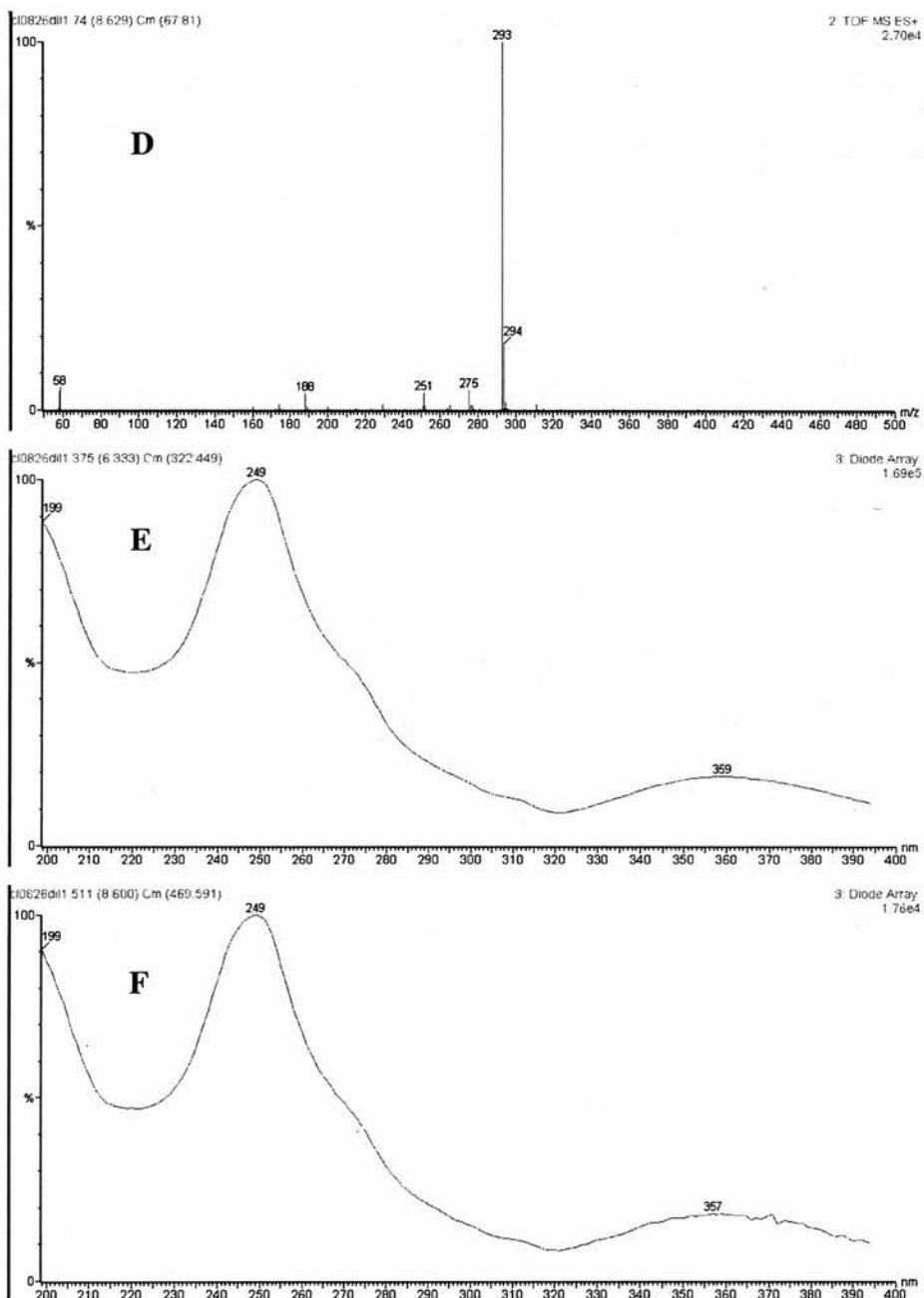


Figure 4. C) ESMS (+ve) of peak $t_R=6.33$ min. $[M+H]^+=293$. D) ESMS (+ve) of peak $t_R=8.60$ min. $[M+H]^+=293$. E) UV-vis spectra of peak $t_R=6.33$ min. max=249 nm. F) UV-vis spectra of peak $t_R=8.60$ min. max=249 nm.

2.3. LC-MASS for *S*-1-(4-bromophenyl)-3 α -hydroxy-6-methyl-2,3,3 α ,4-tetrahydro-1*H*-pyrrolo[2,3-*b*]quinolin-4-one (135)

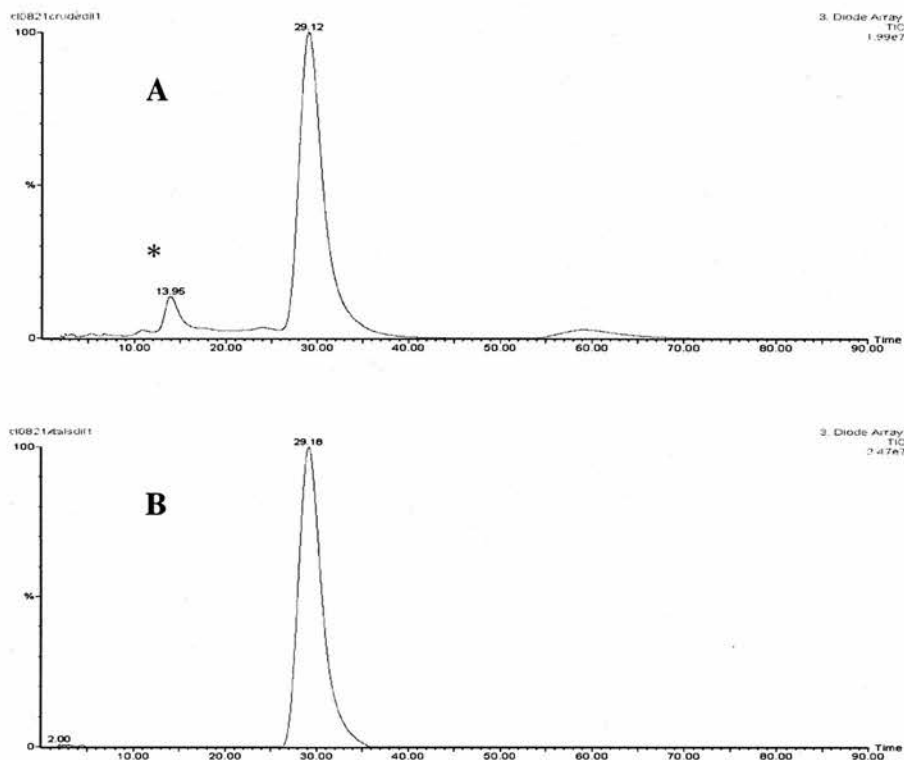
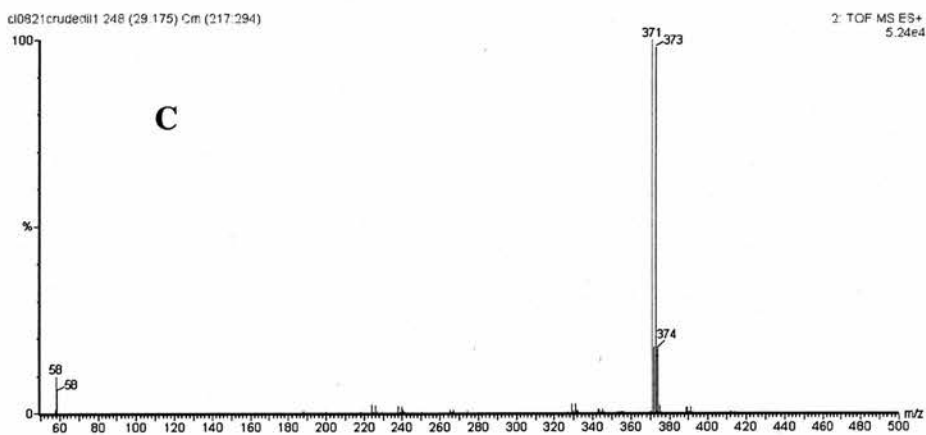


Figure 5. Chiral HPLC analysis. Conditions: Daicel Chiralpak AD-RH, Acetonitrile/Water 50:50, flow rate 0.8 mL min⁻¹, λ =254 nm. A) chromatogram of the crude mixture of **135**: major enantiomer t_R =29.12 min., λ_{max} =244 nm and minor enantiomer t_R =59.25 min., λ_{max} =244 nm. B) chromatogram of the crystallised bromo-blebbistatin analogue (**135**): major enantiomer t_R =29.18 min., λ_{max} =244 nm. * Minor impurity at t_R =13.95 min.



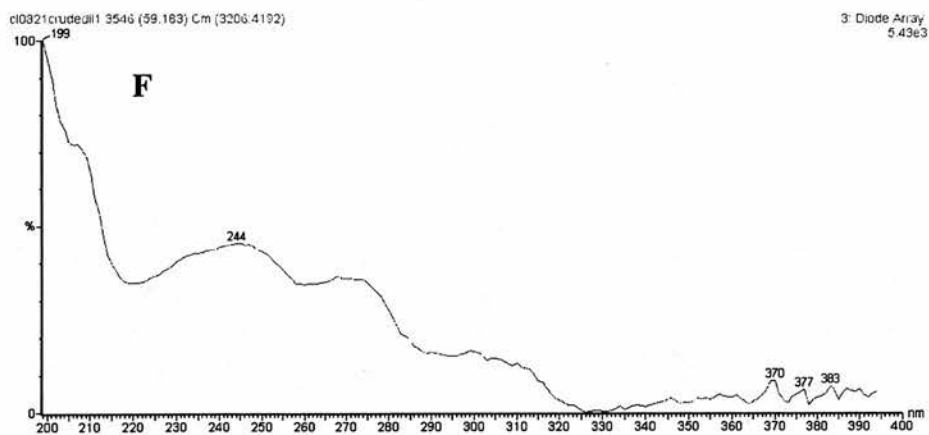
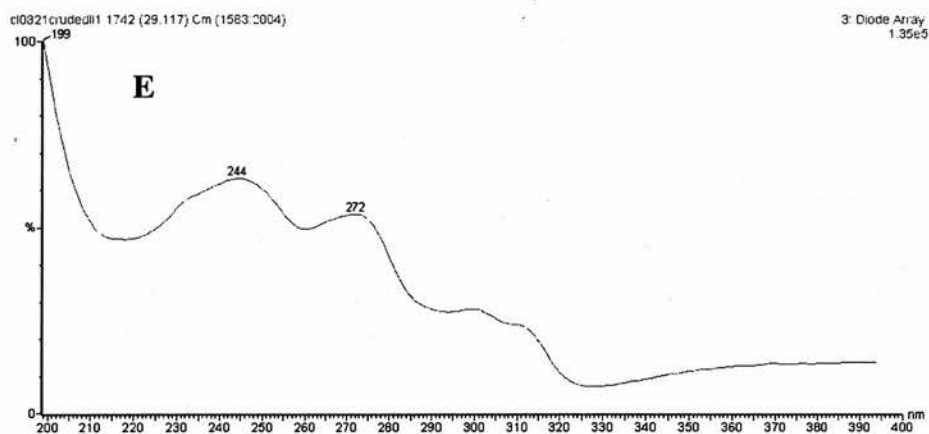
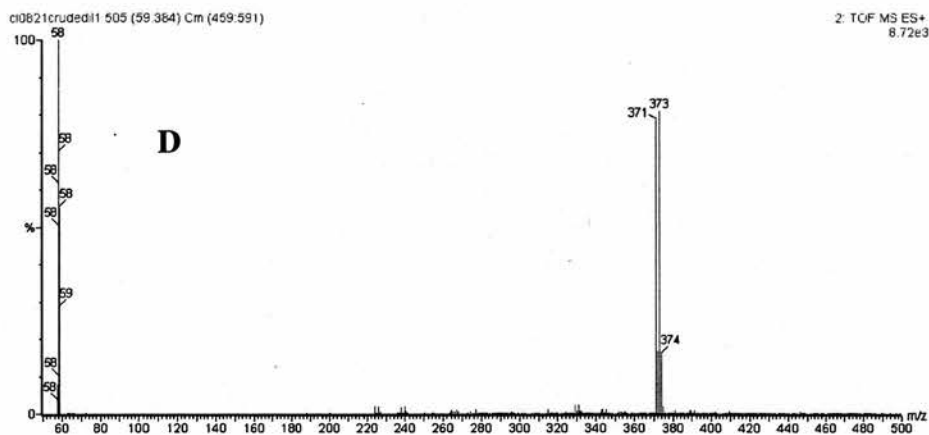


Figure 6. C) ESMS (+ve) of peak $t_R=29.12$ min. $[M+H]^+=371$, $[M+H]^+=373$. D) ESMS (+ve) of peak $t_R=59.25$ min. $[M+H]^+=371$, $[M+H]^+=373$. E), UV-vis spectra of peak $t_R=29.12$ min. max=244 nm. F) UV-vis spectra of peak $t_R=59.25$ min. max=244 nm.